

1152
(NASA-CR-176765) REVIEW AND EVALUATION OF
RECENT DEVELOPMENTS IN MELIC INLET DYNAMIC
FLOW DISTORTION PREDICTION AND COMPUTER
PROGRAM DOCUMENTATION AND USER'S MANUAL
(Kansas Univ. Center for Research, Inc.)

N86-24955

Unclas
G3/34 42988

REVIEW AND EVALUATION OF RECENT DEVELOPMENTS
IN MELIC INLET DYNAMIC FLOW DISTORTION
PREDICTION

and

COMPUTER PROGRAM DOCUMENTATION AND USER'S MANUAL

ESTIMATING MAXIMUM INSTANTANEOUS INLET FLOW
DISTORTION FROM STEADY-STATE TOTAL PRESSURE
MEASUREMENTS WITH FULL, LIMITED, OR NO DYNAMIC
DATA

CRINC



THE UNIVERSITY OF KANSAS CENTER FOR RESEARCH, INC.

2291 Irving Hill Drive-Campus West

Lawrence, Kansas 66045



THE UNIVERSITY OF KANSAS CENTER FOR RESEARCH, INC.

2291 Irving Hill Drive—Campus West
Lawrence, Kansas 66045-2969

Telephone: (913) 864-3441

REVIEW AND EVALUATION OF RECENT DEVELOPMENTS
IN MELIC INLET DYNAMIC FLOW DISTORTION
PREDICTION

and

COMPUTER PROGRAM DOCUMENTATION AND USER'S MANUAL

ESTIMATING MAXIMUM INSTANTANEOUS INLET FLOW
DISTORTION FROM STEADY-STATE TOTAL PRESSURE
MEASUREMENTS WITH FULL, LIMITED, OR NO DYNAMIC
DATA

NASA Grant No. NAG 3-11
FINAL REPORT
Volume II

William G. Schweikhard
Principal Investigator

and

Stephen R. Dennon
Graduate Research Assistant

April 1986

PART I

REVIEW AND EVALUATION OF RECENT DEVELOPMENTS
IN MERLICK INLET DYNAMIC FLOW DISTORTION
PREDICTION

SUMMARY

A brief review of developments in the Melick method of inlet flow dynamic distortion prediction by statistical means is provided. These developments include the general Melick approach with full dynamic measurements, a limited dynamic measurement approach, and a turbulence modelling approach which requires no dynamic rms pressure fluctuation measurements. These modifications are briefly evaluated by comparing predicted and measured peak instantaneous distortion levels from provisional inlet data sets.

A nonlinear mean-line following vortex model is proposed and evaluated as a potential criterion for improving the peak instantaneous distortion map generated from the conventional linear vortex of the Melick method. The model is simplified to a series of linear vortex segments which lay along the mean line. Maps generated with this new approach are compared with conventionally generated maps, as well as measured peak instantaneous maps.

Results of the developments and modifications discussed compare well with experimental measurements, both in the prediction of peak instantaneous distortion levels, and the peak instantaneous maps. Inlet data sets include subsonic, transonic, and supersonic inlets under various flight conditions. The methods discussed can be used in preliminary inlet design phases in the interest of reducing development costs.

TABLE OF CONTENTS

	page
SUMMARY	i
LIST OF SYMBOLS	iii
INTRODUCTION	1
1. REVIEW OF BASIC CONCEPTS AND DEVELOPMENTS	4
A. The Melick Vortex Model	4
B. The Minimum Dynamic Measurement Approach	6
C. The Turbulence Modelling Approach	7
2. A MODIFIED VORTEX MODEL	9
A. Introduction	9
B. Method of Approach	10
C. Mathematical Formulations	13
3. RESULTS AND DISCUSSIONS	19
A. Subsonic Inlet	19
B. Transonic Inlet	20
C. Supersonic Inlet	21
D. General Comments	22
1. The Melick Approach	22
2. The Minimum Dynamic Measurement Approach	24
3. The Segmentes Vortex Approach	24
4. CONCLUSIONS	25
REFERENCES	27
TABLES AND FIGURES (begin)	28

LIST OF SYMBOLS

<u>Symbols</u>	<u>Description</u>
a	vortex core radius (fig. 5)
\bar{a}	mean vortex core size
dP_T	total pressure fluctuation
$dP_{T_{rms}}$	root mean square total pressure fluctuation
e	exponential e^x
erf	error function $\text{erf}(x)$
f	root mean square data cutoff filter frequency
k	distortion factor
\bar{k}	mean instantaneous distortion factor
k_{ss}	steady-state distortion factor
k_{max}	maximum instantaneous distortion factor
P	pressure
P_S	static pressure
P_T	total pressure
$P_{T_{ss}}$	steady-state total pressure
q	dynamic pressure, steady-state
r	radius from vortex centerline
r_{rms}	root mean square
r_p	radial location of probe
r_v	radial location of vortex core
U, U_2	steady-state inlet flow velocity

V	vortex induced velocity
V_T	tangential swirl velocity about vortex
$V_{T_{\max}}$	vortex strength - maximum swirling velocity

Subscripts

f	filtered
$inst$	instantaneous
m	measured
max	maximum
min	minimum
p	predicted
rad	radial
rms	root mean square
T	tangential
ss	steady-state

Superscripts

$-$	mean value \bar{x}
-----	----------------------

Greek Symbols

β, δ	vortex orientation angles
α, β	angle of attack, sideslip angle
ρ	density
σ	standard deviation

INTRODUCTION

Inlet turbulence and other flow nonuniformities have long been known to significantly affect the operational stability of gas turbine engines, especially in high performance military aircraft. This inlet flow distortion is traditionally measured at the compressor face of the engine with an array of total pressure probes mounted on rakes. The time-averaged steady-state pressures at each of the probe locations are processed and combined in such a way as to generate various steady-state distortion factors and an engine face pressure contour map (see Table 1 and Figure 1, respectively). These then correlate to engine surge margins.

The distortion problem is intensified by the time variant component of the total distortion level. Random fluctuations in the total pressure measurements can generate instantaneous distortion levels which can induce engine surges even when the steady-state component is well below compressor stall margins. It becomes important, therefore, to be able to predict the most probable peak instantaneous (dynamic) distortion level early in the inlet design effort.

One method of determining the dynamic distortion level of an inlet is to use an array of high response total pressure probes, with an extensive inventory of support instrumentation and computational equipment to record time histories of the pressure fluctuations for each of the probes. These data are then screened, using the Dynamic Data Editing and Computing (DYNADEC) system, to determine an experimental peak distortion level using the same definitions as the steady-state case. This method is generally quite accurate, compared to statistical methods described later, but it is also extremely expensive in terms of instrumentation and

computational requirements. In order to reduce the cost of inlet distortion tests, several statistical methods have been developed to predict the dynamic distortion component, given the steady-state distortion and limited dynamic data (ref. 1, 2, 3).

Of the many statistical methods of predicting dynamic distortion levels, the most efficient is Melick modelling approach. In the Melick method, it is postulated that the dynamic disturbances in the inlet flow can be modelled by the pressure disturbances resulting from a series of randomly distributed vortices convecting through the inlet duct. Filtered and unfiltered root mean square (rms) total pressure fluctuation levels are used to identify the main variables in this vortex flow model (ref. 2, 3, 4).

The main advantages of the Melick method include low cost relative to other techniques, as well as the fact that it can be used online, while the test is in progress. It has been shown that further cost reduction can be attained by reducing the quantity of dynamic data (ref. 2, 3). In fact, Chen (ref. 3) has derived and demonstrated a new technique for predicting the peak distortion levels with only the steady-state distortion data, that is, with no dynamic data.

One of the main disadvantages of the Melick modelling approach is it is not as accurate as some methods in the generation of the peak dynamic distortion patterns in the engine face contour map. This is due primarily to a limitation in the vortex flow model, namely, the use of a single linear vortex in the generation of the peak instantaneous pressure array. More specifically, the peak instantaneous pressure array is computed by placing a linear vortex along a portion of the mean pressure line in such a way to amplify the distortion pattern pressures (fig. 3). The size and strength of this vortex is determined as a function of the most probable peak instantaneous distortion level. It has

been suggested that a new concept in vortex modelling could improve the accuracy of the predicted peak dynamic distortion pattern (ref. 2).

It is apparent that the mean pressure line in distortion patterns is not generally straight. In most cases, the mean line can be seen to arc across the engine face, frequently forming a distorted ring. One possible solution to the vortex modelling problem is to replace the single straight vortex oriented along a portion of the mean line with a curved mean-line-following vortex. This nonlinear vortex (or vortex ring, where applicable) could provide a more accurate amplification of the pressure levels in the vicinity of the vortex.

In the present work, the concept of replacing the linear vortex model of the traditional Melick model with a nonlinear mean-line-following vortex is proposed and evaluated. For the purposes of demonstrating the concept, this new model is simplified by breaking the vortex into a series of vortex segments, one segment for each of the probe rakes (fig. 4). The radius and strength of these vortex segments is retained from the original Melick dynamic data matching process.

The results of the present method are compared to the original single linear vortex model, as well as the DYNADEC results, for a variety of data sets. These data include example subsonic, transonic, and supersonic inlet configurations at various angles of attack and sideslip.

Major objectives of this study are: 1) to review some of the recent developments in dynamic distortion prediction with the Melick method as a foundation; 2) to demonstrate the utility of a new tool for improving the accuracy of peak instantaneous distortion contour maps; and 3) to evaluate present and recent developments in Melick dynamic distortion analysis.

1. REVIEW OF BASIC CONCEPTS AND DEVELOPMENTS

A. The Melick Vortex Model

The Melick convecting vortex model is a tool used to statistically determine the most probable peak instantaneous distortion level, given the steady-state distortion and the root mean square (rms) total pressure fluctuation level at the engine face. It is formulated around the observation that the total pressure fluctuations exhibit random characteristics, with a near-normal (Beta/Gaussian) distribution (fig. 2). From Bernoulli's flow relationships, it is easily seen that these total pressure fluctuations can be expressed in terms of perturbations in the steady-state flow velocity. These velocity perturbations can in turn be modelled by time-variant vorticity (fig. 5). Thus the Melick method envisions the total pressure fluctuations as being totally attributed to a series of random vortices (random in size, strength, location, and orientation) convecting through the inlet duct (ref. 2).

According to the Melick model, as a vortex passes through the inlet duct, it would create a fluctuation in the steady-state pressure level at all locations in the measurement plane, that is, the engine face. This pressure fluctuation would give rise to an instantaneous distortion level, computed from any of a variety of distortion factors (table 1). Given the properties of an arbitrary vortex, the resulting velocity perturbations can be determined from simple flow relationships (fig. 5). The pressure fluctuation can again be determined from the velocity perturbation, resulting in an instantaneous distortion level.

It is shown in reference 2 that the statistical properties of the convecting vortices of the Melick model are directly related to the statistical properties of the pressure fluctuations. Specifically, the mean vortex size can be determined from the root mean square total pressure fluctuation level. This is accomplished by computing the rms fluctuation level resulting from an assumed vortex size and strength, and then comparing the measured rms level. The vortex size is then adjusted until the analytical and experimental rms levels match.

Once evaluated, the mean vortex properties are then used to compute the mean instantaneous distortion level, which leads to the determination of the most probable maximum instantaneous distortion level. The mean instantaneous distortion is found analytically from the steady-state distortion level and the rms total pressure fluctuation level, along with the mean vortex size (ref. 2). The peak instantaneous value is then statistically extrapolated given the mean instantaneous value, the rms level, and certain statistical parameters (ref. 2). The maximum instantaneous distortion level can be computed for a variety of confidence levels, though the "most probable" (a 50% confidence level) is used in most analyses (fig. 6).

The newly computed maximum instantaneous distortion level is then used to produce the peak dynamic distortion contour map. First, the mean vortex is modified to accommodate the peak dynamic distortion level. This is done by increasing the strength of the vortex until it produces an rms fluctuation level, and consequently a distortion level, which matches the maximum instantaneous distortion level. When this new vortex strength has been established, the resulting pressure disturbances are computed for each of the probe locations, and added to the steady-state pressures. The maximum instantaneous pressure array is then used to generate the peak dynamic distortion map (ref. 2).

B. The Minimum Dynamic Measurement Approach

One of the benefits of the Melick approach to dynamic distortion prediction is its low cost relative to other methods. Traditionally, the Melick method requires steady-state total pressure measurements, along with rms total pressure fluctuation measurements at forty probe locations across the engine face. In the derivation of the mean instantaneous distortion level, the mean value (face-average) rms level is used. The actual number of high-response dynamic probes is not important - just the mean rms value is of interest. In principle, therefore, the Melick method requires only one dynamic rms total pressure measurement, provided an average value is indicated. In the interest of further reducing instrumentation cost, and inlet blockage during a test run, it is desirable to minimise the number of dynamic probes used while retaining the accuracy of the results. Proper placement of a minimum number of dynamic probes is necessary in order to obtain an accurate representation of the average rms level, and the resulting peak dynamic distortion prediction.

Chen (ref. 2) provided a criterion for the selection of dynamic probe locations which yield reasonable accuracies in mean rms level determination. It was observed that there exists an inverse relationship between the rms total pressure fluctuation level and the magnitude of the total pressure. In other words, high rms pressure fluctuations tend to occur in regions of low total pressure, while low rms levels occur in high pressure regions. Furthermore it was noted that average rms levels tend to occur near regions of average pressure. This implies that dynamic probes placed near the steady-state mean pressure line would give rms

total pressure fluctuation levels nearly equal to the face-average value.

Since it is preferred to remain on the conservative side in dynamic distortion prediction, that is it would be more desirable to overpredict rather than underpredict the true peak dynamic distortion in any simplifications, it is suggested that the preferred dynamic probe location should be at or outboard of the mean pressure line (ref. 2). This will allow in most cases an rms level slightly higher than the average value obtained in a 40-probe analysis. In any case, dynamic probe locations selected should avoid regions of very high and very low steady-state pressures.

The accuracy of this criterion is shown herein and in reference 2. It was shown that using 2 probes selected according to the "conservative side" criterion yielded distortion factor errors generally within 5% of the 40-probe prediction. Naturally, if dynamic probes were selected such that the average rms value were exactly equal to the 40-probe average, there would be no error. Conversely, the selection of improper probes can lead to very large errors. Consequently, the careful selection of locations for the placement of dynamic probes is extremely important for the accuracy of the results.

C. The Turbulence Modelling Approach

Because of the sensitivity of the predicted peak distortion level to the indicated mean rms level, which in turn is sensitive to the location of the probes relative to the mean total pressure line, it is desirable to develop an approach which includes the benefits of both the full (40-probe) dynamic data method and the minimum dynamic data approach. In response to this need, Chen (ref. 3) developed a turbulence modelling approach which produces an accurate prediction of the peak instantaneous distortion with no

requirement for dynamic rms total pressure fluctuation data.

In this turbulence modelling approach, the rms total pressure fluctuation levels are simulated from information derived from the steady-state total pressure measurements. First, the axial velocity distribution (relative flow velocity at each steady-state probe location) is calculated from the steady-state measurements. A set of turbulence modelling equations is then employed to compute the turbulent kinetic energy distribution, and the turbulent kinetic energy dissipation rate. These terms represent the turbulence levels required to generate the steady-state distortion. The rms total pressure fluctuation levels are then evaluated from the turbulent kinetic energy and the turbulent kinetic energy dissipation rate. These simulated rms levels are then used to compute the mean vortex properties, the mean instantaneous distortion level, and the peak dynamic distortion in the same manner as the original Melick model (ref. 3).

The advantages of the turbulence modelling approach are obvious. There is no need for rms total pressure fluctuation levels to be measured - hence no high-response dynamic probes are needed. Instrumentation costs are reduced considerably from the fully instrumented 40-probe case. In addition, there is no need for concern over where to most effectively place a minimum number of dynamic probes. The turbulence modelling approach, when coupled with the Melick vortex model, is an efficient tool for determining the most probable peak instantaneous distortion level, given the steady-state measurements.

The accuracy of the turbulence model is demonstrated in reference 3. It is shown that this approach is at least as accurate as the fully instrumented case in comparison to the DYNADEC results for a variety of inlet configurations and operating conditions (ref. 3).

2. A MODIFIED VORTEX MODEL

A. Introduction

Although the original Melick vortex modelling approach (including the modifications summarized in the previous section) is shown to be reasonably accurate in the prediction of peak instantaneous distortion levels, it is not as accurate as some methods in the generation of peak instantaneous distortion maps (ref. 2, 5). It is therefore desirable to develop some modification to the Melick vortex model which can improve the accuracy of the peak instantaneous map.

It has been suggested (ref. 2) that the fault in the Melick peak instantaneous mapping method may lie in one of the vortex modelling assumptions. This modelling approach produces the peak instantaneous pressure distribution by superimposing a linear vortex along the mean shear line of the steady-state distortion pattern (fig. 3). The induced flow velocities produced by this vortex, whose properties are determined from the rms total pressure fluctuation levels, result in an amplification of the total pressure distribution. Both high and low pressure regions are enhanced by this vortex so that the distortion level is magnified.

In reality, the mean shear line of most steady-state distortion patterns is not a straight line, but is instead curved. In fact, often the mean line forms a distorted ring. This suggests that the core of the peak instantaneous vortex should not be a straight line, but should follow the curves of the mean shear line. This will be the basis of the present study.

B. Method of Approach

In the present analysis, a new vortex modelling approach designed to improve the accuracy of Melick peak instantaneous distortion maps is developed. In this new approach, the linear vortex model of the original Melick method (fig. 3) is replaced by a vortex which can have a nonlinear core (fig. 4). This is a justified modification because the mean shear line (the borderline between relatively high and low pressure regions) is generally nonlinear (fig. 4).

There are three general methods in modelling a vortex with a nonlinear core. The first and most complex method would be to formulate a mathematical expression for a curve which fits the desired shape of the vortex core - that is the mean shear line. This expression could be in terms of 2-dimensional cartesian or polar coordinates, derived from a least-squares (or other nonlinear) analysis, or perhaps from an infinite series expansion. This method has the potential of being extremely accurate as far as modelling the vortex is concerned, but would not be very efficient in terms of the computational effort.

A second approach to modelling a nonlinear vortex core might be form a finite element model. The nonlinear vortex would be divided up into a series of linear vortex segments which would lie along the mean line. The number of segments used would depend on amount of curvature in the mean shear line and the desired resolution. This method, depending on the number of divisions selected, could be as accurate as the least squares/infinite series method, with considerably better computational efficiency.

It is clear that these two methods have the capability

of achieving very high resolution in the calculation of the vorticity effects, and in the generation of the peak instantaneous distortion map. This high resolution capability is not necessarily useful, however. It should be kept in mind that the peak instantaneous map is generated by calculating the effect that the vortex has upon the total pressure readings obtained at the steady-state probe locations. Pressures at locations between probes are then interpolated from these new "readings". Consequently any vortex action which occurs between probe locations is ignored, prior to the interpolation process. This limitation in the useable resolution of the vortex model is the basis of the simplifications of the third modelling approach.

The third approach to modelling a nonlinear vortex core is similar to the finite element model, but includes some important simplifying assumptions. First, the vortex is divided up into eight segments, each associated with one of the probe rakes (fig. 4). Each vortex segment is considered the dominant contributor to the pressure disturbances occurring on the rake associated with that vortex segment. It is assumed that each vortex segment affects the pressure only on the rake associated with it. The position of the vortex segment relative to its associated rake is assumed to be at the probe nearest to the mean pressure line where it crosses the rake. The orientation of each vortex segment is assumed to be perpendicular to its associated rake, and coplanar with the measurement plane. Each of these simplifying assumptions are illustrated in figure 4, and are discussed separately.

The first assumption involves the division of the nonlinear vortex into eight linear sub-vortices, or vortex segments. Traditionally, there are eight rakes mounted at 45 degree intervals around the measurement plane (fig. 7). Since all probes on a rake are affected by the induced flow velocity caused by the local vorticity, it makes sense

to divide the probes into rake-groups, and to determine the dominant vortex activity associated with that group. Therefore, in this study the nonlinear vortex system is divided into a set of linear vortex segments, with each segment acting as the dominant vortex activity for one of the rakes. Eight rakes each require one vortex segment, for a total of eight sub-vortices. Each vortex segment is considered by definition to affect only the probes on it's respective rake, and induced vortex activity on adjacent rakes is considered by definition negligible.

The next assumption involves the definition of the location of each of the vortex segments. It is assumed that the vortex segment is placed directly over the probe location nearest to the mean shear line as it crosses over or passes near to the rake. In addition, it is assumed that the vortex segment is oriented perpendicular to the rake. These two simplifying assumptions are illustrated in figure 3. It is suggested that these simplifications introduce only small errors into the analysis, while they allow considerable improvement in computational efficiency. In any case, the error produced by these simplifications will always be less than the error produced in the original Melick single linear vortex model.

Finally, it is assumed that the vortex properties as derived in the Melick linear modelling approach are still valid in the segmented modelling approach. These properties include: 1) the mean vortex radius, and 2) the vortex strength. These terms were derived as a function of the rms total pressure fluctuation level, and the most probable peak instantaneous distortion level.

Each of these assumptions and simplifications are made in the interest of providing a straightforward model and a simplified analysis. None of the assumptions are expected to introduce significant error into the analysis. The nature of the model and the analysis is intended to be preliminary,

in the interest of determining whether further research is warranted in this modelling approach.

In the following section, the development of the mathematical formulations is presented based on the simplifying assumptions.

C. Mathematical Formulations

In the Melick approach to peak instantaneous distortion prediction, there are two distinct sections: 1) the development of the most probable peak instantaneous distortion level; and 2) the generation of the peak instantaneous map. Since the present analysis is concerned primarily with the latter of these two sections, the first section will be presented only in summary form. Details on the derivation of the peak instantaneous distortion level may be found in reference 2.

As described in section 1.A., the random total pressure fluctuations measured at the compressor face are attributed to the convection of a series of random vortices through the measurement plane. The pressure fluctuations are to be expressed in terms of velocity perturbations introduced by these vortices. The velocity profile of a one-dimensional steady and incompressible vortex is given as (fig. 5):

$$V_T = V_{T_{\max}} \frac{r}{a} e^{-\frac{1}{2}[(r/a)^2 - 1]} \quad (1)$$

where: V_T is the tangential velocity at any radius r

$V_{T_{\max}}$ is the maximum vortex swirling velocity at $r=a$;
a measure of vortex strength.

r is the independent variable: radius

a is the radius at the point of maximum swirling velocity - also called the vortex size

e is the exponential

The total pressure fluctuations produced by the vortex are superimposed onto the steady-state total pressure to form a time variant instantaneous pressure:

$$P_T = P_{T_{ss}} + dP_T \quad (2)$$

where: P_T is the instantaneous total pressure

$P_{T_{ss}}$ is the steady-state total pressure

dP_T is the pressure fluctuation produced by the vortex

From the incompressible Bernoulli equation:

$$P_{T_{ss}} = P_S + \frac{1}{2}\rho U^2 \quad (3a)$$

$$P_T = P_S + \frac{1}{2}\rho(U + V_T)^2 \quad (3b)$$

where: P_S is the static pressure

ρ is the flow density

U is the steady-state flow velocity

V_T is the vortex-induced velocity

Let $q = \frac{1}{2}\rho U^2$ be the steady-state dynamic pressure. Then substituting (3) into (2), we obtain:

$$\begin{aligned} dP_T &= P_T - P_{T_{ss}} = \frac{1}{2}\rho(U + V_T)^2 - \frac{1}{2}\rho U^2 \\ &= \frac{1}{2}\rho(U^2 + 2UV_T + V_T^2 - U^2) \\ &= q \left[\left(\frac{2V_T}{U}\right) + \left(\frac{V_T}{U}\right)^2 \right] \doteq \frac{2qV_T}{U} \end{aligned} \quad (4)$$

Second order terms have been neglected for V_T much less than U .

Substituting (1) into (4), we obtain:

$$dP_T = \frac{2q}{Ua} V_{T_{\max}} r e^{-\frac{1}{2}[(r/a)^2 - 1]} \quad (5)$$

Equation (5) represents the total pressure fluctuation level produced by the convection of an arbitrary vortex through the inlet duct in terms the relative size and strength of the vortex, and the position of the probe relative to the vortex.

In the Melick analysis, in order to determine the most probable peak instantaneous distortion level, the mean vortex size must be determined. This parameter is shown (Ref 2) to be a function of the rms total pressure fluctuations:

$$\left(\frac{dP_{T_{\text{rms}}}(f)}{dP_{T_{\text{rms}}}} \right)^2 = \text{erf} \left(7.98 \frac{f\bar{a}}{U} \right) \quad (6)$$

The quantity on the left hand side of equation (6) is the square of the ratio of the root mean square total pressure fluctuation level filtered at cut-off frequency f , to the unfiltered rms level. These quantities may be measured, or simulated as developed in reference 3. Using equation (6), the mean vortex size, \bar{a} , can be solved for iteratively in terms of the filtered and unfiltered rms levels, the filter frequency, and the flow velocity, all of which are known quantities.

The mean vortex size is then used to generate the mean instantaneous distortion level, \bar{k} : (Reference 2)

$$\bar{k} = k_{ss} + f(\bar{a}, dP_T) \quad (7)$$

where: k_{ss} = the steady-state distortion level determined from the steady-state total pressure data and table 1

Since dP_T is a function of the vortex properties, \bar{k} can be determined from them:

$$\bar{k} = f(P_{T_{ss}}, q, U, \bar{a}, V_{T_{max}}) \quad (8)$$

where: $P_{T_{ss}}$, q , and U are measured quantities

\bar{a} is computed from equation (6)

$V_{T_{max}}$ is then determined, using equation (5):

$$V_{T_{max}} = \frac{U \bar{a} dP_T}{2qr} e^{\frac{1}{2}[(r/a)^2 - 1]} \quad (9)$$

For $r = \bar{a}$, equation (9) is simplified to:

$$V_{T_{max}} = \frac{1}{2} \frac{U}{q} dP_{T_{rms}} \quad (10)$$

Equation (8) then becomes:

$$\bar{k} = f(P_{T_{ss}}, q, U, \bar{a}, dP_{T_{rms}}) \quad (11)$$

Since q and U are constants, equations (7) and (11) are seen to be identical.

The most probable peak instantaneous distortion level is then statistically extrapolated as a function of the mean instantaneous distortion level, the rms total pressure fluctuation level, and a set of statistical parameters (ref. 2):

$$k_{max} = f(\bar{k}, dP_{T_{rms}}, \text{statistical parameters}) \quad (12)$$

The vortex strength is then adjusted to match the change from

the mean instantaneous distortion level to the maximum instantaneous distortion level:

$$V_{T_{\max}/pk} = V_{T_{\max}} + f(k_{\max} - \bar{k}) \quad (13)$$

Once the most probable peak instantaneous distortion level and the value of $V_{T_{\max}}$ has been determined, the value for the peak instantaneous total pressure can be determined:

$$P_{T_{pk}} = P_{T_{ss}} + dP_{T_{pk}} \quad (14)$$

where $dP_{T_{pk}}$ is obtained from equations (5) and (13):

$$dP_{T_{pk}} = \frac{2q}{U\bar{a}} V_{T_{\max}/pk} r e^{-\frac{1}{2}[(r/\bar{a})^2 - 1]} \quad (15)$$

The only variable in equation (15) above is the radius, r . Using the simplifications and assumptions given in section 2.B., the value of r can be determined on a rake-by-rake and probe-by-probe basis. Substituting (15) into (14) produces the following relationship (let $V = V_{T_{\max}/pk}$):

$$P_{T_{pk}}(k,p) = P_{T_{ss}}(k,p) + \frac{2qV}{U\bar{a}} r(k,p) e^{-\frac{1}{2}[(r(k,p)/\bar{a})^2 - 1]} \quad (16)$$

The subscripts k and p refer to the rake and probe number, respectively. The value of $r(k,p)$ is defined as the distance between the probe with coordinates (k,p) and the core of the vortex associated with rake k :

$$r(k,p) = r_p(k,p) - r_v(k) \quad (17)$$

where: $r_p(k,p)$ is the radial location of probe (k,p)

$r_v(k)$ is the radial location of the core of the
vortex associated with rake (k)

The final step in generating the peak instantaneous map is to interpolate values for $P_{T_{pk}}$ at each of the discrete points between the probes. This is done in the same manner as with the steady-state map (ref. 6).

3. RESULTS AND DISCUSSIONS

In the following sections, numerical and graphical predictions from the analytical methods described in the present work are provided with three inlet data sets. Data comparisons with the DYNADEC results are also provided with each of the inlet configurations. The three inlet data sets consist of provisional experimental results from subsonic, transonic, and supersonic inlet configurations under various flight conditions. Inlet configurations and measured results of the data sets are provided in figures 8 through 10. Data comparisons of predicted and measured peak instantaneous distortion levels, and graphical comparisons of predicted and measured peak instantaneous distortion maps are also provided.

A. Subsonic Inlet

Configuration of a full-scale short S-shaped subsonic inlet duct is shown in figure 8. The engine centerline is tilted approximately six degrees from the horizontal as shown in the figure. The freestream Mach number was given as subsonic. Six test cases were available for data comparison. These data were provided by the Air Force (AFWAL), Wright-Patterson AFB, Ohio.

Comparison of Melick predicted peak instantaneous distortion levels is given in Table 2 and Figures 11 and 12. Figure 13 shows mapping comparisons for the steady-state, DYNADEC measured peak, Melick predicted peak, and the Modified Vortex predicted peak instantaneous distortion patterns. As described in Reference 3, reasonably good accuracy of the distortion level prediction analyses is indicated. In certain

cases, the peak instantaneous distortion level is underpredicted by the Melick approach. This is attributed to the fact that the Melick approach cannot accurately predict the peak distortion level for inlet flows with separated boundary layers. Unfortunately, the subsonic data set contains separated boundary layers at the engine face (ref. 3) Further study will be required to improve the Melick predictive accuracy in separated flow cases.

The Modified (segmented-nonlinear) Vortex technique compares favorably with the Melick modelling approach in the peak distortion map generation, in certain cases. In cases where the Melick linear vortex model produces an accurate prediction of the peak instantaneous map, the modified approach generally overpredicts the distortion pattern slightly. In cases where the Melick approach yields poor results in the peak distortion map, the modified approach tends to improve the map considerably (fig. 13).

B. Transonic Inlet

Configuration of a 15% subscale long S-shaped transonic inlet duct is shown in Figure 9. Six test cases with a transonic freestream Mach number were available for comparison. These data were provided by the Air Force (AFWAL) Wright-Patterson AFB, Ohio.

Comparisons of predicted and measured peak instantaneous distortion levels are given in Table 3 and Figures 14 and 15. Figure 16 shows mapping comparisons for steady-state, DYNADEC measured peak, Melick predicted peak, and the Modified Vortex predicted peak instantaneous distortion patterns. Good accuracy in predicting peak dynamic distortion levels is indicated for these test cases. The Melick method slightly overpredicts the peak distortion level, which is the desired affect.

The Modified Vortex approach again compares favorably with the Melick linear vortex approach. In examples where the original Melick approach yields poor predictions of the peak instantaneous distortion pattern, the modified approach produces superior results (fig. 16). In cases where the Melick approach produces good peak distortion maps, the modified approach produces comparable results.

A notable exception to this can be seen in the first case (case number 464.12). The steady-state map shows a symmetrical pattern, while the DYNADEC predicted pattern is not symmetrical (fig. 16). The Melick approach produces a fairly symmetrical pattern as expected, while the modified approach produces a pattern almost identical to the steady-state pattern, except for enhanced pressure magnitudes, also as expected from the modelling criteria. This is due to the fact that this particular test case represents an extremely high angle of attack, where asymmetrical vortex shedding is evidently taking place. This inlet "pumping" has the effect of alternating high and low pressure levels on either side of the inlet duct instantaneously, while providing apparently symmetrical patterns in the steady-state. Asymmetrical or alternating vortex shedding is the same phenomenon which is associated with wing "rocking" in highly swept delta wings at high angles of attack.

C. Supersonic Inlet

Configurations for four 25% scale supersonic inlet ducts are shown in Figure 10. These inlet models include data for a variety of supersonic freestream Mach numbers, and angles of attack and yaw. There are thirteen test cases available for comparison. These data were also provided by the Air Force (AFWAL) Wright-Patterson AFB, Ohio. The four inlet configurations, test conditions, and some measured results are given in figure 10.

Comparison of predicted and measured peak instantaneous distortion levels is given in table 4 and figure 17. Figure 18 shows comparisons of steady-state, DYNADEC measured peak, Melick predicted peak, and modified Melick predicted peak instantaneous distortion contour maps. Many of the peak instantaneous distortion levels are underpredicted slightly, primarily because these cases show separated boundary layers. It is recalled that the Melick approach tends to underpredict peak distortion levels when separated boundary layers occur in the inlet duct. It is noted that in many cases the maps generated by the Melick approach appear to have no apparent pattern as far as relatively high and low pressure regions. The steady-state and peak instantaneous maps in these cases exhibit quasi-random characteristics, indicating severe turbulence levels and flow separation. The Melick prediction technique generally requires a reasonably well-defined mean shear line in order to effectively apply the vortex model. The predicted distortion levels and distortion maps are seen to be fair to good in these cases. In certain cases, when the linear Melick vortex model fails to provide a good prediction of the peak distortion map and the measured peak map resembles the steady-state pattern, the segmented vortex model provides a map superior to the one generated by the linear vortex model (fig. 13).

D. General Results and Comments

1. The Melick Approach

The Melick approach to predicting the peak instantaneous distortion levels can be evaluated by examining Tables 2, 3 and 4, comparing peak distortion values as measured from the DYNADEC system, and as predicted by the Melick approach. Figures 11, 14 and 17 show these comparisons in graphical form.

It is seen from Figure 11 that the subsonic peak distortion factors are underpredicted in four out of six cases, and has a percent error of greater than plus or minus twenty percent in three out of six cases. At first glance this may be disturbing, but it is recalled that the subsonic inlet data set indicates a separated boundary layer, as described in Reference 3. Since the Melick approach assumes an attached boundary layer, the results are understandable. Nevertheless it can be said that the Melick approach provided a good ball-park figure in distortion level prediction.

Figure 17 shows peak distortion level predictions within 20 percent in 4 out of 6 cases, with an underprediction of the measured peak distortion in only one case. These results can be considered very good. Near-perfect predictions are seen in two cases, which is encouraging. These transonic inlet data sets show a mean percent error of approximately ten percent for all six test cases.

The supersonic test cases show peak distortion predictions within 20 percent in 11 out of 13 cases. However, it is also noted from Figure 17 that the peak distortion is underpredicted in almost all cases. As seen from Figure 18, the supersonic inlet cases in many cases represent highly turbulent separated flow conditions, for which the Melick technique is known to tend to underpredict. The overall results for the supersonic test cases can be said to be fairly good, and very consistent.

The overall accuracy of the Melick approach can be judged with Figure 19. The overall percent error in the predicted peak instantaneous distortion level with non-separated flow shows a mean value of +19.5%, while the separated flow inlets show a mean percent error of -3.3%. These results are considered good for preliminary engineering purposes.

2. The Minimum Dynamic Measurement Approach

In addition to the results indicated in Reference 2, which shows very good results in the minimum dynamic measurement approach with respect to the full (40-probe) approach, Tables 2 and 3, and Figures 12 and 15 indicate excellent correlations between the two approaches. In addition, as indicated in Reference 3, the turbulence modelling approach shows excellent predictions of peak instantaneous distortion levels, with no dynamic measurements. Predictions well within 20 percent of the 40-probe predicted values are indicated for most of the test cases. These results appear to validate these two low-cost approaches.

3. The Segmented Vortex Approach

The segmented vortex approach can be judged in terms of its performance with respect to theoretical expectations. The segmented vortex approach is, again, a simplified model of the nonlinear mean-line following approach. This model will always produce a predicted peak instantaneous distortion pattern similar to the steady-state pattern, with the pressure levels amplified somewhat. This phenomenon can be easily seen in the distortion map comparisons (figs. 13, 16 and 18). In cases where the peak instantaneous map is not similar to the steady-state map, this approach will produce a poor prediction, while cases where the steady-state and peak instantaneous maps have similar patterns as measured by DYNADEC, the approach will produce a map generally superior to the linear Melick vortex approach. In some cases it is seen that the segmented vortex approach is far superior to the linear, while in most cases, the improvement is only marginal (fig. 13, 16, 18). It is possible that the accuracy of this approach can be improved by removing simplifications, though the overall pattern would not change significantly.

4. CONCLUSIONS

A simplified nonlinear vortex model has been developed in order to improve the quality of predicted peak instantaneous distortion maps. The nonlinear mean-line following vortex model is simplified by dividing the vortex into linear vortex segments, one for each rake of probes, oriented perpendicular to each probe, and each having the characteristics of the mean vortex developed in the original Melick approach.

A review and evaluation of recent developments in the Melick peak instantaneous distortion level prediction technique has been included. A simplified description of the Melick method has also been provided, with references to more detailed reports. Predictions using limited, minimum and no dynamic data have been compared to DYNADEC measurements with favorable results for three inlet data sets. Minimum and no dynamic data approaches have also been compared to full (40-probe) predictions with excellent results.

The Melick approach, along with recent improvements, is shown to be an efficient and accurate design tool for predicting peak instantaneous distortion levels in preliminary analyses. It is noted, however, that the approach does not work well with highly turbulent separated flow inlet conditions, due to limitations in the modelling approach. Further research will be required to develop improvements in separated inlet flow predictions.

The segmented vortex approach is a useful method of improving peak instantaneous distortion maps, provided the Melick peak distortion level has been accurately predicted, and provided the actual peak distortion map does resemble the steady-state map pattern. Further improvements in this

modelling approach are possible by removing simplifications and assumptions, as long as these two conditions are met. At this time there exists no modification to the Melick vortex model which can accurately predict the peak instantaneous distortion pattern when the measured peak pattern is significantly different from the steady-state pattern. Further study will be required to understand and predict this particular problem.

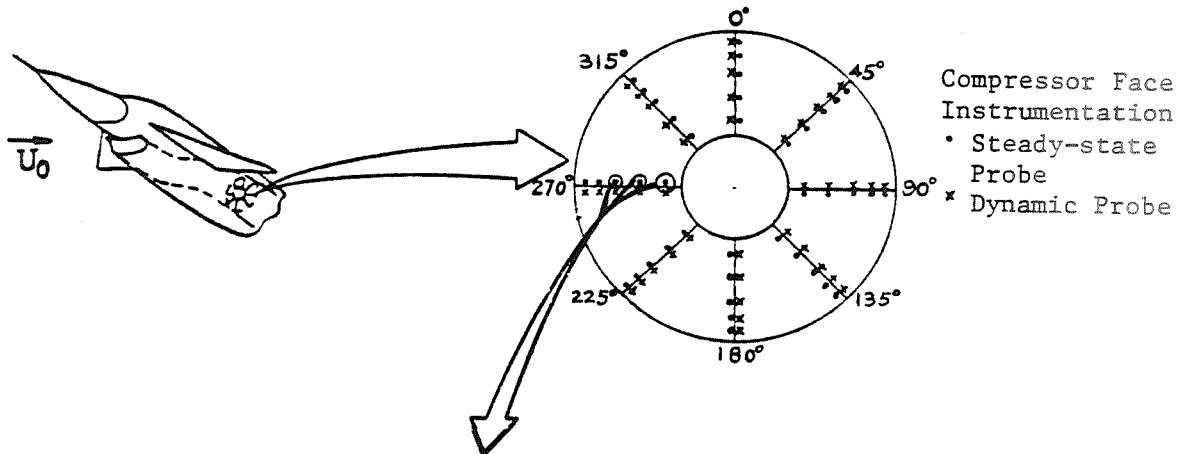
REFERENCES

1. Marous, J. J. and Sedloc, D., DYNAMIC DATA EDITING AND COMPUTING SYSTEM (DYNADEC), Proceedings of the Air Force System Command Science and Engineering Symposium, AFSC-TR-003, vol. 1, October 1973.
2. Chen, Y. S., STATISTICAL PREDICTION OF DYNAMIC DISTORTION OF INLET FLOW USING MINIMUM DYNAMIC MEASUREMENT -- AN APPLICATION TO THE MELICK METHOD, M. S. Thesis, University of Kansas, 1983.
3. Chen, Y. S., INLET FLOW DYNAMIC DISTORTION PREDICTION -- WITHOUT RMS MEASUREMENTS, PhD. Dissertation, University of Kansas, 1985.
4. Melick, H. C. and Ybarra, A. H., ESTIMATING MAXIMUM INSTANTANEOUS DISTORTION FROM INLET TOTAL PRESSURE RMS AND PSD MEASUREMENTS, Vought Systems Division of LTV Aerospace Corporation Technical Report No. 2-57110/5R-3209, 1975.
5. Sanders, M. E., AN EVALUATION OF STATISTICAL METHODS FOR THE PREDICTION OF MAXIMUM INSTANTANEOUS TIME-VARIANT INLET TOTAL PRESSURE DISTORTION, AIAA Paper 80-1110, July, 1980.
6. Dennon, Stephen R., COMPUTER PROGRAM DOCUMENTATION AND USER'S MANUAL - ESTIMATING MAXIMUM INSTANTANEOUS INLET FLOW DISTORTION FROM STEADY-STATE TOTAL PRESSURE MEASUREMENTS WITH FULL, LIMITED, OR NO DYNAMIC DATA, University of Kansas Center for Research, Inc., 1986.

Table 1. Distortion Factor Definitions (Ref. 2)

Factor	Equation	Supplemental equations	Definitions
IDC_{max}	$IDC_{max} = \max \left[\frac{1}{2}(IDC_1 + IDC_2), \frac{1}{2}(IDC_4 + IDC_5) \right]$	$IDC_j = \frac{(\bar{p}_t)_j - (p_{t,min})_j}{\bar{p}_t}$	$(\bar{p}_t)_j$ = average total pressure for ring j $(p_{t,min})_j$ = minimum total pressure reading in ring j
IDR_{max}	$IDR_{max} = \max(IDR_1, IDR_5)$	$IDR_j = \frac{\bar{p}_t - (\bar{p}_t)_j}{\bar{p}_t}$	\bar{p}_t = average total pressure at engine face
K_{D2}	$K_{D2} = \frac{\sum_{j=1}^{NR} \bar{\theta}_j (\Delta p_t / p_t) (OD/D_j)}{\sum_{j=1}^{NR} (OD/D_j)}$	$\frac{\Delta p_t}{p_t} = \frac{(\bar{p}_t)_j - (p_{t,min})_j}{(\bar{p}_t)_j} * 100$	$(\bar{p}_t)_j, (p_{t,min})_j$ = see above $\bar{\theta}_j$ = circumferential extent of largest continuous total pressure depression below $(\bar{p}_t)_j$, degrees D_j = diameter of ring j; NR = number of ring OD = outer duct diameter
K_θ	$K_\theta = \frac{\sum_{j=1}^{NR} (A_1)_j (1/D_j)}{(\bar{q}/\bar{p}_t) \sum_{j=1}^{NR} (1/D_j)}$	$(A_1)_j = (a_1^2 + b_1^2)_j$ $(a_1)_j = \frac{1}{M} \left[\sum_{i=1}^M \frac{p_{t1}}{\bar{p}_t} \cos(\theta_1) \right]_j$ $(b_1)_j = \frac{1}{M} \left[\sum_{i=1}^M \frac{p_{t1}}{\bar{p}_t} \sin(\theta_1) \right]_j$	$\bar{p}_t, (\bar{p}_t)_j, D_j$ = see above \bar{q} = average dynamic pressure at engine face M = number of rakes $(p_{t1})_j$ = individual total pressure; rake 1, ring j θ = angular position of p_{t1}
K_{RAD}	$K_{RAD} = \sum_{j=1}^{NR} \left \frac{\Delta p_{tj}}{\bar{p}_t} \right \frac{\bar{p}_t}{\bar{q}} \frac{1}{D_j}$	$\frac{\Delta p_{tj}}{\bar{p}_t} = \frac{(\bar{p}_t)_j}{\bar{p}_t} - \frac{(p_{t,base})_j}{\bar{p}_t}$	$(p_{t,base})_j$ = base radial profile for ring j; set = 1 for all j b = radial distortion weighting factor=1.0
K_{A2}	$K_{A2} = K_\theta + b K_{RAD}$		
$\frac{\Delta SPR}{Dist}$	$\frac{\Delta SPR}{Dist} = \frac{\Delta SPR}{[(\bar{p}_t - p_{t,min})/\bar{p}_t]} = f(k)$		\bar{p}_t = see above $p_{t,min}$ = minimum total pressure at engine face k = compressor reduced frequency
ID	$ID = k_c (IDC)b + k_r (IDR)$		k_c = circumferential distortion sensitivity factor k_r = radial distortion sensitivity factor b = circumferential distortion weighting factor

ORIGINAL PAGE IS
OF POOR QUALITY



PRESSURE ARRAY

RADIUS	0.	45.0	90.0	135.0	180.0	225.0	270.0	315.0
2.225	0.841	0.851	0.864	0.827	0.774	0.852	0.927	0.876
3.070	0.844	0.857	0.913	0.843	0.770	0.869	0.977	0.894
3.725	0.837	0.869	0.939	0.844	0.759	0.873	1.007	0.901
4.380	0.829	0.858	0.928	0.824	0.741	0.854	0.999	0.890
4.775	0.815	0.830	0.873	0.790	0.722	0.818	0.958	0.864

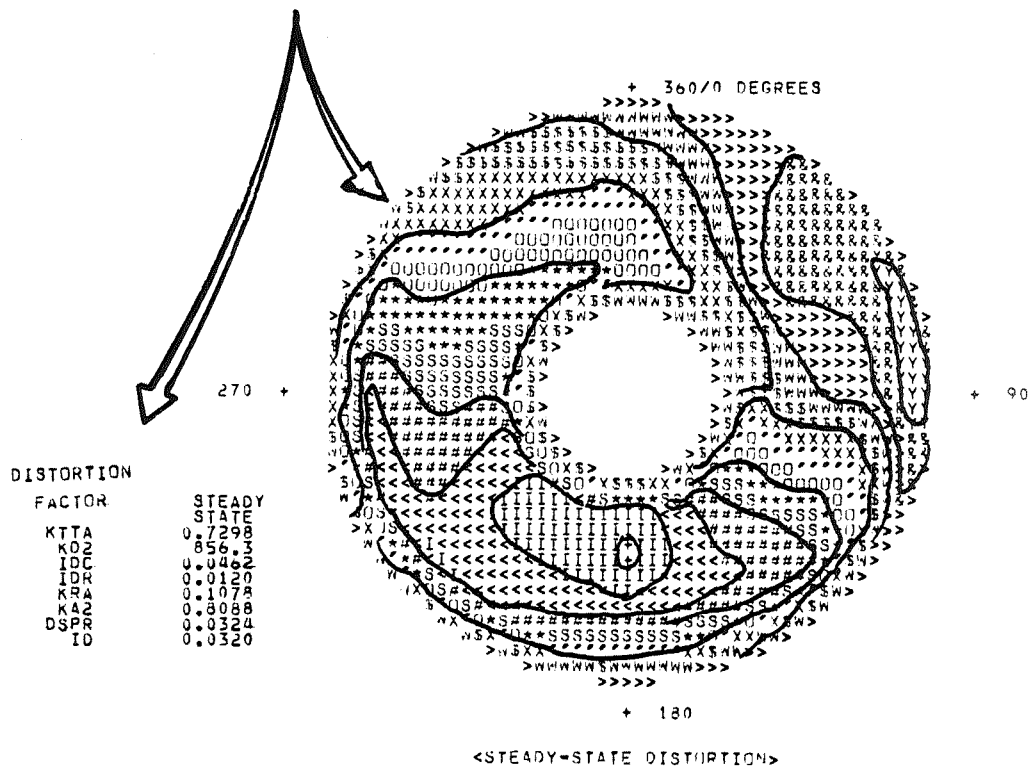


Figure 1. Determination of Steady-State Distortion

ILLUSTRATION OF SOME FEATURES OF THE TIME VARIANT TOTAL PRESSURES AND DYNAMIC DISTORTION:

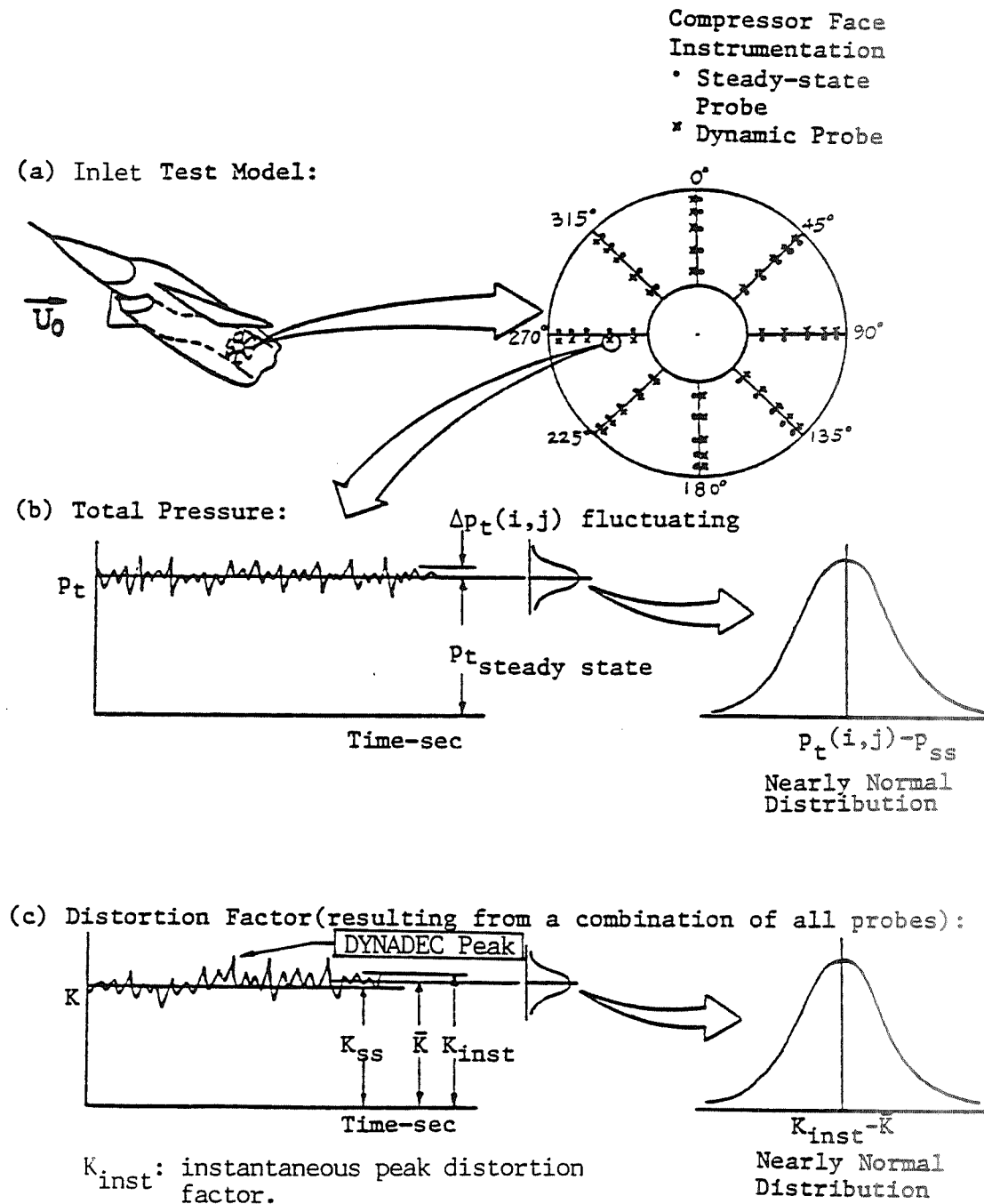
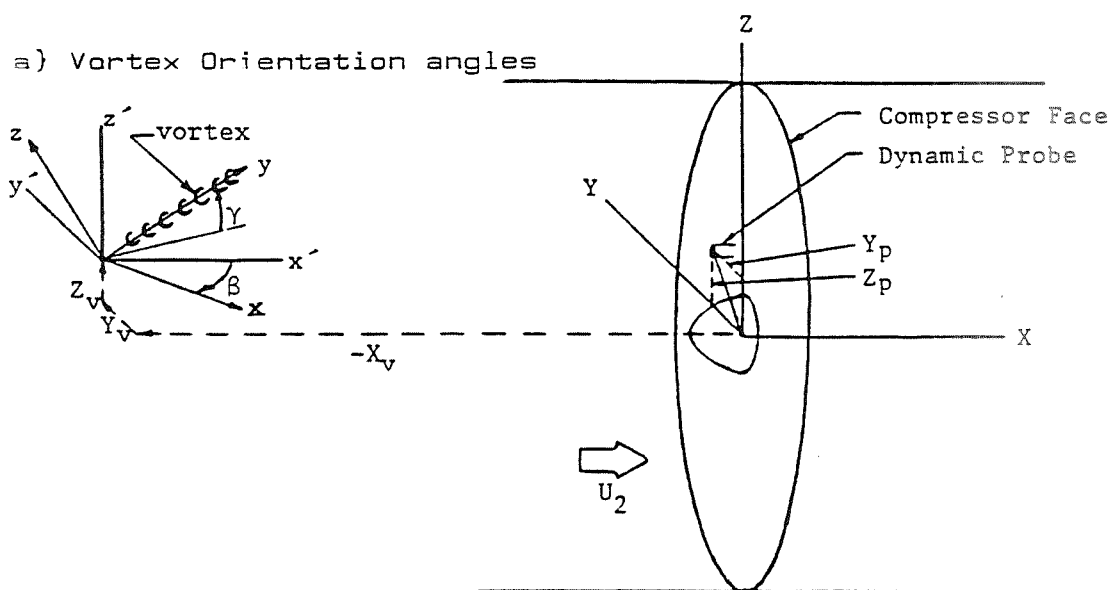


Figure 2. Illustration of a Typical Inlet Test Model and Peak Distortion Factor Measurement



GAMMA = vortex orientation angle between y axis and the $x'-y'$ plane

BETA = vortex orientation angle between x' and x axes, with the x axis in the $x'-y'$ plane

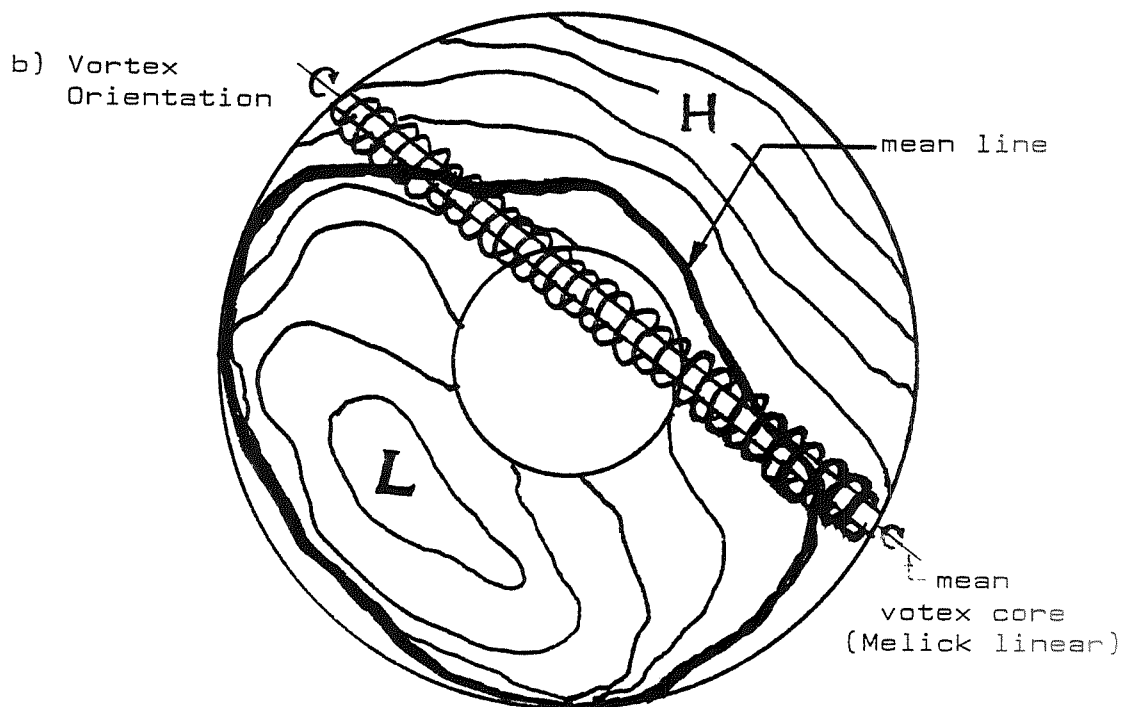


Figure 3. Melick Linear Vortex Model

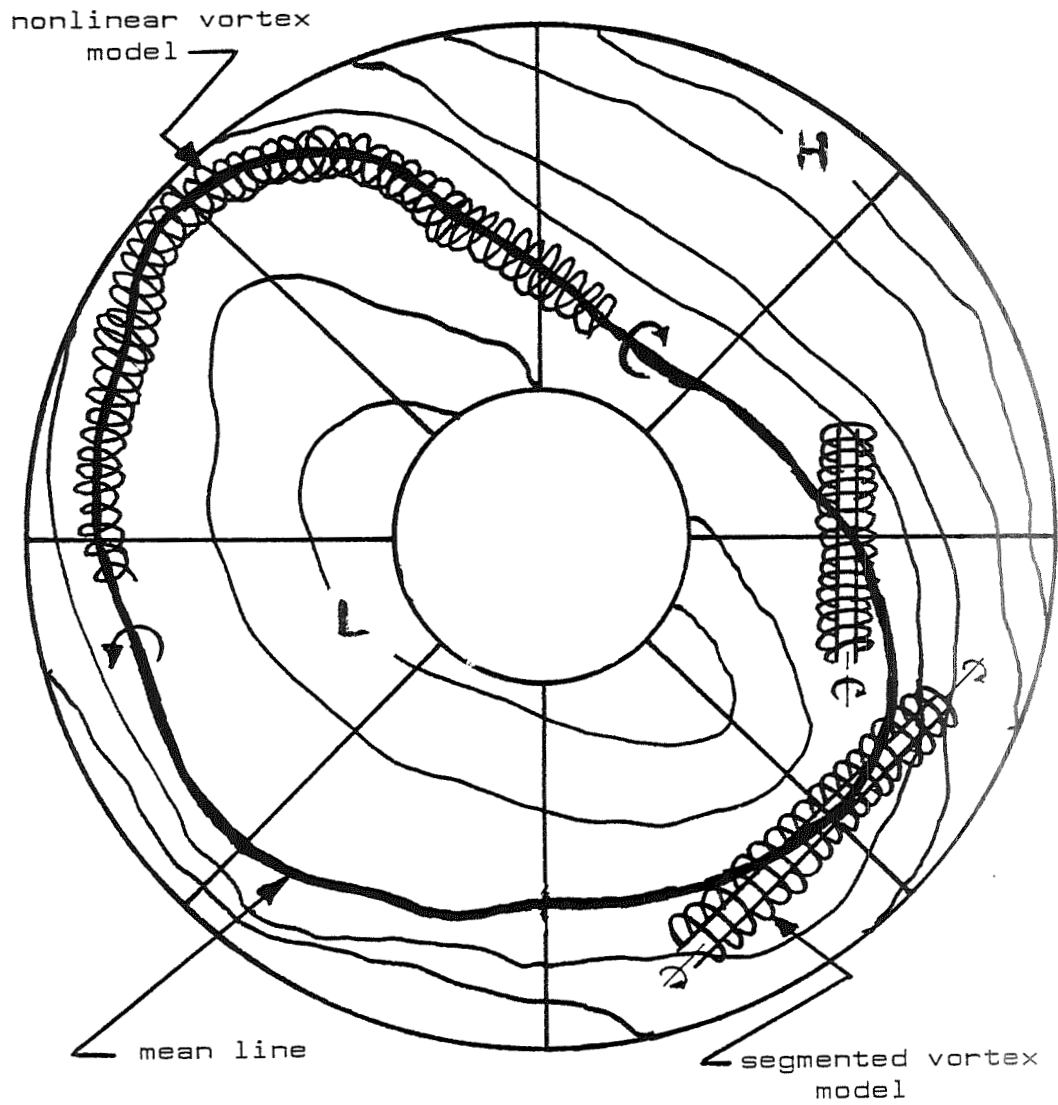


Figure 4. Nonlinear/Segmented Vortex Models

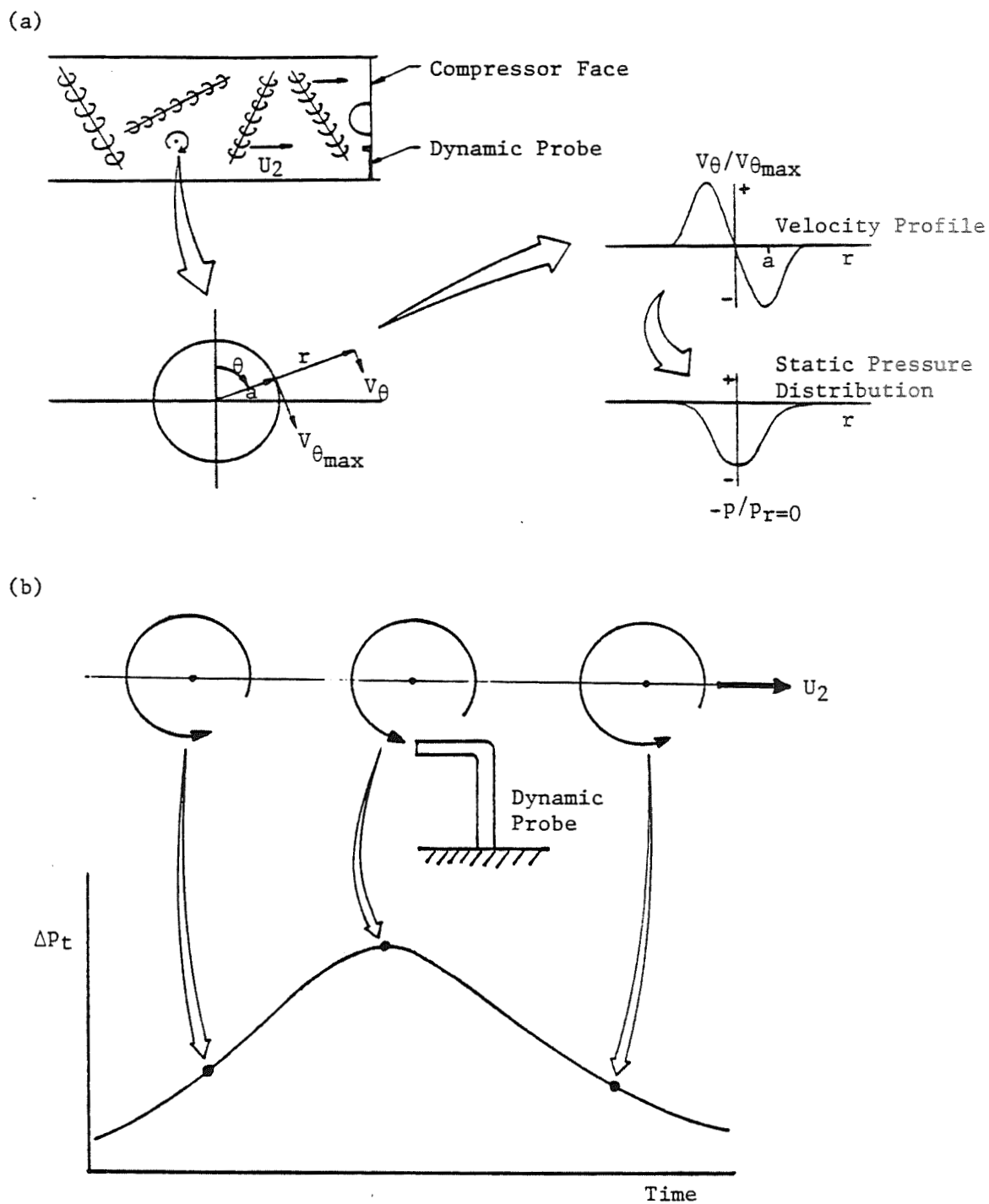


Figure 5. Inlet vortex flow model and perturbation of velocity and static pressure and the time variant total pressure fluctuation caused by a single 1-D vortex (Ref. 2)

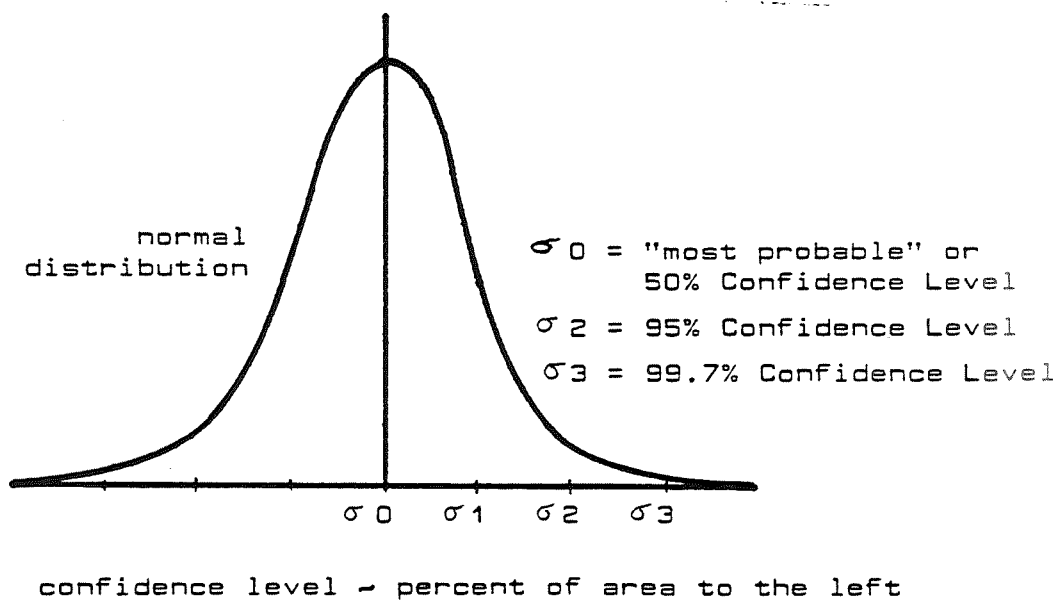
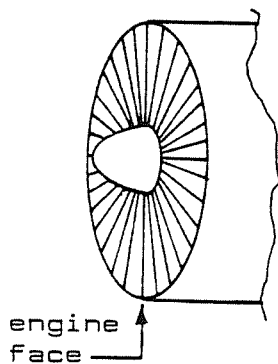
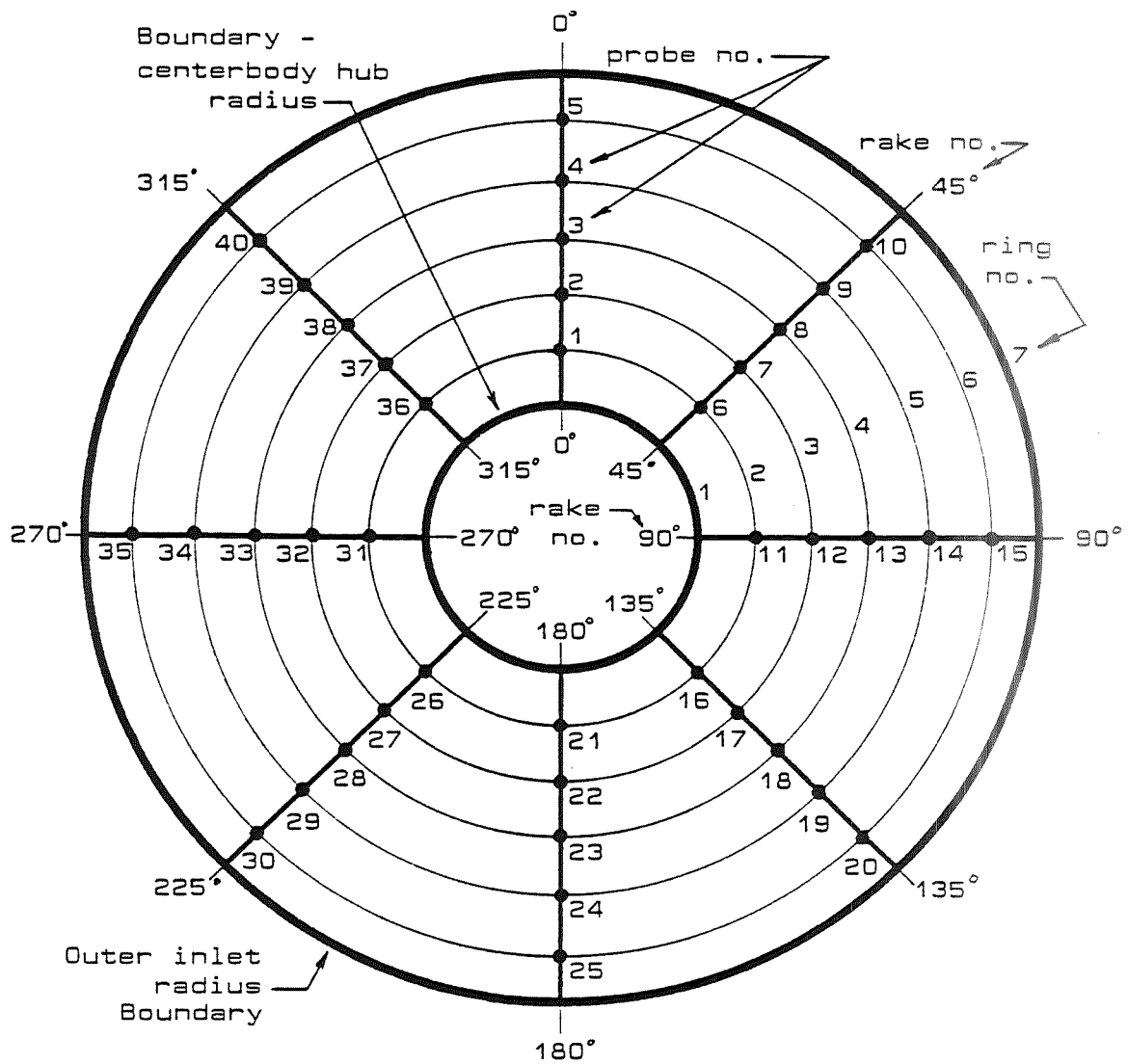


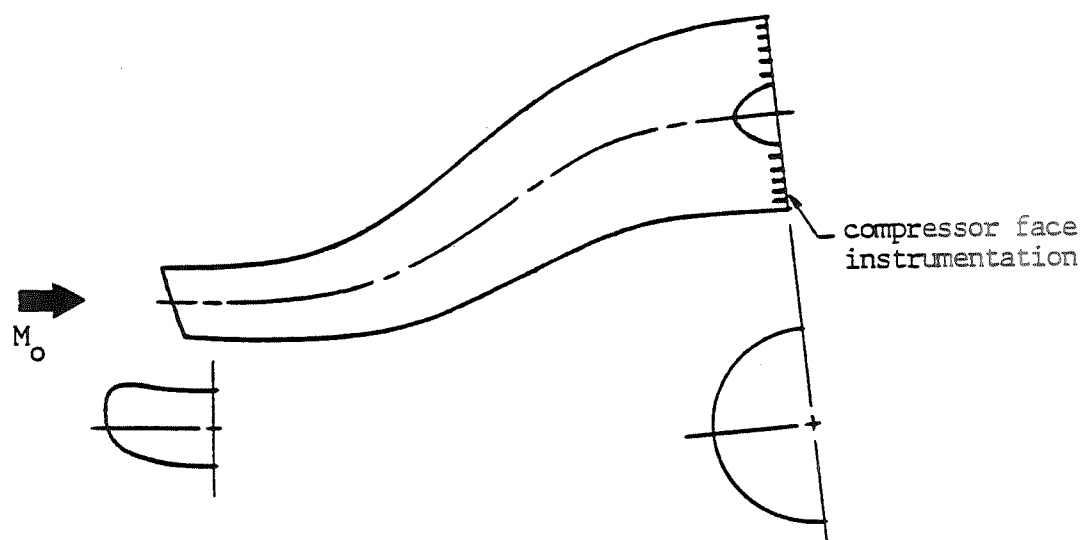
Figure 6. Definition of Confidence Levels



Note: NR = 7 = number of probe rings
NP = 8 = number of probe rakes

Figure 7. Ring, Rake, and Probe Assignments for a typical instrument configuration

(a) Subsonic Full Scale Inlet Model:

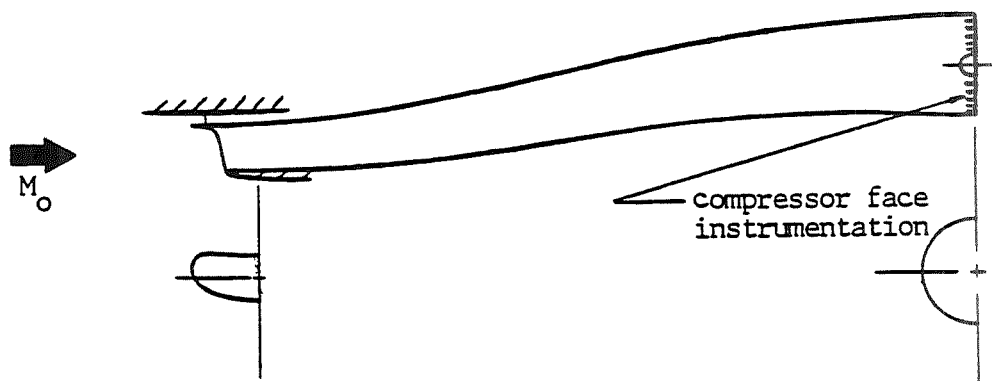


(b) Test Conditions and Some Measured Results:

Data pt.	Mach No.	P_{t2}	\overline{rms}_m	$IDC_{max, peak}$
20.40	subsonic	.887	.0336	.225
54.30	subsonic	.853	.0478	.326
81.40	subsonic	.925	.0337	.127
111.30	subsonic	.868	.0537	.319
112.30	subsonic	.873	.0475	.329
137.50	subsonic	.926	.0360	.144

Figure 8. Illustration of a Subsonic Inlet Test Model and some Test Results (unpublished data from Air Force Flight Dynamics Laboratory, Wright-Patterson Air Force Base, Dayton, Ohio) [Ref. 3]

(a) Transonic .15 scale Inlet Model:

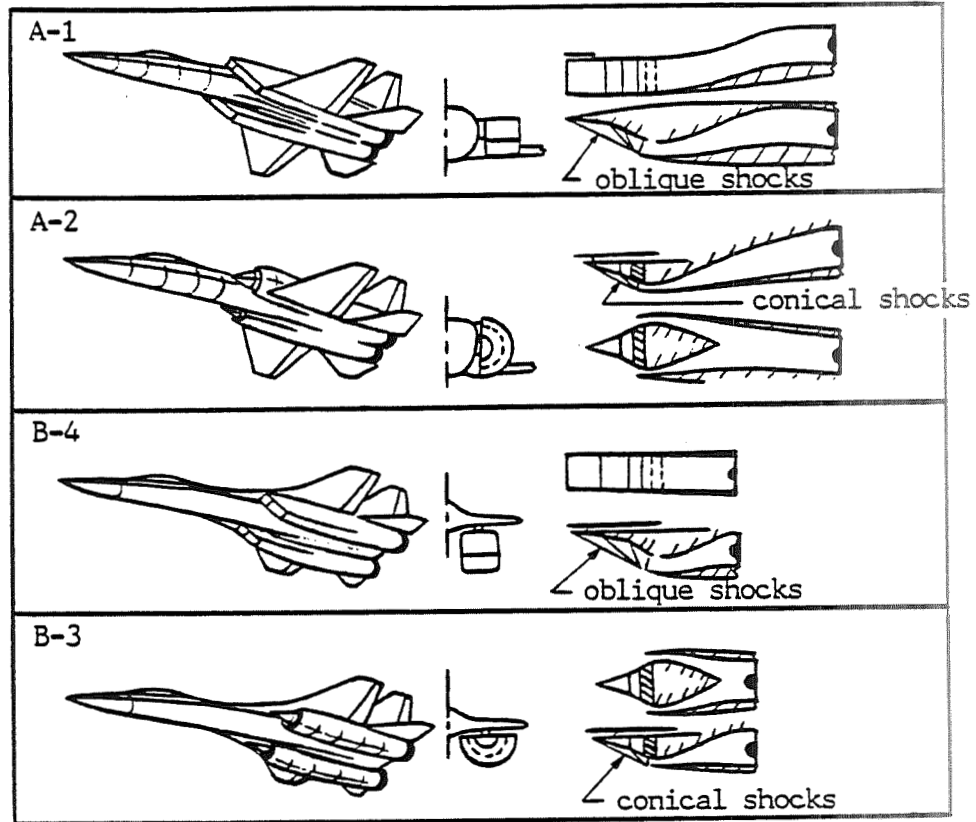


(b) Test Conditions and Some Measured Results:

Data pt.	Mach No.	P_{t2}	\overline{rms}_m	$K_{A2, peak}$
464.12	transonic	.860	.0422	.303
465.11	transonic	.912	.0281	.522
473.12	transonic	.928	.0217	.565
485.10	transonic	.891	.0414	.819
487.80	transonic	.857	.0493	1.025
498.12	transonic	.913	.0299	.777

Figure 9. Illustration of a Transonic Inlet Test Model and some Test Results (unpublished data from Air Force Flight Dynamics Laboratory, Wright-Patterson Air Force Base, Dayton, Ohio)
[Ref. 3]

(a) Configurations of four .25 scale Tailor-Mate Model:



(b) Test Conditions and Some Measured Results:

Inlet	Data pt.	Mach No.	α	β	P_{t2}	IDC_{max}	$K_{A2, peak}$
A-1	182/1	2.2	5	4	.833	.150	1.384
	189/3	2.2	15	0	.829	.076	1.020
	216/3	1.6	10	4	.894	.086	.900
A-2	243/3	2.2	5	4	.768	.078	1.123
	246/3	2.2	15	0	.666	.111	1.446
	247/2	2.2	15	4	.579	.163	1.572
B-4	433/3	2.2	0	0	.814	.090	1.254
	437/3	2.2	5	0	.872	.125	1.511
	1554/4	0.9	20	8	.918	.074	.597
B-3	640/2	2.2	5	-4	.945	.092	.887
	643/3	2.2	15	0	.935	.078	.738
	695/1	1.65	0	-8	.845	.136	1.271
	1334/2	0.9	25	4	.933	.121	.649

Figure 10. Illustration of four Supersonic Inlet Test Model and some Test Results (ref. 3)

DISTORTION FACTOR	STEADY- STATE	DYNADEC PEAK	MELICK PREDICTED PEAK dynamic data input:		
			FULL	MIN.	NONE
CASE#					
20.40					
K-THETA	0.95777	1.48828	1.8486	2.0279	1.9826
KD2	1801.4	3534.1	2712.4	2840.9	2950.7
(IDC)-MAX	0.10759	0.22481	0.1728	0.1813	0.1893
(IDR)-MAX	0.06516	0.06645	0.0761	0.0773	0.0784
KRA	0.30434	0.30659	0.4362	0.4489	0.4689
KA2	1.18085	1.71301	2.0781	2.2580	2.2134
DSPR	0.05760	0.09058	0.1114	0.1221	0.1193
ID	1.26570	2.33132	1.6204	1.6600	1.7002
54.30					
K-THETA	1.19444	2.57046	2.2807	2.5317	2.6086
KD2	2740.2	3937.6	4258.7	4398.5	4620.5
(IDC)-MAX	0.23592	0.32522	0.3381	0.3393	0.3418
(IDR)-MAX	0.09032	0.09262	0.1083	0.1066	0.1117
KRA	0.35968	0.70330	0.5131	0.4885	0.5371
KA2	1.45809	3.08598	2.5518	2.8003	2.8848
DSPR	0.08654	0.11821	0.1644	0.1820	0.1875
ID	2.47579	3.37518	3.1583	3.1545	3.3007
81.40					
K-THETA	0.36337	0.72753	1.1293	1.3249	1.3619
KD2	819.7	1385.4	1864.3	2172.3	2325.0
(IDC)-MAX	0.09355	0.12868	0.1606	0.1787	0.1867
(IDR)-MAX	0.07916	0.08334	0.0901	0.0930	0.0942
KRA	0.40766	0.47655	0.5365	0.5692	0.5852
KA2	0.66219	1.07684	1.4626	1.6637	1.7047
DSPR	0.02406	0.04890	0.0703	0.0816	0.0835
ID	1.29662	1.55624	1.6183	1.7053	1.7424
111.30					
K-THETA	1.06535	1.46101	2.2481	2.0422	2.2327
KD2	2401.7	3728.9	4184.6	3862.5	4146.2
(IDC)-MAX	0.21749	0.31896	0.3373	0.3154	0.3345
(IDR)-MAX	0.08970	0.08782	0.1103	0.1069	0.1098
KRA	0.37629	0.39444	0.5505	0.5224	0.5464
KA2	1.34117	1.75014	2.5291	2.3261	2.5135
DSPR	0.07771	0.10564	0.1628	0.1483	0.1618
ID	2.30509	3.31415	3.0653	2.9376	3.0487
112.30					
K-THETA	0.98200	1.57512	2.0663	2.1201	2.2161
KD2	2142.5	3925.5	3719.7	3749.1	4014.4
(IDC)-MAX	0.18026	0.32841	0.2876	0.2899	0.3090
(IDR)-MAX	0.10505	0.09182	0.1232	0.1235	0.1263
KRA	0.47993	0.41299	0.6332	0.6340	0.6604
KA2	1.33379	1.87784	2.4178	2.4742	2.5783
DSPR	0.07275	0.11616	0.1505	0.1543	0.1610
ID	2.08990	3.41034	2.6794	2.6894	2.7835
137.50					
K-THETA	0.44035	0.72466	1.3124	1.5762	1.4732
KD2	946.7	1999.1	2083.2	2388.4	2444.1
(IDC)-MAX	0.09824	0.14375	0.1725	0.1908	0.1927
(IDR)-MAX	0.08502	0.10058	0.0971	0.1002	0.1002
KRA	0.46385	0.55000	0.6040	0.6355	0.6412
KA2	0.78035	1.12781	1.6853	1.9575	1.8590
DSPR	0.03022	0.04565	0.0838	0.0996	0.0929
ID	1.37968	1.80079	1.7336	1.8218	1.8296

Table 2. Subsonic Inlet Distortion
Factor Comparison

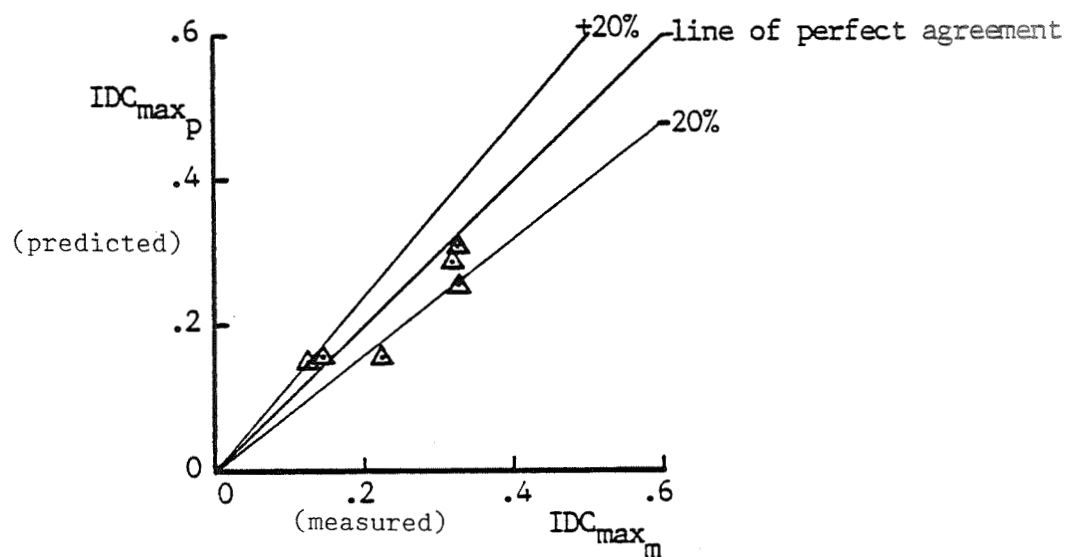
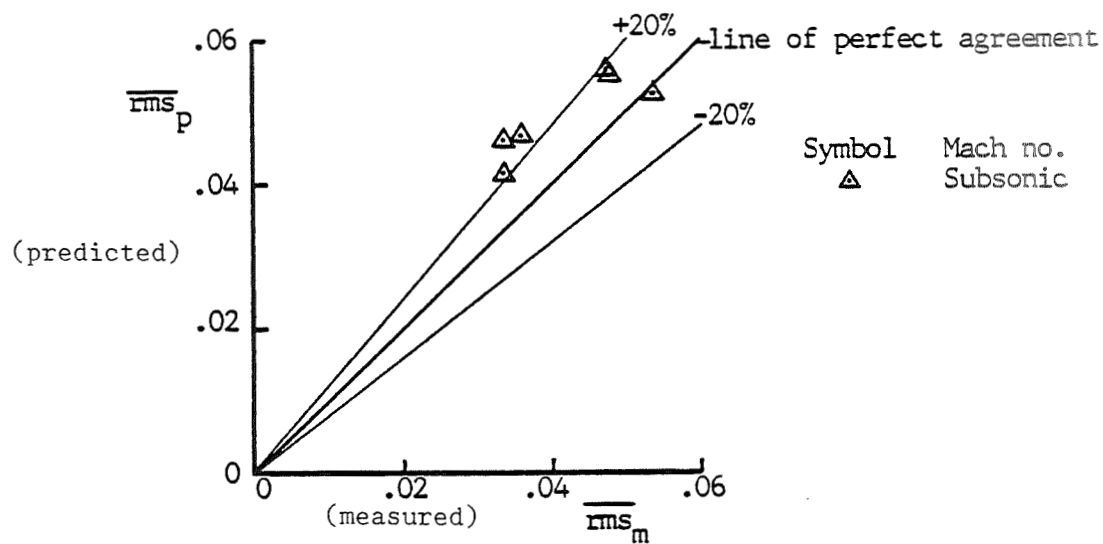


Figure 11. Comparisons of the Predicted and Measured rms Level and Peak Distortion Factor for the Subsonic Inlet Model shown in Figure 8. (unpublished data)

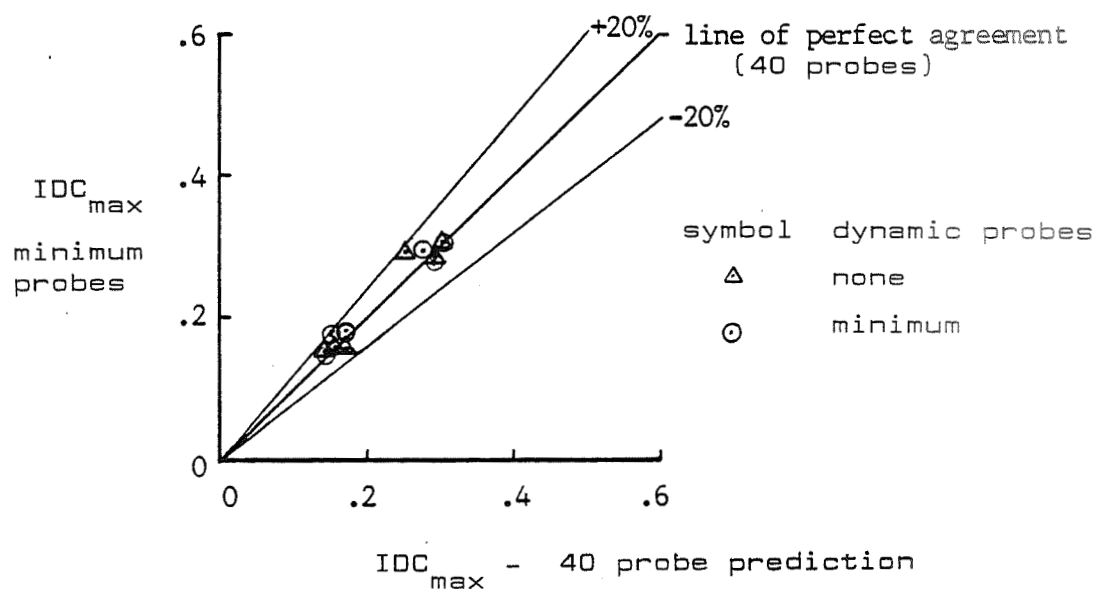
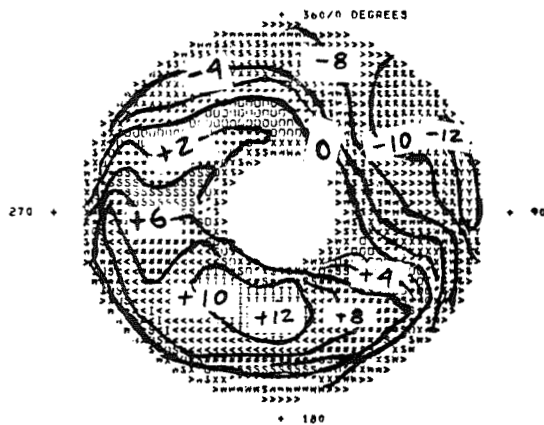


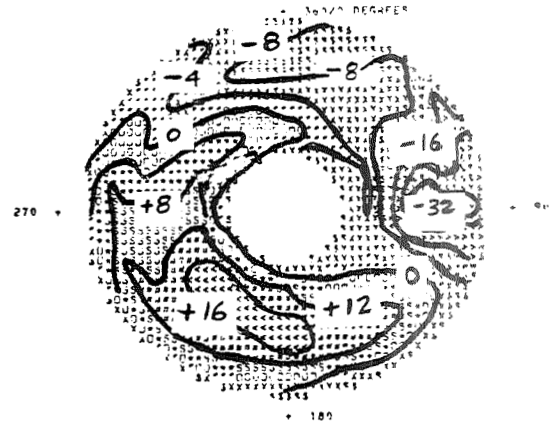
Figure 12. Comparisons of peak distortion factors predicted by the present analyses and the Melick method based on the total pressure rms measurements for the subsonic inlet data set (unpublished data)

(percent from average pressure)



K=THETA	0.95777
KD2	1.80154
(IDC)=MAX	0.10759
(IDR)=MAX	0.06516
KRA	0.30434
KA2	1.10855
DSPR	0.05700
ID	1.26570

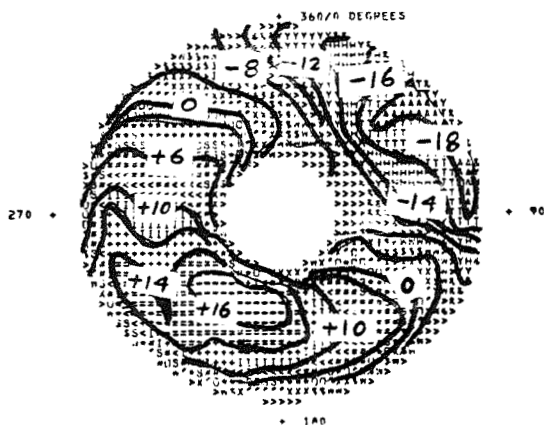
steady-state



K=THETA	1.48828
KD2	3.53021
(IDC)=MAX	0.56645
(IDR)=MAX	0.30659
KRA	1.71501
KA2	0.04955
DSPR	2.33132
ID	

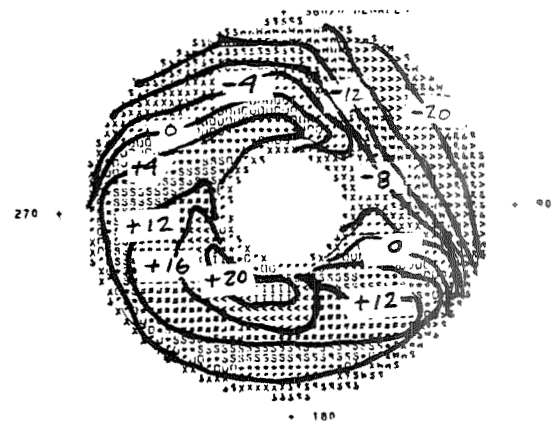
DYNADEC peak

(percent from average pressure)



K=THETA	1.70557
KD2	2.72754
(IDC)=MAX	0.16782
(IDR)=MAX	0.06492
KRA	0.30434
KA2	1.92865
DSPR	0.10343
ID	1.56671

Melick model peak

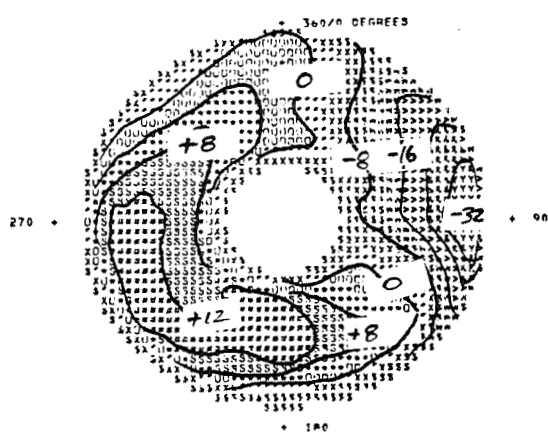


K=THETA	1.59725
KD2	2.92087
(IDC)=MAX	0.16147
(IDR)=MAX	0.12464
KRA	0.65704
KA2	2.07886
DSPR	0.09611
ID	2.19760

segmented vortex peak

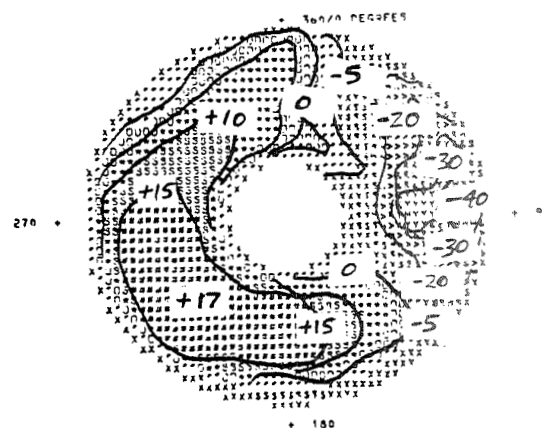
Figure 13a. Subsonic Inlet Map Comparisons (20.40)

(percent from average pressure)



K-THETA	1.19444
KD2	2.74022
(IDC)-MAX	0.235922
(IDR)-MAX	0.090322
KRA	0.359688
KA2	1.45809
DSFR	0.08654
ID	2.47579

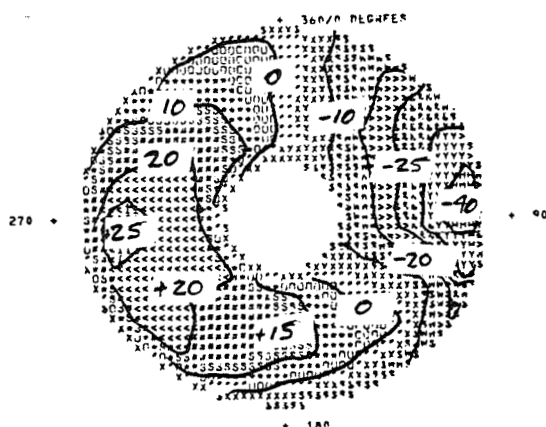
steady-state



K-THETA	2.57046
KD2	3.93716
(IDC)-MAX	0.242022
(IDR)-MAX	0.0713002
KRA	0.005569
KA2	1.1821
DSFR	3.37518
ID	

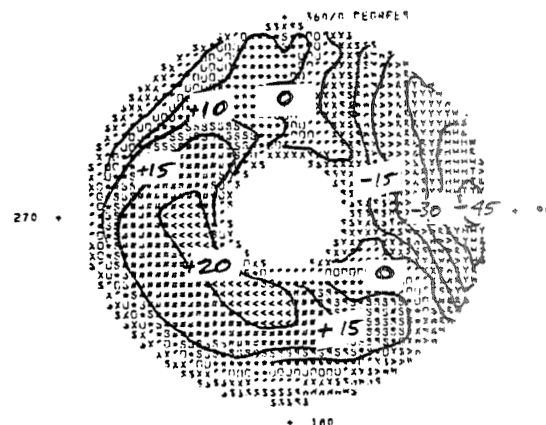
DYNADec peak

(percent from average pressure)



K-THETA	2.27609
KD2	4.9332
(IDC)-MAX	0.34644
(IDR)-MAX	0.09098
KRA	0.35968
KA2	2.53974
DSFR	0.16734
ID	3.17246

Melick model peak

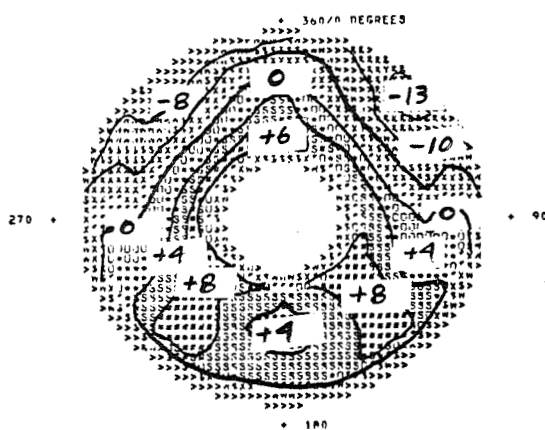


K-THETA	1.88601
KD2	3.89489
(IDC)-MAX	0.33781
(IDR)-MAX	0.15206
KRA	0.67127
KA2	2.37806
DSFR	0.11047
ID	3.79736

segmented vortex peak

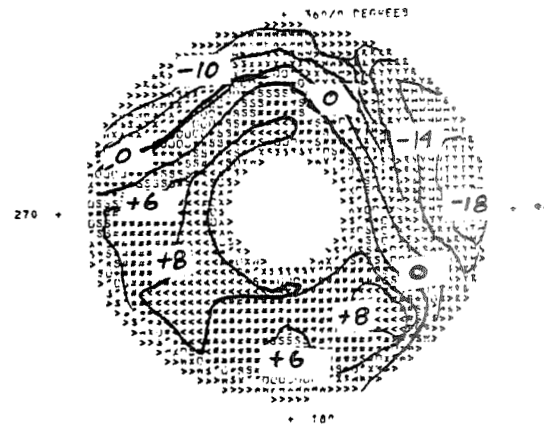
Figure 13b. Subsonic Inlet Map Comparison (54.30)

percent from average pressure



K=THETA	0.36337
KD2	8.197
(IDC)=MAX	0.09355
(IDR)=MAX	0.07916
KRA	0.40766
KA2	0.66219
DSPR	0.02406
ID	1.29662

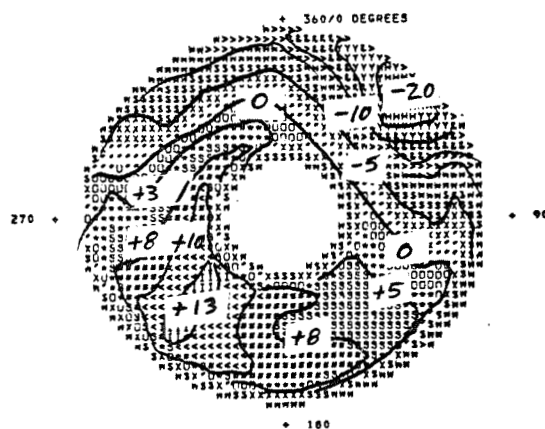
steady-state



K=THETA	0.72753
KD2	1315.7
(IDC)=MAX	0.12868
(IDR)=MAX	0.07354
KRA	0.47655
KA2	1.07664
DSPR	0.04899
ID	1.55624

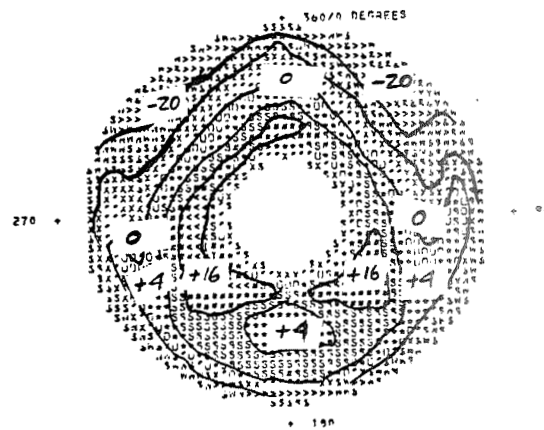
DYNADEC peak

percent from average pressure



K=THETA	1.03546
KD2	2223.2
(IDC)=MAX	0.16101
(IDR)=MAX	0.07888
KRA	0.40766
KA2	1.33427
DSPR	0.06540
ID	1.59487

Mellick model peak

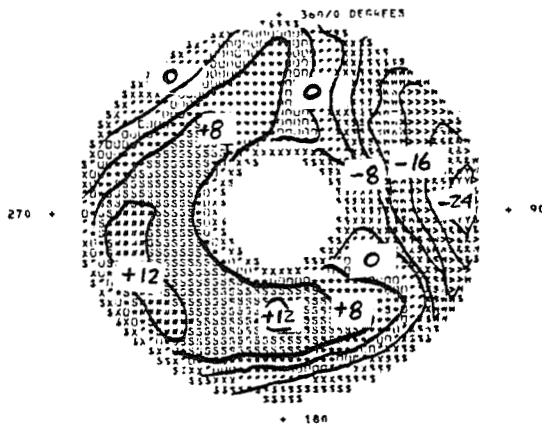


K=THETA	0.74868
KD2	1315.7
(IDC)=MAX	0.15364
(IDR)=MAX	0.17138
KRA	0.99184
KA2	1.47570
DSPR	0.04671
ID	2.58862

segmented vortex peak

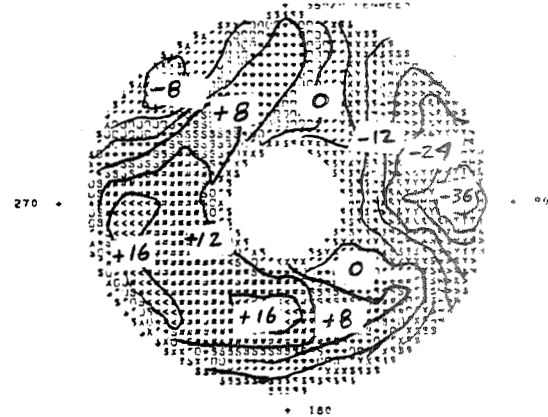
Figure 13c. Subsonic Inlet Map Comparisons (81.40)

percent from average pressure



K-THETA	1.06535
KD2	2.4017
(IDC)-MAX	0.21749
(IDR)-MAX	0.08970
KRA	0.37629
KA2	1.34117
DSPR	0.07771
ID	2.30509

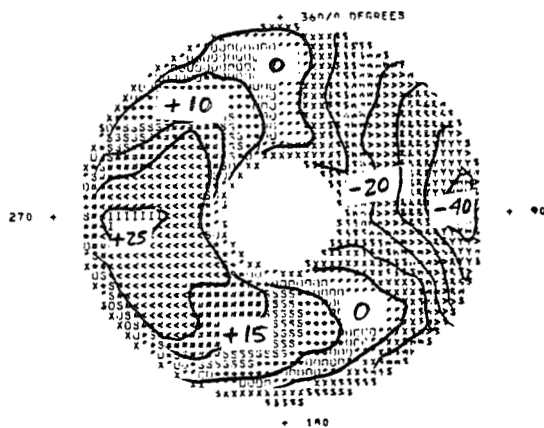
steady-state



K-THETA	1.40101
KD2	3.7269
(IDC)-MAX	0.31496
(IDR)-MAX	0.06752
KRA	0.39444
KA2	1.7504
DSPR	0.10524
ID	3.31415

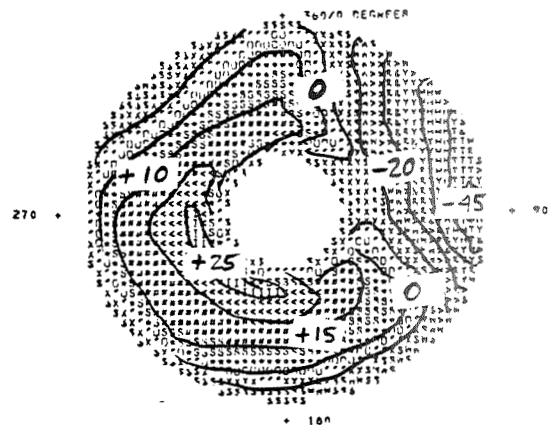
DYNADec peak

percent from average pressure



K-THETA	2.23398
KD2	4.7829
(IDC)-MAX	0.33609
(IDR)-MAX	0.09033
KRA	0.37624
KA2	2.50980
DSPR	0.16524
ID	3.02967

Melick model peak

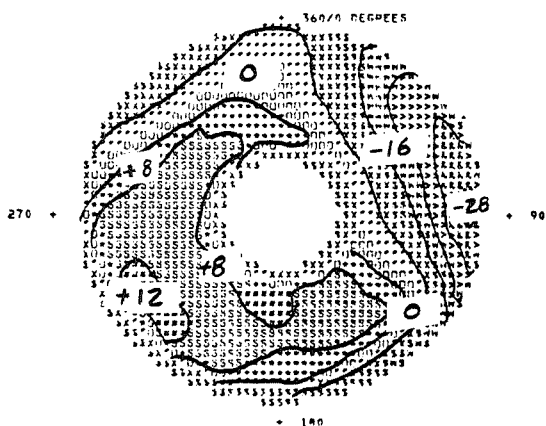


K-THETA	1.81969
KD2	3.4676
(IDC)-MAX	0.33634
(IDR)-MAX	0.17413
KRA	0.95912
KA2	2.50807
DSPR	0.13061
ID	3.95741

segmented vortex peak

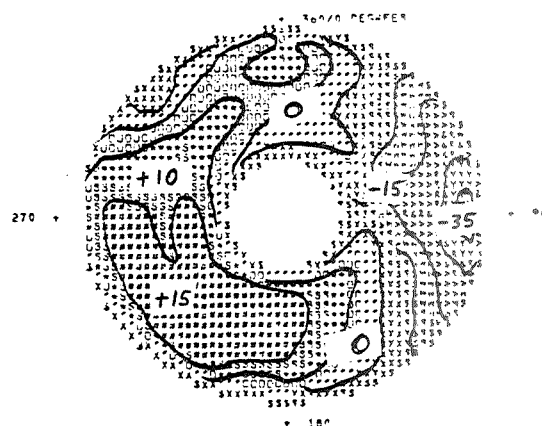
Figure 13d. Subsonic Inlet Map Comparisons (111.30)

percent from average pressure



K=THETA	0.98200
KD2	2.142.5
(IDC)=MAX	0.18026
(IDR)=MAX	0.10505
KRA	0.47993
KA2	1.33379
DSPR	0.07275
ID	2.06990

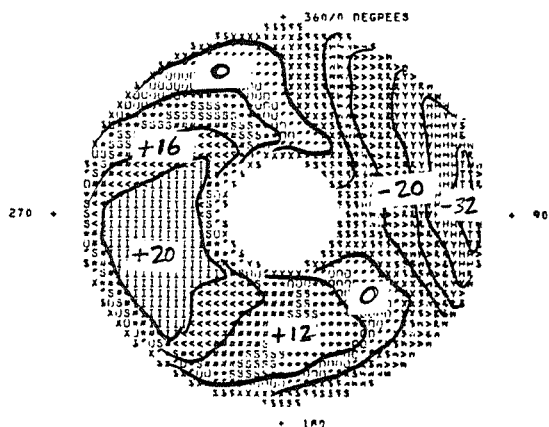
steady-state



K=THETA	1.57512
KD2	3.6512
(IDC)=MAX	0.36512
(IDR)=MAX	0.10505
KRA	0.47993
KA2	1.33379
DSPR	0.07275
ID	3.41034

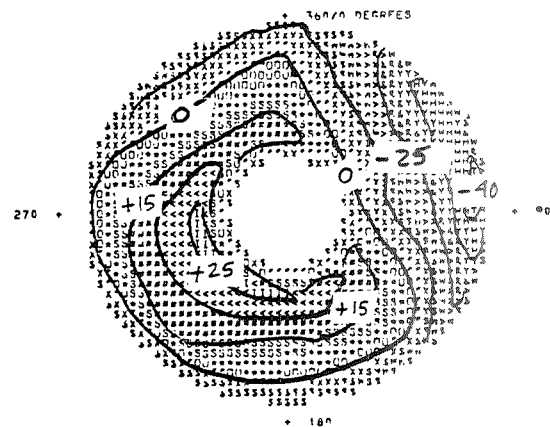
DYNADEC peak

percent from average pressure



K=THETA	2.01448
KD2	4.095.7
(IDC)=MAX	0.28694
(IDR)=MAX	0.10571
KRA	0.47993
KA2	2.36627
DSPR	0.14946
ID	2.64388

Melick model peak

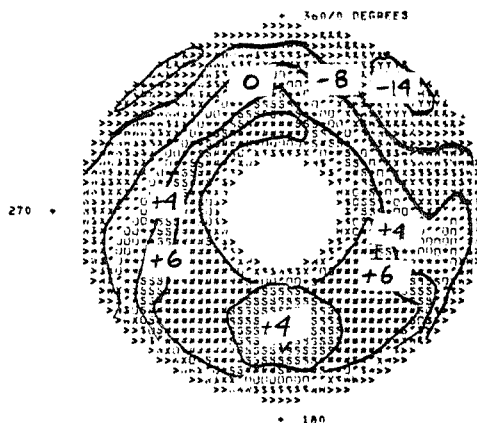


K=THETA	1.69529
KD2	3.057.9
(IDC)=MAX	0.28406
(IDR)=MAX	0.18106
KRA	0.47993
KA2	2.01448
DSPR	0.14946
ID	3.73108

segmented vortex peak

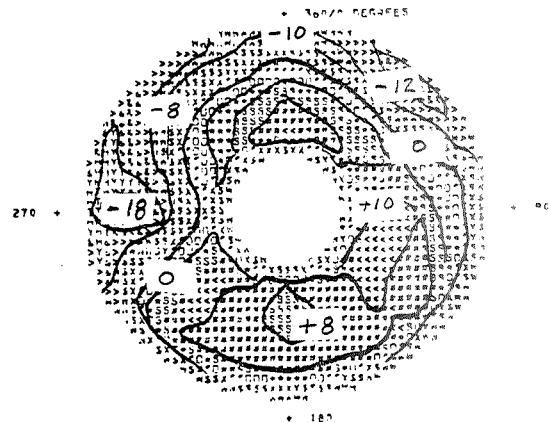
Figure 13e. Subsonic Inlet Map Comparisons (112.30)

percent from average pressure



K=THETA	0.44035
KD2	948.7
(IDC)=MAX	0.09824
(IUR)=MAX	0.08500
KRA	0.46385
KA2	0.76033
USPR	0.03022
ID	1.37968

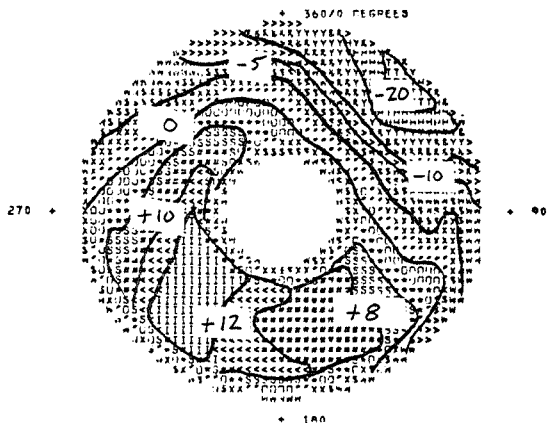
steady-state



K=THETA	0.72606
KD2	1000.1
(IDC)=MAX	0.14375
(IUR)=MAX	0.10056
KRA	0.53000
KA2	1.15781
DSPR	0.04555
ID	1.66070

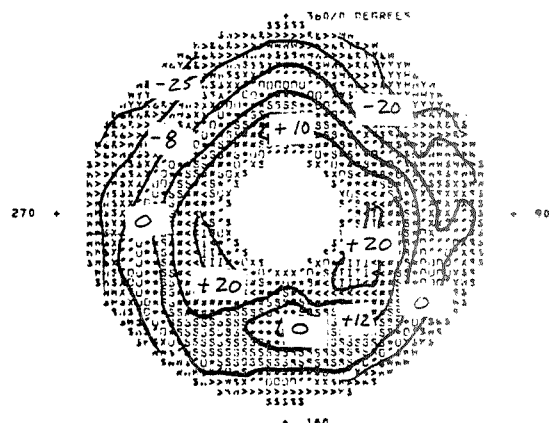
DYNADEC peak

percent from average pressure



K=THETA	1.19054
KD2	2510.5
(IDC)=MAX	0.17302
(IUR)=MAX	0.08468
KRA	0.46385
KA2	1.53054
DSPH	0.07607
ID	1.70783

Melick model peak



K=THETA	0.81925
KD2	1404.3
(IDC)=MAX	0.10546
(IUR)=MAX	0.19300
KRA	1.23500
KA2	1.72493
DSPH	0.05659
ID	2.88571

segmented vortex peak

Figure 13f. Subsonic Inlet Map Comparisons (137.50)

DISTORTION FACTOR	STEADY- STATE	DYNADCC PEAK	MELICK PREDICTED PEAK dynamic data input: FULL MIN. NONE
CASE#			
464.12			
K-THETA	0.03551	0.41514	0.2903
KD2	0.45226	1.19929	1.81126
(IDC)-MAX	0.06052	0.07391	0.07577
(IDR)-MAX	0.03083	0.01520	0.05922
KRA	0.10017	0.07157	0.02833
KAZ	0.11405	0.47126	0.4058
DSPR	0.00258	0.04257	0.0165
ID	0.67161	0.78789	1.3818
465.11			
K-THETA	0.26071	0.37914	0.3868
KD2	0.834.1	1.306.1	1.710.6
(IDC)-MAX	0.05798	0.08741	0.1235
(IDR)-MAX	0.04863	0.03776	0.0661
KRA	0.15727	0.10265	0.2279
KAZ	0.38400	0.45962	0.5211
DSPR	0.02852	0.04038	0.0414
ID	0.79950	0.93361	1.1459
473.12			
K-THETA	0.27191	0.41052	0.3659
KD2	0.748.8	1.157.7	1.432.5
(IDC)-MAX	0.05419	0.08200	0.0947
(IDR)-MAX	0.05092	0.05070	0.0647
KRA	0.17237	0.16923	0.2253
KAZ	0.40705	0.54299	0.5099
DSPR	0.03074	0.04502	0.0400
ID	0.73817	0.84266	1.0000
485.10			
K-THETA	0.51255	0.72939	0.6984
KD2	0.1520.8	0.2181.6	0.2746.1
(IDC)-MAX	0.08006	0.01580	0.0176
(IDR)-MAX	0.06062	0.01041	0.0861
KRA	0.19793	0.07610	0.3059
KAZ	0.66773	0.80480	0.8726
DSPR	0.05478	0.07504	0.0736
ID	1.04356	1.56775	1.5644
487.80			
K-THETA	0.75539	1.05120	0.9839
KD2	1.983.4	3.197.0	3.335.9
(IDC)-MAX	0.10555	0.01770	0.02122
(IDR)-MAX	0.06503	0.03807	0.0944
KRA	0.21478	0.16612	0.3512
KAZ	0.92378	1.18204	1.1757
DSPR	0.07803	0.10784	0.11008
ID	1.25020	1.87747	1.8630
498.12			
K-THETA	0.41709	0.64972	0.5484
KD2	1.258.9	1.902.7	2.143.2
(IDC)-MAX	0.06621	0.01475	0.01348
(IDR)-MAX	0.06127	0.03643	0.07799
KRA	0.21888	0.08764	0.2933
KAZ	0.58869	0.71843	0.7322
DSPR	0.04733	0.06935	0.0614
ID	0.96861	1.16976	1.3266
574.5			
K-THETA	0.41709	0.64972	0.5484
KD2	1.258.9	1.902.7	2.143.2
(IDC)-MAX	0.06621	0.01475	0.01348
(IDR)-MAX	0.06127	0.03643	0.07799
KRA	0.21888	0.08764	0.2933
KAZ	0.58869	0.71843	0.7322
DSPR	0.04733	0.06935	0.0614
ID	0.96861	1.16976	1.3266

Table 3. Transonic Inlet Distortion Factor Comparison

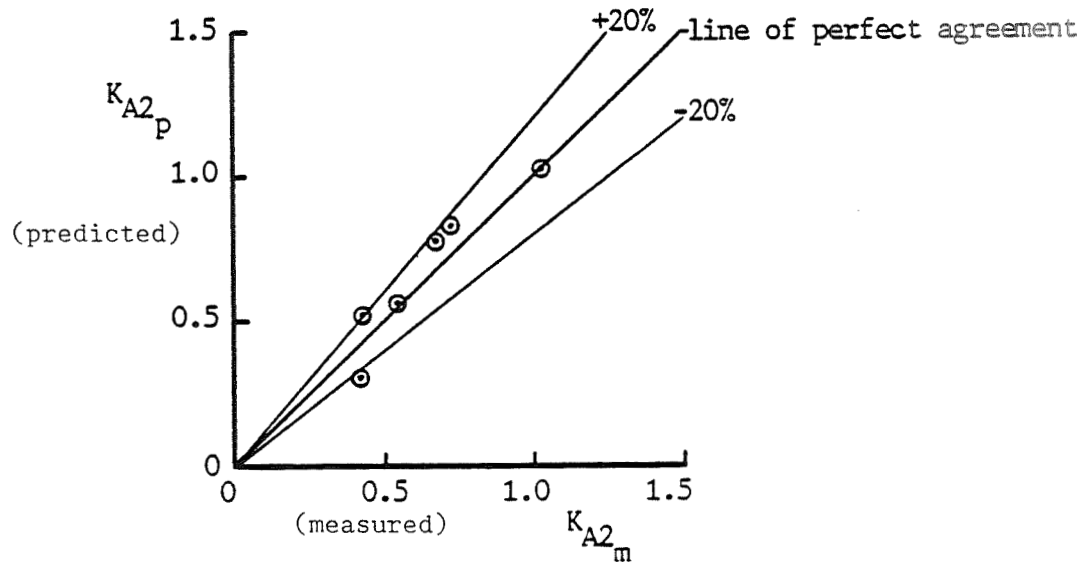
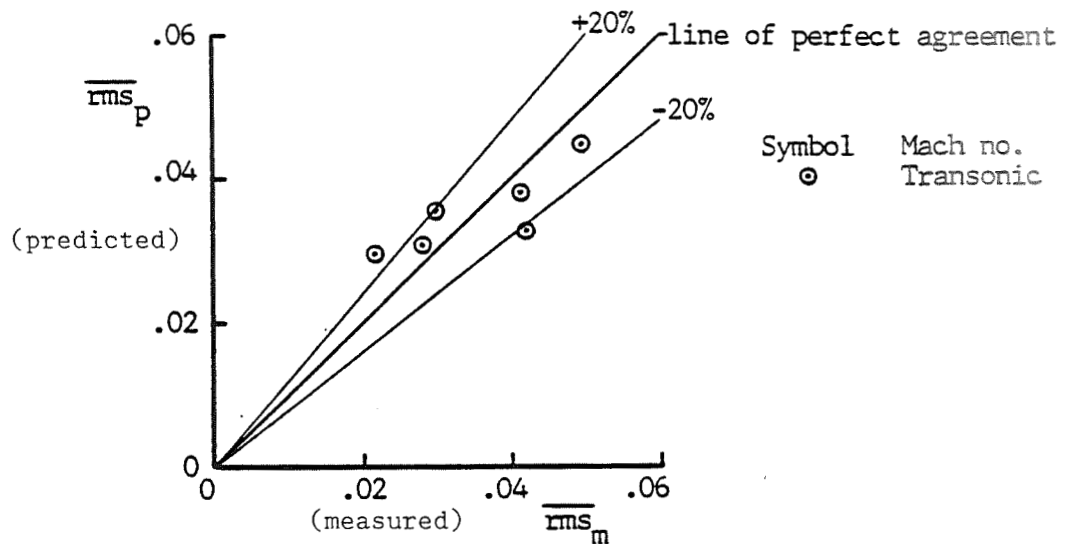


Figure 14. Comparisons of the Predicted and Measured rms Level and Peak Distortion Factor for the Transonic Inlet Model shown in Figure 9. (unpublished data)

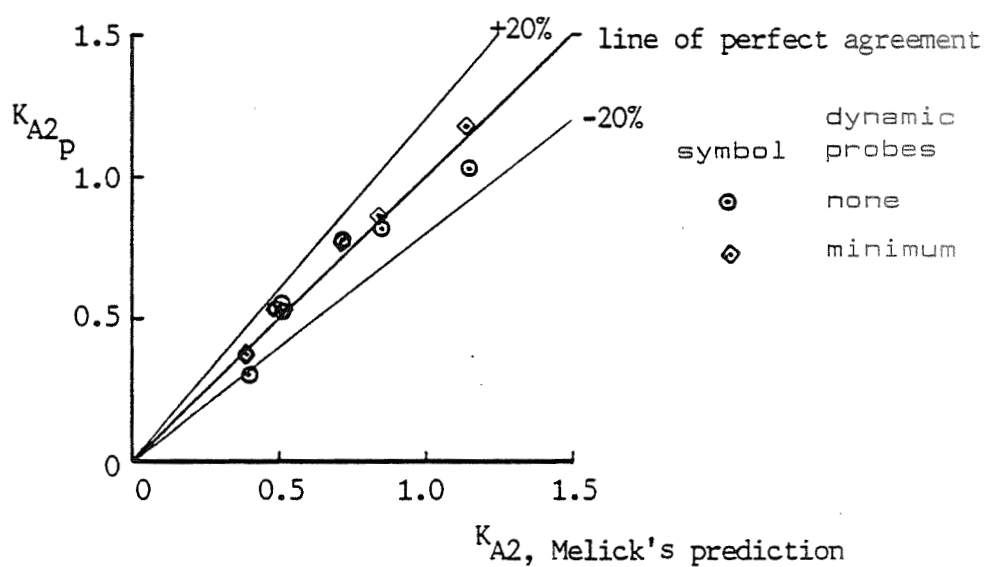
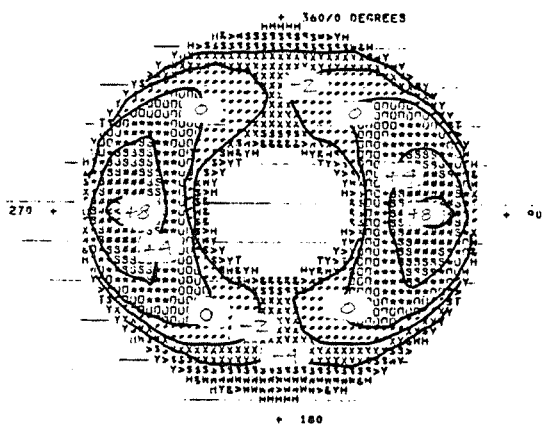


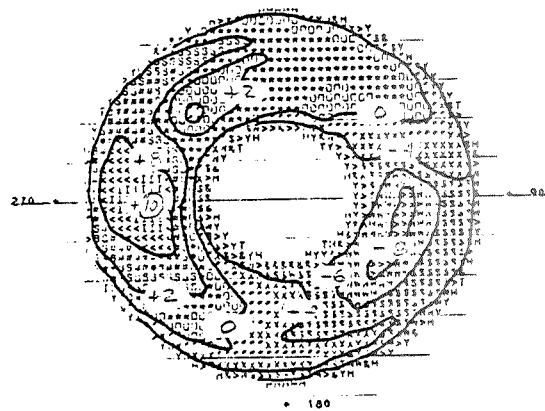
Figure 15. Comparisons of peak distortion factors predicted by the present analysis and the Melick method based on the total pressure rms measurements for the transonic inlet data set (unpublished data)

percent from average pressure



K=THETA	0.03551
KD2	452.6
(IDC)=MAX	0.06052
(IDR)=MAX	0.03083
KRA	0.10017
KAZ	0.11405
DSPR	0.00238
ID	0.67161

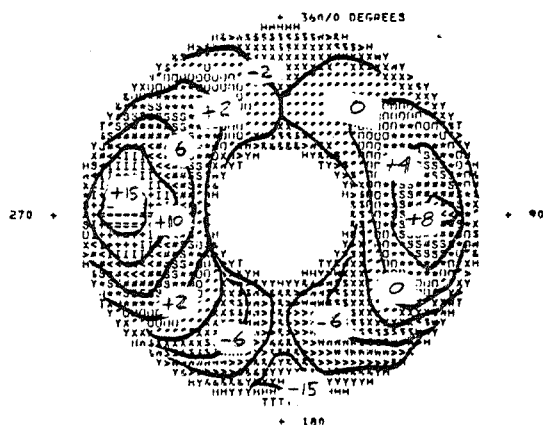
steady-state



K=THETA	0.41514
KD2	1199.5
(IDC)=MAX	0.07391
(IDR)=MAX	0.01520
KRA	0.07157
KAZ	0.41126
DSPR	0.04259
ID	0.76769

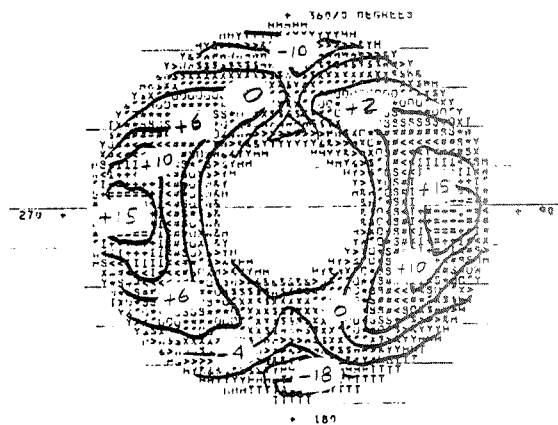
DYNADec peak

percent from average pressure



K=THETA	0.30575
KD2	1348.5
(IDC)=MAX	0.13683
(IDR)=MAX	0.03083
KRA	0.10017
KAZ	0.38428
DSPR	0.03241
ID	1.08694

Melick model peak

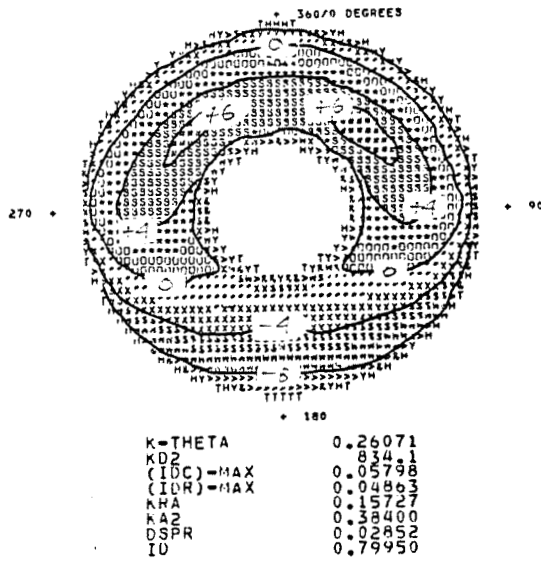


K=THETA	0.18022
KD2	1226.0
(IDC)=MAX	0.15058
(IDR)=MAX	0.05004
KRA	0.27536
KAZ	0.39610
DSPR	0.00733
ID	1.37496

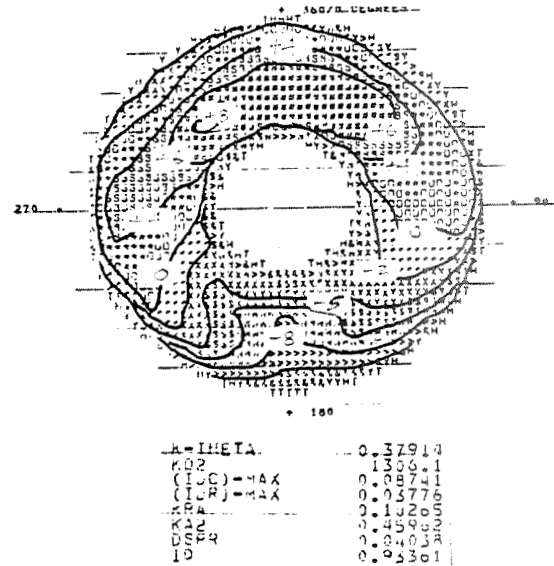
segmented vortex peak

Fig. 16a. Transonic Inlet Map Comparison (464.12)

percent from average pressure

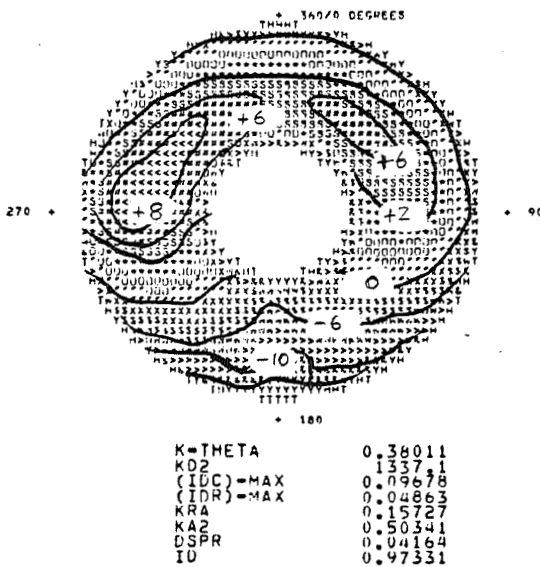


steady-state

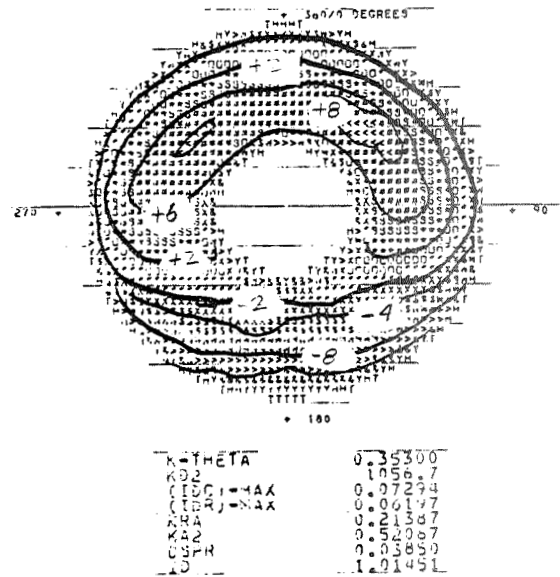


DYNADec peak

percent from average pressure



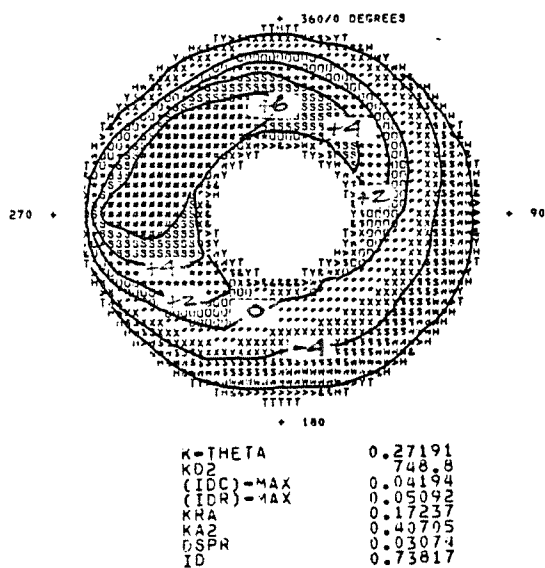
Melick model peak



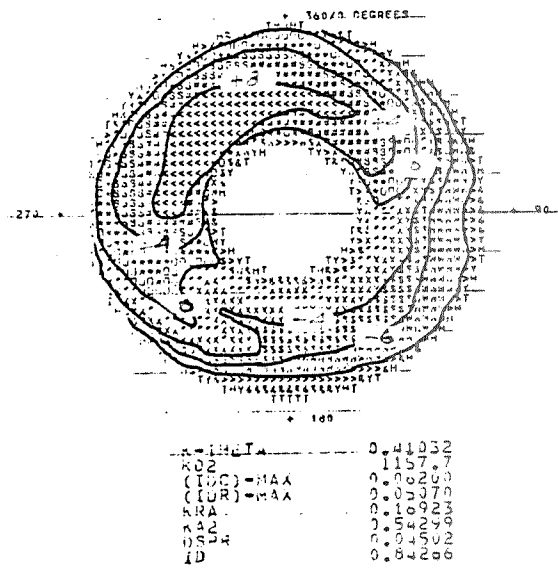
segmented vortex peak

Figure 16b. Transonic Inlet Map Comparison (465.11)

percent from average pressure

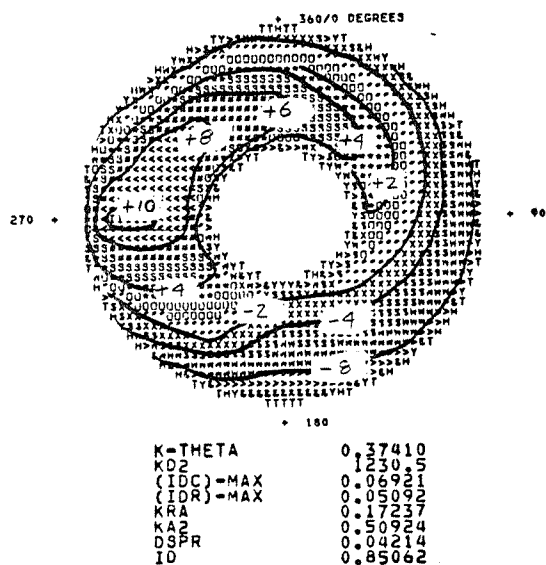


steady-state

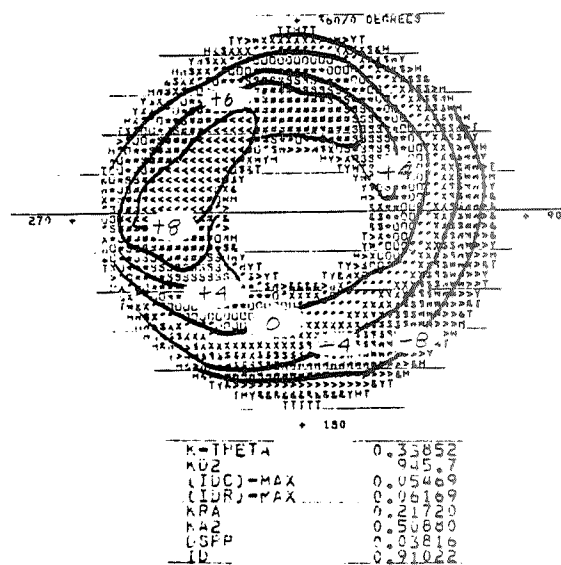


DYNADec peak

percent from average pressure



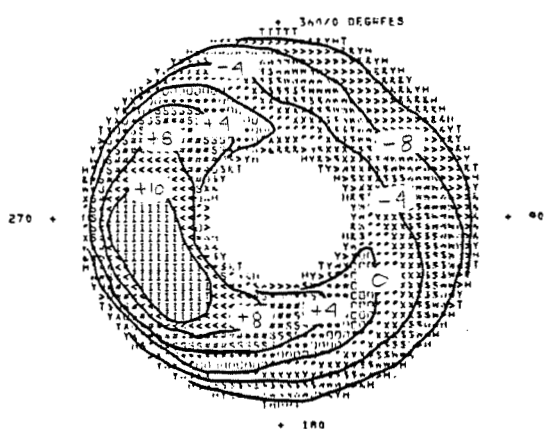
Melick model peak



segmented vortex peak

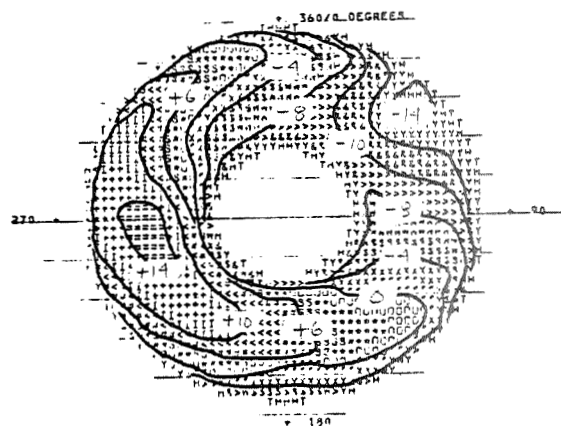
Figure 16c. Transonic Inlet Map Comparison (473.12)

percent from average pressure



K-THETA	0.51255
KDZ	1520 H
(IDC)-MAX	0.08006
(IDR)-MAX	0.06062
KRA	0.19793
KA2	0.66773
DSPR	0.05478
ID	1.04356

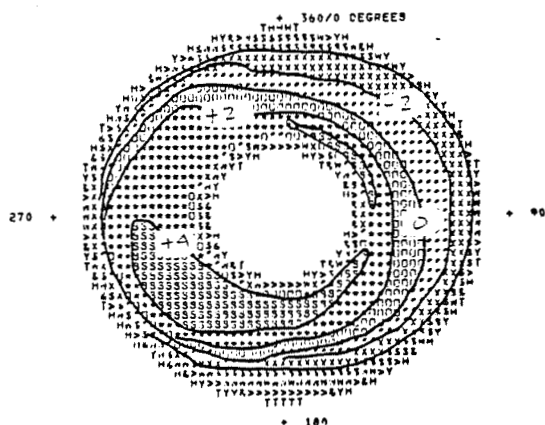
steady-state



K-THETA	0.72939
KDZ	2131.6
(IDC)-MAX	0.13803
(IDR)-MAX	0.01941
KRA	0.03619
KA2	0.80480
DSPR	0.07504
ID	1.56775

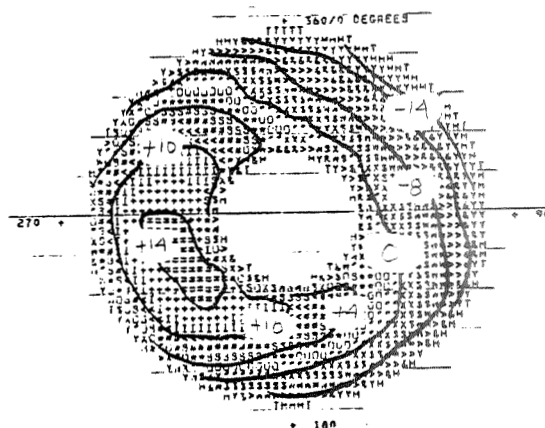
DYNADEC peak

percent from average pressure



K-THETA	0.13204
KDZ	517 S
(IDC)-MAX	0.03954
(IDR)-MAX	0.06062
KRA	0.19793
KA2	0.28722
DSPR	0.00625
ID	0.85547

Melick model peak

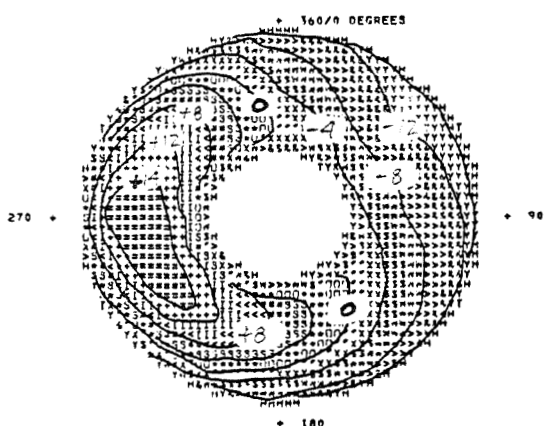


K-THETA	0.65597
KDZ	1804.6
(IDC)-MAX	0.04936
(IDR)-MAX	0.07884
KRA	0.27547
KA2	0.87233
DSPR	0.07006
ID	1.33213

segmented vortex peak

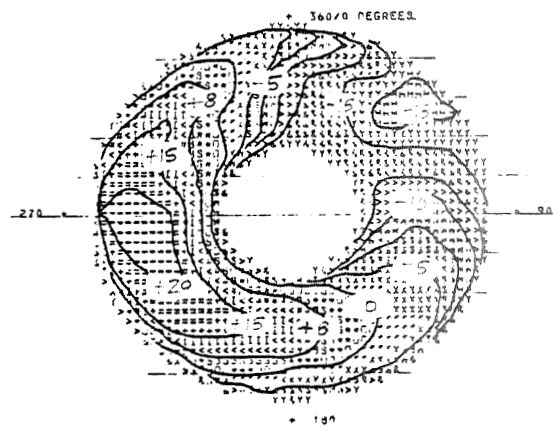
Figure 16d. Transonic Inlet Map Comparison (485.10)

percent from average pressure



K=THETA	0.75539
KD2	0.19834
(IDC)-MAX	0.10555
(IDR)-MAX	0.06503
KRA	0.21478
KA2	0.92378
DSPR	0.07803
ID	1.25020

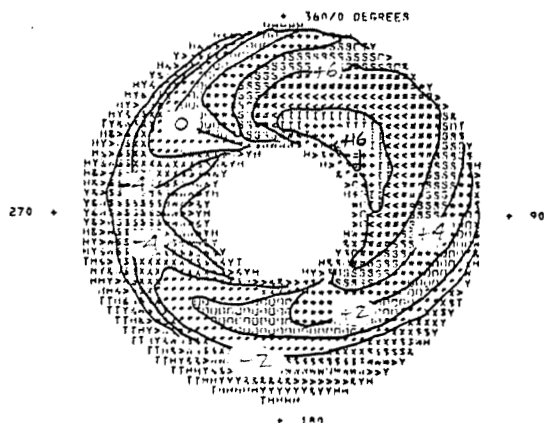
steady-state



K=THETA	1.05180
KD2	0.31940
(IDC)-MAX	0.17707
(IDR)-MAX	0.03807
KRA	0.20612
KA2	1.18204
DSPR	0.10784
ID	1.87747

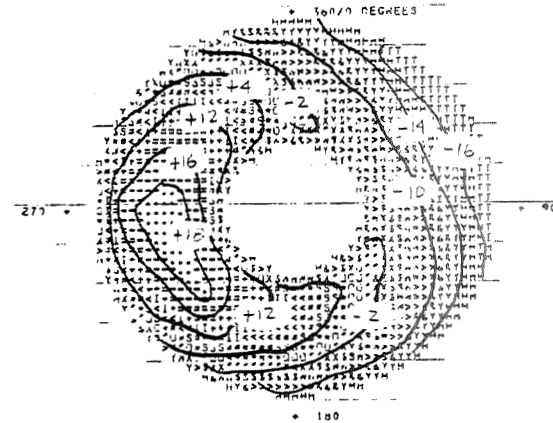
DYNADEC peak

percent from average pressure



K=THETA	0.56445
KD2	0.18620
(IDC)-MAX	0.10969
(IDR)-MAX	0.06503
KRA	0.21478
KA2	0.73204
DSPR	0.05632
ID	1.27092

Melick model peak

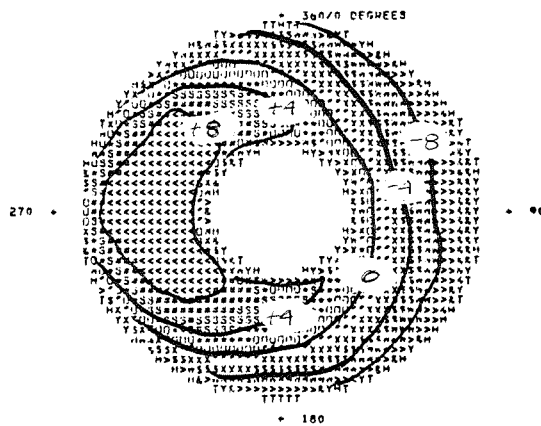


K=THETA	0.93733
KD2	0.23640
(IDC)-MAX	0.12610
(IDR)-MAX	0.06503
KRA	0.20612
KA2	1.17204
DSPR	0.09710
ID	1.57472

segmented vortex peak

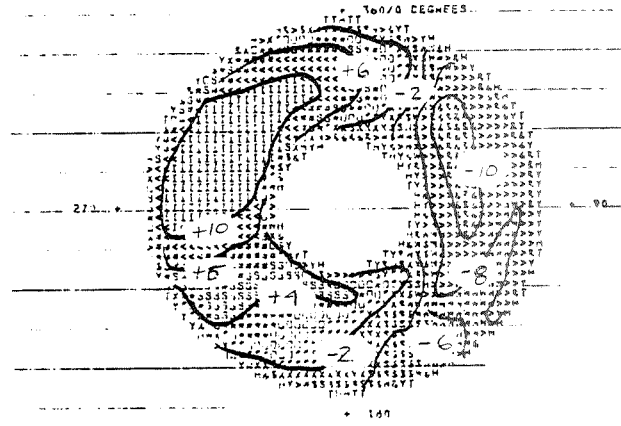
Figure 16e. Transonic Inlet Map Comparison (487.80)

percent from average pressure



K=THETA	0.41709
K02	1258.9
(IDC)=MAX	0.06621
(IDR)=MAX	0.06127
KRA	0.21888
KA2	0.58869
DSPR	0.04733
ID	0.90861

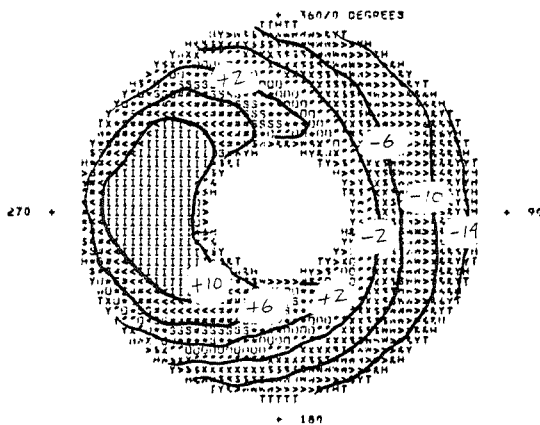
steady-state



K=THETA	0.64922
K02	1992.7
(IDC)=MAX	0.11275
(IDR)=MAX	0.03645
KRA	0.06704
KA2	0.71843
DSPR	0.06939
ID	1.10976

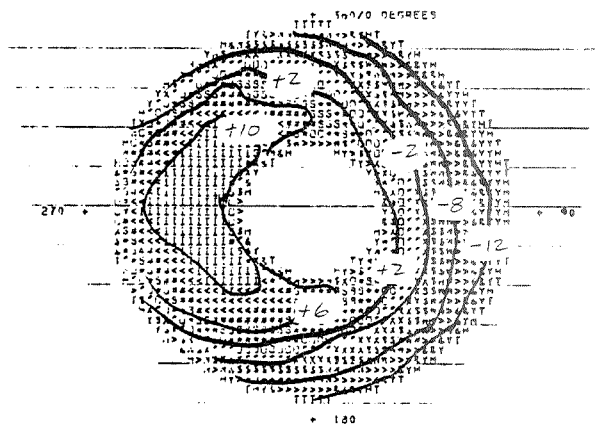
DYNADec peak

percent from average pressure



K=THETA	0.55988
K02	1667.4
(IDC)=MAX	0.08731
(IDR)=MAX	0.06134
KRA	0.21888
KA2	0.73148
DSPR	0.06296
ID	1.06094

Melick model peak



K=THETA	0.51359
K02	1540.2
(IDC)=MAX	0.08236
(IDR)=MAX	0.07514
KRA	0.27740
KA2	0.73107
DSPR	0.05734
ID	1.13403

segmented vortex peak

Figure 16f. Transonic Inlet Map Comparisons (498.12)

DISTORTION FACTOR	STEADY- STATE	DYNADEC PEAK	PREDICTED PEAK
CASE#			
182/1			
K-THETA	1.19729	1.91726	1.5817
KD2	1496.6	2083.6	1836.5
(IDC)-MAX	0.08776	0.14850	0.1161
(IDR)-MAX	0.02588	0.00823	0.0355
KRA	0.26171	0.15219	0.5381
KA2	1.38912	2.02882	1.8198
DSPR	0.05196	0.07252	0.0660
ID	0.06158	0.11609	0.0767
189/3			
K-THETA	0.72977	0.99604	1.0647
KD2	856.3	1317.8	1191.6
(IDC)-MAX	0.04623	0.07602	0.0798
(IDR)-MAX	0.01200	0.01652	0.0218
KRA	0.10781	0.17564	0.3284
KA2	0.80880	1.12478	1.1831
DSPR	0.03236	0.04402	0.0448
ID	0.03198	0.05215	0.0493
216/3			
K-THETA	0.42371	0.77572	0.5765
KD2	1004.2	1550.8	1572.0
(IDC)-MAX	0.05599	0.08596	0.1017
(IDR)-MAX	0.02829	0.02949	0.0416
KRA	0.10789	0.18070	0.2067
KA2	0.50279	0.96817	0.6708
DSPR	0.03187	0.05105	0.0435
ID	0.04657	0.06335	0.0667
243/3			
K-THETA	0.17562	0.29504	0.2777
KD2	840.1	1303.5	2391.7
(IDC)-MAX	0.05782	0.07986	0.1954
(IDR)-MAX	0.02114	0.04603	0.0597
KRA	0.04418	0.09319	0.1126
KA2	0.20800	0.36349	0.3211
DSPR	0.03047	0.05070	0.0461
ID	0.04276	0.07010	0.1114
246/3			
K-THETA	0.35780	0.62345	0.5511
KD2	1089.1	1708.8	2251.2
(IDC)-MAX	0.08957	0.11079	0.1877
(IDR)-MAX	0.03598	0.02923	0.0682
KRA	0.14713	0.12632	0.2814
KA2	0.46565	0.71604	0.6797
DSPR	0.04060	0.06559	0.0587
ID	0.06795	0.07777	0.1150
247/2			
K-THETA	1.43627	1.45223	2.2478
KD2	1163.7	2054.6	1530.2
(IDC)-MAX	0.09133	0.16260	0.1261
(IDR)-MAX	0.03498	0.02580	0.0459
KRA	0.46954	0.35946	1.0524
KA2	1.78044	2.10106	2.6853
DSPR	0.04587	0.06944	0.0657
ID	0.06836	0.11450	0.0853

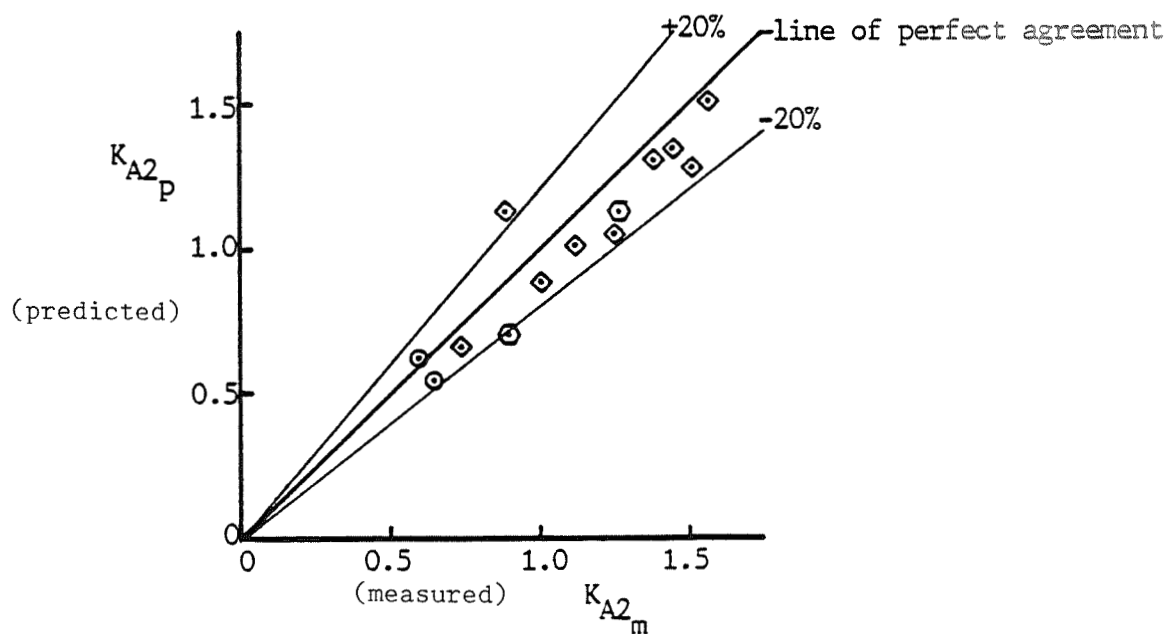
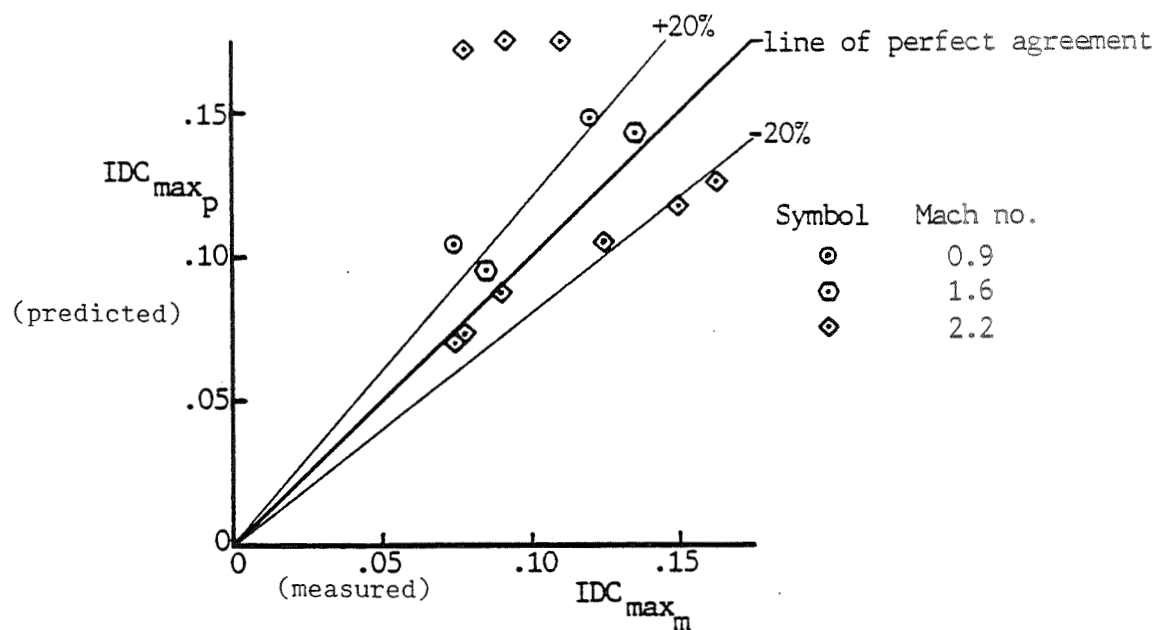
Table 4. Supersonic Inlet Distortion Comparison

DISTORTION FACTOR	STEADY- STATE	DYNADEC PEAK	PREDICTED PEAK
CASE#			
640/2			
K-THETA	0.52739	0.90844	0.7798
KD2	867.7	1089.8	1164.0
(IDC)-MAX	0.08143	0.08115	0.1045
(IDR)-MAX	0.01611	0.02199	0.0243
KRA	0.13391	0.16460	0.3099
KA2	0.62555	1.03275	0.9061
DSPR	0.02388	0.03569	0.0342
ID	0.05671	0.05709	0.0709
643/3			
K-THETA	0.52601	0.87416	0.7126
KD2	745.5	860.2	894.5
(IDC)-MAX	0.06654	0.07828	0.0780
(IDR)-MAX	0.01427	0.02301	0.0184
KRA	0.19070	0.32695	0.3188
KA2	0.66580	1.11381	0.8743
DSPR	0.01783	0.03004	0.0242
ID	0.04631	0.05556	0.0533
695/1			
K-THETA	0.43841	0.72044	0.6187
KD2	987.1	1820.2	1521.4
(IDC)-MAX	0.10020	0.13615	0.1385
(IDR)-MAX	0.05052	0.06602	0.0631
KRA	0.22436	0.26931	0.3362
KA2	0.60287	0.91784	0.8010
DSPR	0.03245	0.05711	0.0445
ID	0.08377	0.11203	0.1019
1334/2			
K-THETA	0.40639	0.52556	0.5013
KD2	1288.8	1415.1	1821.6
(IDC)-MAX	0.10599	0.12034	0.1437
(IDR)-MAX	0.02163	0.02770	0.0341
KRA	0.05386	0.09191	0.1134
KA2	0.44587	0.59292	0.5493
DSPR	0.04740	0.05650	0.0570
ID	0.07595	0.08618	0.0991
433/3			
K-THETA	0.80102	1.81271	1.2175
KD2	852.5	1520.4	1224.7
(IDC)-MAX	0.06253	0.08995	0.0966
(IDR)-MAX	0.02028	0.03254	0.0306
KRA	0.17272	0.41549	0.4572
KA2	0.92762	2.11727	1.3919
DSPR	0.03509	0.05849	0.0495
ID	0.04456	0.06565	0.0615
437/3			
K-THETA	1.20829	2.43519	1.5203
KD2	1379.8	2031.3	1658.9
(IDC)-MAX	0.08946	0.12952	0.1121
(IDR)-MAX	0.02007	0.01100	0.0282
KRA	0.17141	0.15082	0.3996
KA2	1.33393	2.54514	1.6840
DSPR	0.05169	0.07392	0.0633
ID	0.06141	0.09560	0.0748

Table 4. Supersonic Inlet Distortion Comparison
(cont'd)

DISTORTION FACTOR	STEADY- STATE	DYNADEC PEAK	PREDICTED PEAK
CASE#			
1554/4			
K-THETA	0.43895	0.50648	0.5288
KD2	1278.3	1365.6	1725.3
(IDC)-MAX	0.07057	0.07372	0.1036
(IDR)-MAX	0.00489	0.03012	0.0154
KRA	0.03103	0.10038	0.0858
KA2	0.46170	0.58006	0.5599
DSPR	0.04183	0.04993	0.0505
ID	0.05647	0.05731	0.0830

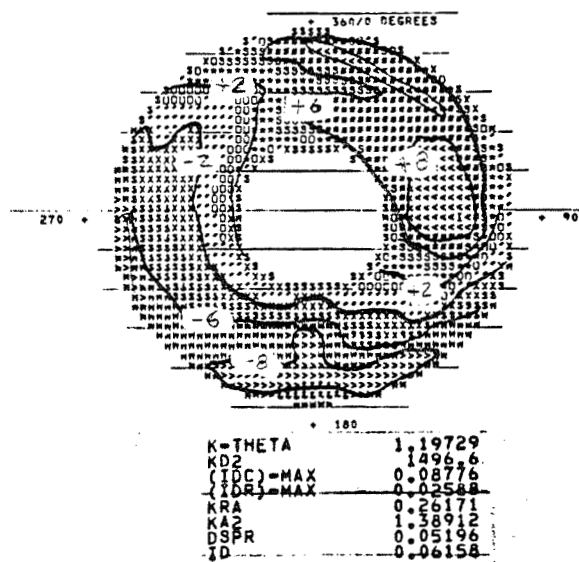
Table 4. Supersonic Inlet Distortion Comparison
(cont'd)



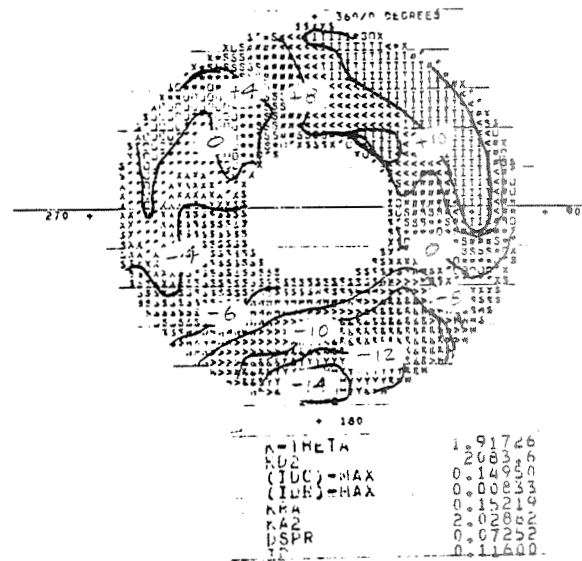
Note: The measured data was screened on K_{A2} for peak distortion

Figure 17. Comparisons of the Predicted and Measured Peak Distortion Factors for four Tailor-Mate Supersonic Inlet Models (ref. 3; see Figure 10)

percent from average pressure

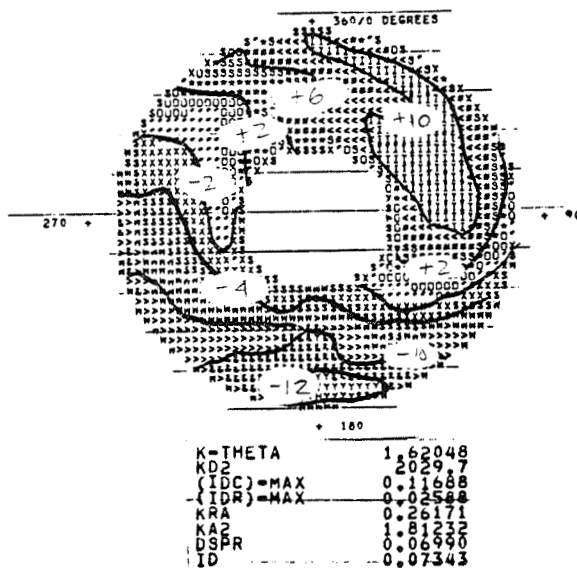


steady-state

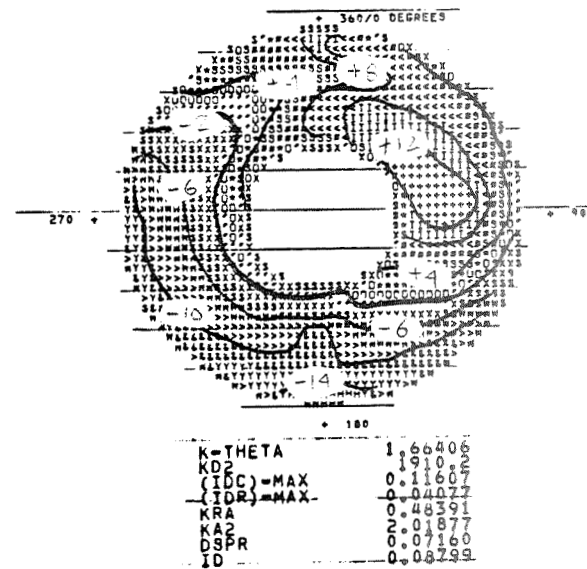


DYNADec peak

percent from average pressure



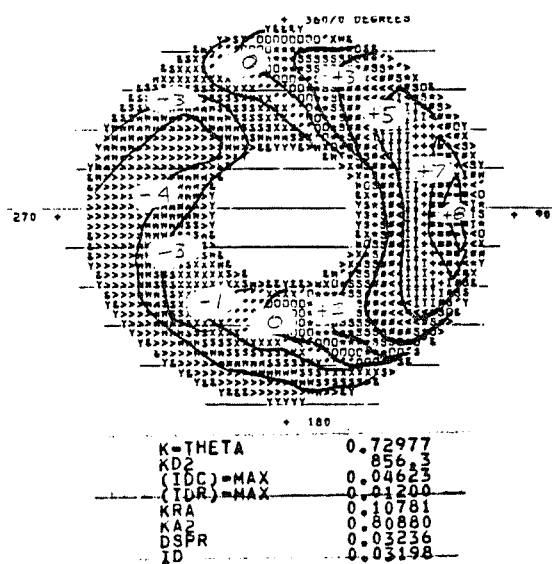
Melick model peak



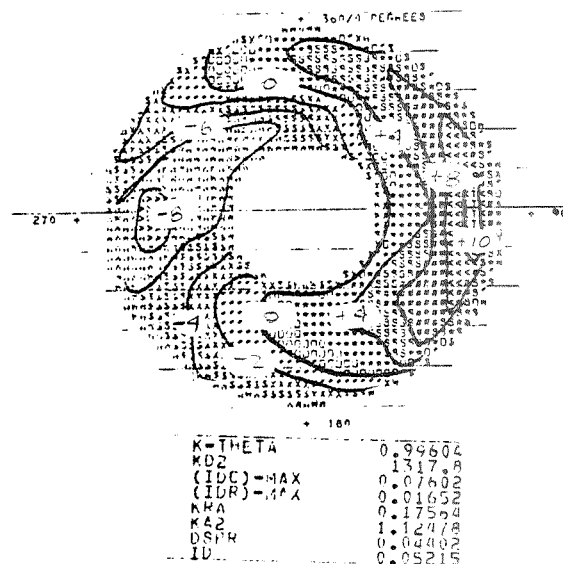
segmented vortex peak

Figure 18a. Supersonic Inlet Map Comparison (182/1)

percent from average pressure

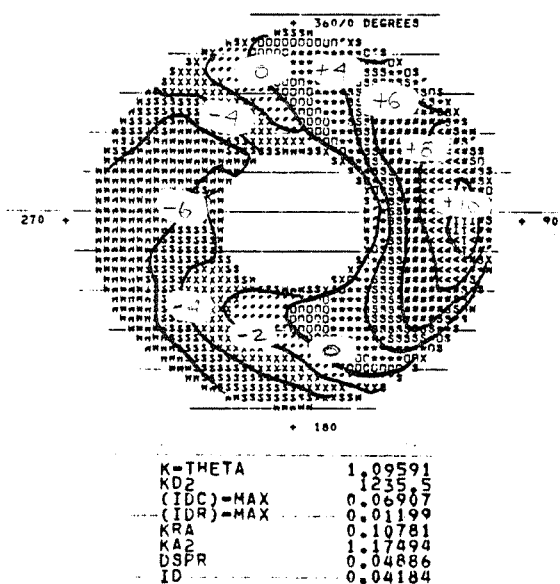


steady-state

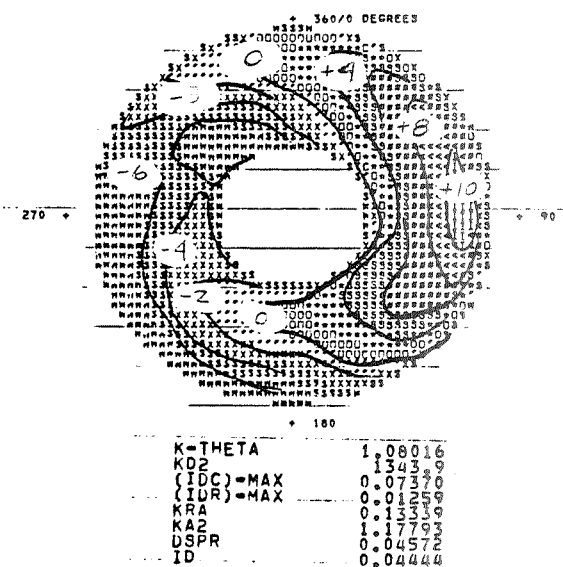


DYNADec peak

percent from average pressure



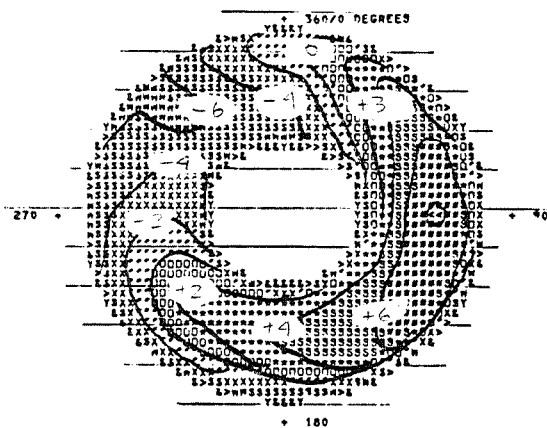
Melick model peak



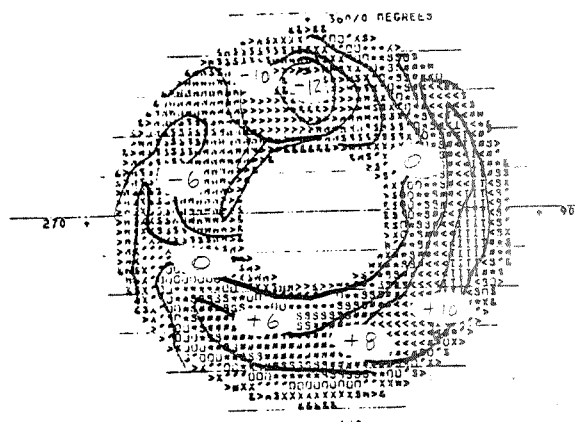
segmented vortex peak

Figure 18b. Supersonic Inlet Map Comparisons (189/3)

percent from average pressure

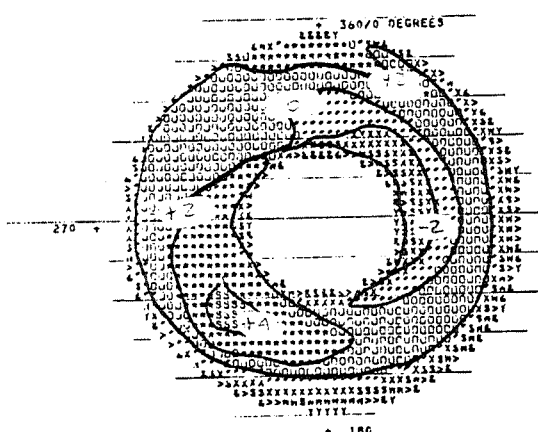


steady-state

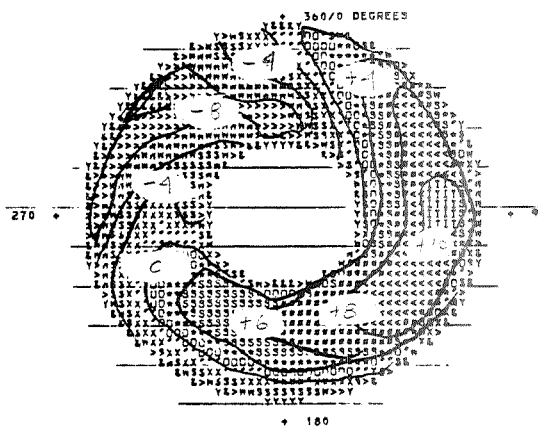


DYNADEC peak

percent from average pressure



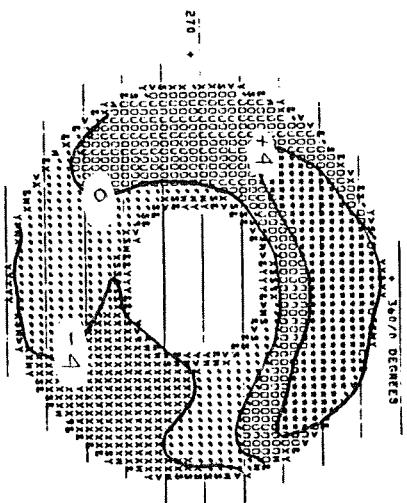
Mellick model peak



segmented vortex peak

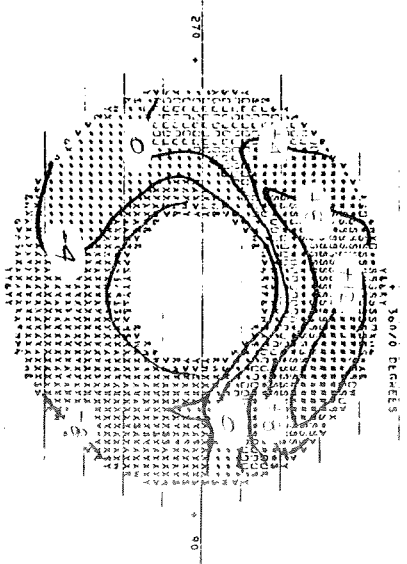
Figure 18c. Supersonic Inlet Map Comparison (216/3)

percent from average pressure



K-THETA 0.47562
 KD2 0.84084
 (IDC)-MAX 0.03184
 KRA 0.04114
 KAZ 0.29810
 DSPR 0.058047
 ID 0.002276

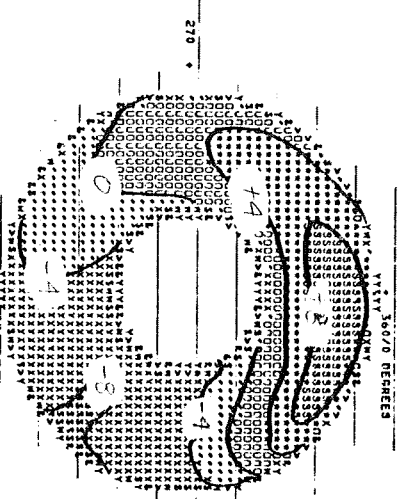
steady-state



K-THETA 0.29704
 KD2 0.130784
 (IDC)-MAX 0.03403
 KRA 0.00339
 KAZ 0.00770
 DSPR 0.03710
 ID 0.007010

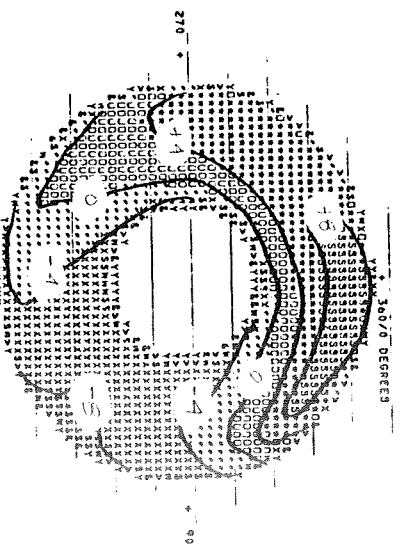
DYNADec peak

percent from average pressure



K-THETA 0.28657
 KD2 0.137948
 (IDC)-MAX 0.008748
 KRA 0.002114
 KAZ 0.044418
 DSPR 0.031895
 ID 0.044920
 0.054400

Melick peak

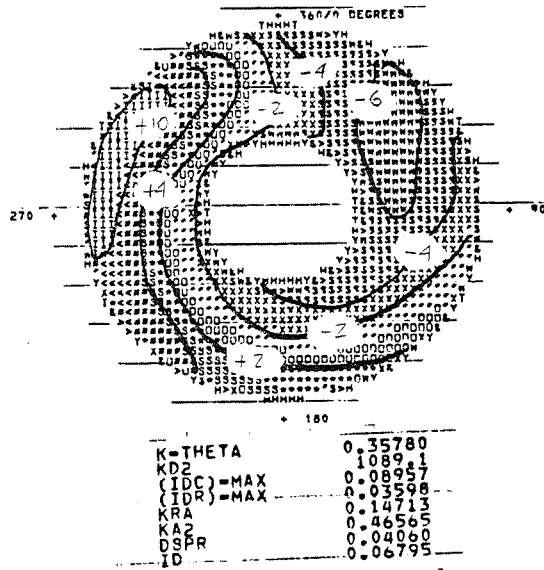


K-THETA 0.28380
 KD2 0.12866
 (IDC)-MAX 0.010405
 KRA 0.005335
 KAZ 0.071268
 DSPR 0.031605
 ID 0.04691
 0.074448

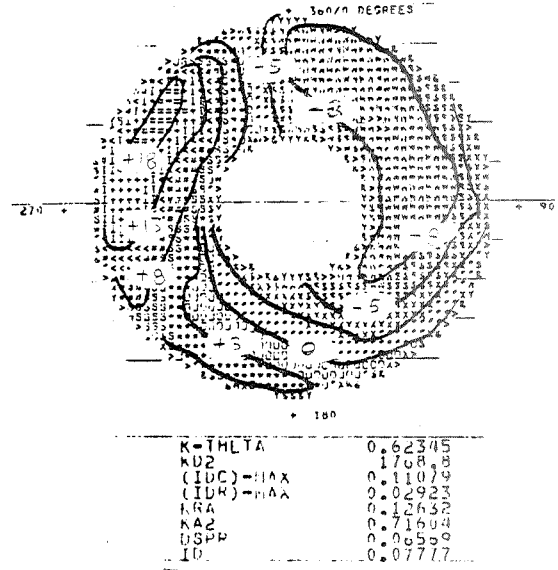
segmented vortex peak

Figure 18d. Supersonic Inlet Map Comparisons (243/3)

percent from average pressure

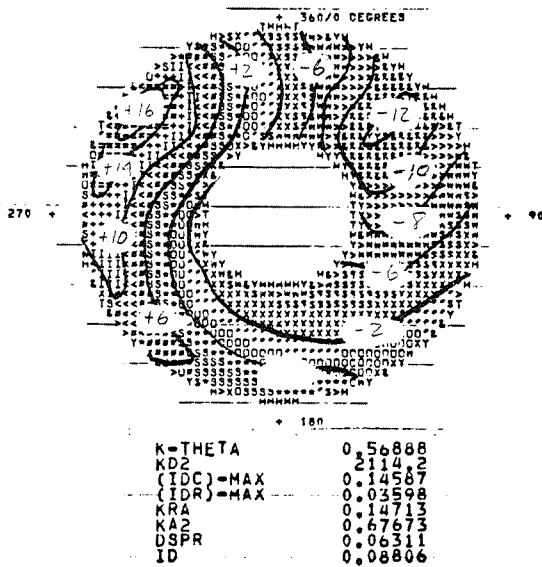


steady-state

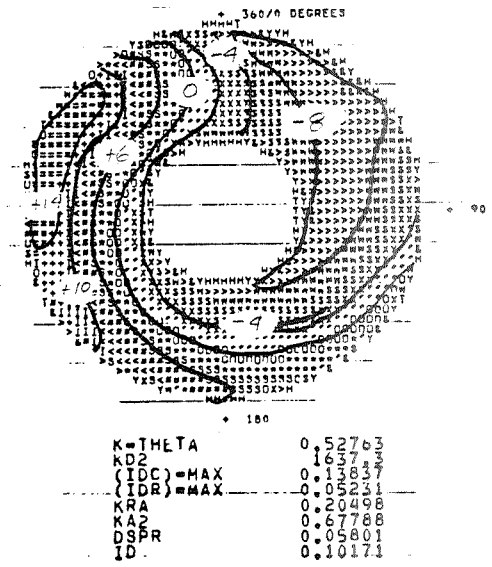


DYNADec peak

percent from average pressure



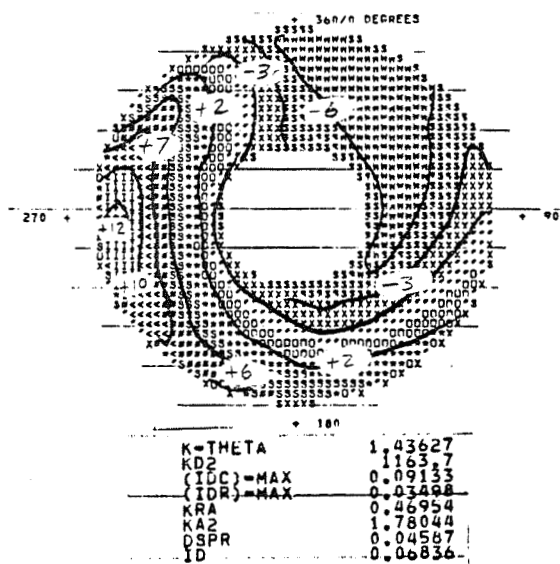
Melick peak



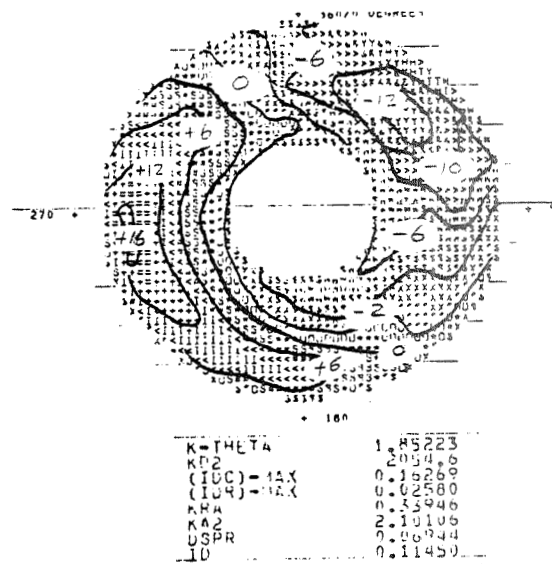
segmented vortex peak

Figure 18e. Supersonic Inlet Map Comparison (246/3)

percent from average pressure

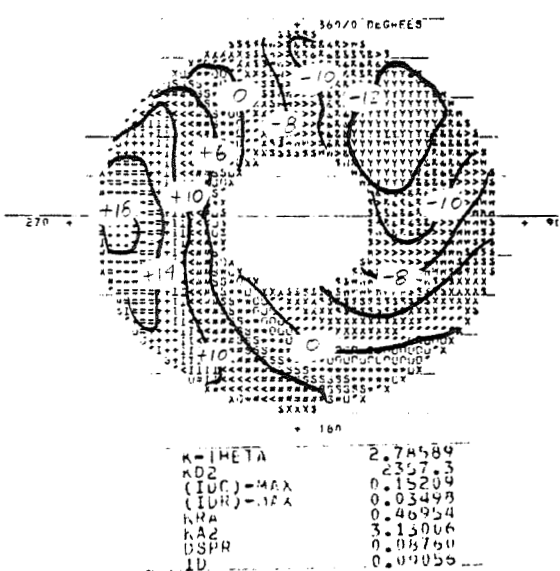


steady-state

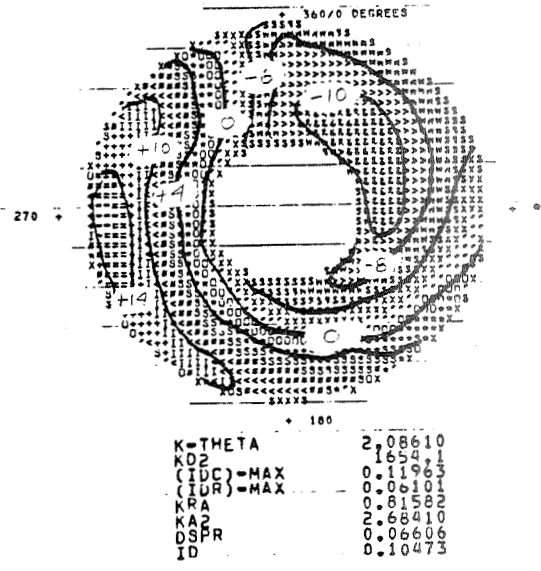


DYNADEC peak

percent from average pressure



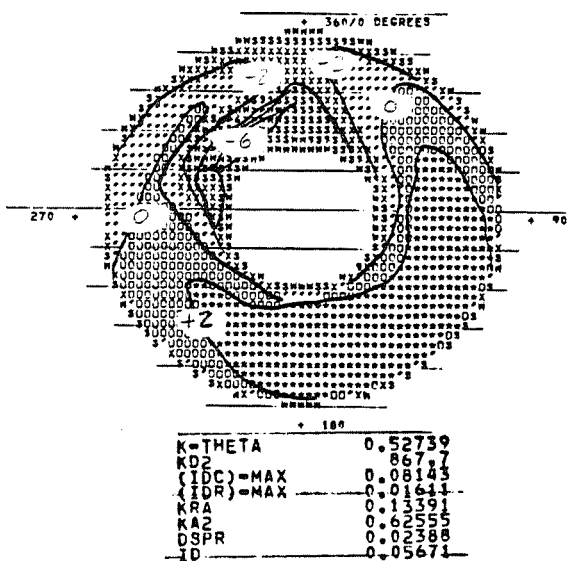
Melick peak



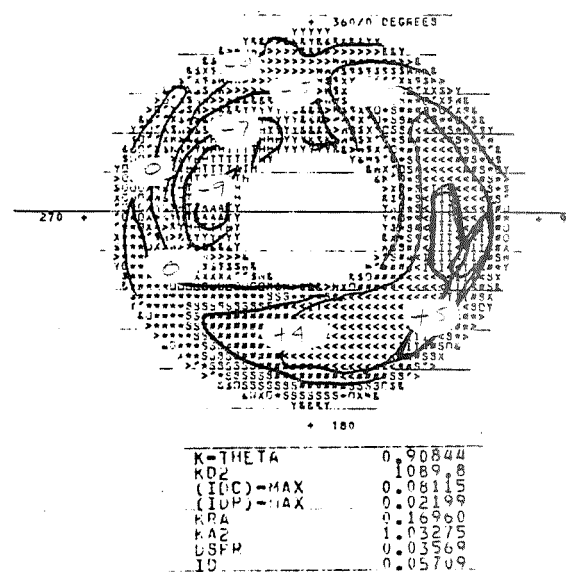
segmented vortex peak

Figure 18f. Supersonic Inlet Map Comparison (247/2)

percent from average pressure

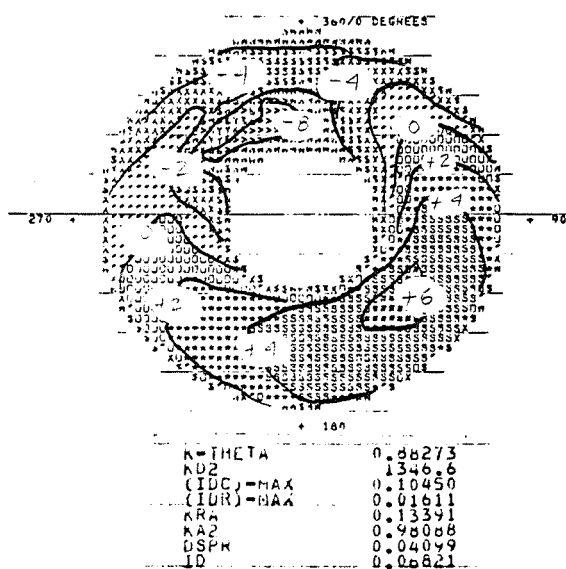


steady-state

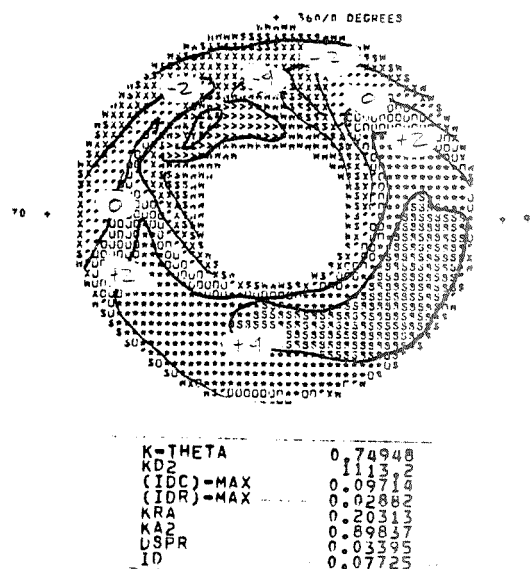


DYNADEC peak

percent from average pressure



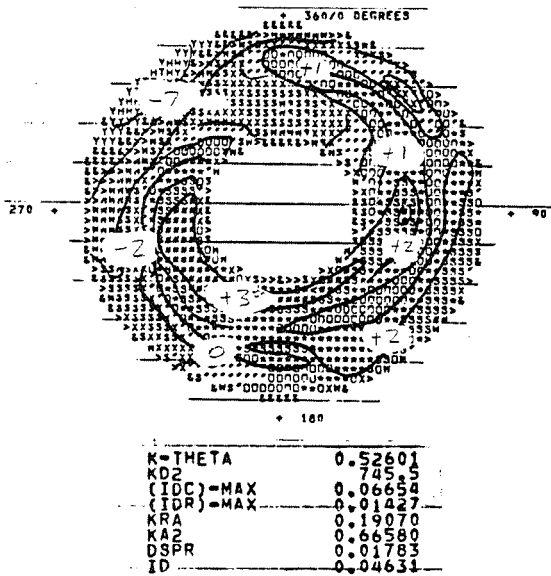
Melick peak



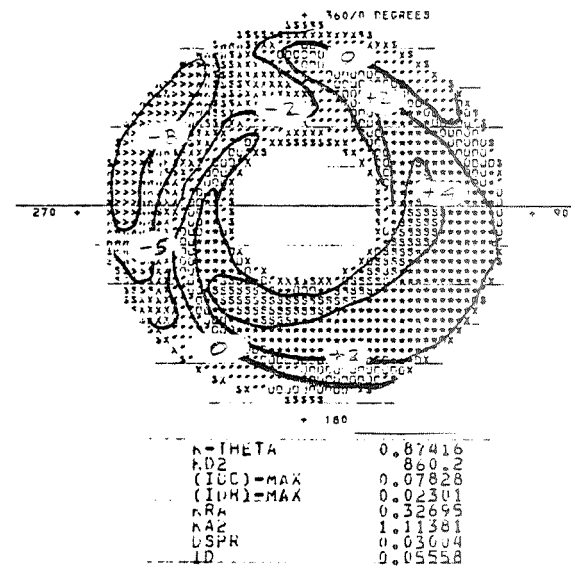
segmented vortex peak

Figure 18g. Supersonic Inlet Map Comparison (640/2)

percent from average pressure

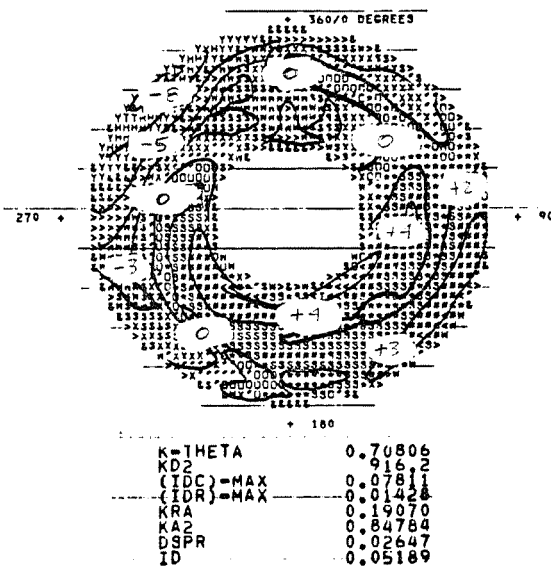


steady-state

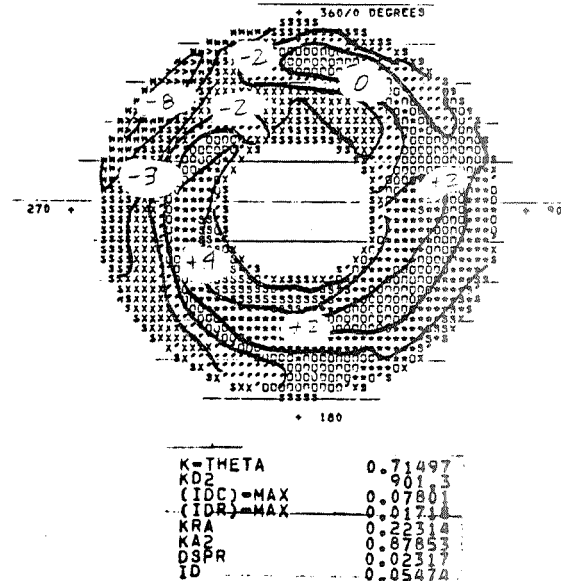


DYNADEC peak

percent from average pressure



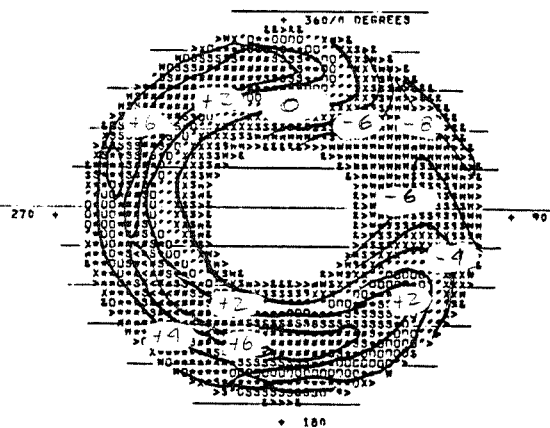
Melick peak



segmented vortex peak

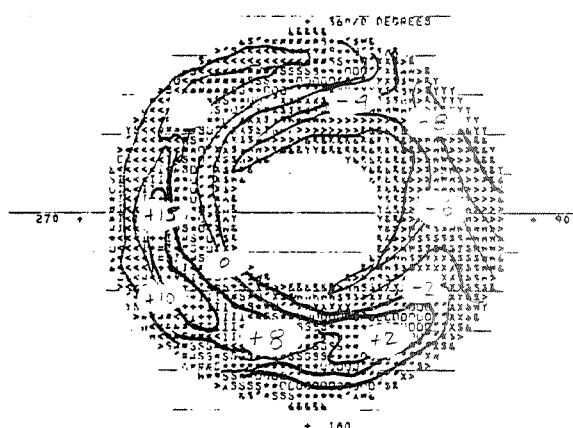
Figure 18h. Supersonic Inlet Map Comparison (643/3)

percent from average pressure



K-THETA	0.43841
KD2	0.98731
(IDC)-MAX	0.10020
(IDR)-MAX	0.05052
KRA	0.22436
KA2	0.60287
DSPR	0.03243
ID	0.08377

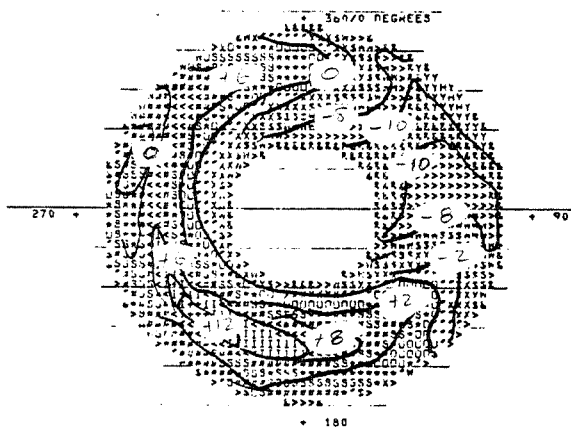
steady-state



K-THETA	0.72044
KD2	1.82040
(IDC)-MAX	0.13609
(IDR)-MAX	0.06602
KRA	0.26931
KA2	0.91784
DSPR	0.05711
ID	0.11263

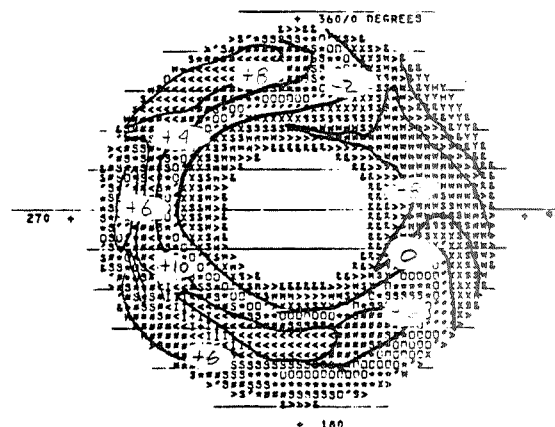
DYNADec peak

percent from average pressure



K-THETA	0.77891
KD2	1.6037
(IDC)-MAX	0.13891
(IDR)-MAX	0.05042
KRA	0.22436
KA2	0.64336
DSPR	0.05823
ID	0.09651

Melick peak

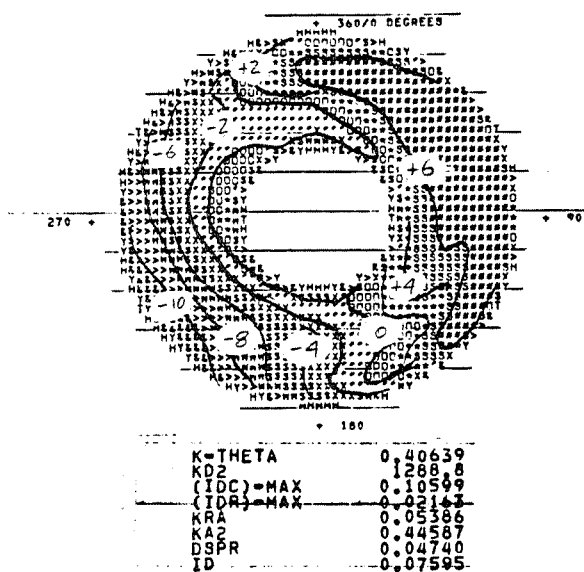


K-THETA	0.55823
KD2	1.4140
(IDC)-MAX	0.13868
(IDR)-MAX	0.07596
KRA	0.33443
KA2	0.80267
DSPR	0.04192
ID	0.12156

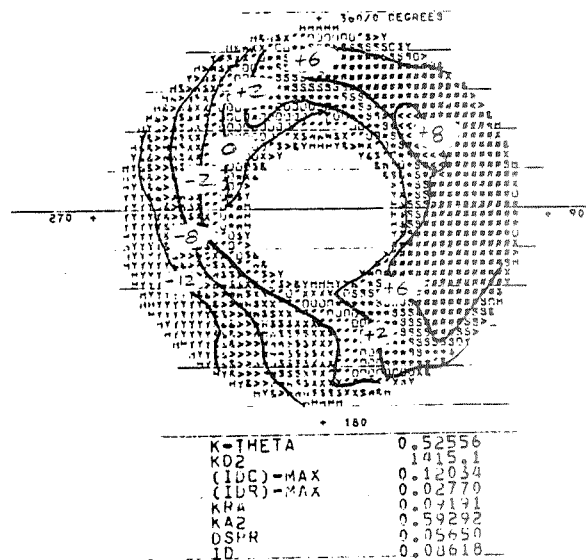
segmented vortex peak

Figure 18i. Supersonic Inlet Map Comparisons (695/1)

percent from average pressure

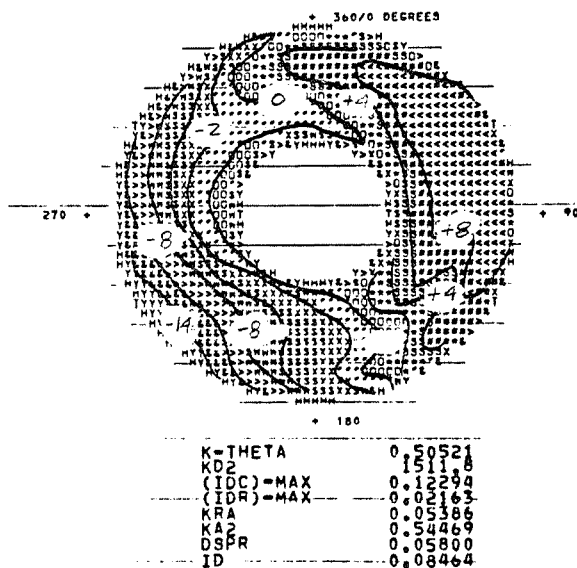


steady-state

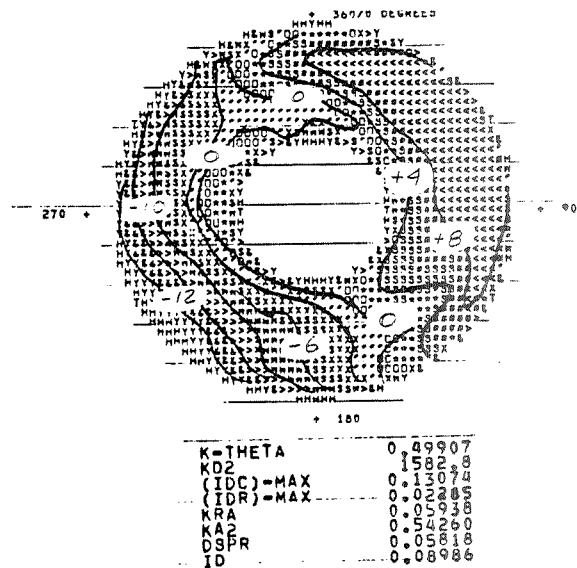


DYNADec peak

percent from average pressure



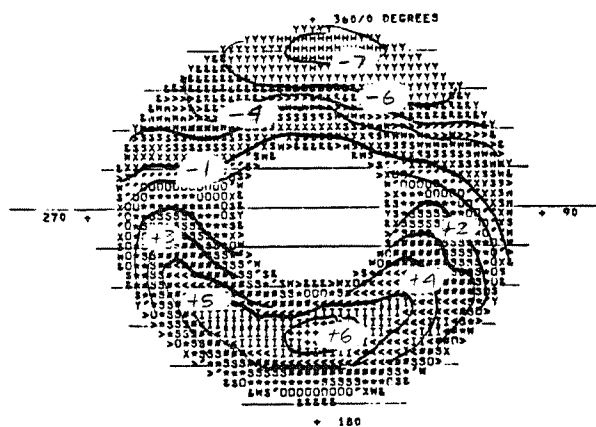
Melick peak



segmented vortex peak

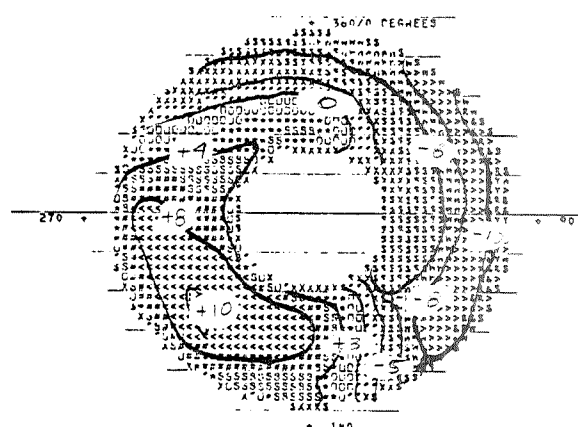
Figure 18j. Supersonic Inlet Map Comparisons (1334/2)

percent from average pressure



K-THETA	0.80102
KD2	0.8526
(IDC)-MAX	0.06235
(IDR)-MAX	0.06235
KRA	0.17272
KA2	0.0277
DSPR	0.0350
ID	0.04456

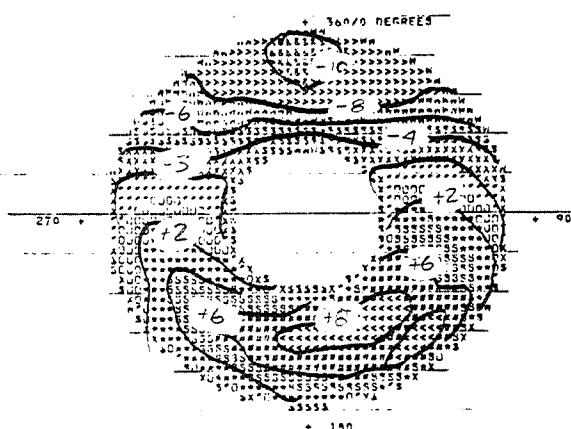
steady-state



K-THETA	1.812/1
KD2	1520.4
(IDC)-MAX	0.08945
(IDR)-MAX	0.03254
KRA	0.41549
KA2	2.11727
DSPR	0.05049
ID	0.00545

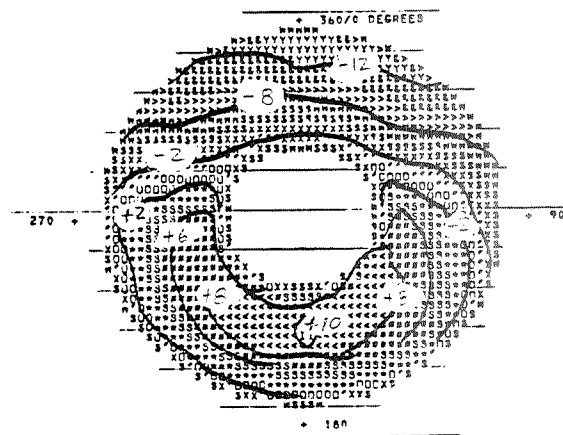
DYNADec peak

percent from average pressure



K-THETA	1.28788
KD2	1425.1
(IDC)-MAX	0.04662
(IDR)-MAX	0.02028
KRA	0.17272
KA2	1.41449
DSPR	0.06510
ID	0.05761

Melick peak

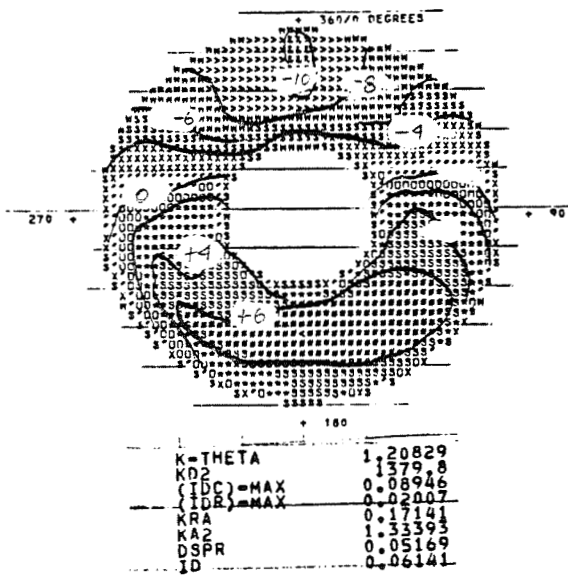


K-THETA	1.37066
KD2	1351.2
(IDC)-MAX	0.09667
(IDR)-MAX	0.04604
KRA	0.45872
KA2	1.70690
DSPR	0.05871
ID	0.08358

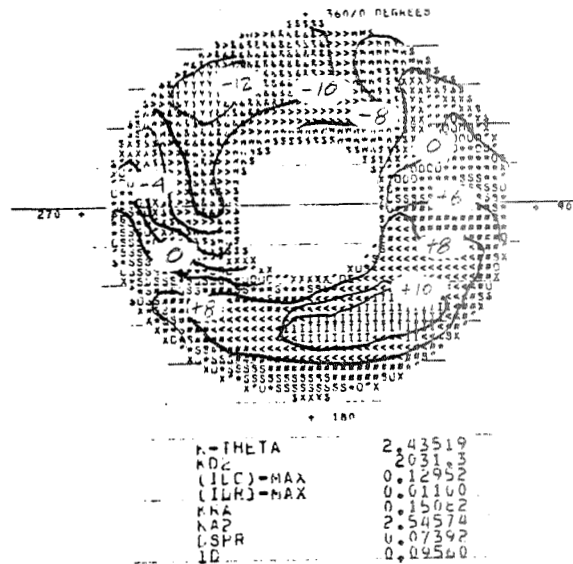
segmented vortex peak

Figure 18k. Supersonic Inlet Map Comparison (433/3)

percent from average pressure

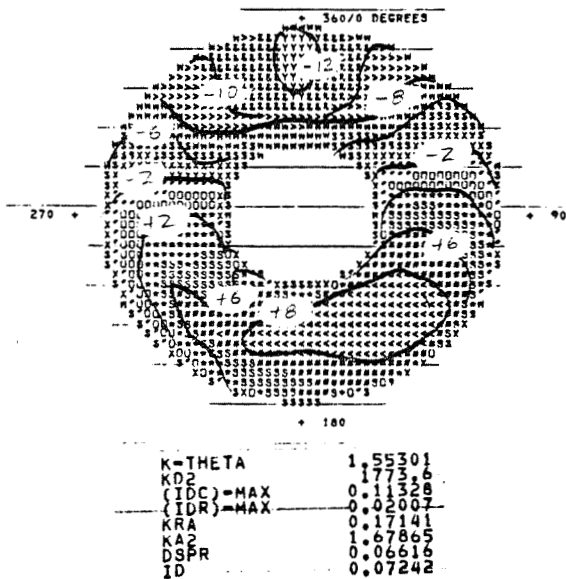


steady-state

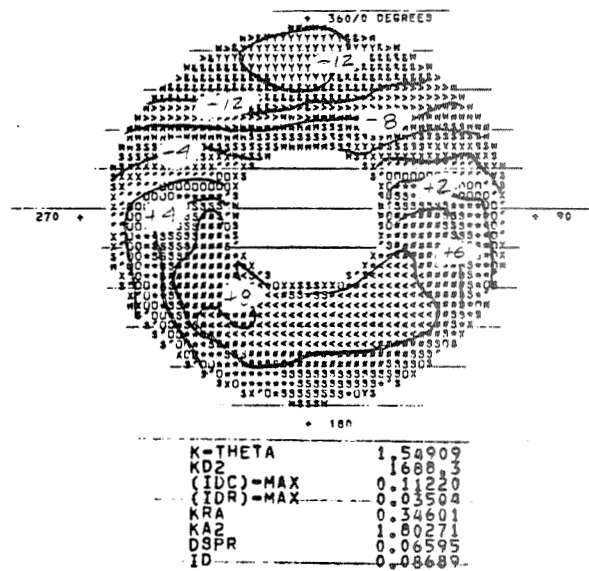


DYNADec peak

percent from average pressure



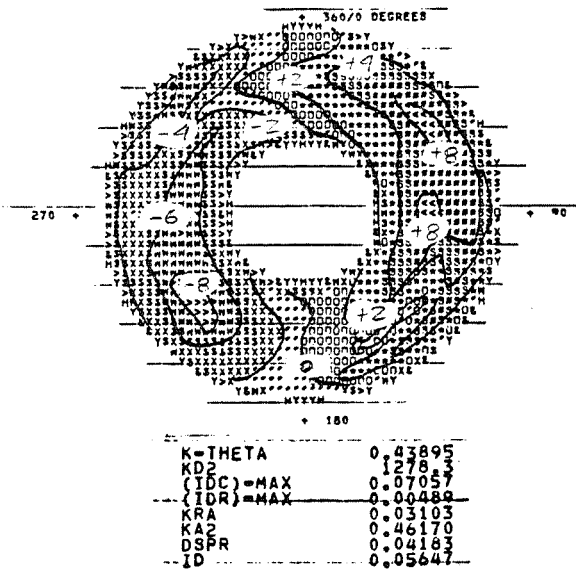
Melick peak



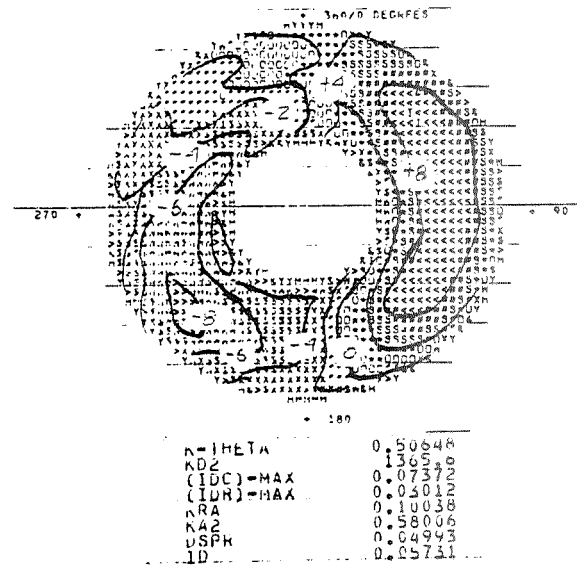
segmented vortex peak

Figure 181. Supersonic Inlet Map Comparison (473/3)

percent from average pressure

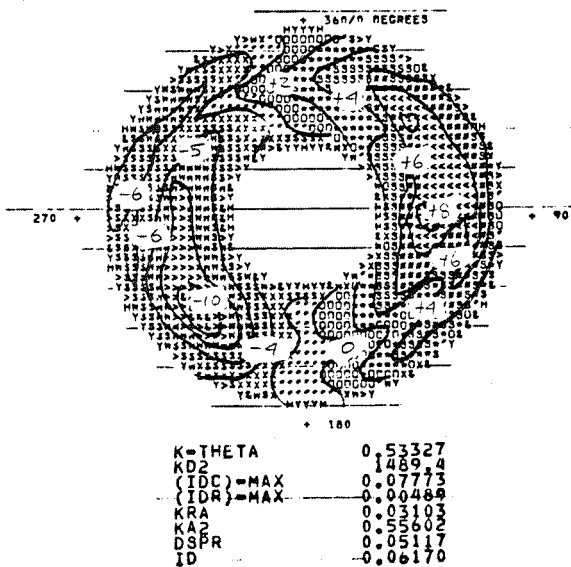


steady-state

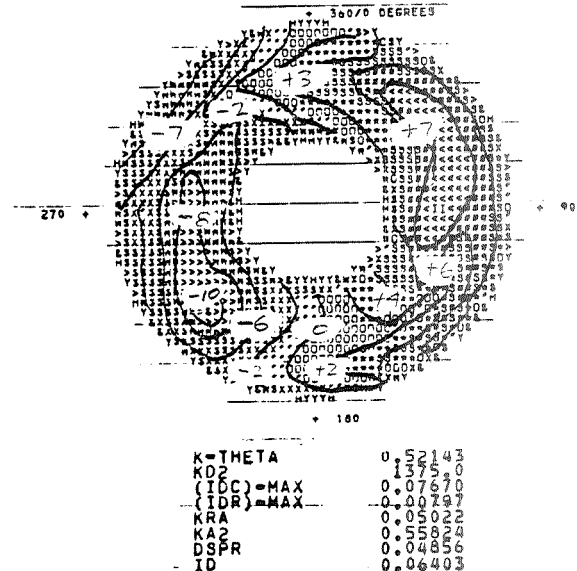


DYNADEC peak

percent from average pressure



Melick peak



segmented vortex peak

Figure 18m. Supersonic Inlet Map Comparison (1554/4)

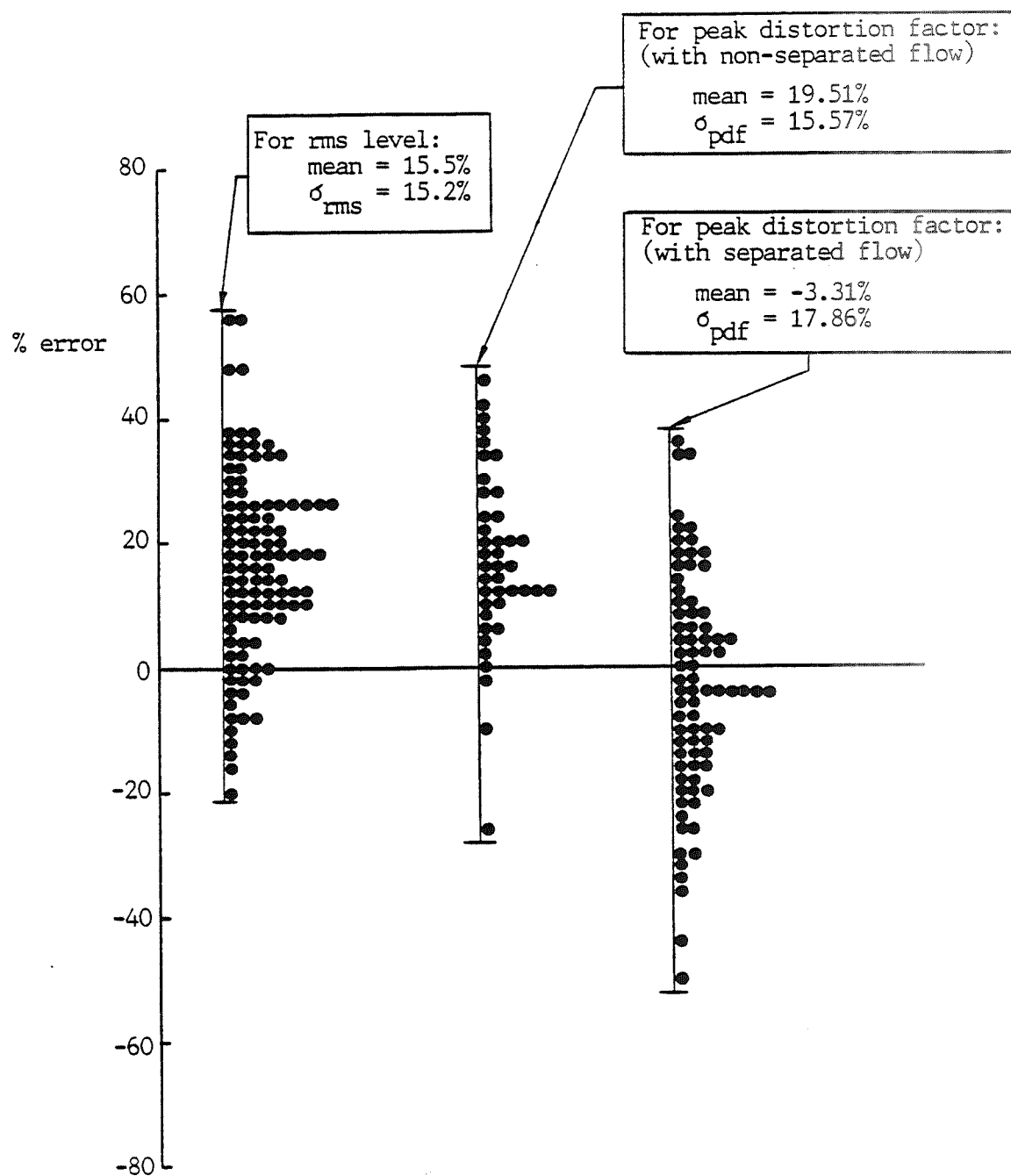


Figure 19. Accuracy of the Present Method in Predicting rms Levels and Dynamic Peak Distortion Factors

PART II

COMPUTER PROGRAM DOCUMENTATION AND USER'S MANUAL

ESTIMATING MAXIMUM INSTANTANEOUS INLET FLOW
DISTORTION FROM STEADY-STATE TOTAL PRESSURE
MEASUREMENTS WITH FULL, LIMITED, OR NO DYNAMIC
DATA

ABSTRACT

A computer program for statistically predicting peak instantaneous dynamic distortion, given steady-state distortion data and dynamic root mean square pressure fluctuation levels in gas turbine inlets, is presented. The statistical approach utilizes a physical flow model which characterizes inlet flow distortion as due to random vorticity convecting through the inlet duct. Characteristics of a mean vortex are statistically determined to match steady-state distortion data and contour map, as measured by steady-state total pressure probes. The mean vortex characteristics are then intensified according to the mean rms fluctuation level as measured by full or limited high response pressure transducer instrumentation, or as simulated by turbulence modeling, to produce the most probable peak instantaneous distortion level. The computer program utilizes this approach to solve for the dynamic distortion and print the results, including contour maps.

FOREWORD

This Report is designed to be a User's Manual and Documentation Guide for the improved Melick (ref. 1-3) dynamic distortion computer program developed at the University of Kansas. This program characterizes the random vortices used to describe the unsteady, turbulent flow in jet engine inlets, and statistically calculates the most probable peak instantaneous (dynamic) distortion level for a particular inlet operating condition. Steady-state distortion levels are computed for eight common distortion factors given the time-averaged steady-state probe pressure array, and the root mean square pressure fluctuation levels are used to project the maximum peak instantaneous distortion for the given conditions.

Details of the derivation and development of the random vortex modelling approach are not included in this User's Guide as the Guide is orientated more towards application than theory. The References, however, provide exhaustive detailing of the general Melick approach, especially References 1 through 3. Reference 4 provides an extensive list of other sources which relate to distortion prediction. Finally References 5, 6, and 8 show details of some specific developments in distortion research at the University of Kansas.

Major segments in this Guide include descriptions of the main program and subprograms as well as input and output data. Sample problems are included for illustration. A listing is provided in an appendix. The fully documented program requires memory capacity for 70,000 characters in 2300 lines. Hardware requirements include, in addition to the mainframe computer, an on-line printer for high speed output.

TABLE OF CONTENTS

	<u>Page</u>
ABSTRACT	ii
FOREWORD	iii
NOMENCLATURE	v
LIST OF FIGURES	xiv
I. INTRODUCTION	1
II. PROGRAM DESCRIPTION	6
III. INPUT DATA DESCRIPTION	24
IV. OUTPUT DATA DESCRIPTION	36
V. SAMPLE PROBLEMS	52
APPENDIX A. FORTRAN SOURCE CODE LISTING	83
APPENDIX B. SEGMENTED VORTEX OPTIONAL ADDITION	149
APPENDIX C. USER QUICK REFERENCE GUIDE	151
VI. CONCLUSION	160
VII. REFERENCES	161

NOMENCLATURE

<u>SYMBOL</u>	<u>OTHER NAMES</u>	<u>DESCRIPTION</u>	<u>PAGE</u>
A		Vortex core radius at point of maximum angular velocity, inches	49
A		Tridiagonal matrix	142
AB	ABAR, \bar{a}	Mean vortex core radius, inches	43
ALPH	alpha	Aircraft/inlet angle of attack, in degrees	29
ANGLOC		Angular position of rakes, deg.	26
ART	A/RT, AYRT, AY/RT	Nondimensionalized vortex core radius (divided by inlet radius)	49
AO		Vortex core size computed from power spectral density function	50
AO/RT		Nondimensionalized PSD vortex radius (divided by inlet radius)	50
A1		Radius of steady-state vortex, inches	40
B	BETA	Vortex orientation angle, deg.	49
BF	B-factor	Radial weighting factor for KA2	29
BRP		Base radial profile	29
BSF		Intermediate weighting factor for ID distortion solution	39
CKP	KC	Circumferential weighting factor for ID distortion solution	29
CUBIC		Subroutine - executes cubic spline interpolations	8

<u>SYMBOL</u>	<u>OTHER NAMES</u>	<u>DESCRIPTION</u>	<u>PAGE</u>
DISPAR		Subroutine - computes primary distortion factors	8
DISTRAT		Subroutine - computes simple distortion parameters	8
DK	K , KD	General distortion factor designator	26
DKBAR		Mean distortion level	46
DKMX	DKMAX	Most probable peak distortion level - 50% probable	46
DKSS		Steady-state distortion level	46
DK950		95% probable distortion level - estimated peak distortion	48
DK997		99.7% probable peak distortion level	48
DRT		Nondimensionalized radial locations of rings	25
DSPR	ΔSPR	Delta stall pressure ratio distortion factor	81
DTH	DTHETA	Angular difference between the pressure rakes with minimum and maximum average total pressure	40
E	TE	Turbulent kinetic energy dissipation rate in ft^2/sec^3	45
ERRE		Error in E in iteration, ft^2/sec^3	44
ERRK		Error in K in iteration, ft^2/sec^2	44
ERRT		Total error in E and K	44
ETA		Face average steady-state total pressure recovery	42
EXTRME		Subroutine - manages distortion factor extreme-value computation	9

<u>SYMBOL</u>	<u>OTHER NAMES</u>	<u>DESCRIPTION</u>	<u>PAGE</u>
FACE	FACP	Element used in discrete point analysis in face contour map	88
FCO	FC	Low-pass cut-off filter frequency in rms fluctuation data	27
FINITE		Subroutine - solves finite difference equations	9
FO	F	Engine rpm filter frequency in hertz	27
FRF		Subroutine - computes by iteration the mean vortex core size	9
G	GAMMA	Vortex orientation angle , deg.	40
GE		Turbulent kinetic energy dissipation rate at each finite element grid point , ft ² /sec ³	44
GK		Turbulent kinetic energy at each grid point , ft ² /sec ²	44
G1		Steady-state GAMMA orientation angle of the vortex , degrees	40
ID		General Electric combined radial/circumferential distortion factor	39
IDC		GE circumferential distortion factor	38
IDC-MAX		Maximum GE circumferential distortion factor	30
IDR		GE radial distortion factor	30
IDR-MAX		Maximum GE radial distortion factor	30
INITL		Subroutine - sets initial values for GE and GK (energies)	10
INIVEL		Subroutine - computes velocity gradients in steady-state data	10

<u>SYMBOL</u>	<u>OTHER NAMES</u>	<u>DESCRIPTION</u>	<u>PAGE</u>
INTERP		Subroutine - interpolates pressure recoveries at discrete element points at engine face	10
K	KD, DK	General distortion factor	26
K	TK	Turbulent kinetic energy in ft^2/sec^2	45
KA2		Pratt & Whitney combined radial and circumferential distortion	39
KD2		P & W circumferential distortion factor	38
KRA		P & W radial distortion factor	38
KTHETA	KTТА	P & W circumferential distortion factor (alternate)	38
LAB	LABEL	Distortion factor name or label	111
LNPOUT		Subroutine - prints pressure distortion contour map and distortion factor tables	11
MAINLP		Subroutine - controls computation of discrete point pressure data for contour mapping	11
MAXDP		Subroutine - calculates projected extreme values of distortion factors	11
MAXIDYN		Main driver computer program	7
MFR		Inlet mass flow ratio - \dot{m}_2/\dot{m}_0	30
MO		Freestream Mach number	29
\dot{m}_0		Mass flow rate in front of inlet	30
\dot{m}_2		Mass flow rate at compressor face measurement plane	30
NEWPSD		Subroutine - inputs dynamic data and evaluates PSD functions	12

<u>SYMBOL</u>	<u>OTHER NAMES</u>	<u>DESCRIPTION</u>	<u>PAGE</u>
NP		Total number of radial rakes	25
NPR	NT, PROBE	Numerical designation of probe	31
NR		Total number of rings, including static pressure rings at hub and outer radius	25
NTUR		Control parameter for selection of dynamic data input or turbulence modelling subroutines	30
P	PI	Local instantaneous total pressure recovery	28
PAVG	PAVE	Average pressure recovery at compressor face measurement plane	37
PFIX		Subroutine - transforms input data into mapping parameters	13
PFX	PFXL	Subroutine - computes vortex flux rate	13
PRNT		Subroutine - prints pressure arrays and other output	13
PROBE	NPR, NT	Numerical designation of probe	31
PS		Local steady-state total pressure recovery	28
PSAVG	SMAVG	Average steady-state total pressure recovery at engine face	37
PSD		Power spectral density function	-
PSI		Aircraft/inlet yaw angle, degrees	29
PSPEC	K, KD, DK	General flow distortion factor designator	26
PT	PT2	Local total pressure recovery at compressor face	37
PTAVG	PTAV, TMAVG	Face average total pressure recovery	37

<u>SYMBOL</u>	<u>OTHER NAMES</u>	<u>DESCRIPTION</u>	<u>PAGE</u>
PTMAX	PTMX, TMMAX	Maximum indicated local total pressure recovery	37
PTMIN	PTMN, TMMIN	Minimum indicated local total pressure recovery	37
QAVG	QAV	Face average dynamic pressure	38
QPT2	Q/PT2	Ratio of dynamic-to-total pressure at engine face	42
RADLOC		Radial position of rings, deg.	25
RATK		Subroutine determines the effect of filter frequencies on distortion factor values	14
RI		Inlet centerbody hub radius in inches (typical units)	41
RKMN		Average total pressure recovery along rake with minimum average pressure	39
RKMX		Average total pressure recovery along rake with maximum average pressure	40
RKP	KR	Radial weighting factor for solution of ID distortion	30
RMS		Root mean square	-
ROUT		Percent difference between the indicated local probe, rake, or ring pressure and the face average pressure	88
RRT	R/RT	Radial location of vortex core (nondimensional)	49
RS		Ratio of filtered-to-unfiltered rms total pressure fluctuations	32
RSIGMA		Subroutine - computes rms value of distortion factors	14

<u>SYMBOL</u>	<u>OTHER NAMES</u>	<u>DESCRIPTION</u>	<u>PAGE</u>
RT		Outer inlet radius (tip) at the compressor face, in	41
SEARCH		Subroutine - controls solution of peak distortion factors	14
SG	SIG	Unfiltered rms total pressure fluctuations	32
SGDK		Filtered rms distortion level	46
SGP		Unfiltered rms distortion level	46
SG/PT2		Ratio of unfiltered rms total pressure fluctuations to average total pressure recovery at engine face	45
SMAVG	PSAVG	Face average static pressure recovery	37
SPTRC		Total pressure recovery through supersonic inlet shock system	30
SUMMER		Subroutine - evaluates error function in vortex core size iterative computations	14
SYMBLE		Subroutine - supplies symbols for distortion contour map generation	15
T	TOP	Time-on-point or data point dwell time - duration of rms pressure fluctuation data measurement, seconds	27
TDP1		Simple distortion parameter: $(PTMAX-PTMIN)/PTMAX$	95
TDP2		Simple distortion parameter: $(PTMAX-PTMIN)/PTAVG$	95
TDP3		Simple distortion parameter: $(PTAVG-PTMIN)/PTAVG$	95
TE	E	Turbulent kinetic energy dissipation rate - ft^2/sec^3	45

<u>SYMBOL</u>	<u>OTHER NAMES</u>	<u>DESCRIPTION</u>	<u>PAGE</u>
THE	THETA	Angular location of the center of the arc DTH, in degrees	40
THMN		Angular location of the rake with minimum rake-average total pressure recovery, degrees	39
THMX		Angular location of the rake with maximum rake-average total pressure recovery, degrees	39
TITLE1		Identification block, also serves to execute end of file	28
TITLE2		Identification title block #2	28
TMAVG	PTAVG	Average total pressure recovery	37
TMMAX	PTMAX	Maximum local total pressure recovery	37
TMMIN	PTMIN	Minimum local total pressure recovery	37
TRIDIA		Subroutine - solves tridiagonal matrix equations	15
TURBUL		Subroutine - manages turbulence modelling predictions and other computations as a subdriver	16
TV	THETA	Angular location of vortex core in degrees	49
UNSTDY		Subroutine - manages dynamic data and peak distortion prediction as a subdriver	15
UU	TUU	Sum of squares of radial and circumferential velocity gradients	45
U		Dimensionless velocity at each probe location	76
U2		Face average flow velocity, fps	29

<u>SYMBOL</u>	<u>OTHER NAMES</u>	<u>DESCRIPTION</u>	<u>PAGE</u>
VBAR		Average vortex strength, in^2/sec	49
VBM	VBMX	Maximum vortex strength, in^2/sec	50
VBO		Approximated vortex strength	50
VL		Vortex core length limit	49

(Nomenclature Addendum)

<u>SYMBOL</u>	<u>OTHER NAMES</u>	<u>DESCRIPTION</u>	<u>PAGE</u>
ANRTU		Function subprogram - computes vortex flux rate	7
KD		Input variable - user selected primary distortion factor	26
NPG		Data run identification code, or "part-point"	31

LIST OF FIGURES

	<u>Page</u>
Figure 1. Program Block Diagram - Subprograms	17
Figure 2. Input Data Arrangement (Batch Input)	33
Figure 3. Input Data Arrangement (Data File)	34
Figure 4. Typical Instrumentation Arrangement	35
Figure 5. Estimation of SPTRC Parameter	47
Figure 6. Definition of "Confidence Levels"	47
Figure 7. Sample Problem Input	59
Figure 8. Sample Problem Output	58
Figure 9. Distortion Factor Definitions	81
Figure 10. Vortex Angle Definitions	82

I. INTRODUCTION

Turbulence and other flow nonuniformities in aircraft engine inlets have long been known to cause an unwanted flow distortion phenomena at the compressor face. These imperfections in the ideally smooth inlet airflow is frequently due to the turning and shaping of the flow as it passes through the inlet duct. Generally the magnitude of the distortion is a function of the angle of attack and sideslip (yaw angle) of the aircraft. The time averaged steady-state distortion level is relatively easy to determine experimentally by locating an array of total pressure probes ahead of the compressor face, and evaluating specific distortion parameters based on these steady-state measurements. Steady-state distortion can be of sufficient magnitude to disrupt the proper operation of the engine by stalling the compressor. Efforts to develop high performance engine and inlet configurations has been hampered because of the inherent sensitivity of highly loaded compressors to flow distortion.

It has also been found that random fluctuations in the distortion level, known as dynamic distortion, can have an even greater effect on engine stability as the steady-state distortion. It has been demonstrated that the dynamic distortion can cause the engine to surge even though the steady state distortion is well below the level at which the engine would be expected to stall. It becomes of particular importance to be able to predict the dynamic distortion levels which could occur at any instant in time.

One of the most common experimental methods of determining the maximum instantaneous distortion is to use fast response (dynamic) probes to produce time histories of the total pressure fluctuations at the compressor face. These

instantaneous pressures are then translated, as in the steady state case, into distortion parameters. These data are then screened by the Dynamic Data Editing and Computing System, DYNADEC, to determine the maximum instantaneous distortion during the test run. An estimation of the most probable peak distortion level is then available for the inlet designer.

The DYNADEC approach to dynamic distortion prediction is generally quite accurate, but is extremely expensive in terms of test instrumentation and computing time. For preliminary design purposes, it becomes difficult to justify the cost of a full DYNADEC test run. It is for this reason that methods of statistically predicting peak distortion levels have been developed. Further information on the DYNADEC and various statistical prediction methods can be obtained with the aid of References 4 and 7.

Of the many statistical approaches for predicting peak dynamic distortion, the Melick random vortex model (Ref. 1 - 3) is of particular interest because of its high efficiency in terms of data requirements and numerical analyses. The basis of the Melick approach is formulated around the observation of the randomness of the total pressure fluctuations during a test run. It was hypothesized that the inlet flow could be modelled as having randomly distributed vortices of random strength, size, and orientation convecting with the steady-state flow, which itself is distorted by a large steady-state vortex. By applying fluid mechanics to convecting vortices, a mathematical model of the inlet turbulence can be generated. The vortices are then translated into dynamic distortion parameters using a statistical criterion.

The distortion level, or the extent to which the flow is distorted, is generally defined in terms of distortion factors. These distortion factors are designed to indicate the distortion relative to some reference value, typically the level at which the engine could be expected to surge.

The maximum dynamic distortion prediction in the Melick approach makes use of rms total pressure fluctuation levels to identify the main variables in the convecting vortex flow model (Ref. 5). Filtered and unfiltered rms levels are required so that any unwanted effects, such as engine speed, can be removed. The rms levels are somewhat easier to process than the instantaneous distortion computations done by DYNADEC, but the instrumentation requirements are much the same. It is seen that instrumentation costs can be reduced by using fewer dynamic probes. The Melick method allows a reduction in probes since it actually uses the face-averaged fluctuation level in the analysis. In principle, the use of very few dynamic probes is feasible, as long as they produce the same face-average rms fluctuation level as the fully instrumented case.

There is some difficulty in choosing the locations for the placement of a limited number of dynamic probes, because it requires some knowledge of the solution before the test begins. Reference 5, however, provides a simplified scheme for locating as few as two dynamic probes at the engine face while retaining sufficient accuracy in the dynamic distortion prediction. It is apparent that even further cost reductions could be achieved if the requirement for dynamic probes and the associated instrumentation could be eliminated entirely. Until recently, however, no methods have been available for reasonably accurate peak dynamic distortion prediction without dynamic data.

Research at the University of Kansas has produced a new technique for estimating maximum instantaneous distortion based only on the steady-state total pressure measurements. Chen (Reference 6) has developed an approach to inlet turbulence modelling which analytically simulates the rms total pressure fluctuation levels using the predicted turbulent kinetic energy distribution at the compressor face. These simulated rms levels replace the rms level data which had to

be measured previously. The simulated rms fluctuation levels are then used to compute the variables of the random vortex model, from which the peak dynamic distortion parameters are derived, just as if the rms levels had been input as data.

The purpose of this work is to present a computer program which statistically computes the most probable peak dynamic distortion level, based on the methods of Chen and Melick. The program is designed to be highly adaptable in that the user may decide on the extent of the dynamic data to be input. There are three main alternatives available to the user. First the user may select a full set of dynamic data, a partial set can be considered (to a minimum of two dynamic probes), or the user can opt to input no dynamic data. In the last case, the program automatically executes the computations related to the turbulence modelling and dynamic data simulation. This flexibility is designed to not only allow the user to select and control the quantity of dynamic data to be processed, but to also allow comparison of different dynamic probe configurations in a single data run.

In summary, the subject computer program solves for an estimation of the maximum instantaneous distortion, given the steady-state distortion data and rms total pressure fluctuation levels. The mathematical and theoretical derivations are well documented in the Melick references (Ref. 1 - 3) and the improvements by Chen are detailed in References 5 and 6. Additional information on inlet flow distortion in general can be found with the aid of Reference 4.

This Users Manual is designed to assist the user toward an understanding of the operational capabilities of the program. The three major sections of the Manual include a breakdown of the program elements, an input and output data section, and a set of sample problems. A listing of the program is included at the end of the Manual. Suggestions for possible future studies in improving the program or the analytical techniques are also included.

COMPUTER PROGRAM DOCUMENTATION
AND USERS MANUAL

II. PROGRAM DESCRIPTION

The subject computer program, the MAXIDYN peak dynamic distortion estimator, is written in FORTRAN IV and can be run as is or with minor modification on most FORTRAN compilers. MAXIDYN requires memory capacity for about 70,000 words in 2300 program lines, including comments. Deletion of the comment lines would reduce the memory space needed to about 45,000 characters and 1600 lines. Appendix A of this work includes a listing of the program and subprograms.

This program is designed to be flexible in nature, and can be used to run with a variety of inlet pressure probe configurations. Individual test cases can be analyzed separately, or groups of data sets can be run in sequence. A set of typical distortion factors are included in the program, though these can be modified by the User. Figure 7 gives the definitions of the distortion factors used in this program.

The program may be used with or without dynamic rms total pressure fluctuation data, with a minimum of two probes in the case that dynamic data is included.

A block diagram of calling sequences of subprograms is given in figure 1. A description of each of the subprograms is given in this section. The subprogram descriptions are alphabetized, for convenience. An operational sequence of events is included to illustrate key events during a data run.

Peripheral requirements are limited to a line printer. The program is suitable for use online while data is being collected, provided format requirements (sect. III) are met.

II.A. SUBPROGRAM DESCRIPTION

1. MAXIDYN main driver

The main driver of the MAXIDYN program controls some of the data input, including the inlet probe configuration, and the steady-state pressure array. In addition, the main driver controls the subprograms which handle the remaining input data, distortion computations, and the output. Specifically, the main driver controls directly the following:

- a. Reading in of pressure probe ring and rake geometry.
- b. Reading in of data titles and identifying comments after checking for an End Of File command which stops program execution.
- c. Reading in of steady-state pressure data.
- d. Controlling the subroutines which control other data input, check for errors, assign default values, and control distortion computations and output.

2. Function ARNTU

This function subprogram computes the vortex flux rate and it's effect on the root mean square distortion level. ARNTU is controlled by subroutine MAXDP.

3. Subroutine CUBIC

This subroutine controls the cubic spline interpolations for subroutines TURBUL and INIVEL. These slope-based cubic spline interpolations are used to compute velocity gradients and turbulent kinetic energies at the fine grid points during turbulence modelling computations.

4. Subroutine DISPAR

This subroutine is used to calculate the eight distortion factors used by the program. These distortion factors are defined in figure 7 and can be modified by the user. DISPAR is controlled by subroutine DISTRT, a subdriver which controls most of the distortion computations. The actual formulas for the distortion factors are contained in DISPAR.

5. Subroutine DISTRT

Subroutine DISTRT is a subdriver which controls the computation of the distortion factors. Some of the duties of DISTRT includes the following:

- a. Calculation of simple distortion parameters; for instance, the locations of the rake or ring with maximum and minimum average pressure.
- b. Calculation of average static pressure at the engine face, and the average Mach number.
- c. Control subroutines INTERP and DISPAR which continue the distortion factor computations.

6. Subroutine EXTRME

This subroutine manages the computation of extreme values of the distortion factors. Called by subroutine MAXDP, EXTRME controls the solution of the most probable peak distortion level for each of the distortion factors. The peak distortion factor is calculated by adding an incremental distortion level to the steady state distortion. The incremental distortion level is computed via the SEARCH subroutine. EXTRME returns the peak distortion level to MAXDP after summing the steady state and incremental distortion values.

7. Subroutine FINITE

FINITE is a subroutine which is used to solve the finite difference equations for subroutine TURBUL. These equations are the turbulence modelling set formed by an implicit tridiagonal matrix scheme. The elements of the tridiagonal matrix equations, which consist of the turbulent kinetic energies and the turbulent kinetic energy dissipation rates, are formed by FINITE and solved by subroutine TRIDIA. FINITE also computes the relative errors in the turbulent kinetic energy and the turbulent kinetic energy dissipation rate for each of the fine grid points at the compressor face.

8. Subroutine FRF

This subroutine evaluates the mean vortex core size by an iterative inverse solution scheme. FRF evaluates the vortex core size as a function of the filtered-to-unfiltered root mean square total pressure fluctuation level. Subroutine SUMMER evaluates the error function of the vortex core size, and the solution is iterated until the error is small.

9. Subroutine INITL

This subroutine solves for the initial values of the turbulent kinetic energy and the turbulent kinetic energy dissipation rate. These initial values are used as a starting point in the iteration of the solution of these parameters. INITL is controlled by the TURBUL subdriver, which uses the turbulent kinetic energies to solve for the turbulent model in the synthesis of the rms pressure fluctuation levels.

10. Subroutine INIVEL

This subroutine calculates the circumferential and radial velocity gradients at each of the grid points at the compressor face. INIVEL is called by TURBUL and uses subroutine CUBIC to carry out spline interpolations of the velocity gradients.

11. Subroutine INTERP

This is an interpolation subroutine which calculates the total pressure recovery at each of the discrete points in the measurement plane. These points are used to generate the pressure contour map. INTERP uses linear interpolation to find the pressure at points between the pressure probe locations. Two linear interpolations are carried out: a radial one and a circumferential one. The final value is taken to be the average of these interpolations. INTERP is called by both MAINLP and DISTAT; when called by MAINLP, the interpolated values are used to generate the contour map, while DISTAT uses the interpolations to compute the distortion factors. A call to subroutine PRNT has been nulled - it had provided a message when interpolations could not be performed.

12. Subroutine LNPOUT

This subroutine controls some of the output from the program. When called by UNSTDY, LNPOUT prints two of the tables in the output: the Overall Flow Descriptors and the Flow Distortion Factors. The Overall Flow Descriptors table gives values for some of the simple distortion parameters, and the Flow Distortion Factors table gives values for the eight user-defined distortion factors. LNPOUT prints these tables for both the steady-state and peak instantaneous case. In addition, LNPOUT prints the distortion contour maps for the steady-state and peak instantaneous case. UNSTDY controls LNPOUT by passing a control parameter; LNPOUT then selects the output to be printed.

13. Subroutine MAINLP

Subroutine MAINLP controls the calculations involved in the development of the pressure distortion contour map. MAINLP calls on INTERP to calculate the pressure at any of the discrete points at the compressor face, given the pressure at the probe locations. Subroutine SYMBLE then assigns a symbol for each of the discrete points, based on the pressure found by INTERP. MAINLP then passes the pressure and symbol information to the main driver, and ultimately to LNPOUT for printing of the distortion map.

14. Subroutine MAXDP

This subroutine is a subdriver which controls the computation of the peak distortion levels for the eight distortion factors. MAXDP computes the mean vortex size and the mean rms pressure fluctuation level, from which the peak

instantaneous distortion is derived. MAXDP also controls the calculations involved in producing the effects of other parameters on the peak distortion, like the vortex flux rate and engine filters, via subroutine RATK. Subroutine RSIGMA is called to compute the filtered and unfiltered rms level of the distortion factors. Subroutine EXTRME then computes the peak instantaneous distortion statistically at 50%, 95%, and 99.7% confidence levels. MAXDP then prints the results in tables, namely the Distortion Factor Extreme Value table and others. The user-selected most probable peak instantaneous distortion factor is also printed. It is this distortion factor that the peak distortion map is based in the iterative matching process.

15. Subroutine NEWPSD

This subroutine is a major subdriver which controls some of the input data and manages most of the computations involved in the prediction of the peak instantaneous distortion. NEWPSD controls the input of the dynamic data, including the filter frequencies, the datapoint dwell time (time on point), identification and program control parameters, and the rms pressure fluctuation data at each of the dynamic probe locations. NEWPSD also passes program execution to the turbulence modelling subroutine, TURBUL, if the user has selected the option of not entering dynamic data. Once the dynamic data has been entered or synthesized, NEWPSD controls subroutines MAXDP and FRF which manage the computations in the peak instantaneous distortion prediction. NEWPSD also prints the dynamic data and the identification and control parameters. NEWPSD is controlled by the main driver and subroutine UNSTDY

16. Subroutine PFIX

This subroutine has two primary functions. The first part of the routine transforms the steady-state or dynamic distortion data from pressure recoveries to percent differences from the average values. These percents are then used by the mapping routines for the plotting of the pressure distortion contour maps. PFIX also calculates the dynamic pressure and Mach number at each of the pressure probe locations as a secondary function. The face-average Mach number is also computed by PFIX. PFIX is called by the main driver in the steady-state case, and UNSTDY in the peak dynamic estimation case.

17. Subroutines PFX and PFXL

These twin subroutines are used in the computation of the eddy (vortex) flux rate as a function of the distortion level. The difference between the two subroutines is in the computation of the vortex flux rate which depends on the magnitude of the ratio of steady-state to root mean square distortion: when this ratio is greater than 2.0, PFX is called, while PFXL is called when the ratio is less than 2. The computational procedure for these two cases is somewhat different and an error would probably occur during computations which involve logarithms and exponentials if the cases were not separated.

18. Subroutine PRNT

This subroutine controls the printing of steady-state and peak instantaneous pressure arrays, the printing of some of the titles and the listing of messages in the output.

19. Subroutine RATK

RATK is a subroutine which evaluates the effect of the engine filter frequency, F_0 , on the root mean square distortion level. The variation of rms distortion with engine filter frequency is analytically determined.

20. Subroutine RSIGMA

This subroutine is called by MAXDP and computes the root mean square distortion level for the eight distortion factors. The routine is divided into separate groups for individual distortion factor evaluations.

21. Subroutine SEARCH

Subroutine SEARCH controls the computation of a peak distortion parameter which is used by EXTRME to form an estimation of the peak instantaneous distortion level. The ratio of the difference between the peak and steady-state to the rms distortion is solved for in an iterative search for the peak distortion level.

22. Subroutine SUMMER

This subroutine evaluates the error function in the iterative calculation of the mean vortex core size. SUMMER is called by FRF.

23. Subroutine SYMBLE

This subroutine supplies the mapping symbols for the generation of the compressor face pressure distortion contour map. Called by MAINLP, SYMBLE assigns a symbol for each discrete point at the engine face, depending on the pressure indicated at that point by the interpolation routine, INTERP. The spelling of SYMBLE was selected to avoid possible conflicts with library functions in some compilers.

24. Subroutine TRIDIA

Subroutine TRIDIA solves the tridiagonal matrix equations in the turbulence modelling computations. TRIDIA is controlled by subroutine FINITE, which sets up the finite difference equations to be solved by TRIDIA.

25. Subroutine UNSTDY

This subroutine is the primary subdriver responsible for the predictive evaluation of the peak instantaneous distortion. Called by the main driver of MAXIDYN, UNSTDY controls the input and output of dynamic data, manages the computations leading to the peak distortion prediction, and controls the output of results. Some of the more important activities and functions of UNSTDY are listed below:

- a. Call NEWPSD to input identification and data control parameters for the test run.
- b. Compute compressor face averaged dynamic pressure and Mach number, inlet vortex properties, and other parameters leading to the peak distortion prediction.

- c. Call subroutine LNPOUT to print some of the tables of distortion data, and the distortion contour map.
- d. Call subdriver NEWPSD to read in and analyse the dynamic data or select the turbulence modelling routines if there is no dynamic data in the input file.
- e. Control the subroutines which iteratively evaluate the most probable peak distortion level and print the results.

26. Subroutine TURBUL

TURBUL is the subdriver responsible for the turbulence modelling prediction when there is no dynamic data in the input file. TURBUL controls subroutines CUBIC, INITL, INIVEL, FINITE, TRIDIA, and PRNT in the synthesis of simulated dynamic data for processing by the subdriver UNSTOY. TURBUL is called by subroutine NEWPSD when the user specifies the "no dynamic data" option in the input data file. TURBUL assigns a finite-element grid to represent the discrete points on the compressor face for the finite difference analytical scheme. The boundary conditions for the turbulence model are estimated based on the total pressure measurements from the steady-state data, and the initial values of the turbulent kinetic energy and dissipation rate are found via INITL. The inlet face velocities are then found via INIVEL, and the turbulent equations are solved by FINITE. These result in estimates for the rms total pressure fluctuation levels, which are then fed back to NEWPSD for the computation of the most probable peak instantaneous distortion.

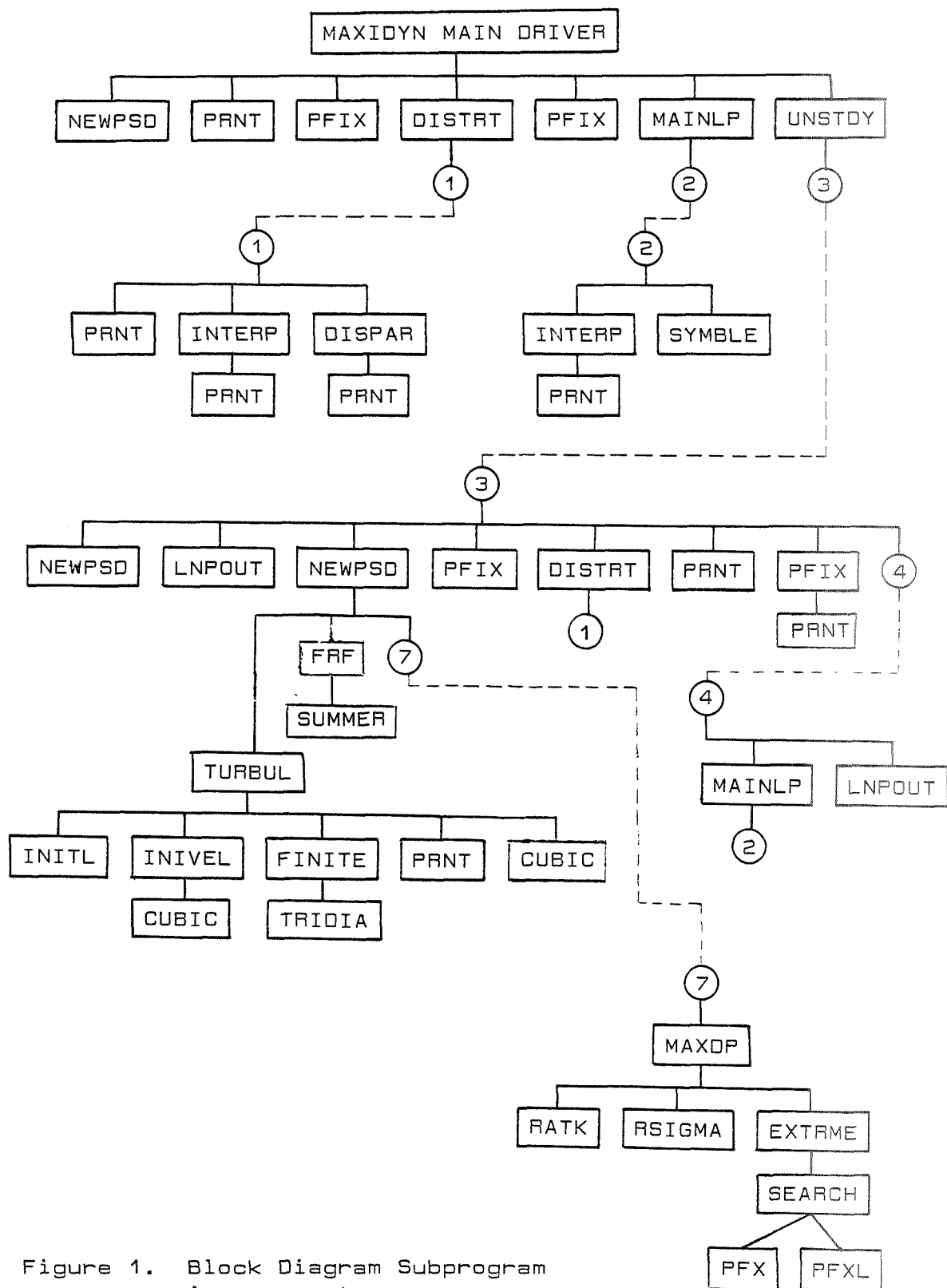


Figure 1. Block Diagram Subprogram Arrangement

II.B. TYPICAL DATA RUN SEQUENCE DESCRIPTION

A typical data run of the MAXIDYN dynamic distortion prediction program can be traced as follows.

The main driver initiates the data input sequence with the reading of control parameters and the inlet pressure probe configuration. After the radial and angular locations of the probe rings and rakes are read in, subroutine NEWPSD is called to read in the engine filter frequency, the rms dynamic data cut-off frequency, the data-point dwell time, or the length of time in which the dynamic data is measured, and the specific distortion factor which the user selects as primary for the peak instantaneous distortion analysis.

The main driver then reads in any data identification titles which the user may elect to input. The resulting set of comments are printed at the top of each page of the output. If an "end of file" or "endjob" instruction is entered at this point, program execution is aborted. After the titles are read in, the main driver reads in the base radial profile and steady-state pressure array. The steady-state pressure recoveries are stored into the instantaneous array as a starting point for the peak instantaneous computations.

Subroutine PRNT is then called to print the table of steady-state pressures and the base radial profile. These items are included on the first page of the output. Subroutine PFIX is called next to compute the face-average Mach number. Subroutine DISTRT is then called to control the computation of the steady-state distortion factors.

Subroutine DISTRT is a subdriver which manages distortion factor computations. DISTRT computes the simple distortion parameters before calling subroutines INTERP and DISPAR to calculate the eight primary distortion factors. Subroutine

PRNT is called if there are an insufficient number of probe rings to allow accurate radial interpolation for some distortion factors, in which case a message to that effect is printed in the output. Subroutine INTERP is called to carry out circumferential interpolations at discrete locations on each of the probe rings, in preparation for the computation of the distortion factors by DISPAR. This subroutine contains a set of sample distortion factor which can be modified by the user as desired. The results of these computations are eight primary steady-state distortion factors used to define the distortion level at the compressor face. After computation of the steady-state distortion level is completed, DISTRT returns control to the main driver.

The main driver then calls subroutine PFIX to set up certain parameters required to develop the distortion contour map for the steady-state case. A "dummy ring" of probes is set up to enable interpolations through the centerbody. PFIX then transforms the input pressure measurements into parameters used by the map-generating subdriver routine MAINLP. MAINLP controls subroutines INTERP and SYMBLE which generate the symbols in the distortion map. INTERP interpolates the pressure at the discrete locations on the engine face based on the steady-state input data, while SYMBLE assigns a character based on the interpolated value at each of the discrete points. After all interpolations and symbol assignments have been completed, MAINLP returns program control to the main driver. At this point the steady-state distortion has been completely defined and the dynamic distortion evaluations are commenced with the calling of the main subdriver, UNSTDY.

UNSTDY controls the subroutines and subdrivers which compute the total pressure fluctuation levels which translate into so-called "delta pressures". These are added to the steady-state pressures to produce the dynamic distortion level and the most likely peak dynamic distortion. After all of the dynamic calculations are completed, UNSTDY returns to

the main driver to start another data run. Before this takes place, however, the main subdriver, UNSTDY, manages all of the dynamic data input and calculations, or the dynamic data simulation if the user selects this option.

After setting initial values for some of the vortex properties, UNSTDY calls on NEWPSD to read in inlet operating parameters and some program control parameters. Most of the inlet parameters are non-functional, that is they are not involved in distortion computations, but rather are of interest for identification and comparison purposes. One control parameter, NTUR, allows the user to select the no-dynamic-data option, or to input the required dynamic data conventionally. After checking the control parameters for errors, assigning default values if necessary, NEWPSD returns to UNSTDY, which evaluates the flow velocity and Mach number, and the vortex properties. LNPOUT is called to print the simple distortion parameters and flow descriptors, and the distortion factors for the steady-state case. After printing the steady-state vortex properties, UNSTDY again calls LNPOUT to print the steady-state distortion contour map. Subroutine NEWPSD is then called to begin the evaluation of the most probable peak instantaneous distortion.

After printing out the identification and control parameters, NEWPSD branches according to the dynamic data option selected by the user. If the no-dynamic-data option has been selected, NEWPSD calls the turbulence modelling subdriver, TURBUL, to compute the rms fluctuation levels which would otherwise be input as data. After setting up a fine grid at the compressor face for finite element modelling of the flow distortion, TURBUL controls subroutines CUBIC, PRNT, INIVEL, FINITE and TRIDIA in the development and solution of the turbulence equations. Subroutine INITL sets initial values for the turbulent kinetic energy, INIVEL computes the velocity gradients, and subroutine FINITE uses finite difference formulations to solve the turbulence model. CUBIC performs cubic spline interpolations and TRIDIA solves tridia-

gonal matrices generated by the finite difference equations. TURBUL then calculates the rms total pressure fluctuation levels at each of the probe locations, and the results are printed. Control is then returned to subdriver NEWPSD, and program execution continues as if the dynamic data had been input, rather than computed.

If the user selects the option for the reading in of dynamic probe data, then these data are input at this point in program execution. In either case, NEWPSD then calls subroutine FRF to evaluate the vortex core size as a function of the filtered-to-unfiltered rms pressure fluctuation level ratio using an iterative scheme. FRF calls subroutine SUMMER to evaluate the error function of the inverse solution. After the vortex core size is found, the results are printed by NEWPSD. When all of the dynamic probe data have been read in, subroutine MAXDP is called to compute the most probable maximum instantaneous distortion levels.

MAXDP is the subdriver which controls the computation of the most probable maximum peak in the distortion level. After determining the mean values for the vortex core size and filtered-to-unfiltered rms pressure fluctuation ratio, and the effects of engine filters and vortex flux rates via subroutines RSIGMA and RATAK, the rms and mean instantaneous levels are computed by adding a "delta" distortion value to the steady-state value. Subroutine EXTRME is then called to evaluate the most probable (50% confidence level) extreme value of the peak instantaneous distortion. EXTRME utilizes subroutine SEARCH which controls the twin subroutines PFXL and PFX in the determination of the "delta" distortion used to find the maximum instantaneous distortion. EXTRME is also used to determine the distortion factor extreme values for the 95% and 99.7% confidence levels, using the same plan as for the 50% confidence level. After printing the results of these computations, program control is returned to NEWPSD, and then back to UNSTDY.

After re-evaluating the vortex properties for the maximum instantaneous case, UNSTDY finds the pressure recoveries at each of the probe locations based on the predicted maximum instantaneous distortion and the steady-state data. Subroutine PRNT is called to print some output, then PFIX is called to compute flow velocities and Mach number at each of the probe locations. The face-average Mach number for the peak instantaneous case is also determined by PFIX. In the same manner as with the steady-state case, subroutine DISTRT manages the computation of the distortion factors given the total pressure recoveries found by UNSTDY for the maximum instantaneous distortion case. Subroutine MAINLP controls the printing of the pressure distortion contour map for the peak instantaneous case as for the steady-state case, and LNPOUT is again called to assist with the printing of output of the peak instantaneous data. After all the output for the test run has been printed, UNSTDY returns to the main driver. The main driver checks for additional sets of data or new test cases. If there data, then program execution begins with the reading in of data titles and the steady-state pressure data for the new case. If an END OF FILE or ENDJOB command is encountered, meaning there is not an additional test case.

In summary, the MAXIDYN dynamic distortion program computes the most probable maximum peak instantaneous distortion given the steady-state distortion data and limited dynamic data. After reading in the steady-state pressure recoveries and computing the steady-state distortion factors, the steady-state distortion contour map is printed along with the distortion data. The average rms pressure fluctuation level is then used to determine the most probable peak instantaneous distortion. The rms fluctuation data may be read in, or simulated by the turbulence modelling routines. After the prediction for the most probable peak distortion level has been made, a new distortion contour map

is generated to represent this case.

The results of the calculations in the MAXIDYN distortion program are printed on several pages of output. This material includes a listing of all input data, the steady-state distortion factors and parameters, the properties of the convecting vortex used to describe the flow in the inlet, the dynamic rms pressure fluctuation data and/or turbulence modelling data, and the pressure distortion contour maps for the steady-state and maximum instantaneous cases. Details on the input and output data are provided in their respective sections.

III. INPUT DATA DESCRIPTION

The input data are divided into three primary groups. The first group defines the inlet pressure probe arrangement at the measurement plane, and some data control parameters. The second group includes identification titles and the steady-state inlet distortion data. The last group is the "dynamic data" - the rms total pressure fluctuation levels - for each of the probe locations. These data may be limited to as few as two probes, or omitted entirely as an option to utilize the turbulence modelling dynamic data simulation capabilities of the program.

The general arrangement and formatting rules for the input data are given in Figures 2 and 3. Further illustration on the arrangement can be found in the sample problems in Section V. The following is a description of the input data items, presented in the order in which they are read by the software. Items marked with an asterisk (*) can be omitted from the input file without disrupting program execution. In this case default values are usually assigned, or simulated in the case of the dynamic data when turbulence modelling has been selected by the user

The first group of input data include specifications for the inlet probe configuration, data filter frequencies, data point dwell time, and a parameter with which the user may select the specific distortion factor used in the generation of the distortion contour maps. NR and NP are the total number of probe rings and rakes, respectively, and RADLOC and ANGLLOC are the radial and angular locations of the probes. KD is the distortion factor key used to select one of the eight distortion factors available in the program.

The time on point, or data point dwell time, T , represents the duration of time in which the rms pressure fluctuations are measured and calculated. FO and FCO are the engine filter and rms dynamic data cutoff frequencies respectively. Further information can be found for each of these variables in the detailed descriptions below:

NR is an integer corresponding to the number of pressure probe rings used in the test run. NR should include static pressure rings located at the centerbody hub and at the outer radius, even if these are not included in the instrumentation, so that the distortion contour map resembles the engine face geometry. If, for example, there are five total pressure probes located along the inlet rakes, NR should be entered as seven to account for the static pressure probes.

NP is an integer corresponding to the number of pressure probe rakes used in the test run. These rakes are generally positioned between the hub and the inside surface of the nacelle, and are evenly spaced along radii around the centerbody hub. NR represents the number of probes along the rakes.

RADLOC is a one-by-NR array of real numbers corresponding to the radial locations of the pressure probes placed along the probe rakes. RADLOC includes the radial location of the centerbody hub, as well as the outer radius of the inlet at the nacelle inner surface. RADLOC may be dimensional, or a dimensionless fraction of the outer inlet radius. Units may be arbitrary in the dimensional case. It is noted, however, that the vortex dimensions will be in terms of the dimensions of RADLOC. See figure 4.

ANGLOC is a one-by-NP array of real numbers which correspond to the angular locations of the probe rakes. The units of ANGLOC are degrees, with the top rake being 'zero' and with the angle increasing clockwise, as viewed from the front. See Figure 4.

KD is an integer with which the user selects the distortion factor of primary interest in the test run. Of eight available distortion factors included in the program, one is selected for use in generating the peak instantaneous distortion contour map which matches and represents the predicted peak distortion level. Definitions of the eight distortion factors provided in the program are given in Figure 9. Below is a key for use in selecting the desired distortion factor. Entering an integer (1 through 8) effects the selection of the distortion factor indicated below:

- 1: KTHETA (Pratt & Whitney circumferential distortion #1)
- 2: KD2 (Pratt & Whitney circumferential distortion #2)
- 3: IDC (General Electric circumferential distortion)
- 4: IDR (General Electric radial distortion factor)
- 5: KRA (Pratt & Whitney radial distortion factor)
- 6: KA2 (Pratt & Whitney combined distortion factor)
- 7: DSPR (Delta [loss in] stall pressure ratio)
- 8: ID (General Electric combined distortion factor)

It is noted that there are two distinct Pratt & Whitney circumferential distortion factors from two distinct definitions (see Figure 9). The combined distortion factors are found by combining the circumferential and radial distortion factors. In the case of KA2, the circumferential distortion factor used in the combination is KTHETA. The distortion factors represented in this program are only examples - the user is free to redefine or modify them at will.

T * This is the dynamic data time on point or "dwell" time during which the total pressure fluctuation level is measured and the root mean square value is determined. The units are seconds, and a default value of one second is assigned if no value is input. T may be omitted if the no-dynamic-data option has been selected for all test cases.

FO * This is the engine filter frequency, in Hertz. FO is used in the computation of the mean peak instantaneous distortion levels. The purpose of the filter is to remove the effect of engine speed on the measured pressure fluctuations. A default value of 500 Hz is assigned if no value is input.

FCO * This is the low pass cutoff filter frequency used when measuring the filtered rms total pressure fluctuation levels. The ratio of filtered-to-unfiltered mean square pressure fluctuations are used to predict the most probable maximum instantaneous distortion. The units of FCO are Hertz, with a default value of 1000 Hz, when no value is input directly.

The second part of the input data includes title blocks, the steady-state total pressure recovery array, and several inlet flow parameters. TITLE1 and TITLE2 provide space for 160 characters of identifying comments. PS is an NR by NP array of steady-state pressure recoveries. The base radial profile BRP is the ratio of ring-average pressures to the face-average pressure. ALPHA and PSI are the angle of attack and sideslip angle respectively, and the freestream Mach number is given by MO. The flow velocity at the engine face is U2. BF, CKP, and RKP are weighting factors used in the computation of combined radial/circumferential distortion factors. The mass flow ratio, MFR, gives an indication of the

**ORIGINAL PAGE IS
OF POOR QUALITY**

the mass flow rate before and after inlet duct bleed-off. NTUR is a control parameter which allows the user to select the option of inputting the dynamic data, or having these data simulated by the turbulence modelling scheme. Finally, SPTRC is the total pressure recovery through the inlet shock system in a supersonic inlet.

More detailed descriptions of the data items in the second group are given below. Most of these data may be deleted from the input data deck, without causing any real difficulties. Many of these are simply included for identification purposes, while others are provided with default values to avoid data errors. Default values are included in the detailed descriptions below:

TITLE1 and TITLE2 are alphanumeric hollerith arrays used for test run identification. Two lines of up to eighty characters each are available for information such as engine/inlet type, Mach number, angle of attack, yaw angle, altitude, and so forth. TITLE1 and TITLE2 are printed at the top of each page of output for easy reference. TITLE1 also is used to check for an END OF FILE or ENDJOB command at the end of the data file, in which case program execution is stopped.

BRP is the compressor face base radial profile. This is defined as the ratio of the average pressure around a ring to the face-average pressure. BRP is a one-by-NR array with a value at each of the radial locations given by RADLOC. BRP has a default value of 1.

PS is an array of steady-state total pressure recoveries. The dimensions of the array are NR rows by NP columns. The rows of PS are pressures at radial locations RADLOC while the columns are at angular locations ANGLOC. The first and last rows of PS are static pressures associated with the static pressure rings located at the

centerbody hub and the surface of the inlet at the engine face. These static pressures can be measured or computed values. The pressure array is eventually used to generate the distortion contour map, and also is the basis for finding the instantaneous pressure array, P .

ALPH is the aircraft/inlet angle of attack relative to the freestream, typically in degrees. ALPH is used for run identification, and does not enter into any computations.

PSI is the aircraft/inlet sideslip or yaw angle relative to the freestream, typically in degrees. Like ALPH, PSI is of interest for identification and analysis, and does not enter into the computations.

MO is the freestream Mach number. Of interest for identification of test runs, MO does not enter into calculations.

U2 is the flow velocity in the inlet at the compressor face, in feet per second.

BF is the b-factor used as a weighting term for the computation of the combined radial and circumferential distortion factor KA2 (Pratt & Whitney). BF is multiplied by the radial contribution, and the result added to the circumferential distortion to get the combined distortion factor. BF has a default value of 1.

CKP is the circumferential weighting factor used in the computation of ID, the General Electric combined radial/circumferential distortion factor. CKP is multiplied by the circumferential distortion, then added to the radial contribution. CKP default value is 16.4.

RKP is the radial weighting factor used in the computation of ID, the General Electric combined radial/circumferential distortion factor. RKP is multiplied by the radial distortion factor, and the result added to the circumferential contribution. The default value for RKP has been set at 11.1 in the program.

MFR is the inlet mass flow reatio, defined in terms of the streamtube geometry. Specifically, MFR is the ratio of actual inlet mass flow rate, to the maximum inlet mass flow rate. The maximum inlet mass flow rate is defined as the product of the freestream velocity times the inlet hilite area. Low MFR implies a large amount of inlet spillage. MFR is generally a function of the engine thrust level and flight velocity.

NTUR is a control parameter which allows the user to select the turbulence modelling dynamic data simulation capabilities of the program as an alternative to using measured dynamic data. Inputting a value of 1.0 for NTUR causes the program to branch to the turbulence modelling routines within the program. A value of zero or defaulting the input of a value causes the program to branch to the routines requiring the input of dynamic data.

SPTRC is the total pressure recovery through the inlet shock system of a supersonic inlet duct. For subsonic and transonic inlets, SPTRC is equal to one. If SPTRC is unknown for an arbitrary supersonic inlet, it can be estimated by using Figure 5, with a value of 0.90 being reasonable as a rough preliminary estimate for most inlet configurations. A default value of 1.0 has been set in the program. It is noted that SPTRC should always be less than or equal to one.

The third part of the input data consists of the dynamic data. These data consist of rms total pressure fluctuation levels from fast-response total pressure probes. The number of dynamic probe data sets in each run is fully under control of the user - within certain limitations. In a normal run, the number of dynamic probes is equal to the number of steady-state total pressure probes. In a reduced dynamic data run, the number of dynamic probes can be anywhere from two to as many as would be used in a normal run. Finally, if the user selects the no dynamic data option by setting NTUR equal to 1.0 (see previous page), these dynamic data may be completely omitted from the input data.

There are four input variables in the dynamic data. NPG is a run identification code, NPR is the probe identification code, RS is the filtered to unfiltered ratio of mean square pressure fluctuation levels, and SIG is the root mean square level of total pressure fluctuations. Further details on these data can be found below.

NPG is a code number for identifying data runs. This user definable integer can be completely arbitrary, though entering a value of zero, or defaulting the input signals the end of the dynamic data set. Therefore NPG can be any integer greater than one. When all of the dynamic data has been input, entering a value of zero for NPG (or leaving it blank) will signal the program to move on to the next phase of computations.

NPR is the numeral designation for the location of the dynamic probe. This identification code can be found with the aid of Figure 4, which is given as an example for the convenience of the user. Other inlet probe and instrumentation configurations may result in a different numeration scheme, so Figure 4 should be used as a guideline.

RS is the ratio of filtered to unfiltered mean square pressure fluctuations. RS is found by squaring the ratio of the rms pressure fluctuation level filtered at the cut-off filter frequency FCO, to the unfiltered level. This ratio is used in the prediction of the maximum instantaneous distortion level, and a default value of 0.50 has been included in the program. In addition, a maximum value of 0.70 has been set to avoid errors in certain computations. These values are easily modified, if necessary, by the user.

SIG is the unfiltered root mean square value of the total pressure fluctuations measured by the dynamic (fast response) total pressure probes. Generally, the units of SIG are identical to those of the PS array, which are nondimensional total pressure recoveries (local total pressure divided by the freestream or inlet lip total pressure).

Sample problems have been included in this manual to illustrate the arrangement of the input data, and to further clarify the utility of the various capabilities of the program. Figures 2 and 3 show formatting rules and the general arrangement scheme of the input data.

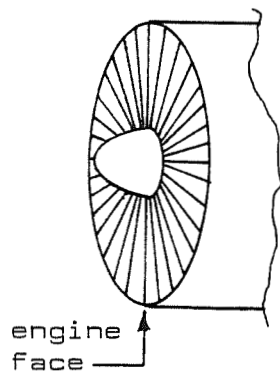
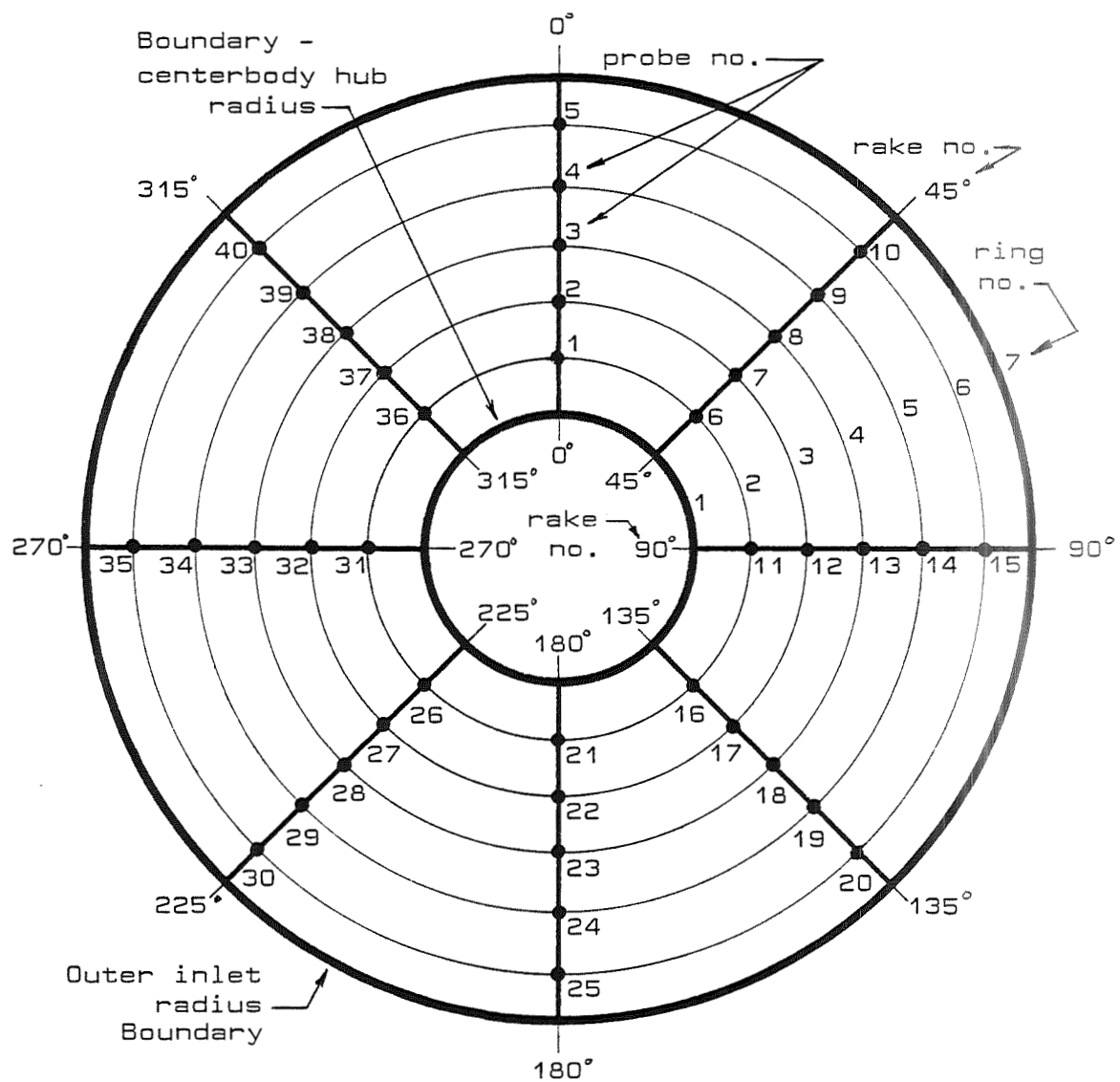
CARD 1										
FIELD	1-5	6-10								
FORMAT	I5	I5								
PARAMETER	NR	NP								
CARD 2										
FIELD	1-10	11-20	21-30	31-40	41-50	51-60	61-70	71-80		
FORMAT	F10.5	F10.5	F10.5	F10.5	F10.5	F10.5	F10.5	F10.5		
PARAMETER	RADLOC(1)	(2)	(3)	(4)	(5)	---	---	RADLOC(NR)		
CARD 3										
FIELD	1-10	11-20	21-30	31-40	41-50	51-60	61-70	71-80		
FORMAT	F10.5	F10.5	F10.5	F10.5	F10.5	F10.5	F10.5	F10.5		
PARAMETER	ANGLOC(1)	(2)	(3)	(4)	(5)	---	---	ANGLOC(NR)		
CARD 4										
FIELD		6-10	11-20	21-30	31-40					
FORMAT		I5	F10.5	F10.5	F10.5					
PARAMETER		KD	T	FO	FCO					
CARD 5,6										
FIELD	1-80									
FORMAT	20A4									
PARAMETER	TITLE1 and TITLE2									
CARD 7.1										
FIELD	1-10	11-20	21-30	31-40	41-50	51-60	61-70	71-80		
FORMAT	F10.5	F10.5	F10.5	F10.5	F10.5	F10.5	F10.5	F10.5		
PARAMETER	BRP(1)	(2)	(3)	(4)	(5)	(6)	(7)	BRP(NR)		
:	:	:	:	:	:	:	:	:		
CARD 7.NR										
FIELD	1-10	11-20	21-30	31-40	41-50	51-60	61-70	71-80		
FORMAT	F10.5	F10.5	F10.5	F10.5	F10.5	F10.5	F10.5	F10.5		
PARAMETER	PS(NR,1)	(NR,2)	(NR,3)	(NR,4)	(NR,5)	---	---	PS(NR,NP)		
CARD 8										
FIELD	6-10	11-15	16-20	21-25	26-30	31-35	36-40	41-45	46-50	51-55
FORMAT	F5.3	F5.3	F5.3	F5.3	F5.3	F5.3	F5.3	F5.3	I5	F5.3
PARAMETER	ALPH	PSI	MO	U2	BF	CKP	RKP	MFR	NTUR	SPTRC
CARD 9										
FIELD		6-10	11-15	16-20	21-26					
FORMAT		I5	I5	F5.3	F6.4					
PARAMETER		NPG	NPR	RS	SIG					
CARD 10										
FIELD										
FORMAT	(BLANK)									
PARAMETER										
CARD 11										
FIELD	1-80									
FORMAT	20A4									
PARAMETER	TITLE1 - for new data point set, or END OF FILE card									

Figure 2. Batch Input Data Deck Formatting Arrangement

ORIGINAL PAGE IS
OF POOR QUALITY

STATEMENT NUMBER		FORTAN STATEMENT		IDENTIFICATION							
NR	NP										
1		RADLOC(1)	RADLOC(2)	RADLOC(3)	RADLOC(4)	RADLOC(5)	RADLOC(6)	RADLOC(7)	RADLOC(8)		
2		ANGLOC(1)	ANGLOC(2)	ANGLOC(3)	ANGLOC(4)	ANGLOC(5)	ANGLOC(6)	ANGLOC(7)	ANGLOC(8)		
3		KD	T	FO	FCO						
4		TITLE1									
5		TITLE2									
6		BRP(1)	BRP(2)	BRP(3)	BRP(4)	BRP(5)	BRP(6)	BRP(7)	BRP(8)		
7		PS(1,1)	PS(1,2)	PS(1,3)	PS(1,4)	PS(1,5)	PS(1,6)	PS(1,7)	PS(1,8)		
8		PS(2,1)	PS(2,2)	PS(2,3)	PS(2,4)	PS(2,5)	PS(2,6)	PS(2,7)	PS(2,8)		
9		PS(NR,1)	PS(NR,2)	PS(NR,3)	PS(NR,4)	PS(NR,5)	PS(NR,6)	PS(NR,7)	PS(NR,8)		
10		ALPH	PSI	MO	U2	BF	GKP	RKP	MFR	NTUR	SPTRG
11		NPG	NPR1	RS	SIG						
12		NPG	NPR2	RS	SIG						
13		NPG	NPRn	RS	SIG						
14		0.	0.	0.	0.						
15		TITLE1 (for next run)									

Figure 3. Input Data File Formatting Arrangement



Note: NR = 7 = number of probe rings
NP = 8 = number of probe rakes

Figure 4. Ring, Rake, and Probe Assignments for a typical instrument configuration

IV. PRINTED OUTPUT DATA DESCRIPTION

The printed output of the MAXIDYN dynamic distortion program consists of from five to seven pages of data (sixty lines on each page) depending on the options selected by the user. The first two pages pertain to the steady-state distortion characteristics, with the steady-state pressure array, vortex properties, distortion factors, and related parameters, along with the steady-state distortion contour map. The next page or two involves the dynamic data, with rms pressure fluctuations levels, turbulence data, and some additional flow parameters. The following page is a listing of a summary of distortion factor extreme values as predicted in the Melick prediction technique. The final two pages are similar to the first two, but pertain to the peak instantaneous distortion level.

The following is a page-by-page description of the output. Since the content of the output depends on the dynamic data input option chosen by the user, some variables described may not apply to a specific case. Data affected by the dynamic data options are so indicated, and all of the affected data are found in the middle pages with the dynamic data groups. Some data are provided with default values as described in the input section, and the default values are repeated here for convenience.

Page 1

The first page of output consists of five tables of steady-state distortion data. Immediately below the title block provided by TITLE1 and TITLE2, the steady-state total pressure recovery array is printed. The rows in this matrix

are identified with the RADLOC radial probe locations, and the columns with the ANGLOC angular rake locations. The static pressure rings associated with the innermost and outermost RADLOCs are not included in the pressure array. The numbers of the pressure array P are otherwise identical to the input array PS.

Beneath the pressure array is a table of base radial profiles. These are defined as the ratio of probe ring average pressures to the average pressure over the entire engine face. For each radial location RADLOC (including static rings) a value of PTR/PTA is given. This BRP array is identical to the input array BRP. A default value of 1.0 is assigned for each term in BRP when no value is input.

The next table is a listing of the overall flow descriptors. These simple distortion parameters are used to evaluate the distortion factors and vortex properties. The terms appearing in this table are defined below:

PTMIN (also PTMN and TMMIN) This is the minimum total pressure recovery value from the pressure array, P , exclusive of the static pressure data.

PTMAX (also PTMX and TMMAX) This is the maximum total pressure recovery value from the pressure array, P , exclusive of the static pressure data.

PTAVG (also PTAV and TMAVG) This is the face-average total pressure recovery from the pressure array, P , exclusive of the static pressure data.

PSAVG (also SMAVG) This is the average value of static pressure from the static pressure data in the pressure array, PS. The two static pressure rings at the centerbody hub and outer radius of the inlet supply these data.

QAVG (also QAV) This is the face-average dynamic pressure recovery, computed as the difference between the average total pressure recovery and the static pressure. Mathematically stated, $QAVG = PTAVG - PSAVG$.

The three remaining terms in the flow descriptors table are algebraic manipulations of PTMAX, PTMIN, and PTAVG. These terms are self explanatory - for example, $(PTMX-PTMN)/PTAV$ is interpreted as the difference between the maximum and minimum total pressure recoveries, divided by the average value.

Following the overall flow descriptors table is a table of flow distortion factors. The eight distortion factors listed in this table are representative of a variety available to the industry, and are intended as examples. The user is free to redefine the distortion factors within the program. Next to the distortion factors in the table are some weighting factors used in calculating combined distortion factors. The eight distortion factors and their weighting factors are described below:

K-THETA (also KTHETA, Kθ, and KTTA) Pratt & Whitney circumferential distortion factor [#1] - see Figure 9.

KD2 Pratt & Whitney circumferential distortion factor [#2] - see Figure 9.

(IDC)-MAX General Electric maximum circumferential distortion factor - see Figure 9.

(IDR)-MAX General Electric maximum radial distortion factor - see Figure 9.

KRA Pratt & Whitney radial distortion factor - see Figure 9.

KA2 Pratt & Whitney combined radial/circumferential distortion factor - see Figure 9.

DSPR Delta (loss in) stall pressure ratio - see Figure 9.

ID General Electric combined radial/circumferential distortion factor - see Figure 9.

B-FACTOR (also BF) Radial weighting factor used in computing KA2 - see Figure 9.

BSF Intermediate weighting factor used in computing ID - see Figure 9.

KC (also CKP) Circumferential weighting factor used in computing ID - see Figure 9.

KR (also RKP) Radial weighting factor used in computing ID - see Figure 9.

Beneath the flow distortion factors table is a list of vortex properties. These properties are described below:

THMN (Theta Min) Angular location of the probe rake with the minimum average total pressure recovery, in degrees. The 'zero' rake is the upper vertical rake. THMN is one of the ANGLOC angular locations, and depends on the steady-state pressure array.

RKMN The average pressure recovery along the rake designated by THMN.

THMX (Theta Max) Angular location of the probe rake with the maximum average total pressure recovery, in degrees. See THMN, above.

RKMX The average total pressure recovery along the rake designated by THMX.

DTH (Delta Theta) The angular difference between THMX and THMN. $DTH = THMX - THMN$.

THETA (also THE) The angular location of the rake midway between the rakes designated by THMX and THMN. $THETA = \frac{1}{2}(THMX + THMN)$.

A1 (also ART, etc.) The vortex core size which fits within the boundaries of the rakes designated by THMN and THMX. A1 represents the size of the steady-state vortex.

G1 (also GAMMA) The orientation angle of the steady-state vortex. This is used to satisfy the amplification of the steady-state distortion level by the vortex field, in determining the peak distortion level.

Page 2

The second page of the printed output is the pressure distortion contour map for the steady-state case. A representation of the high and low pressure regions at the compressor face of the engine, this map is useful in identifying and visualizing the nature of the distortion of the flow through the inlet. Symbols are used for identifying the pressure at any point in the measurement plane, and a key to the mapping symbols is provided. The numbers provided in the key are interpreted to mean the percent difference between the local pressure and the face-average pressure - for example, an indication of -3.0 is interpreted as three percent below the average pressure over the engine face.

The third page of output is related to the dynamic data, which may be included in the input file, or simulated by the turbulence modelling scheme. The content of this page (and sometimes the next page) depends on whether the dynamic data is input or simulated, as described in the cases below:

Case 1: Dynamic Data is Input

Immediately following the title block is a listing of several inlet parameters, along with some parameters used with the dynamic data. These parameters are described below:

I The dynamic data time-on-point, or dwell time during which the dynamic data are measured for each of the dynamic probes. The units are seconds.

FO The engine filter frequency, in Hertz. FO is often associated with the engine rpm speed.

RT The outer radius of the inlet at the compressor face, or the location of the outermost static pressure probes - the maximum value of the RADLOC array.

RI The inner radius of the compressor face, the radius of the centerbody hub, or the minimum value of the RADLOC array.

ALPH (also ALPHA) The inlet angle of attack, relative to the freestream, in degrees.

PSI The sideslip or yaw angle of the inlet in degrees.

SPTRC The total pressure recovery through the inlet shock

SPTRC (cont'd) system in a supersonic inlet configuration. For supersonic inlets SPTRC is less than 1.0, while subsonic and transonic inlets will have SPTRC equal to 1.0.

MO The freestream Mach number.

ETA The face-average total pressure recovery from the steady-state pressure array, PS.

MFR The mass flow ratio of the inlet system. This gives an indication of how much of the inlet air remains after bleed-air has been removed.

U2 The inlet flow velocity at the engine face in feet per second.

QPT2 The dynamic pressure divided by the total pressure. $QPT2 = QAVG/PTAVG$, where QAVG is the face-average dynamic pressure and PTAVG is the face-average total pressure. (see "overall flow descriptors" table description in Page 1 descriptions.)

RS AT FC = The cutoff frequency of the rms dynamic data. (see FCO in input data descriptions)

The next table of data includes the dynamic data as input by the user. For each dynamic probe location selected, values for the rms pressure fluctuations and the resulting vortex core size are given. The specific terms in this table are described below:

PROBE The numerical designation for the location of a dynamic probe. See Figure 4

RS The ratio of the filtered to unfiltered mean square total pressure fluctuation level.

SG/PT2 (also SIG) The unfiltered rms total pressure fluctuation level.

A/RT (also ART) The mean vortex core size, based on the magnitude of SIG. The vortex core size is nondimensionalized to the inlet radius, RT.

Immediately below the dynamic data table, the average value for the rms unfiltered total pressure fluctuation level, SIG, is printed along with the average vortex size. These terms are actually used in the Melick peak distortion prediction technique (Reference 5).

In some cases, specifically when the number of dynamic probes in the dynamic data is relatively few, the distortion factor extreme value table is printed on page three immediately below the dynamic distortion table. The reader should refer to Page 4 output descriptions for identification of the terms in this table.

The following is a description of the terms on page 3 of the output when the no dynamic data option is selected in the input file, that is, when the dynamic data is simulated by the turbulence modelling techniques:

Case 2: Dynamic Data is Simulated

The data appearing on the third page of output includes all of the data appearing in Case 1, excluding the dynamic data listing. The reader should refer to the descriptions in Case 1, except for the dynamic data - PROBE, RS, SIG, and ART. These terms are replaced by three tables of turbulence calculations, and the simulated values of SIG for each of the available dynamic probe locations.

The following is a descriptive listing of the data on the third page of output when the dynamic data are simulated by the turbulence modelling technique. The parameters listed in Case 1 are included in these data, and the reader should refer to the description listing there for details.

The first table following the inlet and control parameter listing gives dimensionless velocities of the flow at the compressor face for each of the pressure probe locations. These velocities are calculated based on the steady-state pressure data from the input file. The rows of the velocity array are associated with the ANGLOC angular locations of the rakes, while the columns are associated with the RADLOC radial probe locations along the rakes. The first and last columns reflect the static pressure probes located at the centerbody hub and outer inlet radius.

Following the table of dimensionless velocities for each of the probe locations is a listing showing the iteration of the turbulent kinetic energy, and the kinetic energy dissipation rate. The relative error in these terms is minimised during the iterations. The first column shows the error in the turbulent kinetic energy; the second, the error in the turbulent kinetic energy dissipation rate, and the third gives the sum of these two. These errors should decrease rapidly within the thirty iterations allowed. Once the errors have been minimized, the turbulent kinetic energy and dissipation rates are used to generate the synthesized dynamic data.

The next table is a listing of the results of the turbulence calculations, including the synthesized dynamic data and the turbulence modelling parameters. This table is similar to the dynamic data table in the Case 1 descriptions, but includes some additional terms. This table is large, and may actually be slipped to the fourth page. The terms appearing in this table are defined on the following page.

PROBE The numerical designation of a dynamic probe, used to define the location of the probe. See Figure 4.

UU The sum of the squares of the radial and circumferential velocity gradients in $(\text{ft}/\text{sec})^2$.

E The turbulent kinetic energy dissipation rate in units of ft^2/sec^3 .

K The turbulent kinetic energy in $(\text{ft}/\text{sec})^2$.

SG/PT2 (or SIG) The synthesized unfiltered rms pressure fluctuation level.

Printed below the synthesized dynamic data table are values for the face-average SIG, and the mean vortex size, ART. These values are used to predict the most probable peak instantaneous dynamic distortion level.

Page 4

The fourth page of output is a table of distortion factors and parameters leading to the most probable peak instantaneous distortion for each of the eight sample distortion factors. The terms and distortion factors appearing in this table are described below:

KTТА (or KTHETA) The Pratt & Whitney circumferential distortion factor, definition #1 (see Fig. 9).

KD2 The Pratt & Whitney circumferential distortion factor, definition #2 (see Fig. 9).

IDC The General Electric circumferential distortion fac-

tor (see Fig. 9).

IDR The General Electric radial distortion factor (see Fig. 9).

KRA The Pratt & Whitney radial distortion factor (see Fig. 9).

KA2 The Pratt & Whitney combined radial/circumferential distortion factor (see Fig. 9).

DSPR The loss in stall pressure ratio (see Fig. 9).

ID The General Electric combined radial/circumferential distortion factor (see Fig. 9)

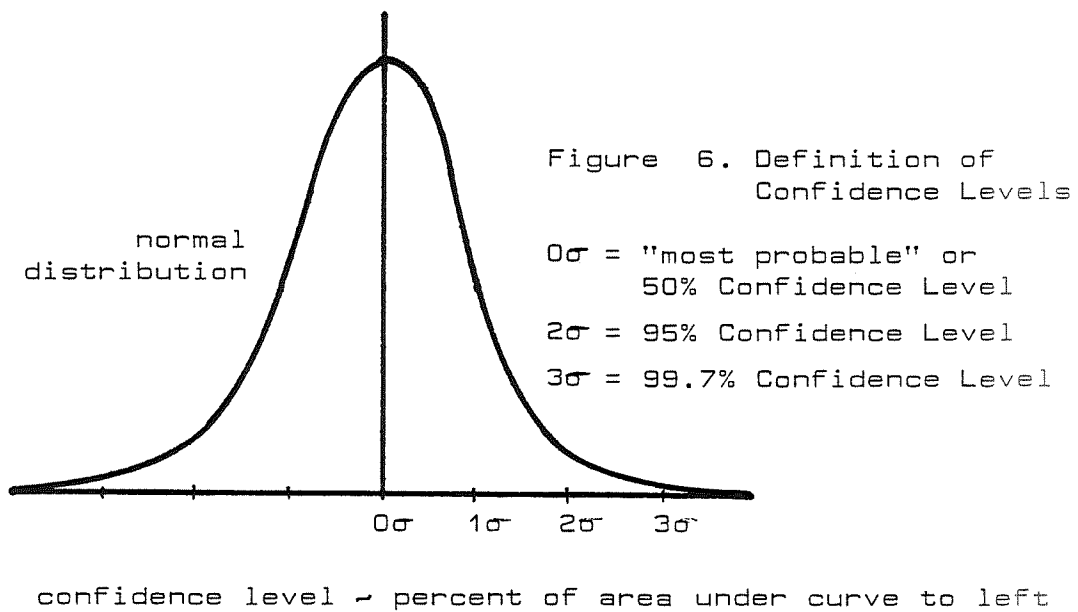
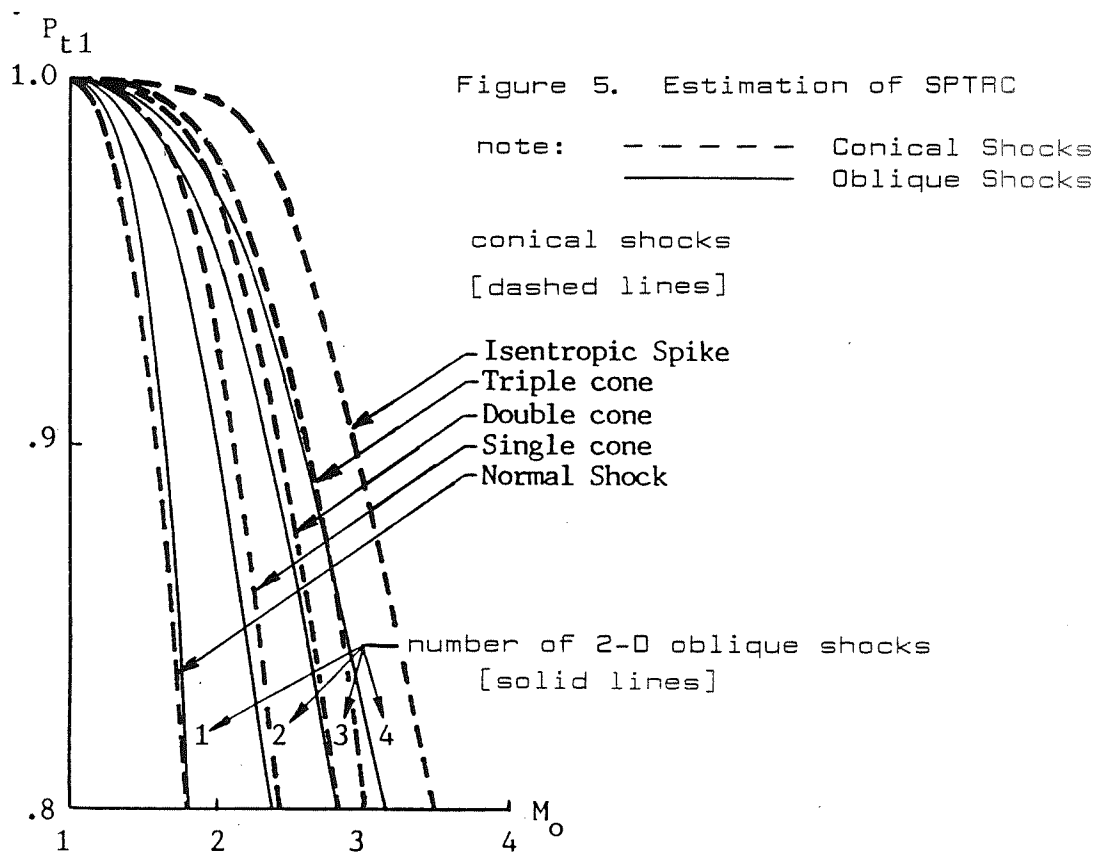
STEADY STATE This column indicates the steady-state values for the distortion factors, as computed from the input distortion data.

MEAN VALUE The mean instantaneous distortion level, computed by adding the mean instantaneous rms fluctuation level to the steady-state distortion.

SIGMA INF The unfiltered rms distortion fluctuation level.

SIGMA FO The rms distortion fluctuation level, filtered at the engine filter frequency, FO.

MOST PROB The most probable peak instantaneous distortion level at a 50% confidence level. Statistically, this is the most likely value for the peak distortion level in the statistical prediction analysis. Moving away from this value decreases the probability.



95% PROB The peak instantaneous distortion level at a 95% confidence level. This is interpreted as meaning there is a 95% chance the actual peak instantaneous distortion level will be less than the indicated level. The likelihood that the actual peak will reach this level is small.

99.7% PROB The peak instantaneous distortion level at a 99.7% confidence level - there is a 99.7% chance that the actual peak will be less than this level. It is very unlikely that the actual peak distortion level will ever be this high.

The most probable peak instantaneous distortion level for the distortion factor selected by the user is printed immediately below the distortion factor extreme value table. This distortion factor is used to develop the peak instantaneous pressure array and contour map.

Page 5

The fifth page of output is much the same as the first page, except the data applies to the peak instantaneous distortion rather than the steady-state. The terms in the tables are defined in the descriptions of Page 1, though any references to the steady-state case are understood to be replaced by the peak instantaneous case.

A major difference between the fifth page and the first page is that the vortex properties table has been replaced by a vortex location table, with some new terms. These are defined on the following page. Many of the terms are similar to some of the steady-state vortex properties, though they apply to the peak instantaneous vortex.

VBAR The average vortex strength in terms of the vortex tangential velocity vector nondimensionalized by dividing by the flow velocity at the engine face. This property is used to define the source of the pressure fluctuations.

A/RT (also ART) The vortex core size in terms of the vortex radius divided by the inlet radius. See AY/RT.

GAMMA A vortex orientation angle in degrees, due to the rotation of the vortex core about the x axis. See Figure 10.

BETA A vortex orientation angle in degrees, due to the rotation of the vortex core about the z axis. See Figure 10.

AY/RT (also AYRT) The vortex core size in terms of the vortex radius (the radius at the maximum tangential velocity of the vortex system) divided by the inlet radius. AY/RT is also the same as A/RT.

VL The nondimensional vortex length limit. VL has been set at 999.999 (infinity for all intents and purposes) in the current program, though this is easily altered. VL should represent the true vortex length limit divided by the inlet radius.

R/RT (also RRT) The radial location of the vortex central core. R/RT is a dimensionless value with a maximum value of unity.

THETA The angular location of the vortex center in degrees. Zero degrees is the top vertical position, with positive THETA being clockwise about the engine face.

VBMAX The maximum vortex strength in terms of the tangential velocity of the vortex divided by the flow velocity at the engine face. VBMAX also appears as VBM in the FORTRAN coding.

VBO The vortex strength as approximated from the total pressure rms fluctuation dynamic data

AO/RT The vortex core size computed from the average of the dynamic data power spectral density (PSD) functions.

Page 6

The sixth and last page of the printed output consists of the pressure distortion contour map for the peak instantaneous case. The terms and parameters appearing with this map are identical to those in the steady-state map. These parameters are described in the Page 2 description in this section.

SUMMARY OF DEFAULT VALUES

The following is a summary list of default values for the input/output variables which have such values:

T	=	1.000	BRP	=	1.000
FO	=	500 Hz	MFR	=	1.000
FCO	=	1000 Hz	SPTRC	=	1.000
BF	=	1.000	VL	=	999.999
RS	=	0.500	max RS	=	0.700
CKP (or KC)	=	16.4	RKP (or KR)	=	11.1

V . SAMPLE PROBLEM

V . SAMPLE PROBLEM

A. Introduction

Four sample data sets are provided to illustrate the input/output capabilities of the MAXIDYN distortion program. These problems are taken from provisional data, and represent a variety of inlet operating conditions. The first and second cases are supersonic inlets with a full set of 40 dynamic probes, and a partial set of 14, respectively. The third case is a subsonic inlet with the minimum number of high-response dynamic probes - 2. The final case is a transonic inlet with no dynamic data input. This case makes use of the turbulence modelling capabilities of the program, which simulates the dynamic data.

Some of the primary data parameters are shown in the table of part B, below. Figure 7 gives a complete listing of the input data files for the sample problems. Figure 8 in part C shows the output from the four sample problems. Definitions of each of the terms in the input and output listings may be found in the input and output data descriptions of section II, parts B and C, respectively.

B. Sample Problem Input

The four test cases provided here have similar probe ring/rake configurations. Figure 4 illustrates the arrangement of the pressure probes at the engine face. Some of the main parameters in the input data are tabulated on the following page, with a complete input data listing in Fig. 7.

PARAMETER	CASE 1	CASE 2	CASE 3	CASE 4
NR	7	7	7	7
NP	8	8	8	8
RI	1.000	1.430	0.283	1.645
RT	5.169	4.346	1.000	5.000
KD	3 (IDC)	3 (IDC)	3 (IDC)	6 (KA2)
T (sec)	30.0	2.0	2.0	2.0
FO (Hz)	500.0	500.0	1000.0	1000.0
FCO (Hz)	1000.0	400.0	500.0	500.0
ALPH (deg)	4.0	5.0	-	-
PSI (deg)	0.0	0.0	-	-
MO	1.36	2.5	-	-
U2 (fps)	514.3	278.5	432.4	575.8
BF	0.733	0.733	0.733	0.784
CKP/KC	1.0	1.0	-	-
RKP/KR	1.0	1.0	-	-
MFR	-	1.0	-	-
NTUR	-	0	-	1
SPTAC	-	1.0	-	-
probes	40	14	2	0

[A dash "-" indicates a defaulted entry, or zero. The program assigns default values in these cases.]

C. Sample Problem Output

The line-printer generated output for the four test cases is presented in Figure 8. The number of pages of output varies with the dynamic data content, but never exceeds seven pages, unless there are run-time errors (exponential overflows, negative square root radicals, etc.) or compile-time errors. Run-time errors can occur with bad data. The terms given in the output are defined in Section II, part C.

[illegible]

54


```

7 0.283 0.419 0.599 0.737 0.852 0.953 1.000 315.
  0.0 0.45 1.00 1.35 1.80 2.25 2.70 --
  -- SAMPLE PROBLEM #3 - USAF SURSONIC INLET - 22 DEC 1983 --
  -- PART-POINT = 20.40 1.000 1.000 1.000 1.000 1.000 1.000
1.000 1.000 1.000 1.000 1.000 1.000 1.000 1.000
.804 .804 .804 .804 .804 .804 .804 .804
.902 .861 .846 .835 .822 .810 .800 .800
.886 .790 .785 .785 .785 .785 .785 .785
.857 .785 .785 .785 .785 .785 .785 .785
.825 .785 .785 .785 .785 .785 .785 .785
.804 .804 .804 .804 .804 .804 .804 .804
0.0 0.0 0.0 0.0 0.0 0.0 0.0 0.0
2040 12 432.4 432.4 432.4 432.4 432.4 432.4
2040 34 0.0 0.0 0.0 0.0 0.0 0.0 0.0
0 0 0 0 0 0 0 0
ENDJOB

```

Figure 7. (cont'd)

```

7 1.645 2.225 3.070 3.725 4.280 4.775 5.000 315.
0.0 45. 100. 500. 180. 325. 370.
-- SAMPLE PRUAFM #4 - 464.12 22 DEC 1983 --
PART-PUINT = 464.12 M0 = TRANSONIC
1.000 1.000 1.000 1.000 1.000 1.000 1.000
.721 .721 .721 .721 .721 .721 .721
0.83700 0.85100 0.86800 0.85600 0.84000 0.8200 0.8100
0.84000 0.86700 0.91700 0.87200 0.83600 0.8200 0.8100
0.83300 0.86900 0.94300 0.87300 0.86900 0.85400 0.84100
0.82500 0.85800 0.93200 0.87300 0.82500 0.81800 0.8100
0.81100 0.83000 0.87700 0.81900 0.80700 0.78800 0.72060
0.72060 0.72060 0.72060 0.72060 0.72060 0.72060 0.72060
0.0 0.0 0.0 0.0 0.0 0.0 0.0
0.0 0.9 575.8 578.4 0.0 0.0 0.0
ENDJOB

```

Figure 7. (cont'd)

```

---      SAMPLE PROBLEM #1      ---
MU = 1.36      ALPHA = 4.0
PRESSURE ARRAY
RADIUS      ANGULAR POSITION OF INPUT MEASUREMENTS, DFG
0.          45.0      90.0      135.0      180.0      225.0      270.0      315.0
1.331      0.978      0.981      0.979      0.978      0.978      0.978      0.981
2.585      0.942      0.968      0.948      0.978      0.977      0.978      0.970
3.615      0.951      0.965      0.949      0.978      0.977      0.978      0.960
4.469      0.954      0.971      0.969      0.978      0.976      0.979      0.967
4.962      0.949      0.948      0.951      0.960      0.937      0.958      0.947

```

```

BASE RADIAL PROFILE
RADI      1.000      1.331      2.585      3.615      4.469      4.962      5.169
PTR/PTA    1.0000      1.0000      1.0000      1.0000      1.0000      1.0000      1.0000

```

```

OVERALL FLOW DESCRIPTIONS
PTMIN= 0.937      (PTMX-PTMIN)/PTMX= 0.0446
PTMAX= 0.981      (PTMX-PTMIN)/PTMX= 0.0452
PTAVG= 0.966      (PTAV-PTMIN)/PTAVE= 0.0298
PSAVG= 0.860      QAVG= 0.1015

```

```

FLOW DISTORTION FACTORS
K-THETA      0.06314
KD2          138.2
(TDC)-MAX      0.01563
(TDR)-MAX      0.01397
KRA          0.07476
KA2          0.11794
DSPR          0.00470
ID           0.01816
B-FACTOR      0.73300
BSF 0.26821    KC      1.000      KR      1.000

```

```

VORTEX PROPERTIES
THMN      RKMN      THMX      RKMV      DTH      THFA      A1      C1
0.        0.955      135.00      0.975      135.00      67.50      1.178      90.00

```

ORIGINAL PAGE IS
OF POOR QUALITY

Figure 8. Sample Problem Output

--- SAMPLE PROBLEM #1 ---
 MU = 1.36 KEY TO MAPPING SYMBOLS
 BURDEN (PI-PAVG)/PAVG 18.0 16.0 14.0 12.0 10.0 8.0 6.0 4.0 2.0 0.0
 IN PERCENT

 X/S X/W W/> >/R R/Y Y/H H/T T/A
 -2.0 -4.0 -6.0 -8.0 -10.0 -12.0 -14.0 -16.0 -18.0
 (PI-PAVG)/PAVG PROFILE

AVERAGE PRESSURE = 0.906

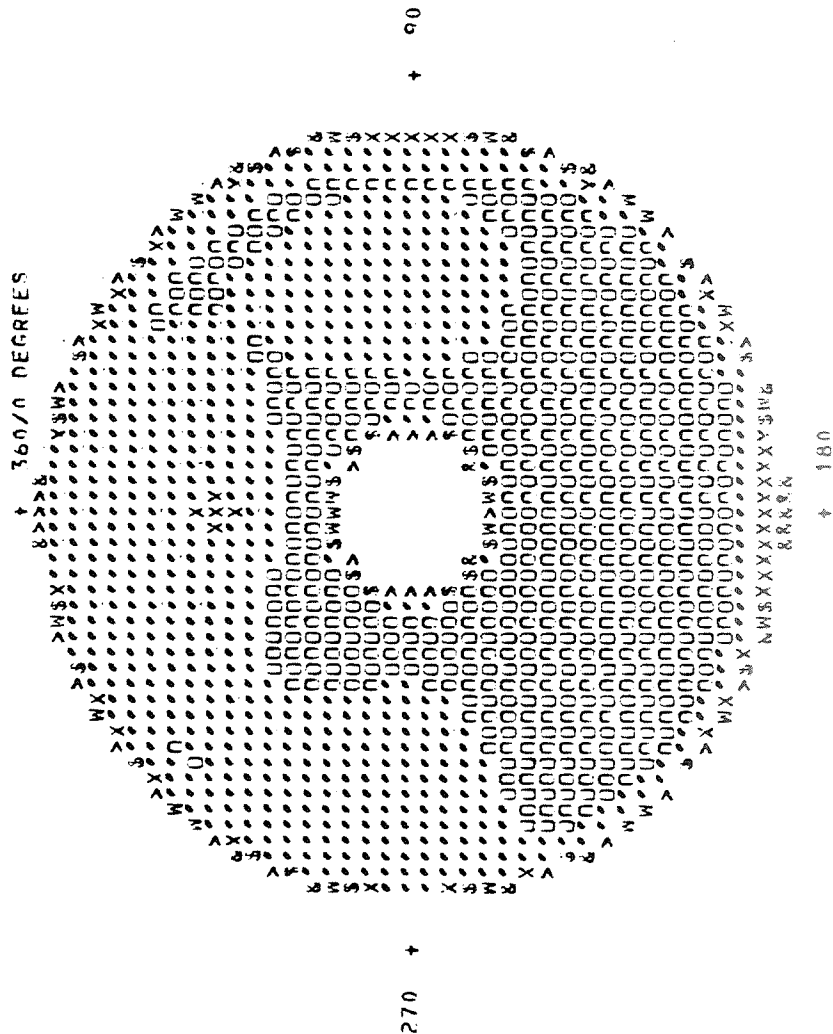


Figure 8. (cont'd)

ORIGINAL PAGE IS
OF POOR QUALITY

SAMPLE PROBLEM #1
ALPHA = 4.0
MN = 1.36

T 30.000 500.0 5.169 1.000 1.000
ALPH 4.000 0. 1.360 0.966 1.000 510.3 0.1051
PST MN ETA MFR H2 GPI2

RS AT FC = 1000.0

PROBE	RS	SG/PI2	A/RT
1	0.3380	0.0022	0.0463
2	0.4030	0.0027	0.0560
3	0.4460	0.0026	0.0626
4	0.4600	0.0032	0.0649
5	0.5380	0.0032	0.0779
6	0.4880	0.0012	0.0694
7	0.4110	0.0028	0.0572
8	0.3890	0.0029	0.0538
9	0.4180	0.0029	0.0583
10	0.4380	0.0023	0.0614
11	0.3630	0.0015	0.0500
12	0.3820	0.0029	0.0528
13	0.4300	0.0035	0.0601
14	0.4510	0.0022	0.0634
15	0.4580	0.0031	0.0645
16	0.5370	0.0010	0.0777
17	0.5200	0.0010	0.0748
18	0.4950	0.0011	0.0706
19	0.4790	0.0011	0.0679
20	0.4180	0.0021	0.0583
21	0.5170	0.0010	0.0743
22	0.4110	0.0011	0.0572
23	0.4690	0.0003	0.0663
24	0.5100	0.0012	0.0731
25	0.4480	0.0020	0.0630
26	0.5880	0.0010	0.0868
27	0.5310	0.0010	0.0766
28	0.4240	0.0003	0.0592
29	0.4970	0.0011	0.0709
30	0.4040	0.0021	0.0561
31	0.4970	0.0011	0.0709
32	0.4030	0.0022	0.0560
33	0.3800	0.0023	0.0525
34	0.4320	0.0021	0.0604
35	0.4690	0.0021	0.0663
36	0.5600	0.0010	0.0817
37	0.4250	0.0026	0.0594
38	0.4240	0.0025	0.0592
39	0.4550	0.0028	0.0641
40	0.4450	0.0026	0.0625

FACE-AVERAGE RMS (SG/PI2) = 0.00212

MEAN VORTEX SIZE (A0/RT) = 0.06473

Figure 8. (cont'd)


```

---          SAMPLE PROBLEM #1          ---
              MD = 1.36          ALPHA = 4.0

              PRESSURE ARRAY

RADIUS      0.      ANGULAR POSITION OF INPUT MEASUREMENTS, DEG
1.331      0.975    45.0    90.0    135.0    180.0    225.0    270.0    315.0
2.585      0.939    0.979    0.980    0.981    0.979    0.979    0.979    0.979
3.615      0.948    0.967    0.949    0.981    0.979    0.979    0.959    0.968
4.469      0.951    0.964    0.951    0.981    0.979    0.979    0.956    0.959
4.962      0.946    0.969    0.970    0.981    0.977    0.980    0.955    0.965
              0.947    0.952    0.963    0.939    0.959    0.968    0.945

              BASE RADIAL PROFILE

RADIUS      1.000    1.331    2.585    3.615    4.469    4.962    5.169
PTR/PTA     1.0000    1.0000    1.0000    1.0000    1.0000    1.0000    1.0000

              OVERALL FLOW DESCRIPTORS

PTMIN= 0.939    (PTMX-PTMN)/PTMX= 0.0429
PTMAX= 0.981    (PTMX-PTMN)/PTAV= 0.0436
PTAVG= 0.966    (PTAV-PTMN)/PTAV= 0.0279
PSAVG= 0.860    QAVG= 0.1015

              B=FACTOR      0.73300

RSF 0.26821    KC      1.000    KR      1.000

              FLOW DISTORTION FACTORS

A-THETA      0.07663
KD2           176.0
(IDC)=MAX     0.01607
(TDR)=MAX     0.01397
KRA           0.07476
KA2           0.13143
DSPR          0.00624
ID            0.01828

              VORTEX LOCATION

VBAR      A/RT    GAMMA    BETA      AY/RT      VI      R/RT      THETA
0.013     1.178    90.0    0.      1.178    999.999    0.597    67.50
VBMX      VRQ     A0/RT
1.063     0.027    0.0647

```

Figure 8. (cont'd)

--- MU = 1.36 SAMPLE PROBLEM #1 ---
 BURDER (PI-PAVG)/PAVG 18.0 16.0 14.0 12.0 10.0 8.0 6.0 4.0 2.0 0.0
 IN PERCENT
 -/ = + I/K </# #/S S/X
 -2.0 -4.0 -6.0 -8.0 -10.0 -12.0 -14.0 -16.0 -18.0
 (PI-PAVG)/PAVG PRFTLF Y/H H/T I/A
 AVERAGE PRESSURE = 0.964

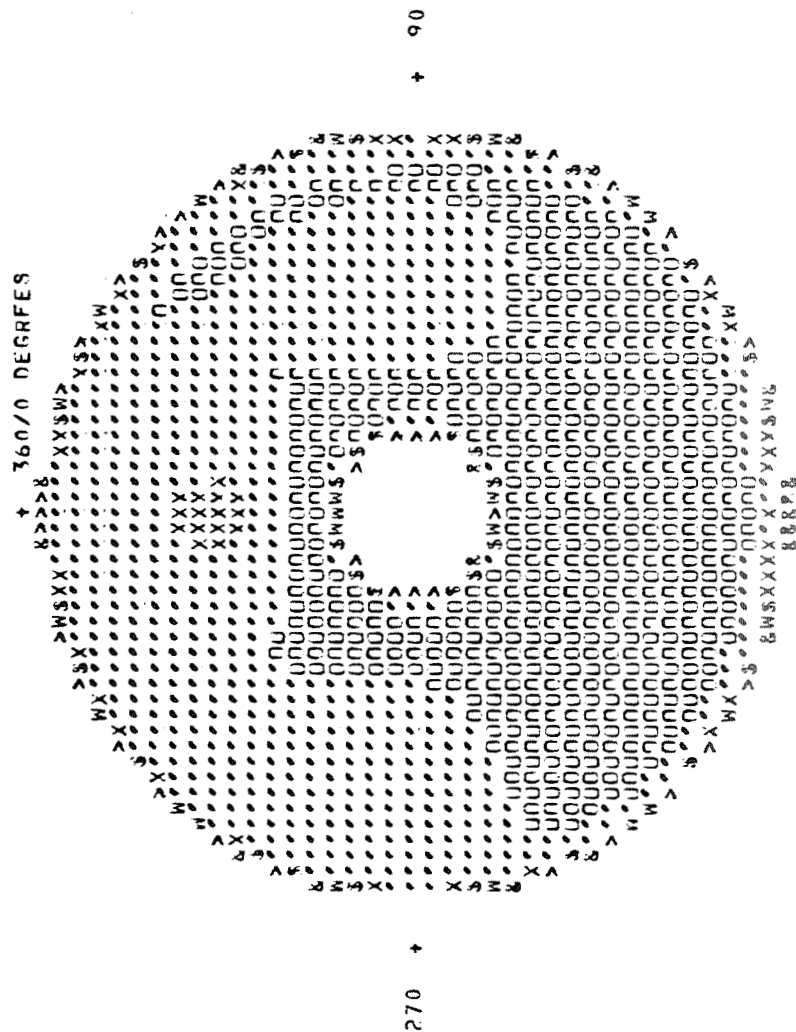


Figure B. (cont'd)

ORIGINAL PAGE IS
OF POOR QUALITY

```

-- SAMPLE PROBLEM NO. 2 MAR. 14, 1981 --
M0 = 2.5 ALPHA = 5.0

PRESSURE ARRAY

RADIUS      0.      ANGULAR POSITION OF INPUT MEASUREMENTS, DEG
1.934      0.905    45.0    90.0    135.0    180.0    225.0    270.0    315.0
2.669      0.904    0.908    0.885    0.883    0.881    0.888    0.874    0.883
3.238      0.893    0.894    0.890    0.887    0.871    0.871    0.865    0.879
3.721      0.894    0.890    0.896    0.870    0.849    0.859    0.860    0.870
4.151      0.886    0.889    0.882    0.847    0.842    0.851    0.858    0.877
          0.886    0.889    0.857    0.835    0.837    0.850    0.858    0.877

BASE RADIAL PROFILE

RADI    1.430    1.934    2.669    3.238    3.721    4.151    4.346
PIR/PIA 1.0000    1.0000    1.0000    1.0000    1.0000    1.0000    1.0000

OVERALL FLOW DESCRIPTORS

PTMIN= 0.835    (PTMX-PTMIN)/PTMX= 0.0804
PTMAX= 0.908    (PTMX-PTMIN)/PTMX= 0.0834
PTAVG= 0.875    (PTMX-PTMIN)/PTMX= 0.0855
PSAVG= 0.842    (PTMX-PTMIN)/PTMX= 0.0824

FLOW DISTORTION FACTORS

K-THETA    0.58596
KD2        462.7
(IDC)-MAX  0.02979
(IDR)-MAX  0.01563
KRA        0.27757
KA2        0.78942
DSPR       0.01518
ID         0.02539

H-FACTOR    0.73300
BSF 0.32740 KC 1.000 KR 1.000

VORTEX PROPERTIES

THMN  KMIN  THMX  RKMX  DTH  THETA  A1  G1
180.00 0.856 0. 0.896 180.00 90.00 1.571 -90.00

```

Figure 8. (cont'd)

-- SAMPLE PROBLEM NO. 2 MAR. 14, 1981 --
 RUMBER (PT-PAVG)/PAVG 9.0 8.0 7.0 6.0 5.0 4.0 3.0 2.0 1.0 0.0
 KEY TAPPING SYMBOLS
 ALPHA = 5.0
 T/I 1/2
 S/W 6.0
 W/> 5.0
 </# 4.0
 #/S 3.0
 S/* 2.0
 H/T -8.0
 T/A -9.0
 AVERAGE PRESSURE = 0.075

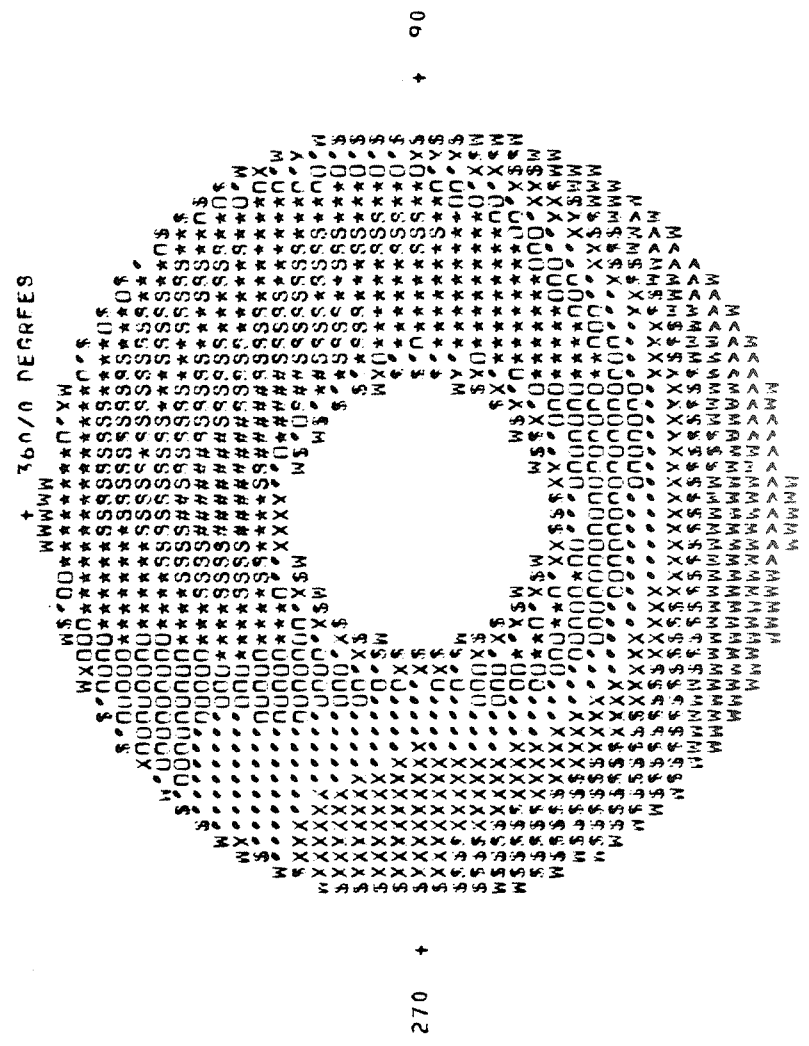


Figure 8. (cont'd)

ORIGINAL PAGE IS
 OF POOR QUALITY

<STEADY-STATE DISTORTION>

-- SAMPLE PROBLEM NO. 2 MAR. 14, 1981 --
 M0 = 2.5 ALPHA = 5.0

T 2.000 FO 500.0 RT 4.346 RT 1.430 SPTRC 1.000
 ALPH 5.000 PSI 0. MN 2.500 ETA 0.875 MFR 1.000 U2 278.5 UPI2 0.0370
 RS AT FC = 400.0

PROBE	RS	SG/PT2	A/RT
1	0.4900	0.0079	0.1123
4	0.3900	0.0140	0.0869
6	0.4630	0.0127	0.1052
17	0.3940	0.0081	0.0879
18	0.3610	0.0078	0.0800
19	0.3420	0.0108	0.0754
20	0.4220	0.0265	0.0948
21	0.6670	0.0139	0.1650
22	0.5170	0.0129	0.1196
23	0.4160	0.0078	0.0933
24	0.4720	0.0128	0.1076
36	0.5210	0.0109	0.1206
37	0.4990	0.0098	0.1147
38	0.4990	0.0079	0.1147

FACE-AVERAGE RMS (SG/PT2) = 0.01261

MEAN VORTEX SIZE (A0/RT) = 0.10779

DISTORTION FACTOR EXTREME VALUE

FACTOR	STEADY STATE	MEAN VALUE	9 SIGMA INF	STGMA FC	MAXIMUM INSTANTANEOUS
KTTA	0.5860	0.5999	0.1069	0.0801	99.7%
KD2	462.7	475.7	34.7	26.0	PROB 1.0450
IDC	0.0298	0.0312	0.0025	0.0018	614.0
IDR	0.0156	0.0157	0.0007	0.0005	0.0412
KRA	0.2776	0.2811	0.0541	0.0405	0.0180
KAZ	0.7894	0.8060	0.1140	0.0854	0.5095
DSPR	0.0152	0.0153	0.0023	0.0018	1.2701
TU	0.0254	0.0259	0.0011	0.0008	0.0249
					0.0297

MAXIMUM INSTANTANEOUS DISTORTION FACTOR

IDC = 0.0389

Figure 8. (cont'd)

```

-- SAMPLE PROBLEM NO. 2 MAR. 14, 1981 --
M0 = 2.5 ALPHA = 5.0
PRESSURE ARRAY
RADIUS      0.  ANGULAR POSITION OF INPUT MEASUREMENTS, DEG  270.0  315.0
1.934      0.914  0.885  0.877  0.872  0.881  0.870  0.890
2.669      0.913  0.890  0.881  0.862  0.864  0.861  0.886
3.238      0.902  0.896  0.864  0.840  0.852  0.856  0.881
3.721      0.903  0.892  0.841  0.833  0.844  0.854  0.881
4.151      0.895  0.857  0.829  0.828  0.843  0.854  0.884

```

```

BASE RADIAL PROFILE
RADI  1.430  1.934  2.669  3.238  3.721  4.151  4.346
PTR/PTA 1.0000 1.0000 1.0000 1.0000 1.0000 1.0000 1.0000

```

```

OVERALL FLOW DESCRIPTORS
PTMIN= 0.828 (PTMX-PTMIN)/PTMX= 0.0937
PTMAX= 0.914 (PTMX-PTMIN)/PTMX= 0.0980
PTAVG= 0.874 (PTAV-PTMIN)/PTAV= 0.0524
PSAVG= 0.842 QAVG= 0.0324

```

```

FLOW DISTORTION FACTORS
K-THETA  0.83940
KD2      568.8
(IDC)-MAX 0.03786
(YDR)-MAX 0.01564
KRA      0.27757
KA2      1.04286
DSPR     0.02184
ID       0.02803
R-FACOR  0.73300
RSF 0.32740 KC 1.000 KR 1.000

```

```

VORTEX LOCATION
VBAK  A/RT GAMMA BETA AY/RT VL R/RT THETA
0.131 1.571 -90.0 0. 1.571 999.999 0.665 90.00
VRMX  VRU A0/RT
1.402 0.464 0.1078

```

Figure 8. (cont'd)

ORIGINAL PAGE IS
OF POOR QUALITY

-- SAMPLE PROBLEM NO. 2 MAR. 14, 1981 --
 BUREAU (PI-PAVG)/PAVG 9.0 8.0 7.0 6.0 5.0 4.0 3.0 2.0 1.0 0.0
 IN PERCENT
 -- ALPHA = 5.0
 KEY TO MAPPING SYMBOLS
 +/I I/< </# #/S
 -/X X/\$ \$/W W/> >/R R/Y Y/H H/I T/A
 -1.0 -2.0 -3.0 -4.0 -5.0 -6.0 -7.0 -8.0 -9.0
 (PI-PAVG)/PAVG PROFILE
 AVERAGE PRESSURE = 0.870

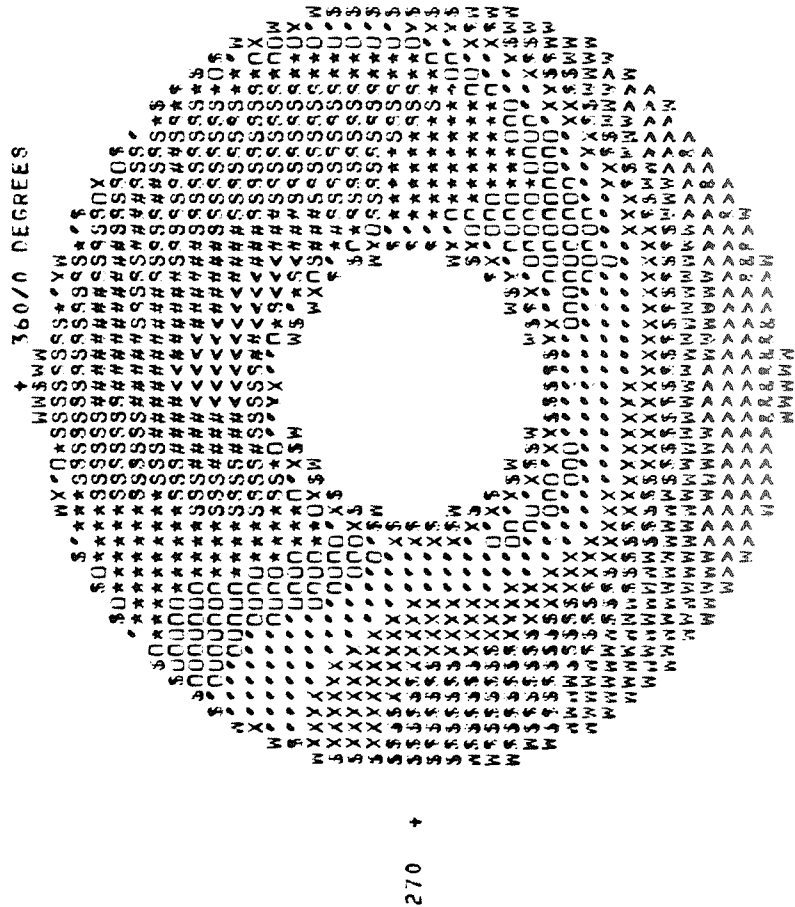


Figure 8. (cont'd)

```

-- SAMPLE PROBLEM #3 -- USAF SUBSONIC INLET - 22 DEC 1983 --
PART-POINT = 20.40 MD = SUBSONIC

PRESSURE ARRAY

RADIUS      0.  ANGULAR POSITION OF INLET MEASUREMENTS, DEG  270.0  315.0
0.419      0.902  0.861  0.846  0.935  0.992  0.985  0.940  0.920
0.599      0.866  0.790  0.817  0.936  0.995  0.980  0.930  0.900
0.737      0.857  0.783  0.814  0.955  0.965  0.962  0.946  0.871
0.852      0.835  0.786  0.785  0.944  0.920  0.985  0.962  0.863
0.953      0.825  0.786  0.758  0.830  0.820  0.882  0.881  0.852

BASE RADIAL PROFILE

RADI  0.283  0.419  0.599  0.737  0.852  0.953  1.000
PTR/PTA 1.0000 1.0000 1.0000 1.0000 1.0000 1.0000 1.0000

OVERALL FLOW DESCRIPTIONS

PTMIN= 0.758 (PTMX-PTMN)/PTMX= 0.2382
PTMAX= 0.995 (PTMX-PTMN)/PTMX= 0.2672
PTAVG= 0.897 (PTAV-PTMN)/PTAV= 0.1455
PSAVG= 0.804 GAVG= 0.0802

FLOW DISTORTION FACTORS

K-THETA  0.95777
KD2      1801.4
(TDC)-MAX 0.10759
(TDR)-MAX 0.06516
KPA      0.30434
KA2      1.18085
DSPR     0.05760
ID       1.26570
B-FACIOR 0.73300
RSF 0.30742 KC 16.400 KR 11.100

VORTEX PROPERTIES

THMN  RKMN  THMY  RKMY  PTH  THFA  A1  G1
45.00 0.801 225.00 0.959 180.00 135.00 1.571 90.00

```

Figure 8. (cont'd)

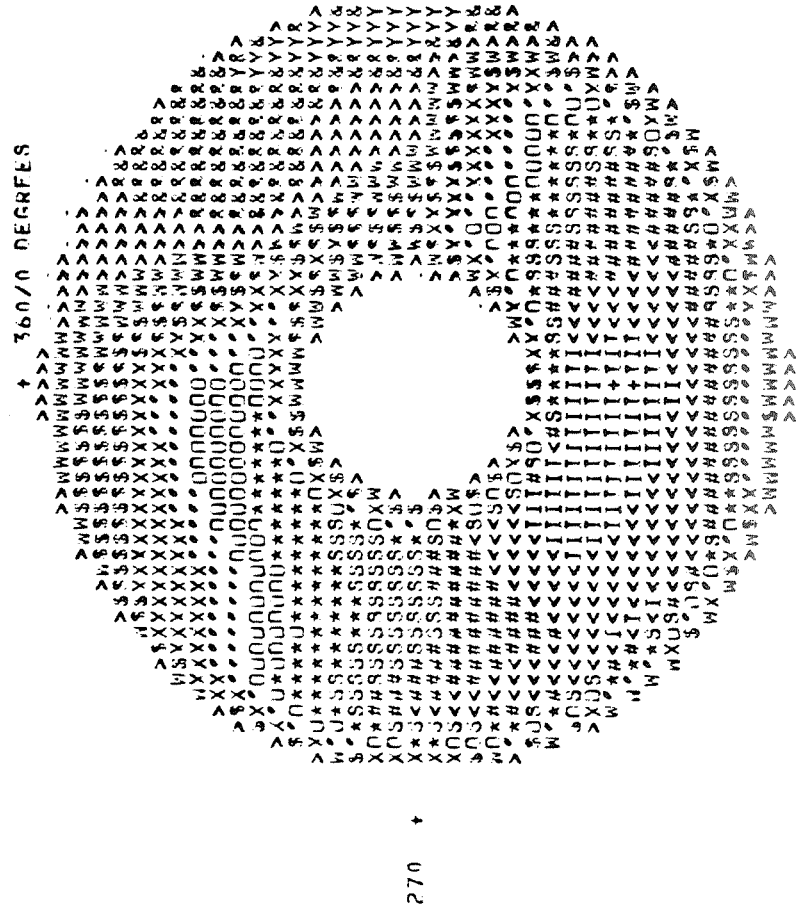

```

-- SAMPLE PROBLEM #3
PART-POINT = 20.40
-- USAF SUBSONIC INLET--22 DEC 1983
KEY TO MAPPING SYMBOLS
--
RURDK (PT-PAVG)/PAVG 10.0 --/3 14.0 --/4 12.0 10.0 8.0 6.0 4.0 2.0 0.0
IN PERCENT
--
--/X --/S --/W --/Z --/Y --/H --/T --/A
-2.0 -4.0 -6.0 -8.0 -10.0 -12.0 -14.0 -16.0 -18.0
{PT-PAVG}/PAVG PROF YLF

```

AVERAGE PRESSURE = 0.887

ORIGINAL PAGE IS
OF POOR QUALITY



<STEADY-STATE DISTORTION>

Figure 6. (cont'd)

-- SAMPLE PROBLEM #3 -- USAF SURSONIC INLET - 22 DEC 1983 --
 PART-POINT = 20.40 MO = SUBSONIC

T FO RT RI SPTC
 2.000 1000.0 1.000 0.283 1.000
 ALPH PSI MN FTA MFR U2 QPI2
 0. 0. 0. 0.887 1.000 432.4 0.0904

RS AT FC = 500.0

PROBE R3 SG/PT2 A/RT
 12 0.3840 0.0500 0.4614
 34 0.2100 0.0240 0.2450

FACE-AVERAGE RMS (SG/PT2) = 0.03922

MEAN VORTEX SIZE (A0/RT) = 0.36942

DISTORTION FACTOR EXTREME VALUE

FACTOR	STEADY STATE	MEAN VALUE	SIGMA INF	STGMA EN	MAXIMUM INSTANTANEOUS	MINIMUM INSTANTANEOUS
KITA	0.9578	0.9740	0.2082	0.1568	1.6787	0.9977
KD2	1.8014	1.5562	0.3141	0.2365	2.8293	1.8604
IDC	0.1076	0.1162	0.0201	0.0151	0.1784	0.1407
IDR	0.0652	0.0662	0.0033	0.0025	0.0776	0.0789
KRA	0.3043	0.3184	0.0419	0.0315	0.4455	0.4857
KA2	1.1809	1.2074	0.2105	0.1585	1.8614	2.0712
DSPR	0.0576	0.0583	0.0126	0.0095	0.0985	0.1120
TD	1.2657	1.3208	0.1076	0.0810	1.6058	1.7028

MAXIMUM INSTANTANEOUS DISTORTION FACTOR

IDC = 0.1786

Figure 6. (cont'd)

-- SAMPLE PROBLEM #3 -- USAF SUBSONIC INLET - 22 DEC 1983 --
 PART-POINT = 20.40 MN = SUPSONIC

RADIUS	PRESSURE ARRAY					DEG	
	0.	45.0	90.0	135.0	180.0	225.0	270.0
0.419	0.851	0.798	0.800	0.935	1.038	1.048	0.991
0.599	0.835	0.727	0.771	0.936	1.041	1.043	0.981
0.737	0.806	0.720	0.768	0.955	1.011	1.025	0.997
0.852	0.784	0.723	0.739	0.944	0.966	1.048	1.013
0.953	0.774	0.723	0.712	0.830	0.866	0.945	0.932
							0.880

BASE RADIAL PROFILE

RADII	0.283	0.419	0.599	0.737	0.852	0.953	1.000
PIR/PIA	1.0000	1.0000	1.0000	1.0000	1.0000	1.0000	1.0000

OVERALL FLOW DESCRIPTIONS

PTMIN=	0.712	(PTMX-PTMIN)/PTMX=	0.3210
PTMAX=	1.048	(PTMX-PTMIN)/PTAV=	0.3779
PTAVG=	0.891	(PTAV-PTMIN)/PTAV=	0.2007
PSAVG=	0.804	QAVG=	0.0002

FLOW DISTORTION FACTORS

K-THETA	1.77307	R-FACTOR	0.73300
KD2	2820.4	RSF	0.30742
(TDC)-MAX	0.17394	KC	16.400
(TDR)-MAX	0.06490	KR	11.100
KRA	0.30434		
K42	1.99615		
USPR	0.10752		
ID	1.59735		

VORTEX LOCATION

VORX	A/R	GAMMA	BETA	AY/RT	VI	R/RT	THETA
0.395	1.571	90.0	0.	1.571	999.999	0.642	135.00
VRMX	VRU	A0/RT					
1.461	0.590	0.3694					

Figure 6. (cont'd)


```

-- SAMPLE PROBLEM #4 - USAF TRANSONIC INLET - 22 DEC 1983 --
PART=PUTNT = 464.12 MO = TRANSONIC

PRESSURE ARRAY

RADIUS      0.      ANGULAR POSITION OF INPUT MEASUREMENTS, DEG      315.0
2.225      0.837  0.851  0.868  0.854  0.840  0.852  0.861  0.847
3.070      0.840  0.867  0.917  0.872  0.836  0.869  0.911  0.865
3.725      0.833  0.869  0.943  0.873  0.825  0.873  0.941  0.872
4.280      0.825  0.858  0.932  0.853  0.807  0.854  0.933  0.861
4.775      0.811  0.830  0.877  0.819  0.788  0.818  0.892  0.835

-- BASE RADIAL PROFILE

RADI  1.645  2.225  3.070  3.725  4.280  4.775  5.000
PTR/PTA  1.0000  1.0000  1.0000  1.0000  1.0000  1.0000  1.0000

OVERALL FLOW DESCRIPTIONS

PTMNE= 0.788 (PTMX-PTMNI)/PTMX= 0.1644
PTMAX= 0.943 (PTMX-PTMNI)/PTMX= 0.1802
PTAVG= 0.860 (PTMX-PTMNI)/PTMX= 0.0840
PSAVG= 0.721 GAVG= 0.1308

FLOW DISTORTION FACTORS

K-THETA      0.03551
KD2          452.6
(TDC)-MAX    0.06052
(TDR)-MAX    0.03083
KRA          0.10017
KA2          0.11405
USPR         0.00238
ID           0.67161

B=FACTOR      0.78400
BSF 0.33185 KC 16.400 KR 11.100

VORTEX PROPERTIES

THMN  RKMN  THMX  RKMX  DTH  YHFTA  A1  C1
180.00 0.819 270.00 0.908 90.00 -135.00 0.785 90.00

```

Figure 6. (cont'd)

```

-- SAMPLE PROBLEM #4 - USAF TRANSONIC INLET - 22 DEC 1983 --
PART-POINT = 464.12 M0 = TRANSONIC
KEY TO MAPPING SYMBOLS
BURDER (PI-PAVG)/PAVG 18.0 16.0 14.0 12.0 10.0 8.0 6.0 4.0 2.0 0.0
I/H PERCENT 18.0 16.0 14.0 12.0 10.0 8.0 6.0 4.0 2.0 0.0
X/S X/W W/> >/K R/Y Y/H H/T I/A
-2.0 -4.0 -6.0 -8.0 -10.0 -12.0 -14.0 -16.0 -18.0
(PI-PAVG)/PAVG PROFILE

```

AVERAGE PRESSURE = 0.960

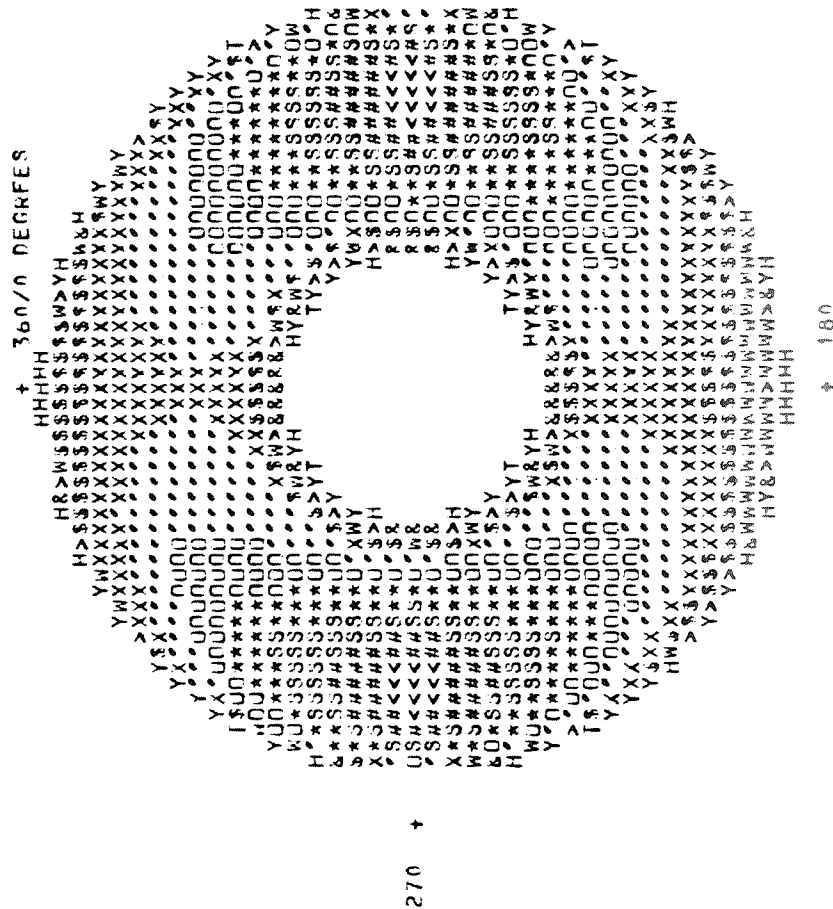


Figure 6. (cont'd)

ORIGINAL PAGE IS
OF POOR QUALITY

-- SAMPLE PROBLEM #1 - IISAF TRANSONIC INLET - 22 DEC 1983 --
 PART-POINT = 464.12 M0 = TRANSONIC

T 2.000 1000.0 5.000 1.645 1.000
 ALPH 0. PSI 0.900 0.860 1.000 575.8 0.1520

RS AT FC = 500.0

TURBULENCE CALCULATIONS :

DIMENSIONLESS VELOCITY AT EACH	PROBE LOCATION:	
26.93	25.93	23.37
27.87	29.57	25.60
27.87	35.85	30.30
27.87	29.94	24.34
27.87	25.04	20.29
27.87	35.50	24.22
27.87	29.85	31.62
27.87	28.81	26.15

ERRORS IN K, F AND (K+E) OF EACH ITERATION:		
52.56748	67.93246	
8.42651	16.60464	
3.57977	4.87612	
1.64211	3.47984	
0.97559	2.64657	
0.78194	2.08359	
0.63496	1.67382	
0.51999	1.36140	
0.42829	1.11619	
0.35419	0.92011	
0.29379	0.76138	
0.24422	0.63179	
0.20336	0.52534	
0.16955	0.43751	
0.14150	0.36480	
0.11819	0.30440	
0.09877	0.25429	
0.08258	0.21249	
0.06807	0.17745	
0.05778	0.14857	
0.04835	0.12426	
0.04046	0.10398	
0.03387	0.08700	
0.02835	0.07281	
0.02373	0.06094	
0.01986	0.05101	
0.01664	0.04270	
0.01392	0.03575	
	0.02992	

Figure 6. (cont'd)

-- SAMPLE PROBLEM #4 -- USAF TRANSONIC INLET -- 22 DEC 1983 --
 PART-POINT = 464.12 M0 = TRANSONIC

RESULTS OF TURBULENCE CALCULATIONS:

PRDRE	UII	E	K	SG/PT2
1	1.4448	2236.3714	120.9109	0.031157
2	9.2138	2486.2515	128.6876	0.032748
3	53.8775	2745.8098	135.8546	0.032908
4	157.1708	3020.2345	142.8482	0.032833
5	5434.5535	3315.1465	149.8993	0.031811
6	88.5994	2093.5900	98.7376	0.029223
7	90.7128	2476.5374	105.5357	0.032221
8	107.7528	2923.0317	113.1623	0.033786
9	411.0606	3447.4029	121.6877	0.033907
10	10674.3311	4066.7809	131.2077	0.031811
11	3228.9029	1603.9231	71.0785	0.025860
12	363.1044	1933.3533	73.3018	0.030837
13	532.8087	2435.1411	78.3018	0.034355
14	20992.1580	3170.0668	86.2044	0.035154
15	532.8087	4222.9423	97.1550	0.031811
16	67.8584	4407.4271	104.9544	0.030784
17	101.2175	2888.3006	111.5637	0.035539
18	185.5759	3464.7780	120.4113	0.034695
19	790.1339	4157.9947	130.4113	0.031811
20	13829.8063	4995.9947	141.6099	0.033772
21	6.9553	2893.2974	135.3699	0.034959
22	39.2705	3342.0105	146.9025	0.034903
23	207.7453	3794.7266	157.3540	0.033573
24	519.1988	4269.7131	167.4694	0.033573
25	8048.2910	4780.7404	177.6324	0.031811
26	82.4443	2409.1980	103.2728	0.030112
27	107.1068	2409.1115	111.1357	0.033433
28	160.3528	3554.2982	120.2175	0.035479
29	802.5839	4311.6639	130.6608	0.034863
30	14972.7083	5235.0960	142.6111	0.031811
31	335.7476	1476.2798	70.4834	0.025077
32	442.0766	1707.2749	71.8314	0.029771
33	21.0620	2052.2888	75.8039	0.033483
34	320.6582	2543.4345	81.1118	0.034095
35	14572.3848	3223.6260	89.0140	0.031811
36	69.7910	2023.5076	90.0392	0.028819
37	130.0550	2348.8047	104.6667	0.031811
38	120.1257	2734.4349	111.1492	0.033783
39	396.8805	3189.9798	118.5119	0.033746
40	9608.6600	3729.7290	126.8308	0.031811

FACE-AVERAGE RMS (SG/PT2) = 0.03249

MEAN VORTEX SIZE (A0/RT) = 0.16525

Figure 6. (cont'd)

-- SAMPLE PROBLEM #4 -- USAF TRANSONIC INLET - 22 DEC 1983 --
 PART-POINT = 464.12 MO = TRANSONIC

DISTORTION FACTOR EXTREME VALUE

FACTOR	STEADY STATE	MEAN VALUE	SIGMA INF	SIGMA EN	MAXIMUM	INSTANTANEOUS
KT TA	0.0355	0.1158	0.0385	0.0335	0.2627	0.2853
KD2	0.4526	0.8335	0.1011	0.3564	2.3417	2.5095
IDC	0.0605	0.0854	0.0293	0.0255	0.1971	0.2139
IDR	0.0308	0.0314	0.0061	0.0053	0.0546	0.0587
KRA	0.1002	0.1042	0.0299	0.0260	0.2189	0.2382
KA2	0.1140	0.1974	0.0451	0.0392	0.3682	0.3978
DSPK	0.0024	0.0066	0.0021	0.0018	0.0147	0.0159
ID	0.0716	0.8136	0.1736	0.1508	1.4685	1.5834

MAXIMUM INSTANTANEOUS DISTORTION FACTOR

KA2 = 0.3682

ORIGINAL PAGE IS
 OF POOR QUALITY

Figure 6. (cont'd)

-- SAMPLE PROBLEM #4 -- USAF TRANSONIC INLET - 22 DEC 1983 --
 PART-POINT = 464.12 M0 = TRANSONIC

RADIUS	PRESSURE ARRAY					
	0.	45.0	90.0	135.0	180.0	225.0
2.225	0.840	0.851	0.865	0.830	0.783	0.852
3.070	0.843	0.867	0.914	0.846	0.779	0.869
3.725	0.836	0.869	0.940	0.847	0.768	0.873
4.280	0.828	0.858	0.929	0.827	0.750	0.854
4.775	0.814	0.830	0.874	0.793	0.731	0.818
						0.918
						0.968
						0.998
						0.990
						0.949
						0.861

BASE RADIAL PROFILE					
RADII	1.645	2.225	3.070	3.725	4.280
PTIR/PTA	1.0000	1.0000	1.0000	1.0000	1.0000
					5.0000
					1.0000

OVERALL FLOW DESCRIPTORS

PTMINE	0.731	(PTMX-PTMN)/PTMX	0.2678
PTMAXE	0.998	(PTMX-PTMN)/PTAV	0.3107
PTAVGE	0.860	(PTMX-PTMN)/PTAV	0.1505
PSAVGE	0.721	WAVE	0.1308

FLOW DISTORTION FACTORS

K-THETA	0.26719		
KD2	1221.98		
(TDC)-MAX	0.12698		
(TDR)-MAX	0.03083		
KRA	0.10017		
KA2	0.34573	B-FACTOR	0.78400
DSPR	0.02846		
ID	1.03333	BSF	0.33185
		KC	16.400
		KR	11.100

VORTEX LOCATION

VBAR	A/RT	GAMMA	BETA	AY/RT	VI	R/RT	THETA
0.218	0.785	90.0	0.	0.785	999.999	0.664	-135.00
VBEK	VRU	A0/RT					
1.225	0.291	0.1653					

Figure 6. (cont'd)

-- SAMPLE PROBLEM #4 -- USAF TRANSONIC INLET - 22 DEC 1983 --
 PART-PUTNT = 404.12 M0 = TRANSONIC
 KEY TO MAPPING SYMBOLS
 BURDER (PI-PAVG)/PAVG 18.0 16.0 14.0 12.0 10.0 8.0 6.0 4.0 2.0 0.0
 IN PERCENT
 --/X X/\$ \$/W W/> >/& &/Y Y/H H/T T/A
 -2.0 -4.0 -6.0 -8.0 -10.0 -12.0 -14.0 -16.0 -18.0
 (PI-PAVG)/PAVG PROFILE

AVERAGE PRESSURE = 0.860

+ 360/0 DEGREES

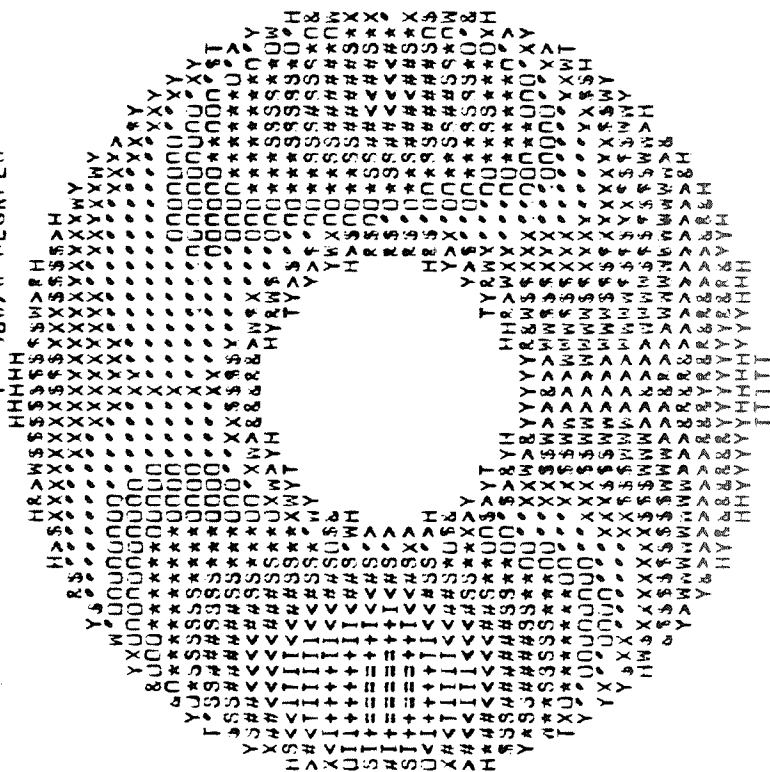
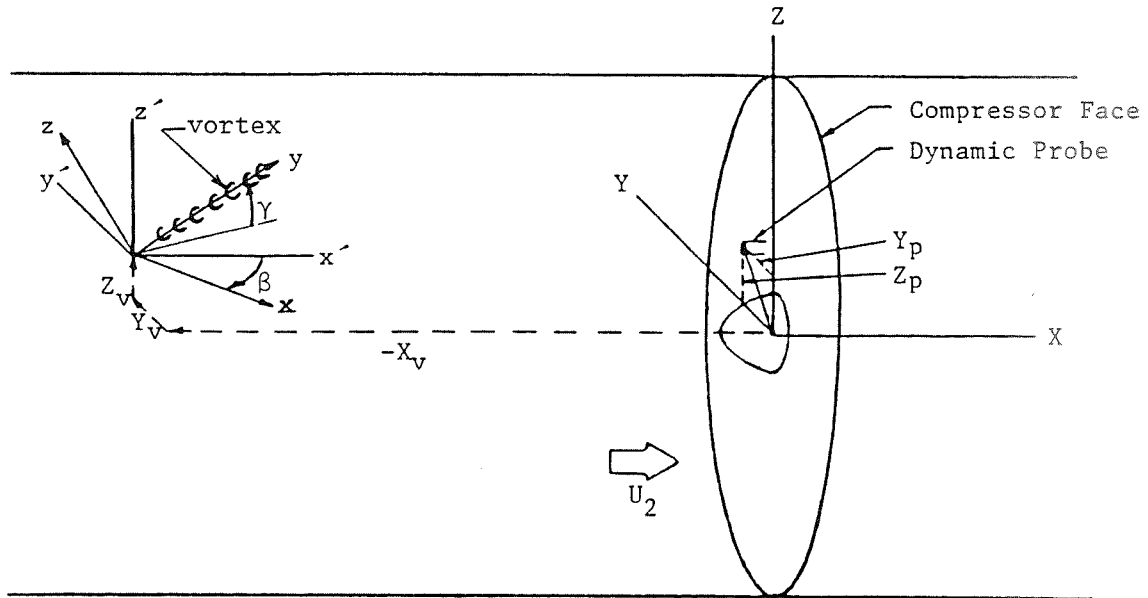


Figure 6. (cont'd)

ORIGINAL PAGE IS
 OF POOR QUALITY

Factor	Equation	Supplemental equations	Definitions
IDC_{max}	$IDC_{max} = \max \left\{ \frac{1}{2}(IDC_1 + IDC_2), \frac{1}{2}(IDC_4 + IDC_5) \right\}$	$IDC_j = \frac{(\bar{p}_t)_j - (p_{t,min})_j}{\bar{p}_t}$	$(\bar{p}_t)_j$ = average total pressure for ring j $(p_{t,min})_j$ = minimum total pressure reading in ring j
IDR_{max}	$IDR_{max} = \max(IDR_1, IDR_5)$	$IDR_j = \frac{\bar{p}_t - (\bar{p}_t)_j}{\bar{p}_t}$	\bar{p}_t = average total pressure at engine face
K_{D2}	$K_{D2} = \frac{\sum_{j=1}^{NR} \bar{\theta}_j (\Delta p_t / p_t) (OD/D_j)}{\sum_{j=1}^{NR} (OD/D_j)}$	$\frac{\Delta p_t}{p_t} = \frac{(\bar{p}_t)_j - (p_{t,min})_j}{(\bar{p}_t)_j} * 100$	$(\bar{p}_t)_j, (p_{t,min})_j$ = see above $\bar{\theta}_j$ = circumferential extent of largest continuous total pressure depression below $(\bar{p}_t)_j$, degrees D_j = diameter of ring j; NR = number of ring OD = outer duct diameter
K_θ	$K_\theta = \frac{\sum_{j=1}^{NR} (A_1)_j (1/D_j)}{(\bar{q}/\bar{p}_t) \sum_{j=1}^{NR} (1/D_j)}$	$(A_1)_j = (a_1^2 + b_1^2)_j$ $(a_1)_j = \frac{1}{M} \left[\sum_{i=1}^M \frac{p_{t1}}{\bar{p}_t} \cos(\theta_1) \right]_j$ $(b_1)_j = \frac{1}{M} \left[\sum_{i=1}^M \frac{p_{t1}}{\bar{p}_t} \sin(\theta_1) \right]_j$	$\bar{p}_t, (\bar{p}_t)_j, D_j$ = see above \bar{q} = average dynamic pressure at engine face M = number of rakes $(p_{t1})_j$ = individual total pressure; rake 1, ring j θ = angular position of p_{t1}
K_{RAD}	$K_{RAD} = \sum_{j=1}^{NR} \left \frac{\Delta p_{tj}}{\bar{p}_t} \right \frac{\bar{p}_t}{\bar{q}} \frac{1}{D_j}$	$\frac{\Delta p_{tj}}{\bar{p}_t} = \frac{(\bar{p}_t)_j - (p_{t,base})_j}{\bar{p}_t}$	$(p_{t,base})_j$ = base radial profile for ring j; set = 1 for all j b = radial distortion weighting factor=1.0
K_{A2}	$K_{A2} = K_\theta + b K_{RAD}$		\bar{p}_t = see above $p_{t,min}$ = minimum total pressure at engine face k = compressor reduced frequency
$\frac{\Delta SPR}{Dist}$	$\frac{\Delta SPR}{Dist} = \frac{\Delta SPR}{[(\bar{p}_t - p_{t,min})/\bar{p}_t]} = f(k)$		k = circumferential distortion sensitivity factor k = radial distortion sensitivity factor b ^r = circumferential distortion weighting factor
ID	$ID = k_c (IDC)b + k_r (IDR)$		

Figure 9. Distortion Factor Definitions



GAMMA = vortex orientation angle between y axis
and the $x'-y'$ plane

BETA = vortex orientation angle between x' and x
axes, with the x axis in the $x'-y'$ plane

Figure 10. Definition of Vortex Angles

APPENDIX A.

PROGRAM SOURCE CODE LISTING (FORTRAN)

```

0001C MAXIMUM DISTORTION PROGRAM - MAIN DRIVER
0002C
0003C
0004C PRELIMINARY DECLARATIONS AND DESIGNATIONS
0005C
0006      COMMON AB,ANGLOC(20),AUD,BETA2,BF,CDPOP3(10),CMAY6(10),FD,ISHFT,
0007      & CMMIN(10),DKMX(10),DKSS(10),FACE(39,65),FACTOR,FARCE(39,65),BSF,
0008      & J1,J2,KEY,KD,LCNTFL,NH,NP,P(11,20),PR(10),PS(11,20),CKP,
0009      & PSPEC(20),PVALUE,QAV,QPT2,R,RADLOC(11),RANGE,RI,RNAV,BRP(11),
0010      & RT,SGDK(10),SGP(10),SIG,SMAY6,STAT1,STATD,I,TDPI,TDPI2,TMMIN,
0011      & TDP3,THETA,THMIN(10),TITLE1(20),TITLE2(20),TNAV5,TMAX,RKP,U2
0012C
0013      LOGICAL STAT1,STATD,LCNTFL
0014      LCNTFL=.FALSE.
0015      STAT1=.TRUE.
0016      STATD=.TRUE.
0017      DIMENSION DRT(11)
0018C
0019C INPUT PDEE CONFIGURATION.
0020C NP IS NUMBER OF RINGS; PLUS 2 TO INCLUDE CENTERBODY AND OUTER RADIUS
0021C NP IS THE NUMBER OF RADIAL RAKES
0022C RADLOC IS RADIAL LOCATION OF CENTERBODY; RINGS AND OUTER INLET RADIUS
0023C ANGLOC IS ANGULAR LOCATION OF RAKES IN DEGREES. TOP RAKE IS 0
0024C
0025      READ (5,100) NR,NP
0026      READ (5,101) (RADLOC(I), J=1,NR)
0027      READ (5,101) (ANGLOC(I), I=1,NP)
0028      J1=1
0029      IF (STAT1) J1=2
0030      J2=NR
0031      IF (STATD) J2=NR-1
0032      FACTOR=RADLOC(NR)/19.1
0033C
0034C CALL NEWPSD TO INPUT DISTORTION KEY, DWELL TIME AND FILTER FREQUENC.
0035C
0036      CALL NEWPSD (1)
0037 10  ISHFT=1
0038C
0039C INPUT DATA TITLES AND COMMENTS; CHECKING FIRST FOR END OF FILE.
0040C

```

```

0041      READ(5,124,END=999) TITLE1
0042 20    READ(5,124) TITLE2
0043C
0044C      INPUT BASE RADIAL PROFILE
0045C
0046      READ(5,101) (BRP(J),J=1,NR)
0047      DO 25 J=1,11
0048 25    IF (BRP(J).EQ.0.0) BRP(J)=1.0
0049C
0050C      INPUT STEADY STATE PRESSURE AND PLACE INTO ARRAY 'P'
0051C
0052      DO 30 J=1,NR
0053      DRT(J)=(RADLOC(J)-RADLOC(1))/(RADLOC(7)-RADLOC(1))
0054      READ(5,101) (PS(J,I), I=1,NP)
0055      DO 30 I=1,NP
0056 30    P(J,I)=PS(J,I)
0057      WRITE(7) (DRT(J),J=1,NR), (BRP(J),J=1,NR)
0058      BF=1.0
0059C
0060C      CALL PANT TO PRINT STEADY STATE PRESSURE ARRAY.
0061C
0062      CALL PNT(2)
0063C
0064C      CALL SUBROUTINES WHICH CALCULATE DISTORTION PARAMETERS.
0065C
0066      CALL PPIX(.TRUE.)
0067      CALL DISTRT
0068C
0069C      CALL PPIX TO TRANSFORM INPUT MEASUREMENTS INTO MAPPING PARAMETERS.
0070C
0071      CALL PPIX(.FALSE.)
0072C
0073C      MAINLP CONTROLS INTERPOLATION PROCESS IN INPUT MEASUREMENT PLANE
0074C
0075      CALL MAINLP
0076      ISHFT=2
0077C
0078C      CALL SUBROUTINE TO COMPUTE MAXIMUM INSTANTANEOUS DISTORTION VALUES
0079C      AND INSTANTANEOUS PRESSURE MAPS. UNSTDY ALSO CONTROLS THE OUTPUT.
0080C

```



```

0081      CALL UNSTDY
0082      GO TO 10
0083C
0084 999  STOP
0085 100  FORMAT (2I5)
0086 101  FORMAT (8F10.5)
0087 124  FORMAT (20H4)
0088      END
0089C
0090C

```

```

0091C
0092C SUBROUTINE PFXL (AKS,DKS,ANT)
0093C
0094C THIS SUBROUTINE SOLVES (KMAX-KEAR)/SIGMA K FOR KEAR/SIGMA K.LE. 2.0
0095C
0096C DKS=0.0
0097C IF (ANT.LE.1.0) GO TO 200
0098C IF (AKS.LE.0.0) GO TO 200
0099C X=ALD5 (ANT)
0100C A=2.9564*AKS**0.8641
0101C B=0.0047+0.3865/AKS
0102C XD=0.6909+0.1817/AKS
0103C AN=0.5625+0.58/AKS**0.707
0104C DX=X-XD
0105C IF (DX.LE.0.0) GO TO 200
0106C DKS=A*(1.0-EXP(-B*DX**AN))
0107C
0108C 200 RETURN
0109C END
0110C
0111C -----

```

```

0112C
0113
0114C
0115C
0116C
0117C
0118C
0119C
0120
0121
0122
0123
0124
0125
0126C
0127
0128
0129
0130 20
0131
0132C
0133C
0134C
0135
0136 22
0137
0138
0139
0140
0141
0142
0143
0144
0145
0146 100
0147
0148 10
0149
0150
0151 30

SUBROUTINE LAPOUT(KY)

THIS SUBROUTINE CONTROLS THE OUTPUT
SOME OUTPUT IS CONTROLLED BY 'CARDAD' AND 'PREFIX'.
NP,RADLOC,ANGLOC,AND P HAVE FIRST ARRAY DIMENSION EQUAL TO 11. TEN OF
THESE ARE AVAILABLE FOR USE. 11TH IS NEEDED FOR INTERNAL PROCESSING.

COMMON AB,ANGLOC(20),AUD,BETA2,BF,CDFOP3(10),CMAVG(10),FD,LSHFT,
* CMIN(10),DKMX(10),DKSS(10),FACE(39,65),FACTOR,FARCE(39,65),BSF,
* J1,J2,KEY,KD,LCNTFL,NA,NP,P(11,20),PR(10),PS(11,20),CKP,
* PSPEC(20),PVALUE,QAV,OPT2,R,RADLOC(11),RANGE,RI,RMAV,BRP(11),
* RT,SGDK(10),SGP(10),SIG,SMAYG,STAT1,STATD,T,TDP1,TDP2,TMIN,
* TDP3,THETA,THMIN(10),TITLE1(20),TITLE2(20),TMAVG,TMMAX,RKP,U2

DIMENSION ROUT(19),FACP(65),FACE(65)
LOGICAL STAT1,STATD,LCNTFL
IF (KY-2) 30,20,20
WRITE (6,190) TITLE1,TITLE2
WRITE (6,105)

OUTPUT SECTION FOR (PI-PAVG)/PAVG MAP

DO 22 I=1,19
ROUT(I)=FLOAT(10-I)*(RANGE/20.0)
WRITE (6,107)
WRITE (6,110) (ROUT(I),I=1,10)
WRITE (6,109)
WRITE (6,407)
WRITE (6,111) (ROUT(I),I=11,19)
WRITE (6,128) TMAVG
WRITE (6,120)
DO 10 I=1,39
DO 100 J=1,51
FACP(J)=FACE(I,J)
IF (I.NE.20) WRITE (6,101) (FACP(J), J=1,51)
IF (I.EQ.20) WRITE (6,121) (FACP(J), J=1,51)
WRITE (6,122)
GO TO 16
WRITE (6,219) TMIN,TDP1,TMMAX,TDP2,TMAVG,TDP3,SMAYG,PAV

```

```

0152C
0153C OUTPUT SECTION FOR USER-DEFINED DISTORTION PARAMETERS.
0154C
0155 WRITE (6,301) (PSPEC(I), I=1,6), BF, PSPEC(7)
0156 WRITE (6,302) PSPEC(8),BSF,CKP,RKP
0157C
0158 101 FORMAT (14X,51A1)
0159 105 FORMAT (37X,22HKEY TO MAPPING SYMBOLS)
0160 107 FORMAT (2X,6HORDER,11X, 57H, /- -/+ =/+ 1/X </# #/
0161 108 $S $/ ♦ ♦/0 0//)
0162 109 FORMAT (2X,10HIN PERCENT)
0163 110 FORMAT (2X,14H(P1-PAVG)/PAVG,20(1X,F5.1))
0164 111 FORMAT (22X,10F6.1)
0165 120 FORMAT (/39X,16H+ 360/0 DEGREES/)
0166 121 FORMAT ( 6X,6H270 +,2X,51A1,2X,5H+ 90)
0167 122 FORMAT ( /39X,6H+ 180)
0168 128 FORMAT (32X,23H(P1-PAVG)/PAVG PROFILE32X,16HAVERAGE PRESSURE
0169 129 1H=F7.3)
0170 190 FORMAT (1H1,6X,20A4/6X,20A4)
0171 219 FORMAT (/33X,24HVERALL FLOW DESCRIPTORS//
0172 25X,6HPTMIN=F7.3,3X,17H(PTMX-PTMN)/PTMX=F7.4/
0173 25X,6HPTMAX=F7.3,3X,17H(PTMX-PTMN)/PTAV=F7.4/
0174 25X,6HPTAVG=F7.3,3X,17H(PTAV-PTMN)/PTAV=F7.4/
0175 25X,6HPSAVG=F7.3,15X,5H0AVG=F7.4)
0176C
0177C SECTION FOR FORMATS FOR THE OUTPUT OF USER DEFINED DISTORTION FACTORS
0178C
0179 301 FORMAT (/11X,23HFLOW DISTORTION FACTORS//
0180 11X,11HK-THETA ,F11.5/11X,11HKD2 ,F11.1/
0181 11X,11H(IDC)-MAX ,F11.5/11X,11H(IDR)-MAX ,F11.5/
0182 11X,11HKRA ,F11.5/11X,11HKA2 ,F11.5,
0183 3X,11HB-FACTOR ,F11.5/11X,11HDSR ,F11.5)
0184 302 FORMAT (11X,2HID,9X ,F11.5,3X,2HDSR,10.5X,
0185 5H KR,F8.3)
0186 407 FORMAT (/25X, 51H/X X/X $/W W/> >/# #/Y Y/H H/
0187 8T T/A)
0188C
0189 16 RETURN
0190 END
0191C

```

```

0192C -----
0193C
0194      SUBROUTINE RATAK (RKFK,FABUD)
0195C
0196C      THIS IS THE FILTER ROUTINE.
0197C
0198      RKFK=0.0
0199      IF (FABUD.EQ.0.0) GO TO 40
0200      B=11.76
0201      RKFK=1.0
0202      E=-B*FABUD
0203      IF (ABS(E).GT.650.0) GO TO 40
0204      RKFK=SQRT(1.0-EXP(E))
0205C
0206 40      RETURN
0207      END
0208C
0209C -----

```

```

0210c SUBROUTINE SUMMER (X,ERF,KODE)
0211
0212c THIS SUBROUTINE SOLVES THE ERROR FUNCTION.
0213c
0214c
0215     DIMENSION XT( 30)
0216     DATA J/1/
0217     IF (J-2) 10,30,30
0218 10    DO 20 K=1,30
0219     N=2*(K-1)+1
0220     E=303.0/N
0221     IF (E .GT. 38.) E=38.0
0222 20    XT(K)=10.0**E
0223     J=2
0224     CHECK=0.00001
0225 30    SUM=0.0
0226     IF (X.LT.2.5) 60 TO 40
0227     ERF=1.0
0228     60 TO 70
0229 40    D=1.0
0230     AN=1.0
0231     DO 50 I=1,30
0232     IF (X.5T.XT(I)) 60 TO 60
0233     N=I-1
0234     AN=2.0*AN
0235     IF (N.EQ.0) AN=1.0
0236     ND=2*N+1
0237     D=D*ND
0238     XX=X**ND
0239     TERM=AN*XX/D
0240     IF (TERM.LT.CHECK) 60 TO 60
0241     SUM=SUM+TERM
0242     R=TERM/SUM
0243     IF (R.LT.CHECK) 60 TO 60
0244 50    CONTINUE
0245 60    ERF=1.12838*EXP(-X*X)**SUM
0246 70    IF (KODE-2) 90,80,80
0247 80    ERF=1.0-ERF
0248c
0249 90    RETURN
0250    END

```

```

0251C
0252C
0253C
0254 SUBROUTINE MAINLP
0255C
0256C DRIVING SUBROUTINE WHICH INDEXES THROUGH THE GRID POINTS
0257C IN THE INPUT MEASUREMENT PLANE.
0258C NP, RADLOC, ANGLOC, AND P HAVE THE FIRST
0259C ARRAY DIMENSION EQUAL TO 11. TEN OF THE
0260C 11 POSITIONS ARE AVAILABLE FOR USE. THE
0261C REMAINING POSITION IS NEEDED FOR INTERNAL PROCESSING.
0262C
0263C COMMON AB,ANGLOC(20),AUG,BETA2,BF,CDPOP3(10),CMAYG(10),FD,LSHFT,
0264C % CMIN(10),DKMX(10),DKSS(10),FACE(39,65),FACTOR,FARCE(39,65),BSF,
0265C % J1,J2,KEY,KD,LCONTFL,NN,NP,NR,P(11,20),PR(10),PS(11,20),CKP,
0266C % PSPEC(20),PVALUE,QAV,QPT2,R,RADLOC(11),RANGE,R1,RMAX,BRP(11),
0267C % RT,S6DK(10),S6P(10),SIG,SMAYG,STAT1,STATD,T,TDP1,TDP2,TMIN,
0268C % TDP3,THETA,THTMIN(10),TITLE1(20),TITLE2(20),TMAYG,TMAX,RKP,U2
0269C
0270C DATA BLANK/1H /,PLUS/1H+/
0271C
0272C CALCULATION OF R AND THETA
0273C APPROX. 1.0R(OUTER) <-- Y --> APPROX. -1.0R(OUTER)
0274C APPROX. -1.0R(OUTER) <-- X --> APPROX. 1.0R(OUTER)
0275C FACTOR% SEE LINE 39 OF SUBROUTINE CARDRD
0276C
0277C DO 10 IO=1,39
0278C DO 10 JO=1,51
0279C Y=(FLOAT(20-IO))*FACTOR
0280C X=((FLOAT(JO-26))/1.306)*FACTOR
0281C R=SQRT(X*X+Y*Y)
0282C IF (X.EQ.0.0) GO TO 26
0283C OMEGA=ATAN(ABS(Y/X))
0284C GO TO 27
0285C 26 OMEGA=1.5708
0286C
0287C CHANGING FROM CONVENTIONAL R-OMEGA SYSTEM TO THE
0288C R-THETA SYSTEM USED IN THE INTERPOLATION PROCESS.
0289C
0290C 27 IF (X.GE.0.0.AND.Y.LE.0.0) THETA=1.5708-OMEGA

```

```

0291 IF (X.GE.0.0.AND.Y.LT.0.0) THETA=1.5708+OMEGA
0292 IF (X.LT.0.0.AND.Y.LT.0.0) THETA=4.71239-OMEGA
0293 IF (X.LT.0.0.AND.Y.GE.0.0) THETA=4.71239+OMEGA
0294 IF (THETA.GE.6.28318) THETA=6.28318
0295 IF (THETA.LT.0.0) THETA=0.0
0296 THETA=THETA*(360.0/6.28318)
0297C
0298C MAKE MAP ROUND OR ELSE
0299C
0300 IF (R.LT.RADLOC(1).OR.R.GT.RADLOC(NR)) GO TO 9
0301C
0302C CALLING INTERPOLATION AND SYMBOL SUBROUTINE.
0303C
0304 CALL INTERP
0305 CALL SYMBL
0306 FACE(ID,JD)=PVALUE
0307 GO TO 10
0308 9 FACE(ID,JD)=BLANK
0309 10 CONTINUE
0310C
0311 RETURN
0312 END
0313C
0314C -----

```



```

0315c
0316      SUBROUTINE DISTRT
0317c
0318c      SUBROUTINE WHICH CALCULATES SIMPLE DISTORTION PARAMETERS.
0319c      NP, RADLOC, ANGLC, AND P HAVE THE FIRST
0320c      ARRAY DIMENSION EQUAL TO 11. TEN OF THE
0321c      11 POSITIONS ARE AVAILABLE FOR USE. THE
0322c      REMAINING POSITION IS NEEDED FOR INTERNAL PROCESSING.
0323c
0324      COMMON AB, ANGLC(20), AUD, BETA2, BF, CDPOP3(10), CMAVG(10), FO, ISHFT,
0325      & CMMIN(10), DKMX(10), DKSS(10), FACE(39,65), FACTOR, FARCE(39,65), BSF,
0326      & J1, J2, KEY, KD, LCNTFL, NN, NP, NR, P(11,20), PR(10), PS(11,20), CKP,
0327      & PSPEC(20), PVALUE, QAV, QPT2, R, RADLOC(11), RANGE, RI, RMAV, BRP(11),
0328      & RT, SGDK(10), SGP(10), SIG, SMAVG, STAT1, STATO, T, TDP1, TDP2, TMIN,
0329      & TDP3, THETA, THTMIN(10), TITLE1(20), TITLE2(20), TMAVG, TMMAX, RKP, U2
0330c
0331      DIMENSION SEG(10), RADP(8,10), THTTOT(10), CMMAX(10)
0332      LOGICAL STAT1, STATO, LCNTFL, LADD
0333c
0334c      CALCULATION OF SIMPLE CIRCUMFERENTIAL DISTORTION PARAMETERS.
0335c
0336      DO 10 I=J1, J2
0337c
0338c      CALCULATION OF CMMAX, CMMIN, AND CMAVG FOR EACH RING
0339c
0340      CMMAX(I)=0.0
0341      CMMIN(I)=50000.0
0342      CMAVG(I)=0.0
0343      DO 11 J=1, NP
0344      CMMAX(I)=AMAX1(P(I, J), CMMAX(I))
0345      CMMIN(I)=AMIN1(P(I, J), CMMIN(I))
0346 11  CMAVG(I)=CMAVG(I)+(P(I, J)/FLOAT(NP))
0347c
0348c      CALCULATION OF CDPOP'S FOR EACH RING.
0349c
0350 10  CDPOP3(I)=(CMAVG(I)-CMMIN(I))/CMAVG(I)
0351c
0352c      CALCULATION OF TMMAX AND TMIN.
0353c
0354      TMMAX=0.0

```

```

0355 TMIN=50000.0
0356 DO 7 I=J1,J2
0357 TMAX=AMAX1(CMAX(I),TMAX)
0358 7 TMIN=AMIN1(CMIN(I),TMIN)
0359C
0360C CALCULATION OF TMAVG
0361C
0362 DIV=0.0
0363 PTSUM=0.0
0364 DO 33 I=J1,J2
0365 DO 33 J=1,NP
0366 PTSUM=PTSUM+P(I,J)
0367 33 DIV=DIV+1.0
0368 TMAVG=PTSUM/DIV
0369C
0370C CALCULATION OF TDP'S
0371C
0372 TDP1=(TMAX-TMIN)/TMAX
0373 TDP2=(TMAX-TMIN)/TMAVG
0374 TDP3=(TMAVG-TMIN)/TMAVG
0375C
0376C SECTION TO CALCULATE THTMIN FOR EACH RING.
0377C
0378 DO 9 I=J1,J2
0379 DO 13 LL=1,10
0380 13 SE6(LL)=0.0
0381 IF (NP.EQ.1) GO TO 8
0382 L=1
0383 LADD=.FALSE.
0384 DO 12 J=1,NP
0385 K0=J-1
0386 IF (K0.EQ.0) K0=NP
0387 K1=J
0388 A1=AM6LOC(K1)
0389 K2=J+1
0390 IF (K2.GT.NP) K2=K2-NP
0391 A2=AM6LOC(K2)
0392 IF ((J+1).GT.NP) A2=A2+360.0
0393 IF (J.GT.1) GO TO 14
0394 IF (P(I,K1).LT.CMAVG(I)) GO TO 21

```

```

0395 IF (P(I,K1).EQ.CMAVG(I).AND.P(I,K2).LT.CMAVG(I)) GO TO 22
0396 GO TO 14
0397 22 IF (P(I,K0).GE.CMAVG(I)) GO TO 14
0398 21 LADD=.TRUE.
0399C
0400C LOGIC DETERMINES EACH SEGMENT'S CONTRIBUTION TO THMIN ON EACH RING
0401C
0402 14 RINC=0.0
0403 IF (P(I,K2).LT.CMAVG(I).AND.P(I,K1).LT.CMAVG(I)) RINC=R2-A1
0404 IF (P(I,K2).LT.CMAVG(I).AND.P(I,K1).EQ.CMAVG(I)) RINC=R2-A1
0405 IF (P(I,K2).EQ.CMAVG(I).AND.P(I,K1).LT.CMAVG(I)) RINC=R2-A1
0406 IF (P(I,K2).GT.CMAVG(I).AND.P(I,K1).LT.CMAVG(I))
0407 % RINC=((R2-A1)/(P(I,K2)-P(I,K1)))♦CMAVG(I)-P(I,K1))
0408 IF (P(I,K2).LT.CMAVG(I).AND.P(I,K1).GT.CMAVG(I))
0409 % RINC=((R2-A1)/(P(I,K1)-P(I,K2)))♦CMAVG(I)-P(I,K2))
0410C
0411C LOGIC DETERMINES HOW TO ADD TOGETHER THE CONTRIBUTIONS OF EACH SECTION
0412C
0413 IF (RINC.EQ.0.0) GO TO 20
0414 IF (P(I,K2).LT.CMAVG(I).AND.P(I,K1).GT.CMAVG(I)) GO TO 23
0415 24 SEG(L)=SEG(L)+RINC
0416 GO TO 12
0417 23 IF (P(I,K0).GE.CMAVG(I)) GO TO 24
0418 IF (J.EQ.1) GO TO 24
0419 L=L+1
0420 GO TO 24
0421 20 IF (J.EQ.1) GO TO 12
0422 IF (SEG(L).EQ.0.0) GO TO 12
0423 L=L+1
0424 12 CONTINUE
0425 K3=0
0426 THTTOT(I)=0.0
0427 DO 18 K=1,10
0428 IF (SEG(K).NE.0.0) K3=K3+1
0429 18 THTTOT(I)=THTTOT(I)+SEG(K)
0430 IF (LADD) SEG(I)=SEG(I)+SEG(K3)
0431 IF (LADD) K3=K3-1
0432C
0433C SEARCH FOR LARGEST DEPRESSION BELOW AVERAGE ON EACH RING
0434C THIS WILL BECOME THMIN FOR THAT RING

```

```

0435C      THTMIN(I)=0.0
0436      DO 19 K=1,K2
0437      IF (SEG(K).GT.THTMIN(I)) THTMIN(I)=SEG(K)
0438 19      GO TO 9
0439      CALL PRNT(3)
0440 8      THTMIN(I)=0.0
0441      THTMIN(I)=0.0
0442 9      CONTINUE
0443C
0444C      CALCULATION OF AVERAGE STATIC PRESSURE.
0445C
0446      DIV=0.0
0447      STATSM=0.0
0448      IF (.NOT.STATI) GO TO 29
0449      DO 30 I=1,NP
0450 30      STATSM=STATSM+P(I,I)
0451      DIV=DIV+FLOAT(NP)
0452 29      IF (.NOT.STATO) GO TO 31
0453      DO 32 I=1,NP
0454 32      STATSM=STATSM+P(NR,I)
0455      DIV=DIV+FLOAT(NP)
0456 31      IF (DIV.EQ.0.0) DIV=1.0
0457      SMAVG5=STATSM/DIV
0458C
0459C      CALCULATION OF AVERAGE MACH NUMBER WHEN NO STATIC PRESSURES ARE INPUT
0460C
0461      AMACH=5.0*((ABS(TMAVG/SMAVG5))**.286-1.0)
0462      RMAVG=SQRT(ABS(AMACH))
0463C
0464C      CALCULATION OF SIMPLE RADIAL DISTORTION PARAMETERS.
0465C
0466      DO 40 IR=1,NR
0467      DO 40 ITH=1,8
0468      R=RADLOC(IR)
0469      THETA=45*(ITH-1)
0470C
0471C      CALL INTERPOLATION SUBROUTINE TO OBTAIN INTERPOLATED VALUES
0472C      OF MEASUREMENTS ON EACH RING AT DISCRETE THETA LOCATIONS.
0473C      NOTICE THAT SUBROUTINE /INTERP/ WILL GO THROUGH THE PROCESS OF RADIAL
0474C      INTERPOLATION EVEN THOUGH IT IS NOT NECESSARY. THIS REDUNDANCY IS NOT

```

0475c EXTREME SINCE THE RADIAL INTERPOLATION IS NOT EXECUTED TOO MANY TIMES
0476c
0477 CALL INTERP
0478 40 RADP(ITHT,IR)=PVALUE
0479c
0480c CALL SUBROUTINE TO CALCULATE SPECIFIC DISTORTION PARAMETERS.
0481c
0482 CALL DISPAR
0483c
0484 RETURN
0485 END
0486c
0487c -----

```

0488c
0489      SUBROUTINE EXTRME (SGK,KSS,KMAX,T,FLUR)
0490c
0491c      SUBROUTINE WHICH MANAGES COMPUTATION OF EXTREME VALUES
0492c      SGKF IS DISTORTION FACTOR SIGMA
0493c      KSS IS MEAN VALUE
0494c      KMAX IS EXTREME VALUE
0495c      T IS TIME ON POINT, SECONDS
0496c      FLUR IS VORTEX FLUX RATE.
0497c
0498      REAL KSS,KMAX
0499      SGKF=SGK
0500 110   AKS=KSS/SGKF
0501      FLUX=T*FLUR
0502      DKS=0.0
0503      KMAX=0.0
0504      IF (SGKF.EQ.0.0) GO TO 120
0505      IF (AKS.GT.64.0) AKS=64.0
0506      CALL SEARCH (AKS,DKS,FLUX)
0507      KMAX=KSS+DKS*SGKF
0508c
0509 120   RETURN
0510      END
0511c
0512c -----

```

```

0513C
0514 SUBROUTINE PPIX(LQ)
0515C
0516C SUBROUTINE TO TRANSFORM INPUT MEASUREMENTS INTO MAPPING PARAMETERS.
0517C SUBROUTINE ALSO CONTROLS SOME OUTPUT
0518C
0519C NP, RADLOC, ANGLOC, AND P HAVE THE FIRST
0520C ARRAY DIMENSION EQUAL TO 11. TEN OF THE
0521C 11 POSITIONS ARE AVAILABLE FOR USE. THE
0522C REMAINING POSITION IS NEEDED FOR INTERNAL PROCESSING
0523C
0524C COMMON AB,ANGLOC(20),AUD,BETA2,BF,CDPOP3(10),CNAV5(10),FO,ISHFT,
0525C % CMMIN(10),DKMX(10),DKSS(10),FACE(39,65),FACTOR,FARCE(39,65),BSF,
0526C % J1,J2,KEY,KD,LCNTFL,NN,NP,NR,P(11,20),PR(10),PS(11,20),CKP,
0527C % PSPEC(20),PVALUE,QAV,QPT2,R,RADLOC(11),RANGE,RI,RNAV,BRP(11),
0528C % RT,S6DK(10),SGP(10),SIG,SMWV5,STAT1,STATO,T,TDP1,TDP2,TMIN,
0529C % TDP3,THETA,TMIN(10),TITLE1(20),TITLE2(20),TNAV5,TMAX,RKP,U2
0530C
0531C DIMENSION DPC(6)
0532C LOGICAL STAT1,STATO,LCNTFL,LQ
0533C DATA DPC(1),DPC(2),DPC(3)/10.,20.,25./
0534C DATA DPC(4),DPC(5),DPC(6)/40.,50.,100./
0535C IF (LQ) 60 TO 55
0536C
0537C SECTION THAT ENABLES INTERPOLATION THROUGH THE CENTER OF THE CONTOUR MAP
0538C SHIFT RADIAL LOCATIONS OUTWARD IF THE CENTER IS TO BE FILLED IN
0539C
0540C IF (.NOT.LCNTFL) 60 TO 50
0541C IF (ISHFT.EQ.2) 60 TO 50
0542C DO 51 I=1,NR
0543C NR1=NR+2-I
0544C RADLOC(NR1)=RADLOC(NR1-1)
0545C
0546C K --> ORIGINAL NO. OF POINTS ON THIS RING
0547C SHIFT ANGULAR POSITIONS OUTWARD; SHIFT DATA OUTWARD
0548C
0549C DO 51 J=1,NP
0550C P(NR1,J)=P(NR1-1,J)
0551C NR=NR+1
0552C

```

```

0553C SET UP 8-POINT DUMMY INNER RING, AND FIND AVERAGE PRESSURE ON THE RING
0554C
0555 49 RADLOC(1)=0.01
0556 PSUM=0.0
0557 DO 54 I=1,NP
0558 I1=I-1
0559 IF (I1.EQ.0) I1=NP
0560 A1=ANGLOC(I1)
0561 IF (I-1).EQ.0) A1=A1-360.0
0562 I2=I+1
0563 IF (I1.GT.NP) I2=1
0564 A2=ANGLOC(I2)
0565 IF ((I+1).GT.NP) A2=A2+360.0
0566 DELTHT=((A2-A1)/2.0)/360.0
0567 54 PSUM=PSUM+(DELTHT*P(2,I))
0568C
0569C DUMMY RING DATA AND POSITION SET-UP
0570C
0571 DO 53 I=1,8
0572 TH=(I-1)*45
0573 ANGLOC(I)=TH
0574 53 P(1,I)=PSUM
0575 50 PCMN=0.0
0576 PCMX=0.0
0577C
0578C MAPPING PARAMETERS GENERATED FROM INPUT MEASUREMENTS
0579C
0580 DO 12 I=1,NR
0581 DO 12 J=1,NP
0582 P(I,J)=((P(I,J)/TMAVG)-1.0)*100.0)
0583 IF (PCMN.GT.P(I,J)) PCMN=P(I,J)
0584 12 IF (PCMX.LT.P(I,J)) PCMX=P(I,J)
0585C
0586C SECTION TO WRITE OUT MAPPING PARAMETERS.
0587C MAPPING PARAMETERS PUT INTO PROPER FORM FOR SYNEOL SUBROUTINE
0588C
0589 PCMN=-PCMN
0590 PMX=AMAX1(PCMN,PCMX)
0591 DO 130 I=1,6
0592 IF (PMX.LT.DPC(I)) GO TO 131

```



```

0593 130 CONTINUE
0594      I=6
0595 131 RANGE=2.0*DPG(I)
0596      DO 13 I=1,NR
0597      DO 13 J=1,NP
0598C
0599C      CONVERT DELTA PERCENT TO DELTA RANGE INCREMENTS -10.0 TO +10.0
0600C
0601 13   P(I,J)=(P(I,J)/(RANGE/20.0))-10.0
0602C
0603      RETURN
0604C
0605C      ENTRY POINT FOR CALCULATION OF BLOC.
0606C
0607 55   RMSUM=0.0
0608      KMSUM=0
0609      DO 30 I=J1,J2
0610      DO 30 J=1,NP
0611      PC=P(I,J)+(P(NR,J)-P(I,J))*((RADLOC(I)-RADLOC(1))/(RADLOC(NR)-
0612      %   RADLOC(1)))
0613C
0614C      NACH NUMBER IS CALCULATED FOR EACH INPUT MEASUREMENT LOCATION.
0615C
0616      GAM=0.286
0617      IF (PC.EQ.0.0) PC=0.00001
0618      AMACH=5.0*((ABS(P(I,J)/PC))*GAM-1.0)
0619      IF (AMACH) 610,630,620
0620 610   AMACH=-SORT(ABS(AMACH))
0621      GO TO 630
0622 620   AMACH=SORT(AMACH)
0623 630   RMSUM=RMSUM+AMACH
0624 30   KMSUM=KMSUM+1
0625C
0626C      CALCULATION OF AVERAGE NACH NUMBER.
0627C
0628      RMAY=RMSUM/FLOAT(KMSUM)
0629C
0630      RETURN
0631      END
0632C
0633C

```

```

0634C
0635 SUBROUTINE FRF(RS,FAUF)
0636C
0637C SUBROUTINE TO EVALUATE FUNCTION OF AREA/UD VS SIGMA RATIO,
0638C USES AN ITERATIVE SCHEME FOR INVERSE SOLUTION
0639C
0640 TOL=0.0001
0641 FAUL=0.5
0642 RSL=.5205
0643 FAU=0.5+.96061*(RS-.5205)
0644 K=1
0645 DO 100 J=1,100
0646 CALL SUMMER (FAU,RSC,K)
0647 ABE=ABS(RSC-RS)
0648 IF (ABE.LT.TOL) GO TO 110
0649 SLOPE=(FAU-FAUL)/(RSC-RSL)
0650 FAUL=FAU
0651 RSL=RSC
0652 100 FAU=FAUL+SLOPE*(RS-RSL)
0653 110 FAUF=FAU
0654C
0655 RETURN
0656 END
0657C
0658C -----

```

```

0659C SUBROUTINE SYMELE
0660
0661C SUBROUTINE TO SUPPLY THE SYMEOLS FOR THE LINE PRINTER CONTOUR MAP
0662C
0663C
0664C COMMON AB,ANGLOC(20),AUD,BETA2,BF,CDPOP3(10),CMAVG(10),FD,ISHFT,
0665C % CMMIN(10),DKMX(10),DKSS(10),FACE(39,65),FACTOR,FARCE(39,65),BSF,
0666C % J1,J2,KEY,KD,LCONTFL,NN,NP,NR,P(11,20),PR(10),PS(11,20),CKP,
0667C % PSPEC(20),PVALUE,QAV,QPT2,R,RADLOC(11),RANGE,RI,RNAV,BRP(11),
0668C % RT,SGDK(10),SGP(10),SIG,SMAVG,STATI,STATD,T,TDP1,TDP2,TMIN,
0669C % TDP3,THETA,THMIN(10),TITLE1(20),TITLE2(20),TMAVG,TMAX,RKP,U2
0670C
0671C DIMENSION OUTSYM(20),OUTSIN(20)
0672C
0673C TWO LISTS OF SYMEOLS COVER ALL POSSIBLE TYPES OF CONTOUR MAPS.
0674C
0675C DATA OUTSYM/1H.,1H-,1H=,1H+,1H1,1H<,1H#,1H$,1H0,1H',1Hx,1H$,
0676C % 1H0,1H>,1H$,1Hy,1Hh,1Ht,1Ha/
0677C
0678C IF BETA EXCEEDS MAX OR MIN RANGE INCREMENTS, ASSIGN MAX OR MIN TO IT
0679C
0680C IF (PVALUE.GE.0.0) PVALUE=-.0001
0681C IF (PVALUE.LE.-20.0) PVALUE=-19.9999
0682C
0683C SECTION TO DETERMINE THE PROPER SYMEOL FOR THE CONTOUR MAP.
0684C
0685C DO 10 I=1,20
0686C UP=1-I
0687C IN=UP-1.0
0688C IF (PVALUE.LE.UP.AND.PVALUE.GT.IN) GO TO 11
0689C 10 CONTINUE
0690C 11 PVALUE=OUTSYM(I)
0691C
0692C RETURN
0693C END
0694C
0695C

```

```

0696C
0697
0698C
0699C
0700C
0701
0702
0703
0704
0705
0706
0707C
0708
0709
0710C
0711C
0712C
0713C
0714C
0715C
0716C
0717C
0718C
0719C
0720C
0721C
0722C
0723
0724
0725
0726
0727
0728
0729
0730C
0731
0732C
0733C
0734C
0735C

SUBROUTINE NEWPSD(KY)

SUBROUTINE TO EVALUATE RMS AND PSD FUNCTIONS FROM DYNAMIC PRESSURES.

COMMON AB,ANGLOC(20),AUG,BETA2,BF,CIDPOF3(10),CMAY5(10),FO,ISHFT,
& CMMIN(10),DKMX(10),DKSS(10),FADE(39,65),FACTOR,FARCE(39,65),BSF,
& J1,J2,KEY,KD,LCONTFL,NN,NP,NR,P(11,20),PR(10),PS(11,20),CKP,
& PSPEC(20),PVALUE,QAY,OPT2,R,RADLOC(11),RANGE,RI,RMAY,BRF(11),
& RT,S6DK(10),SGP(10),SIG,SMAY5,STAT1,STAT0,T,TDP1,TDP2,TNMIN,
& TDP3,THETA,THMIN(10),TITLE1(20),TITLE2(20),TMAV5,TMAX,RKP,U2

REAL MD,MFR

DIMENSION NODRD(40),RVSIZ(40),ENDPRD(40)

ON CALL FROM MAIN (KY=1) INPUT DISTORTION FACTOR KEY; TIME ON POINT,
AND FILTER FREQUENCIES. DISTORTION FACTORS ARE DEFINED BRIEFLY BELOW:

'1' KTHETA - PRATT & WHITNEY CIRCUMFERENTIAL DISTORTION FACTOR
'2' KD2 - PRATT & WHITNEY CIRCUMFERENTIAL DISTORTION FACTOR
'3' IDC - GENERAL ELECTRIC CIRCUMFERENTIAL DISTORTION FACTOR
'4' IDR - GENERAL ELECTRIC RADIAL FLOW DISTORTION FACTOR
'5' KRA - PRATT & WHITNEY RADIAL FLOW DISTORTION FACTOR
'6' KAZ - PRATT & WHITNEY COMBINED CIRCUMFERENTIAL/RADIAL DISTORTION
'7' DSPR - DELTA (LOSS IN) STALL PRESSURE RATIO
'8' ID - GENERAL ELECTRIC COMBINED CIRCUMFERENTIAL/RADIAL DISTORTION

IF (KY-2) 100,250,255
READ (5,130) KD,T,FO,FCD
IF (T.EQ. 0) T = 1.
IF (FO.LT. 1) FO = 500.
IF (FCD.LT. 1) FCD = 1000.
RT=RADLOC(NR)
PI=PRADLOC(1)

RETURN

ON 1ST CALL FROM UNSTDY, INPUT IDENTIFICATION AND CONTROL PARAMETERS
AND SET STEADY STATE DISTORTION FACTORS.

```

```

0736 250 READ (5,70) ALPH,PSI,MD,U2,BF,CKP,RKP,MFR,NTUR,SPTRC
0737 IF (SPTRC.EQ. 0) SPTRC = 1.
0738 IF (PSPEC(3)) 101,102,101
0739 101 RD=PSPEC(4)/PSPEC(3)
0740 BSF=0.24+0.76/EXP(3.6*RD**0.79)
0741 IF (CKP.EQ.0.0) CKP=16.4
0742 IF (RKP.EQ.0.0) RKP=11.1
0743 PSPEC(8)=BSF*CKP*PSPEC(3)+RKP*PSPEC(4)
0744 102 IF (BF.EQ.0.0) BF=1.0
0745 ETA=TNAV6
0746 OPT2=QAV/TNAV6
0747 PSPEC(6)=PSPEC(1)+BF*PSPEC(5)
0748 DO 241 I=1,10
0749 241 DKSS(I)=PSPEC(I)
0750C
0751 RETURN
0752C
0753C ON 2ND CALL FROM UNSTDY COMPUTE MAX INSTANTANEOUS DISTORTION FACTORS
0754C
0755 255 NN=0
0756 IF (MFR.EQ. 0) MFR = 1
0757 WRITE (6,10) TITLE1,TITLE2
0758 WRITE (6,20) T,FO,RT,RI,SPTRC
0759 WRITE (6,30) ALPH,PSI,MD,ETA,MFR,U2,OPT2
0760 WRITE (6,120) FCD
0761C
0762C BRANCH TO TUREULNCE MODELLING SUBROUTINE IF THERE IS NO DYNAMIC DATA
0763C
0764 IF (NTUR.EQ. 1) GO TO 500
0765 WRITE (6,50)
0766 DO 258 I=1,10
0767 258 SSP(I)=0.0
0768C
0769C INPUT DYNAMIC DATA
0770C MFS IS RUN CODE. IF ZERO IS ENTERED, THE INPUT SEQUENCE IS EXITED
0771C MFR IS A DYNAMIC PRESSURE PROBE NUMBER
0772C RS IS RATIO OF FILTERED/UNFILTERED MEAN SQUARE VALUE OF DYNAMIC
0773C PRESSURE FLUCTUATIONS.
0774C SIG IS RMS VALUE OF DYNAMIC PRESSURE FLUCTUATION.
0775C

```

```

0776 260 READ (5,90) NPG,NPR,RS,SIG
0777 IF (RS.EQ. 0) RS = 0.5
0778 IF (RS.GT. 0.7) RS = 0.7
0779 IF (NPG.NE.0) GO TO 300
0780C
0781C CALL MAXDP TO COMPUTE MAXIMUM DISTORTION VALUES.
0782C
0783 CALL MAXDP
0784 DO 372 I=1,NN
0785 AVSIZ(I)=AVSIZ(I)/(AB)
0786 372 FNDPRD(I)=FLOAT(NDPRD(I))
0787 WRITE (7) (FNDPRD(I),I=1,NN), (AVSIZ(I),I=1,NN)
0788 RETURN
0789C
0790C COMPUTE MEAN VORTEX CORE SIZE FOR EACH PROBE AND SUM REAR AND SIG.
0791C NN IS COUNTER FOR NUMBER OF DYNAMIC PRESSURE PROBES.
0792C
0793 300 CALL FFF (RS,FAUF)
0794 AUO=FAUF/(7.976*PCO)
0795 AB=12.0*AUO*U2
0796 AB=AB/RT
0797 WRITE (6,60) NPR,RS,SIG,AB
0798 SGP(1)=SGP(1)+SIG*SIG
0799 SGP(2)=SGP(2)+AB*AB
0800 NN=NN+1
0801 NDPRD(NN)=NPR
0802 AVSIZ(NN)=AB
0803 GO TO 260
0804 500 CONTINUE
0805C
0806C CALL TURBULENCE SUBPROGRAM, TURBUL, TO COMPUTE THE RMS LEVELS.
0807C SPTRC IS THE TOTAL PRESSURE RECOVER THROUGH INLET SHOCK SYSTEM,
0808C (SPTRC=1. FOR SUBSONIC AND TRANSONIC SPEED).
0809C RS IS RATIO OF FILTERED/UNFILTERED MEAN SQUARE VALUE OF DYNAMIC
0810C PRESSURE FLUCTUATIONS.
0811C SIG IS RMS VALUE OF DYNAMIC PRESSURE FLUCTUATION.
0812C
0813 CALL TURBUL (PS,RAIDLOC,NR,NP,U2,OPT2,TNAV6,ND,SPTRC,SIG)
0814 RS=0.5
0815 CALL FFF (RS,FAUF)

```

```

0816 AUD=FAUF/(7.976*FCD)
0817 AB=12.0*AUD*U2/RT
0818 NN=1
0819 AVSIZ(NN)=AB
0820 NOPRO(NN)=1
0821 SGP(1)=S16
0822 SGP(2)=AB*AB
0823C
0824C
0825C
0826
0827
0828
0829
0830 375
0831
0832C
0833
0834C
0835 10
0836 20
0837
0838 30
0839
0840 50
0841 60
0842 70
0843 80
0844 90
0845 120
0846 130
0847C
0848
0849C
0850C

```

CALL MAXDP TO COMPUTE MAXIMUM DISTORTION VALUES.

CALL MAXDP

DO 375 I=1,NN

AVSIZ(I)=AVSIZ(I)/(AB)

FNOPRO(I)=FLOAT(NOPRO(I))

CONTINUE

WRITE (7) (FNOPRO(I), I=1,NN), (AVSIZ(I), I=1,NN)

RETURN

FORMAT (1H1,19X,20A4/19X,20A4)

FORMAT (/14X,1HT,6X,2HFO,6X,2HRT,6X,2HRI,5X,5HSPTRC/5X,F12.3,
F8.1,3F8.3)

FORMAT (/13X,4HALPH,5X,3HPS1,4X,2HMD,5X,3HETA,4X,3HMER,4X,2HU2,
5X,4HOPT2/10X,F7.3,F8.3,3F7.3,F7.1,F8.4)

FORMAT (/10X,5HPRBE,3X,2HRS,3X,6HSG/PT2,3X,4HA/RT)

FORMAT (10X,13,1X,4F7.4)

FORMAT (5X,8F5.3,15,F5.3)

FORMAT (5X,215,2F5.3,11F5.2)

FORMAT (5X,215,F5.3,F6.4)

FORMAT (/11X,10HRS AT FC =,F8.1)

FORMAT (5X,15,7F10.5)

END

```

0351C
0352 SUBROUTINE MAXDP
0353C
0354 COMMON AB,ANGLOC(20),AUD,BETA2,BF,CDPOP3(10),CMAY5(10),FO,ISHFT,
0355 % CMIN(10),DMX(10),DKSS(10),FACE(39,65),FACTOR,FARCE(39,65),BSF,
0356 % J1,J2,KEY,KD,LCHTFL,NN,NP,NR,P(11,20),PR(10),PS(11,20),CKP,
0357 % PSPEC(20),PVALUE,QAV,OPT2,R,RADLOC(11),RANGE,R1,RNAV,BRP(11),
0358 % RT,SGDK(10),SGP(10),SIG,SMAY5,STAT1,STATD,T,TDP1,TDP2,TMMIN,
0359 % TDP3,THETA,THMIN(10),TITLE1(20),TITLE2(20),TNAV5,TMMAX,RKP,U2
0360C
0361 DIMENSION LAB(8),FO(10),DKBAR(10)
0362 DATA LAB(1),LAB(2),LAB(3),LAB(4)/4HKTTA,4H KD2,4H IDC,4H IDR/
0363 DATA LAB(5),LAB(6),LAB(7),LAB(8)/4H KRA,4H KA2,4H DSPR,4H ID/
0364C
0365 FO(1)=1.0
0366 FO(2)=1.0
0367 FO(3)=1.0
0368 FO(4)=OPT2
0369 FO(5)=OPT2
0370 FO(6)=OPT2
0371 FO(7)=1.0
0372 FO(8)=1.0
0373 FO(9)=OPT2
0374 FO(10)=1.0
0375 RTUD=RT/U2/12.0
0376 400 AN=NN
0377C
0378C FIND MEAN VALUES OF SIGMA AND AREA
0379C
0380 S16=SQRT(SGP(1)/AN)
0381 AB=SQRT(SGP(2)/AN)
0382 SGP(1)=S16/OPT2
0383C
0384C FIND FLUX AND ENGINE FILTER EFFECTS
0385C
0386 FL=ANRTU(AB)/RTUD
0387 TFL=T*FL
0388 FAEUD=FO*RTUD*AB
0389 CALL RATA (REFK,FAEUD)
0390 VB=0.949*SGP(1)*REFK/SQRT(AB)

```



```

0891      SIGF=SIG*RKFK
0892C
0893C      FIND MAXIMUM VALUES FOR EACH DISTORTION FACTOR.
0894C
0895      DO 450 I=3,10
0896      J=1-2
0897C
0898C      GET SIGMA RATIOS AND DELTAS FOR ALL FACTORS EXCEPT KA2 AND ID
0899C
0900      IF (1.E0.8) GO TO 404
0901      IF (1.E0.10) GO TO 406
0902      CALL RSIGMA (J,R1,RK,RE,DKSS(J),NP,OPT2,VB,SIGF)
0903      SGP(I)=R1*SGP(1)*FQ(I)
0904      GO TO 410
0905C
0906C      FORMULAS FOR KA2 AND ID SIGMAS
0907C
0908 404      SGP(I)=SQRT(SGP(3)*♦2+(BF*SGP(7))*♦2)
0909      GO TO 410
0910 406      SGP(I)=SQRT((BSF*CKP*SGP(5))*♦2+(RKP*SGP(6))*♦2)
0911C
0912C      FILTERED RMS LEVEL (SGDK) OF DISTORTION FACTOR.
0913C
0914 410      SGDK(I)=SGP(I)*RKFK
0915      IF (1.E0.8) GO TO 424
0916      IF (1.E0.10) GO TO 426
0917C
0918C      COMPUTE MEAN INSTANTANEOUS VALUE (DKBAR) OF DISTORTION FACTOR.
0919C
0920      DKBAR(J)=RK*SGDK(I)+DKSS(J)
0921      GO TO 450
0922C
0923C      FORMULAS FOR KA2 AND ID DELTAS.
0924C
0925 424      DKBAR(6)=DKBAR(1)+BF*DKBAR(5)
0926      GO TO 450
0927 426      DKBAR(8)=BSF*CKP*DKBAR(3)+RKP*DKBAR(4)
0928C
0929C      TO FIND MOST PROBABLE EXTREME VALUES.
0930C

```

```

0931 450 CALL EXTRE (SGDK(I),DKBAR(I),DKMX(I),T,FL)
0932 WRITE (6,60) SIG
0933 WRITE (6,70) AB
0934 IF (NM.LT.2) GO TO 459
0935 IF (NM.LT.25) GO TO 460
0936 459 WRITE (6,130) TITLE1,TITLE2
0937 460 WRITE (6,100)
0938 DO 500 I=1,8
0939 J=1+2
0940 IF (I.GT.1) GO TO 470
0941 PP=1.0-EXP(-0.051293294/TFL)
0942 IF (PP.EQ.0.) GO TO 999
0943 997 FL1=1.0/(PP+T)
0944 PP=1.0-EXP(-0.003004509/TFL)
0945 IF (PP.EQ.0.) GO TO 996
0946 995 FL2=1.0/(PP+T)
0947C
0948C FIND INSTANTANEOUS VALUES AT 95.0 AND 99.7 CONFIDENCE LEVELS
0949C
0950 470 CALL EXTRE (SGDK(I),DKBAR(I),DK950,T,FL1)
0951 CALL EXTRE (SGDK(I),DKBAR(I),DK997,T,FL2)
0952 IF (I-2) 480,490,480
0953 480 WRITE (6,110) LAB(I),DKSS(I),DKBAR(I),SGP(I),SGDK(I),DKMX(I),
0954 & DK950,DK997
0955 GO TO 500
0956 490 WRITE (6,120) LAB(I),DKSS(I),DKBAR(I),SGP(I),SGDK(I),DKMX(I),
0957 & DK950,DK997
0958 500 CONTINUE
0959 WRITE (6,75) LAB(KD), DKMX(KD)
0960C
0961 60 FORMAT (/13X,"FACE-AVERAGE RMS (SG/PT2) =",F8.5)
0962 70 FORMAT (/13X,"MEAN VORTEX SIZE (A0/RT) =",F8.5)
0963 75 FORMAT (/25X,39HMAXIMUM INSTANTANEOUS DISTORTION FACTOR//
0964 & 30X,1A10,1H=F13.4)
0965 100 FORMAT (/22X,31HDISTORTION FACTOR EXTREME VALUE//59X,21HMAXIMUM I
0966 NSTANTANEOUS/12X,6HFACTOR,4X,6HSTEADY,3X,4HMEAN,5X,5HSIGMA,4X,
0967 8SHSIGMA,5X,4HMOST,4X,5H95.0%,4X,5H99.7%/22X,5HSTATE,4X,5HVALUE,5X,
0968 83HINF,7X,2HFD,6X,4HPRDB,5X,4HPRDB,5X,4HPRDB)
0969 110 FORMAT (10X,A4,6X,F7.4,6F9.4)
0970 120 FORMAT (10X,A4,6X,F7.1,6F9.1)

```

```

0971 130  FORMAT (1H1,19%,20H4/19%,20H4)
0972C
0973      RETURN
0974C
0975 999  PP=.0000001
0976      WRITE (6,998)
0977 998  FORMAT (//10%,29HCONFIDENCE LEVEL IS INCORRECT)
0978      GO TO 997
0979 996  PP=.0000001
0980      WRITE (6,998)
0981      GO TO 995
0982C
0983      END
0984C
0985C -----

```

```

0986C
0987      FUNCTION ANRTU (ART)
0988C
0989C      FUNCTION FOR FINDING VORTEX FLUX RATE.
0990C
0991      ANRTU=1.0E+06
0992      IF (ART.EQ.0.0) GO TO 100
0993      ANRTU=0.254/(ART*ART)
0994C
0995 100      RETURN
0996      END
0997C
0998C -----

```

```

0999C
1000 SUBROUTINE R(SIGMA (J,E1,RK,AB,DKS,NP,OPT,VB,S6F)
1001C
1002C THIS ROUTINE IS USED NOW TO COMPUTE THE RATIO OF SIGMA KD
1003C TO SIGMA DFT AND THE RATIO (KEAR-KES)/SIGMA K.
1004C EF IS RATIO OF SIGMA-OPT/R
1005C PN IS NUMBER OF PROBES PER RING
1006C DT IS ANGULAR APC PER PROBE
1007C
1008 SP=1.0537*SQRT(AB)
1009 PN=NP
1010 DT=6.28319/PN
1011 GO TO (10,20,30,40,50,60,70), J
1012C
1013C THIS BRANCH APPLIES TO KTHETA.
1014C
1015 10 DKSS=DKS/VB
1016 SDKIS=1.65*SQRT(AB/PN)/EXP(40.0*(AB/DT)**4.0)
1017 SDKIL=2.106*(1.0-1.0/EXP(1.1*(AB**1.5)))
1018 SDKI=SDKIS+SDKIL*SDKIL
1019 DKTS=(1.408*AB/EXP(76.67*(AB/DT)**4))/SQRT(1.0+99.0*DKSS*DKSS)
1020 DKTL=(2.0*(1.0-1.0/EXP(1.05*(AB**1.5))))/SQRT(1.0+5.25*(0.9*DKSS/
1021 AB)**2.3)
1022 DKT=SQRT(DKTS*DKTS+DKTL*DKTL)
1023 SIGK=SQRT(SDKI-2.0*DKSS*DKT-DKT*DKT)
1024 R1=SIGK/SP
1025 RK=DKT/SIGK
1026 IF (J.EQ.7) GO TO 71
1027 GO TO 90
1028C
1029C THIS BRANCH APPLIES TO KD2.
1030C
1031 20 DKSS=DKS/(OPT*VB)
1032 IF (AB-0.45) 21,21,22
1033 21 R1=10847.0*(1.0-1.0/EXP(4.0*AB))
1034 GO TO 23
1035 22 R1=9054.0*(AB-0.45)*(1164.0+14052.0*(1.0-1.0/EXP(2.5*DKSS/
1036 97627.0)))
1037 23 RK=25763.0*(1.0-1.0/EXP(4.82*(.125*PN*AB)**1.4))/EXP(DKSS/
1038 17627.0)

```

```

1039      RK=RK/R1
1040      R1=R1*OPT/(0.1475*SP)
1041      GO TO 90
1042C
1043C      THIS BRANCH APPLIES TO IDC.
1044C
1045 30      DKSS=DKS/(OPT*VB)
1046      R11=1.01*AB**0.63
1047      R10=SQRT((0.5356*AB**0.26)**2+(1.2271*SQRT(8.0*AB/PN)/
1048      *      EXP(5.42*(AB/DT)**2))**2)
1049      RS=SQRT(1.0-1.0/EXP(0.17*(DKS/SGF)**2))
1050      IF (R11-R10) 31,31,32
1051 31      R1=R10-RS*(R10-R11)
1052      GO TO 33
1053 32      R1=R10+RS*(R11-R10)
1054 33      RK=1.458*(1.0-1.0/EXP(9.0*(.125*PN*AB)**1.4))/EXP(DKSS/1.424)
1055      *      **0.75)
1056      RK=RK/R1
1057      R1=R1*OPT/(0.1475*SP)
1058      GO TO 90
1059C
1060C      THIS BRANCH APPLIES TO IDR.
1061C
1062 40      R1=0.1324*(1.0-1.0/EXP(4.0*(AB**1.4142)))
1063      IF (AB.GT.0.3) GO TO 45
1064      RS=0.2713*SQRT(AB)-1.6528*AB*AB
1065      R1=SQRT(RS*RS+R1**R1)
1066 45      RK=0.0830*(1.0-1.0/EXP(4.0*AB*AB))
1067      RK=RK/R1
1068      R1=R1*OPT/(0.1397*SP)
1069      GO TO 90
1070C
1071C      THIS BRANCH APPLIES TO HRA
1072C
1073 50      R1=0.0825*(1.0-1.0/EXP(6.0*AB**1.475))
1074      IF (AB.GT.0.35) GO TO 55
1075      RS=0.192*SQRT(AB)-0.9253*AB*AB
1076      R1=SQRT(RS*RS+R1**R1)
1077 55      RK=0.0542*(1.0-1.0/EXP(3.75*(AB**1.6667)))
1078      RK=RK/R1

```

```

1079 R1=R1/SP
1080 GO TO 90
1081C
1082C THIS BRANCH WHICH APPLIED TO K&2 HAS BEEN NULLED.
1083C
1084 60 GO TO 90
1085C
1086C THIS BRANCH APPLIES TO D&PR.
1087C
1088 70 DKS=1.4809+DKS/QPT
1089 GO TO 10
1090 71 DKS=0.6753+DKS+QPT
1091 DKS=DKS/VB
1092 IF (AB-0.6) 72,72,75
1093 72 RR1=0.0996+(0.047/EXP(8.0+DKSS+0.8)-0.008)+ (AB-0.6)
1094 A=0.0992+1.15+(1.0-1.0/EXP(4.0+DKSS+3))
1095 IF (AB-0.28) 73,73,74
1096 73 S=0.5+DKSS
1097 AP=A/(0.28+S)
1098 RRK=AP+AB+S
1099 GO TO 76
1100 74 S=(A-0.0996)/0.42
1101 RRK=0.0996-S+(AB-0.6)
1102 GO TO 76
1103 75 RR1=0.0996
1104 RRK=0.0996
1105 76 R1=R1+RR1/0.1475
1106 RK=RK+RRK/.1475
1107C
1108 90 RETURN
1109 END
1110C
1111C -----

```

```

1112C SUBROUTINE SEARCH (AKS,DKS,ANT)
1113
1114C
1115C THIS SUBROUTINE CONTROLS SOLUTION OF (KMAX-KEAR)/SIGMA K.
1116C
1117 IF (AKS,5E,2.0) GO TO 40
1118 CALL PFXL (AKS,DKS,ANT)
1119 GO TO 120
1120 40 DKS=2.6+0.283*(ALD5(ANT)-4.60517)
1121 SLOPP=7.5
1122 DKS=DKS+0.25
1123 DO 100 J=1,100
1124 IF (DKS,LT,2.3) GO TO 120
1125 CALL PFX (AKS,DKS,PX)
1126 ERR=ABS(PX-ANT)/ANT
1127 IF (ERR,LT,0.001) RETURN
1128 IF (J,EQ,1) GO TO 60
1129 DDK=ABS(DKS2-DKS)
1130 IF (DDK,LT,0.00001) RETURN
1131 SLOPE=(ALD5(PX2)-ALD5(PX))/(DKS2-DKS)
1132 IF (SLOPE,EQ,0.0) SLOPE=SLOPP
1133 DKS=DKS+(ALD5(ANT)-ALD5(PX))/SLOPE
1134 60 PX2=PX
1135 DKS2=DKS
1136 DKS=DKSN
1137 100 SLOPP=SLOPE
1138C
1139 120 RETURN
1140 END
1141C
1142C -----

```



```

1143C SUBROUTINE PFX (AKS,DKS,PX)
1144
1145C
1146C THIS SUBROUTINE SOLVES (KMAX-KBAR)/SIGMA K FOR KBAR/SIGMA K.GT.
1147C
1148     UND=(-1)♦(8.0♦ABS(AKS-2.0))
1149     UND1=-5.♦ABS(AKS-2.5)
1150     UND2=-5.♦ABS(AKS-3.)
1151     IF (UND1.LT. -38.) UND1=-38.
1152     IF (UND2.LT. -38.) UND2=-38.
1153     IF (UND.LT. -38.) UND=-38.
1154     B=((AKS+15.)♦.023)/(ABS(AKS-1.5)♦♦1.2)♦2.4
1155     AM=1.16-(15.5♦(AKS-1.4)/(AKS+.4)♦♦4)
1156     Y1=-.66-.140♦(EXP(-.30♦ABS(AKS-6.5)))
1157     ♦+.440♦(EXP(-.99♦ABS(AKS-2.0)))
1158     ♦-.035♦(EXP(-1.2♦ABS(AKS-4.7)))
1159     ♦-.062♦(EXP(-0.7♦ABS(AKS-16.)))
1160     A=.13-(.031♦(AKS-2.7)♦.5♦(ABS(AKS-2.7)♦♦.15)♦EXP(AKS-5.)♦
1161     ♦(-.45)))-.0299♦(EXP(-.08♦ABS(AKS-16.)))
1162     ♦+.04♦(EXP(UND1))-0.177♦(EXP(-ABS(AKS-4.)))
1163     ♦-.0172♦(EXP(-ABS(AKS-6.0)))-.0534♦(EXP(UND))
1164     ♦-.0017♦(EXP(UND2))
1165     CH1=AM♦AKS+Y1+A♦(DKS-2.3)♦♦B)
1166     IF (CH1.GT. 38.) CH1=38.0
1167     IF (CH1.LT. -38.) CH1=-38.0
1168     PX=10.♦♦CH1
1169C
1170     RETURN
1171     END
1172C
1173C

```

```

1174C
1175
1176C
1177C
1178C
1179C
1180C
1181C
1182C
1183
1184
1185
1186
1187
1188
1189C
1190C
1191C
1192C
1193
1194
1195
1196
1197C
1198C
1199C
1200
1201
1202 26
1203
1204 27
1205 25
1206
1207 28
1208C
1209C
1210C
1211
1212
1213

SUBROUTINE DISPAR
      SUBROUTINE TO CALCULATE SPECIFIC DISTORTION PARAMETERS.
      NP, RADLOC, ANSLOC, AND P HAVE THE FIRST ARRAY DIMENSION EQUAL TO 11.
      TEN OF THE 11 POSITIONS ARE AVAILABLE FOR USE. THE
      REMAINING POSITION IS NEEDED FOR INTERNAL PROCESSING.

      COMMON AB,ANGLOC(20),AUG,BETA2,BF,CDPOP3(10),CMAVG(10),FO,ISHFT,
     & CMMIN(10),DKMX(10),DKSS(10),FACE(39,65),FACTOR,FARCE(39,65),BSF,
     & J1,J2,KEY,KD,LCNTFL,NH,NP,PR,P(11,20),PR(10),PS(11,20),CKP,
     & PSPEC(20),PVALUE,QAV,QPT2,R,RADLOC(11),RANGE,RI,RNAV,BRP(11),
     & RT,SGDK(10),SGP(10),SIG,SMAGS,STAT1,STATD,T,TDP1,TDP2,TMIN,
     & TDP3,THETA,THMIN(10),TITLE1(20),TITLE2(20),TMAX5,TMAX,RKP,U2

      COMMON BLOCK FOR TRANSFERRING SPECIFIC DISTORTION
      PARAMETERS TO THE OUTPUT SUBROUTINE 'LNFOUT'

      DIMENSION PT(20), QD(10), DTHETA(20), RIDC(5), RIDR(5)
      LOGICAL STAT1,STATD,LCNTFL
      DATA IT/0/
      IF (IT.EQ.1) GO TO 25

      CALCULATION OF KD2
      DINVS=0.0
      DO 26 I=J1,J2
      DINVS=DINVS+(1.0/RADLOC(I))
      DO 27 I=J1,J2
      QD(I)=(1.0/RADLOC(I))/DINVS
      RKD2=0.0
      DO 28 I=J1,J2
      RKD2=RKD2+(CDPOP3(I)*THMIN(I)*QD(I)*100.0)

      CALCULATION OF K-THETA.
      IF (IT.EQ.1) GO TO 37
      DO 36 J=1,NP
      K1=J-1

```

```

1214 IF (K1.EQ.0) K1=NP
1215 A1=ANGLOC(K1)
1216 IF ((J-1).EQ.0) A1=A1-360.0
1217 K2=J+1
1218 IF (K2.GT.NP) K2=1
1219 A2=ANGLOC(K2)
1220 IF ((J+1).GT.NP) A2=A2+360.0
1221 36 DTHETA(J)=(A2-A1)/2.0
1222 RGAM=.285714
1223 RKHT=0.0
1224 TTTT=DTHETA(1)
1225 DTHT=TTTT
1226 IF (ISHT.EQ.1) QAV=(SMAGV/RGAM)*((ABS(TMAV6/SMAGV))*RGAM)-1.0)
1227 DO 35 I=J1,J2
1228 RISIN=0.0
1229 RICOS=0.0
1230 DO 34 J=1,NP
1231 PHI=0.017453*ANGLOC(J)
1232 RISIN=RISIN+(P(I,J)/TMAV6)*SIN(PHI)*DTHETA(J)
1233 34 RICOS=RICOS+(P(I,J)/TMAV6)*COS(PHI)*DTHETA(J)
1234 35 RKHT=RKHT+PD(I)*SQRT(ABS((ABS(RISIN))*2)+(ABS(RICOS))*2))
1235 IF (QAV.EQ.0.0) QAV=1.0
1236 RKHT=(RKHT/(180.0*QAV))*TMAV6
1237C
1238C CALCULATION OF IDC-MAX AND IDR-MAX.
1239C
1240 NCHK=NR
1241 IF (STAT) NCHK=NCHK-1
1242 IF (STAT) NCHK=NCHK-1
1243 IF (NCHK.EQ.5) GO TO 39
1244 CALL PRNT(3)
1245 GO TO 39
1246 39 DO 41 J=J1,J2
1247 RIDC(J)=(CMAGV(J)-CMIN(J))/TMAV6
1248 41 RIDR(J)=(TMAV6-CMAV6(J))/TMAV6
1249 RIDCX1=(RIDC(J)+RIDC(J1+1))/2.0
1250 RIDCX2=(RIDC(J1+3)+RIDC(J1+4))/2.0
1251 RIDCMX=AMAX1(RIDCX1,RIDCX2)
1252 RIDRMX=AMAX1(RIDR(J1),RIDR(J1+4))
1253C

```

```

1254C  CALCULATION OF ID
1255C
1256      RID=RIDCMX*BSF*CKP+RIDCMX*CKP
1257C
1258C  CALCULATION OF KRA2 AND KA2
1259C
1260      SPTR=0.0
1261      DO 100 I=J1,J2
1262          PTAVR=CMHVS(I)
1263          DPTR=ABS(PTAVR/THAV5-BEP(I))/BEP(I)
1264      100  SPTR=SPTR+DPTR*DD(I)
1265          AKRA2=THAV5*SPTR/DAV
1266          AKRA2=RKTHT+AKRA2*BF
1267C
1268C  CALCULATION OF DELTA STALL MARGIN -DSM
1269C  FIRST FIND THE AVERAGE RADIAL PRESSURE AND MINIMUM PRESSURE
1270C
1271      PTR=0.0
1272      PTRM=50000.
1273      AK=NP
1274      ANR=J2-J1+1
1275      DO 300 J=1,NP
1276          PT(J)=0.0
1277      DO 200 I=J1,J2
1278      200  PT(J)=PT(J)+P(I,J)
1279          PT(J)=PT(J)/ANR
1280          PTR=PTRA+PT(J)
1281      300  PTRM=AMIN1(PT(J),PTRM)
1282          PTRA=PTRA/AK
1283          RISIN=0.0
1284          RICOS=0.0
1285      DO 400 J=1,NP
1286          PHI=0.017453*ANGLOC(J)
1287          RISIN=RISIN+(PT(J)/PTRA)*SIN(PHI)*DHT
1288      400  RICOS=RICOS+(PT(J)/PTRA)*COS(PHI)*DHT
1289          DSM=0.675*SQRT(RISIN+RICOS*RICOS)/180.0
1290C
1291C  SPECIFIC DISTORTION PARAMETERS STORED IN ARRAY 'PSPEC'
1292C  IN PREPARATION TO BEING TRANSFERRED TO 'LNFOUT'.
1293C

```

```
1294 PSPEC(1)=PKTHT  
1295 PSPEC(2)=PKD2  
1296 PSPEC(3)=RIDCMX  
1297 PSPEC(4)=RIDRMX  
1298 PSPEC(5)=HKRH2  
1299 PSPEC(6)=HKH2  
1300 PSPEC(7)=DSM  
1301 PSPEC(8)=RID  
1302C  
1303 RETURN  
1304 END  
1305C  
1306C -----
```

```

1307c SUBROUTINE PRINT (KP)
1308
1309c
1310 COMMON AB,ANGLOC(20),AUD,BETA2,BF,CDPOP3(10),CMAVG(10),FO,ISHFT,
1311 % CMMIN(10),DKMX(10),DKSS(10),FACE(39,65),FACTOR,FARCE(39,65),BSF,
1312 % J1,J2,KEY,KD,LCONTFL,NA,NP,PR,P(11,20),PS(11,20),CKP,
1313 % PSPEC(20),PVALUE,QAV,OPT2,R,RADLOC(11),RANGE,R1,RMAX,BRP(11),
1314 % RT,S6DK(10),SGP(10),SIG,SMAGS,STAT1,STATD,T,TDP1,TDP2,TMMIN,
1315 % TDP3,THETA,THMIN(10),TITLE1(20),TITLE2(20),TMAVG,TMAX,RKP,U2
1316c
1317 LOGICAL STAT1,STATD,LCONTFL
1318 GO TO (9,2,3,9,9,9,8,9), KP
1319 2 WRITE (6,125) TITLE1,TITLE2
1320c
1321c SECTION THAT WRITES THE ANGULAR POSITIONS OF THE INPUT MEASUREMENTS
1322c
1323 WRITE (6,113)
1324 WRITE (6,121)
1325 WRITE (6,123) (ANGLOC(I), I=1,NP)
1326 WRITE (6,109)
1327c
1328c SECTION THAT WRITES THE INPUT MEASUREMENTS
1329c
1330 DO 40 J=J1,J2
1331 40 WRITE (6,110) RADLOC(J), (P(J,I), I=1,NP)
1332c
1333c SECTION THAT WRITES THE BASE RADIAL PROFILES.
1334c
1335 WRITE (6,104) (RADLOC(J),J=1,NR)
1336 WRITE (6,105) (BRP(J),J=1,NR)
1337 GO TO 1000
1338 3 WRITE (6,100)
1339 9 GO TO 1000
1340 8 WRITE (6,125) TITLE1,TITLE2
1341 GO TO 1000
1342c
1343 100 FORMAT (/10X,40HIDC-MAX AND IDR-MAX CANNOT BE CALCULATED,
1344 % 10X,51HTHERE ARE NOT EXACTLY 5 RINGS OF TOTAL MEASUREMENTS)
1345 104 FORMAT (/30X,19HBASE RADIAL PROFILE//10X,8HRADI ,SF8.3)
1346 105 FORMAT (/10X,8HPT/PTA ,SF8.4)

```

```

1347 109 FORMAT (1H )
1348 110 FORMAT (5X,F6.3,4X,10F8.3/15X,10F8.3)
1349 113 FORMAT (/30X,14HPRESSURE ARRAY)
1350 121 FORMAT (1X/4X,6HRADIUS,15X,43HANGULAR POSITION OF INPUT MEASUREMEN
1351      &TS, DEG)
1352 123 FORMAT (15X,10F8.1)
1353 125 FORMAT (1H1,6X,20A4/6X,20A4)
1354C
1355 1000 RETURN
1356      END
1357C
1358C -----

```

```

1359C
1360
1361C
1362C
1363C
1364C
1365C
1366C
1367C
1368C
1369
1370
1371
1372
1373
1374
1375C
1376
1377
1378
1379
1380C
1381C
1382C
1383
1384
1385
1386 11
1387C
1388C
1389C
1390 12
1391
1392C
1393C
1394C
1395C
1396C
1397C

SUBROUTINE INTERP
INTERPOLATION SUBROUTINE
NP, RADLOC, ANGLOC, AND P HAVE THE FIRST
ARRAY DIMENSION EQUAL TO 11. TEN OF THE
11 POSITIONS ARE AVAILABLE FOR USE. THE
REMAINING POSITION IS NEEDED FOR INTERNAL PROCESSING.
COMMON AR,ANGLOC(20),AUD,BETA2,BF,CDPOP3(10),CMAY5(10),FD,ISHFT,
% CMMIN(10),DKMX(10),DKSS(10),FACE(39,65),FACTOR,FARCE(39,65),BSF,
% J1,J2,KEY,KD,LCONTFL,NA,NP,NR,P(11,20),PR(10),PS(11,20),CKP,
% PSPEC(20),PVALUE,QAV,OPT2,R,RADLOC(11),RANGE,RI,RNAV,BRP(11),
% RT,SGDK(10),SGP(10),SIG,SMAY5,STAT1,STATD,T,TDP1,TDP2,TMMIN,
% TDP3,THETA,THMIN(10),TITLE1(20),TITLE2(20),TNAV5,TMMAX,RKP,U2
DIMENSION NFIT(2),NRFIT(2),RADFIT(2),Z(2),F(2)
LOGICAL STAT1,STATD,LCONTFL
IF (NR.LT.2) CALL PRNT (3)
NR1=NR-1
DETERMINE THE CORRECT TWO RINGS TO USE IN THE INTERPOLATION PROCESS.
DO 11 I=1,NR1
  I1=I
  IF (R.GE.RADLOC(I1).AND.R.LT.RADLOC(I1+1)) 60 TO 12
  CONTINUE
INTERPOLATION BOUNDARY RING NOS.
NFIT(1)=I1
NFIT(2)=I1+1
SET-UP FOR CIRCUMFERENTIAL INTERPOLATION
DETERMINE THE TWO MEASUREMENTS ON EACH RING TO USE
IN THE CIRCUMFERENTIAL INTERPOLATION PROCESS.
INTERPOLATION RING ONE TO INTERPOLATION RING TWO

```



```

1398      DO 15 I=1,2
1399      K=NRFIT(I)
1400      IF (NP.NE.1) GO TO 21
1401C
1402C      IF ONLY ONE POINT ON RING, NO CIRCUMFERENTIAL INTERPOLATION
1403C
1404      RDRFIT(I)=P(K,1)
1405      GO TO 15
1406C
1407C      IF 0. < THETA < ANGLOC(K,1) REQUIRES SPECIAL INTERPOLATION
1408C
1409 21      IF (THETA.LT.ANGLOC(1)) GO TO 19
1410C
1411C      SEARCH FOR ANGULAR BOUNDS
1412C
1413      DO 16 J=1,NP
1414      N2=J
1415      IF (J.EQ.NP) GO TO 20
1416C
1417C      IF ANGLOC(K,NP) < THETA < 360. REQUIRES SPECIAL INTERPOLATION
1418C
1419      IF (THETA.GE.ANGLOC(J).AND.THETA.LT.ANGLOC(J+1)) GO TO 20
1420 16      CONTINUE
1421      GO TO 20
1422 19      N2=NP
1423C
1424C      NUMBERS OF INTERPOLATION BOUNDARY ANGLES
1425C
1426 20      NRFIT(1)=N2
1427      NRFIT(2)=N2+1
1428      DO 18 I=1,2
1429      IF (THETA.LT.ANGLOC(1)) GO TO 7
1430      IF (NRFIT(1).LT.1) GO TO 23
1431      IF (NRFIT(1).GT.NP) GO TO 24
1432      L=NRFIT(1)
1433      Z(I)=ANGLOC(L)
1434      F(I)=P(K,L)
1435      GO TO 18
1436 7      IF (NRFIT(1).LE.NP) GO TO 6
1437      L=NRFIT(1)-NP

```

```

1438      Z(I)=ANGLOC(L)
1439      F(I)=P(K,L)
1440      GO TO 18
1441C
1442C      SET UP SPECIAL INTERPOLATION EXTERIOR POINT
1443C
1444 6      L=NRFIT(I)
1445      Z(I)=ANGLOC(L)-360.0
1446      F(I)=P(K,L)
1447      GO TO 18
1448 23      L=NRFIT(I)+NP
1449      Z(I)=ANGLOC(L)-360.0
1450      F(I)=P(K,L)
1451      GO TO 18
1452 24      L=NRFIT(I)-NP
1453      Z(I)=360.0+ANGLOC(L)
1454      F(I)=P(K,L)
1455 18      CONTINUE
1456C
1457C      LINEAR INTERPOLATION IN THE CIRCUMFERENTIAL DIRECTION.
1458C
1459      RADFIT(I)=(F(2)-F(1))*((THETA-Z(1))/(Z(2)-Z(1)))+F(1)
1460 15      CONTINUE
1461C
1462C      LINEAR INTERPOLATION IN THE RADIAL DIRECTION.
1463C
1464      DO 30 I=1,2
1465      L=NRFIT(I)
1466      Z(I)=RADLOC(L)
1467 30      F(I)=RADFIT(I)
1468C
1469C      FINAL INTERPOLATED VALUE
1470C
1471      PVALUE=(F(2)-F(1))*((R-Z(1))/(Z(2)-Z(1)))+F(1)
1472C
1473      RETURN
1474      END
1475C
1476C

```

```

1477C
1478
1479C
1480C
1481C
1482C
1483C
1484C
1485
1486
1487
1488
1489
1490
1491C
1492
1493
1494C
1495C
1496C
1497
1498
1499
1500C
1501C
1502C
1503
1504C
1505C
1506C
1507
1508
1509
1510
1511
1512
1513
1514C
1515C
1516C

SUBROUTINE UNSTDY

THIS SUBROUTINE PERFORMS THE TOTAL PRESSURE FLUCTUATION COMPUTATIONS

THE DELTA PRESSURES ARE ADDED TO THE STEADY STATE PRESSURES; THEN THE
DISTORTION FACTOR ROUTINES AND THE CONTOUR MAP ROUTINES ARE CALLED.

COMMON AR,ANGLOC(20),AUD,BETA2,RF,CDPOP3(10),CMAY5(10),FO,LSHFT,
& CMMIN(10),DKMX(10),DKSS(10),FACE(39,65),FACTOR,FARCE(39,65),BSF,
& J1,J2,KEY,KD,LONTFL,NN,NP,NR,P(11,20),PR(10),PS(11,20),CKP,
& PSPEC(20),PVALUE,QAV,QPT2,R,RADLOC(11),RANGE,RI,RNAV,BFP(11),
& RT,SGDK(10),SGP(10),SIG,SMAY5,STAT1,STATD,T,TDP1,TDP2,TMMIN,
& TDP3,THETA,THMIN(10),TITLE1(20),TITLE2(20),TMAY5,TMMAX,RKP,U2

DIMENSION AR(11)
CON=1.0/57.29577951

SET INITIAL AND/OR DEFAULT VALUES.

VL=999.999
XA=0.0
R1=0.0

CALL SUBROUTINE NEWPSD: INPUT IDENTIFICATION AND: CONTROL PARAMETERS

CALL NEWPSD(2)

DEFINE PROBE RADIAL LOCATION IN RATIO FORM.

NRG=0
DO 50 I=1,NP
IF (1.6E.J1.AND.1.LE.J2) NRG=NRG+1
AR(I)=RADLOC(I)/RADLOC(NR)
RRAR=0.5*(1.0+AR(I))
RRT=RRAR
DOPT=0.7*RNAV+RNAV/(1.0+0.2*RNAV+RNAV)**3.5

COMPUTE AVERAGE AND MAXIMUM MACH NUMBER AND VELOCITY AT ENGINE FACE.

```

```

1517 TMAVG6=TMAVG
1518 AMA=SQRT(5.♦♦((TMAVG/SMAG6)♦♦.286)-1.0)
1519 AMN=SQRT(5.♦♦((TMMA6/SMAG6)♦♦.286)-1.0)
1520 VBM=AMN♦SQRT(1.0+0.2♦AMA♦AMA)/SQRT(1.0+0.2♦AMN♦AMN)/AMA
1521 NV=2
1522 OKD=PSPEC(KD)
1523 VB1=1.0
1524c
1525c SEARCH FOR VORTEX LOCATION AND ORIENTATION.
1526c
1527 RKM=TMMIN
1528 RKM=TMMA6
1529 DO 68 I=1,NP
1530 RKA=0.0
1531 DO 66 J=J1,J2
1532 66 RKA=RKA+PS(J,I)
1533 RKA=RKA/NRG
1534 IF (RKA.LT.RKM) GO TO 67
1535 RKM=RKA
1536 THM=ANGLOC(I)
1537 67 IF (RKA.GT.RKM) GO TO 68
1538 RKM=RKA
1539 THM=ANGLOC(I)
1540 68 CONTINUE
1541 DTH=ABS(TMN-THM)
1542 THE=0.5♦(TMN+THM)
1543 IF (DTH.LE.180.0) GO TO 69
1544 DTH=360.0-DTH
1545 THE=THE+180.0
1546 69 IF (THE.GE.360.0) THE=THE-360.0
1547 ART=DTH/114.592
1548 61=-90.0
1549 IF (TMN.GT.THE) GO TO 71
1550 61=90.0
1551 71 IF (THE.GT.180.0) THE=THE-360.0
1552c
1553c TV IS THE VORTEX CIRCUMFERENTIAL LOCATION
1554c
1555 TV=THE
1556 CALL LNPUT(1)

```

```

1557 WRITE (6,1996)
1558 WRITE (6,1998) THMN,RKMN,THMX,RKMX,DTH,THE,ART,GI
1559 CALL LNPOUT(2)
1560 WRITE (6,1800)
1561C
1562C CALL SUBROUTINE TO COMPUTE MAXIMUM INSTANTANEOUS DISTORTION FACTORS
1563C
1564 CALL NEWPSD(3)
1565 A0=AB
1566 VB0=1.36*SIG/OPT2
1567 72 VBAR=VB1
1568C
1569C LOOP 600 IS THE VORTEX STRENGTH (VBAR) ITERATION.
1570C VBAR VARIES FROM VB1 TO VB2 BY DVB, NV TIMES.
1571C
1572 VBAR=VB1
1573 DO 600 IV=1,NV
1574 IF (IV-2) 73,721,722
1575 721 DNKD=PSPEC(KD)
1576 722 VBAR=(DKMX(KD)-DKD)/(DNKD-DKD)
1577C
1578C WHEN A SPECIFIC PRESSURE CONTOUR IS NEEDED A/RT IS COMPUTED FROM VBAR
1579C
1580 73 AYRT=ART
1581 RAV=1.0/AYRT
1582C
1583C VORTEX ORIENTATION ANGLES AND FUNCTIONS.
1584C
1585 G=61
1586 COSG=COS(CON*G)
1587 SING=SIN(CON*G)
1588 B=B1
1589 COSB=COS(CON*B)
1590 SINB=SIN(CON*B)
1591 CBG=COSB*SING
1592 SBG=SINB*SING
1593 CBG=COSB*COBG
1594 SBG=SINB*COBG
1595C

```

1596C LOOP 90 IS THE PROBE RADIAL LOCATION ITERATION. FOR A GIVEN VORTEX
 1597C THE PRESSURE FLOWFIELD IS FOUND AT EACH PROBE RADIUS AND THETA.
 1598C THERE ARE NR RINGS AND NP PROBES PER RING.

```
1599C
1600   DO 90 J=1,NR
1601     IF (J-J1) 78,65,63
1602     63   IF (J-J2) 65,65,78
1603     65   ZA=(AR(J)-RRT)/HYRT
1604     IF (ABS(ZA).GT.100.0) ZA=$16N(100.0,ZA)
1605     IF (ABS(TV).GT.180.0) TV=$16N(180.0,TV)
1606C
```

1607C LOOP 80 IS THE PROBE CIRCUMFERENTIAL LOCATION ITERATION.

```
1608C
1609   DO 80 I=1,NP
1610     PHI=ANGLOC(I)-TV
1611     IF (PHI.GT.180.0) PHI=PHI-360.0
1612     IF (PHI.LT.-180.0) PHI=PHI+360.0
1613     YA=CON*PHI*RAV
1614     Y=-XA*SBOSG+YA*CBOSG+ZA*SING
1615     IF (ABS(Y/VL).LT.1.0) GO TO 70
1616     DPT1=0.0
1617     GO TO 75
1618   70   BASE=YA*SING-ZA*COSG+COSB
1619     RAD=(XA*COSB+YA*SINB)*2+(-XA*SBOSG+YA*CBOSG-ZA*COSG)*2-1.0
1620     IF (RAD.GT.670.0) RAD=670.0
1621C
```

1622C DET1 IS THE PRESSURE FLUCTUATION AT PROBE AR(J) AND ANGLOC(J,I)

```
1623C
1624   DPT1=2.0*VBAR*BASE/EXP(0.5*PI*DI)
1625   75   P(J,I)=PS(J,I)+DPT1*ODPT*TMAY55
1626   80   CONTINUE
1627   GO TO 90
1628C
```

1629C RESET STATIC PRESSURE RINGS TO STATIC PRESSURE.

```
1630C
1631   78   DO 79 I=1,NP
1632   79   P(J,I)=PS(J,I)
1633   90   CONTINUE
1634   IF (IV-I) 91,91,92
1635   91   CALL PFI(X,TRUE.)
```

```

1636 CALL DISTRT
1637 GO TO 600
1638 92 CALL PRNT (2)
1639 CALL PFIY(.TRUE.)
1640 CALL DISTRT
1641 CALL PFIY(.FALSE.)
1642 CALL MAINLP
1643 CALL LNPOUT (1)
1644 WRITE (6,1995)
1645 WRITE (6,2000)
1646 WRITE (6,1999)
1647 CALL LNPOUT (2)
1648 WRITE (6,1805)
1649 600 CONTINUE
1650c
1651 RETURN
1652c
1653 1800 FORMAT (//27X,"<STEADY-STATE DISTORTION>")
1654 1805 FORMAT (//31X,"<PEAK DISTORTION>")
1655 1995 FORMAT (//25X,15HVORTEX LOCATION)
1656 1996 FORMAT (//25X,17HVORTEX PROPERTIES)
1657 1998 FORMAT (/12X,4HTHMN,3X,4HRKMN,4X,4HTHMX,3X,4HRKMX,4X,3HDTN,3X,
1658 % 5HTHETA,5X,2HA1,6X,2HG1/8X,2(F8.2,F7.3),F7.2,F8.2,F8.3,F7.2)
1659 1999 FORMAT (/11X,4HVBMX,4X,3HVB0,3X5HHA0/RT/8X,2F7.3,F8.4)
1660 2000 FORMAT (/10X,4HVBAP,4X,4HA/RT,1X,5HGAMMA,2X,4HBETA,3X,5HAY/RT,
1661 % 5X,2HVL,4X,4HR/RT,4X,5HTHETA/6X,2F8.3,2F6.1,3F8.3,F8.2)
1662c
1663 END
1664c
1665c

```

```

1666C SUBROUTINE TURBUL (PT1,RS1,NR1,NP1,U2,02,PT2,XM0,PTT0,RMSHG)
1667
1668C
1669C TURBULENCE PROGRAM
1670C BY: YEN-SEN CHEN
1671C (MAR. 17, 1984)
1672C
1673C THIS SUBROUTINE IS A SUBDRIVER FOR THE COMPUTATION OF RMS LEVELS
1674C AT THE COMPRESSOR FACE BY SOLVING THE K-E TURBULENCE MODEL.
1675C
1676C SUBROUTINE INITL IS USED TO SET INITIAL VALUES OF K AND E AT EACH
1677C GRID POINT (GK AND GE RESPECTIVELY).
1678C SUBROUTINE INIVEL IS USED TO CALCULATE VELOCITY GRADIENTS.
1679C SUBROUTINE CUBIC IS USED TO DO THE CUBIC SPLINE INTERPOLATIONS.
1680C SUBROUTINE TRIDIA IS USED TO SOLVE THE TRIDIAGONAL MATRIX EQUATION.
1681C SUBROUTINE FINITE SOLVES FOR THE K-E TURBULENCE MODEL USING A FINITE
1682C DIFFERENCE FORMULATION.
1683C
1684C
1685C DIMENSION PT(11,20),PT1(11,20),U(11,20),WK(20),WE(20),WUR(20),
1686C & RS1(20)
1687C COMMON /CUB/ NGR,NGP,NPW,NRW,NR,NP,RS(20),THA(20),DR(20),C1(20),
1688C & C2(20),C3(20),THG
1689C COMMON /VELGR/ URG(80,80),URRG(80,80),UTG(80,80),UTT6(80,80),
1690C & UUG(80,80),UG(80,80)
1691C COMMON /INIKE/ GK(80,80),GE(80,80),GP(80),GT(80),ERRK,ERRE
1692C COMMON /PARA/ PMU,NPR,NPP,NRG,NP6,NSHT,FACT
1693C
1694C SET GRID SIZE PARAMETERS (NGR & NGP), ITERATION LIMITER (NSHT),
1695C RELAXATION FACTOR (FACT) AND OTHER CONSTANTS.
1696C
1697C NGR=4
1698C NGP=4
1699C NSHT=30
1700C FACT=1.0
1701C AMU=1.75E-4
1702C PI=3.141592654
1703C NR=NR1
1704C NP=NP1
1705C DO 18 I=2,NR

```



```

1706 18      RS(I)=RS1(I)
1707      RS(I)=0.0
1708      WRITE(6,400)
1709 400      FORMAT(//1X,"TURBULENCE CALCULATIONS :")
1710      DO 10 I=2,NR
1711      DO 12 J=1,NP
1712 12      PT(I,J)=PT1(I,J)
1713 10      CONTINUE
1714C
1715C      COMPUTE RING AVERAGE PRESSURES FOR ESTIMATING BOUNDARY CONDITIONS.
1716C
1717      SUM=0.0
1718      SUM5=0.0
1719      SUM7=0.0
1720      SUM1=0.0
1721      DO 20 J=1,NP
1722      SUM=SUM+PT(2,J)
1723      SUM5=SUM5+(PT10-PT(6,J))
1724      SUM7=SUM7+PT(7,J)
1725      SUM1=SUM1+2.*PT(NR-2,J)-PT(NR-1,J)
1726 20      CONTINUE
1727      AVG=SUM/NP
1728      AVG5=SUM5/NP
1729      PT7A=SUM7/NP
1730      AVGP=SUM1/2.0/NP
1731      DO 30 J=1,NP
1732      PT(1,J)=AVG
1733 30      CONTINUE
1734C
1735C      NONDIMENSIONALIZE RADIAL COORDINATE AND GENERATE GRID POINTS.
1736C
1737      DO 40 I=2,NR-1
1738      RS(I)=RS(I)/RS(NR)
1739      DR(I-1)=(RS(I)-RS(I-1))/NSR
1740      DO 40 II=1,NSR
1741      L=(I-2)*NSR+II
1742      GR(L)=RS(I-1)+(II-1)*DR(I-1)
1743 40      CONTINUE
1744      THF=2.*PI/NP
1745      THG=THE/NSF

```

```

1746 NRH=(NR-2)*NHR+1
1747 NRM=NR*NSP
1748 GP(NRM)=RS(NR-1)
1749 DO 50 J=1,NP
1750 THA(J)=(J-1)*THE
1751 DO 50 JJ=1,NSP
1752 L=(J-1)*NSP+JJ
1753 GT(L)=THA(J)+(JJ-1)*THG
1754 50 CONTINUE
1755C
1756C ESTIMATE BOUNDARY RMS LEVEL AND CALCULATE VELOCITY DISTRIBUTIONS.
1757C
1758 DA=RS(NR)/6.
1759 RS(NR)=1.0
1760 CK=0.115*(PTT0-PT2)*(-0.2587)
1761 RED=U2*DA/AMU
1762 VELR=0.1275*(ALOG10(RED))*(-2.5)
1763 AMUR=SQRT(VELR)*U2*DA/AMU/2.
1764 PMU=1./AMUR
1765 CENK=10.0
1766 CENE=0.164*CENK**1.5/0.12
1767 WRMS=CK*AV65
1768 IF(WRMS.LT. 0.01) FACT=0.7
1769 DO 5 JJ=1,NP
1770 SUMP=0.0
1771 DO 15 I=1,NR-1
1772 DENR=(PT(I,J)/PT7A)**0.714286
1773 P1=PT(I,J)/DENR-PT7A
1774 P1=3.5*P1/02/VELR/PT2
1775 U(I,J)=SQRT(ABS(P1))
1776 IF(P1.LT. 0.) U(I,J)=-U(I,J)
1777 IF(I.LT. NR-2) GO TO 15
1778 SUMP=SUMP+(1.-PT(I,J))
1779 15 CONTINUE
1780 P0=CK*SUMP/2.0/AV6P
1781 P1=1./3.*U(NR-1,J)**2
1782 P2=1.75*WRMS/02/VELR/DENR
1783 WP(J)=-P1+SQRT(P1*P1+P2*P2)
1784 U(NR,J)=0.0
1785 WUR(J)=-2.0*U(NR-1,J)/(1.0-P3(NR-1))

```

```

1786 5  CONTINUE
1787  WRITE(6,300)
1788 300  FORMAT(//5X,"DIMENSIONLESS VELOCITY AT EACH PROBE LOCATION:")
1789  DO 35 J=1,NP
1790  WRITE(6,500)  U(I,J),I=1,NR
1791 500  FORMAT(1X,12F10.2)
1792 35  CONTINUE
1793  C1(1)=0.
1794C
1795C  SET INITIAL VALUES FOR TURBULENCE KINETIC ENERGY, GK.
1796C
1797  CALL CUBIC(NP,NK,THA,C1,C2,C3)
1798  CALL INITL(CENK,NK,GK)
1799C
1800C  CALCULATE THE RADIAL AND CIRCUMFERENTIAL VELOCITY GRADIENTS.
1801C
1802  CALL INIVEL(U,RS,THA,IR,THG,NPW,NRM,WUR,GR,NP,NR,NRP,NRP)
1803  DO 65 J=1,NP
1804  JNP=(J-1)*NGP+1
1805  WE(J)=0.3*WK(J)*SQRT(UUG(NPW,JNP))
1806 65  CONTINUE
1807  C1(1)=0.
1808C
1809C  SET INITIAL VALUES FOR TURBULENT KINETIC ENERGY DISSIPATION RATE,
1810C  GE.
1811C
1812  CALL CUBIC(NP,WE,THA,C1,C2,C3)
1813  CALL INITL(CENE,WE,GE)
1814 600  FORMAT(13X,"*****")
1815  WRITE(6,200)
1816 200  FORMAT(//5X,"ERRORS IN K, E AND (K+E) OF EACH ITERATION:")
1817  UUM=UUG(1,1)
1818  DO 45 J=2,NPW
1819  IF(UUG(1,J).GT. UUM) UUM=UUG(1,J)
1820 45  CONTINUE
1821  DO 55 J=1,NPW
1822  UUG(1,J)=UUM
1823 55  CONTINUE
1824  NRP5=NRP
1825  NRP5=NRP

```

```

1826      NRP=NP
1827      NRP=NP
1828C
1829C      CALL FINITE SUBROUTINE TO SOLVE FOR THE TURBULENCE MODEL USING
1830C      FINITE DIFFERENCE FORMULATIONS.
1831C
1832      CALL FINITE(UUG,DR,THG,NPW,NPW)
1833      CALL PRNT (8)
1834      WRITE(6,100)
1835 100    FORMAT(//4X,"RESULTS OF TURBULENCE CALCULATIONS:")
1836      WRITE(6,800)
1837 800    FORMAT(//13X,"PROBE",5X,"UU",10X,"E",11X,"K",9X,"SG/PT2")
1838C
1839C      COMPUTE RMS LEVEL AT EACH PROBE.
1840C
1841      SUMF=0.0
1842      DO 60 J=1,NP
1843      JJ=(J-1)*NGP+1
1844      DO 60 I=1,NR-2
1845      II=I*NGR+1
1846      TK=GK(II,JJ)
1847      TE=GE(II,JJ)
1848      TUU=UUG(II,JJ)
1849      TU=U(II,J)
1850      TR=RS(II+1)
1851      NT=(J-1)*(NR-2)+I
1852      DENR=(PT(II+1,J)/PT7H)**0.714286
1853      PRO=0.09*TK*TK+TUU*TE/TE
1854      P0=2./3.
1855      P1=2.*02*DENR*VELR/3.5
1856      P2=P0+TU*TU
1857      RMS=P1*SQRT(P2*TK+TK*TK)
1858      SUMF=SUMF+RMS**2
1859      WRITE(6,700) NT,TUU,TE,TK,RMS
1860 700    FORMAT(11X,15,3F12.4,F12.6)
1861 60    CONTINUE
1862      RMSH5=SUMF/NT
1863      RETURN
1864      END
1865C

```

```

1866C -----
1867C
1868      SUBROUTINE INITL(CE,WA,GA)
1869C
1870C      THIS SUBROUTINE GIVES THE INITIAL VALUES OF GK AND GE.
1871C
1872      DIMENSION WA(20),GA(80,80)
1873      COMMON /CUB/ NGR,NGP,NPW,NRM,NR,NP,RS(20),THA(20),DR(20),C1(20),
1874      & C2(20),C3(20),TH5
1875      DO 1 J=1,NP
1876      DO 1 I=1,NGP
1877      JJ=(J-1)*NGP+I
1878      T1=THA(J)+(I-1)*TH5
1879      P1=T1-THA(J)
1880      GA(NRW,JJ)=(C1(J)*P1+C2(J))*P1+C3(J))*P1+WA(J)
1881 1      CONTINUE
1882      DO 2 J=1,NPW
1883      DA=(GA(NRW,J)-CE)/RS(NR-1)
1884      DO 2 I=1,NR-2
1885      DO 2 K=1,NGR
1886      KK=(I-1)*NGR+K
1887      R1=RS(I)+(K-1)*DR(I)
1888      GA(KK,J)=CE+R1*DA
1889 2      CONTINUE
1890      RETURN
1891      END
1892C -----
1893C

```

```

1894C SUBROUTINE INIVEL(U,R,T,DR,TG,NPW,NPW,MUR,GR,NR,NR,NGR,NGR)
1895
1896C
1897C THIS SUBROUTINE COMPUTES THE RADIAL AND CIRCUMFERENTIAL VELOCITY
1898C GRADIENTS AT EACH GRID POINT USING CUBIC SPLINE INTERPOLATIONS.
1899C
1900 DIMENSION U(11,20),R(20),T(20),C1(60),C2(60),C3(60),A(60),DR(20),
1901 & MUR(20),MUR5(80),RA(60),GR(NRW)
1902 COMMON /VELGR/ UR5(80,80),URR5(80,80),UT5(80,80),UTT5(80,80),
1903 & UUG(80,80),UG(80,80)
1904 DO 1 I=2,NR-1
1905 DO 2 J=1,NP
1906 A(J)=U(I,J)
1907 CONTINUE
1908 C1(I)=0.
1909 CALL CUBIC(NP,A,T,C1,C2,C3)
1910 T1=(I-1)*NGR+1
1911 DO 1 J=1,NP
1912 DO 1 K=1,NGP
1913 KK=(J-1)*NGP+K
1914 T1=(K-1)*T5
1915 U5(I1,KK)=(C1(J)*T1+C2(J))*T1+C3(J)*T1+U(I,J)
1916 CONTINUE
1917 DO 3 J=1,NP
1918 DO 3 K=1,NGP
1919 KK=(J-1)*NGP+K
1920 U5(I,KK)=U(I,J)
1921 CONTINUE
1922 C1(I)=0.
1923 CALL CUBIC(NP,MUR,T,C1,C2,C3)
1924 DO 4 J=1,NP
1925 DO 4 K=1,NGP
1926 KK=(J-1)*NGP+K
1927 T1=(K-1)*T5
1928 MUR5(KK)=(C1(J)*T1+C2(J))*T1+C3(J)*T1+MUR(J)
1929 CONTINUE
1930 MP=NPW/2
1931 MR=2*NR-1
1932 DO 5 J=1,NP
1933 JJ=NP+J

```

```

1934      DO 6 I=1,NR
1935      IF (I .GT. NR) GO TO 8
1936      IF (I .EQ. 1) GO TO 7
1937      II=(NR-I) *N5R+1
1938      A(I)=U5(I,I,J)
1939      RA(I)=R(NR-I+1)
1940      GO TO 6
1941      C1(I)=999.
1942      C1(2)=WUR5(J)
1943      A(I)=0.
1944      RA(I)=R(NR)
1945      GO TO 6
1946      CONTINUE
1947      IF (I .EQ. NR) GO TO 9
1948      II=(I-NR) *N5R+1
1949      A(I)=U5(II,JJ)
1950      RA(I)=-R(I-NR+1)
1951      GO TO 6
1952      C1(3)=-WUR5(JJ)
1953      A(I)=0.
1954      RA(I)=-R(NR)
1955      CONTINUE
1956      CALL CUBIC(MR,A,RA,C1,C2,C3)
1957      DO 11 I=2,NR-1
1958      IF (I .GT. NR-1) GO TO 12
1959      DO 13 K=1,N5R
1960      II=(NR-I) *N5R+2-K
1961      IK=NR-I
1962      R1=-(K-1) *DR(IK)
1963      U5(II,J)=(C1(I) *R1+C2(I)) *R1+C3(I) *R1+A(I)
1964      UR5(II,J)=C3(I) *R1+2. *C2(I) *R1+C3(I)
1965      URR5(II,J)=6. *C1(I) *R1+2. *C2(I)
1966      CONTINUE
1967      GO TO 11
1968      CONTINUE
1969      DO 22 K=1,N5R
1970      II=(I-NR) *N5R+K
1971      IK=I-NR+1
1972      R1=-(K-1) *DR(IK)
1973      U5(II,JJ)=(C1(I) *R1+C2(I)) *R1+C3(I) *R1+A(I)

```

```

1974      UR6(I,JJ)=-C3.♦C1(I♦R1+2.♦C2(I)♦R1+C3(I)
1975      UR6(I,JJ)=6.♦C1(I♦R1+2.♦C2(I)
1976      CONTINUE
1977      CONTINUE
1978      U5(I,J)=U5(I,JJ)
1979      UR6(I,J)=-UR6(I,JJ)
1980      UR6(I,J)=UR6(I,JJ)
1981      CONTINUE
1982      DO 14 J=1,NPW
1983      UT5(I,J)=0.
1984      UT5(I,J)=0.
1985      DO 14 I=2,NPW
1986      IF(J.EQ. 1) GO TO 15
1987      IF(J.EQ. NPW) GO TO 16
1988      B=U5(I,J-1)
1989      D=U5(I,J+1)
1990      GO TO 17
1991      B=U5(I,NPW)
1992      D=U5(I,2)
1993      GO TO 17
1994      B=U5(I,NPW-1)
1995      D=U5(I,1)
1996      UT5(I,J)=(D-B)/2./T5/GR(I)
1997      UT5(I,J)=(D+B-2.♦U5(I,J))/T5/T5/GR(I)/GR(I)
1998      CONTINUE
1999      DO 20 J=1,NPW
2000      DO 20 I=1,NPW
2001      U05(I,J)=UR6(I,J)♦♦2+UT5(I,J)♦♦2
2002      CONTINUE
2003      RETURN
2004      END
2005c
2006c

```



```

2007c SUBROUTINE CUBIC(N,Y,X,C1,C2,C3)
2008
2009c THIS SUBROUTINE PERFORMS CUBIC SPLINE INTERPOLATIONS (SLOPE-BASED).
2010c
2011c
2012c DIMENSION Y(N),X(N),C1(N),C2(N),C3(N),G(60),H(60),S(60),B(60)
2013 DO 5 I=1,N-1
2014 G(I)=Y(I+1)-Y(I)
2015 H(I)=X(I+1)-X(I)
2016 5 S(I)=SORT(G(I)/Y(3))**2+H(I)**2)
2017 H(N)=1.
2018 IF(C1(1) .NE. 0.) GO TO 7
2019 G(N)=Y(1)-Y(N)
2020 H(N)=X(N)-X(N-1)
2021 S(N)=SORT(G(N)**2+H(N)**2)
2022 7 CONTINUE
2023 DO 10 I=1,N
2024 IF(I .EQ. 1) GO TO 1
2025 IF(I .EQ. N) GO TO 2
2026 P1=G(I-1)**S(I)/H(I-1)
2027 P2=G(I)**S(I-1)/H(I)
2028 B(I)=(P1+P2)/(S(I)+S(I-1))
2029 GO TO 10
2030 1 CONTINUE
2031 P1=G(N)**S(1)/H(N)
2032 P2=G(1)**S(N)/H(1)
2033 B(1)=(P1+P2)/(S(1)+S(N))
2034 IF(C1(1) .EQ. 999.) B(1)=C1(2)
2035 GO TO 10
2036 2 CONTINUE
2037 P1=G(N-1)**S(N)/H(N-1)
2038 P2=G(N)**S(N-1)/H(N)
2039 B(N)=(P1+P2)/(S(N)+S(N-1))
2040 IF(C1(1) .EQ. 999.) B(N)=C1(3)
2041 10 CONTINUE
2042 B(N+1)=B(1)
2043 M=N-1
2044 IF(C1(1) .EQ. 0.) M=N
2045 DO 50 I=1,M
2046 P1=H(I)**H(I)

```

```

2047      C1(I)=(B(I)+B(I+1))/P1-2.*5(I)/P1/H(I)
2048      C2(I)=- (2.*B(I)+B(I+1))/H(I)+3.*5(I)/P1
2049      C3(I)=B(I)
2050      CONTINUE
2051      RETURN
2052      END
2053c
2054c -----

```

ORIGINAL PAGE IS
OF POOR QUALITY

```

2055C
2056      SUBROUTINE TRIDIA(N,A,B,C,F,X)
2057C
2058C      THIS SUBROUTINE SOLVES THE TRIDIAGONAL MATRIX EQUATION.
2059C
2060      DIMENSION A(N),B(N),C(N),F(N),X(N)
2061      DO 10 I=1,N
2062      IF (I.EQ. 1) GO TO 5
2063      A(I)=A(I)-B(I)*C(I-1)
2064      C(I)=C(I)/A(I)
2065      F(I)=(F(I)-B(I)*F(I-1))/A(I)
2066      GO TO 10
2067 5      C(I)=C(I)/A(I)
2068      F(I)=F(I)/A(I)
2069 10      CONTINUE
2070      X(N)=F(N)
2071      DO 20 I=1,N-1
2072      J=N-I
2073      X(J)=F(J)-C(J)*X(J+1)
2074 20      CONTINUE
2075      RETURN
2076      END
2077C
2078C

```

ORIGINAL PAGE IS
OF POOR QUALITY

```

2079C
2080
2081C
2082C
2083C
2084C
2085
2086
2087
2088
2089C
2090C
2091C
2092
2093
2094
2095
2096
2097
2098
2099
2100
2101
2102
2103
2104
2105
2106
2107
2108
2109
2110C
2111C
2112C
2113
2114
2115
2116C
2117C
2118C

SUBROUTINE FINITE(UU,DR,THG,NPW,NRW)

THIS SUBROUTINE SOLVES FOR THE FINITE DIFFERENCE SCHEME USING
IMPLICIT TRIDIAGONAL MATRIX FORMULATIONS.

      DIMENSION DR(20),UU(80,80),A(160),B(160),C(160),F(160),XK(160),
      & XE(160),VMEFF(80,80),DRG(80),A1(160),B1(160),C1(160),F1(160)
      COMMON /PARA/ PMU,NRR,NPP,NRG,NPG,NSHT,FACT
      COMMON /INIK/ GK(80,80),GE(80,80),GR(80),GT(80),ERRK,ERRE

SET INITIAL PARAMETER AND CONSTANTS.

      NSH=1
      SIGK=1.0
      SIGE=1.3
      CE1=1.45
      CE2=2.0
      DO 1 I=1,NRR-2
      PDR=DR(I)/NRG
      DO 1 K=1,NRG
      KK=(I-1)*NRG+K
      DRG(KK)=PDR
      CONTINUE
      DO 2 I=1,NRW
      DO 2 J=1,NPW
      VMEFF(I,J)=0.09*GK(I,J)*2/GE(I,J)+PMU
      CONTINUE
      NP=NPW/2
      NR=2*NRW-1
      NM=NR-2

START ITERATIONS.

      CONTINUE
      EPPK=0.0
      ERPE=0.0

COMPUTE ELEMENTS OF TRIDIAGONAL MATRIX EQUATIONS OF K AND E.

```

2119	DO 3 J=1,MP	
2120	DO 7 I=1,NM	
2121	IF (I .GT. NRM-1) GO TO 5	
2122	II=NRM-I	
2123	JJ=J	
2124	K=1	
2125	L1=0	
2126	L2=1	
2127	JP=JJ-1	
2128	J0=JJ+1	
2129	IF (J .EQ. 1) JP=NPM	
2130	GO TO 6	
2131	CONTINUE	5
2132	II=I-NRM+2	
2133	JJ=J+MP	
2134	K=-1	
2135	L1=1	
2136	L2=0	
2137	JP=JJ-1	
2138	J0=JJ+1	
2139	IF (J .EQ. MP) J0=1	
2140	CONTINUE	6
2141	I0=II	
2142	GR0=GR(I1)	
2143	GRB=GR(I1+K)	
2144	GRA=GR(I1-K)	
2145	THG0=THG	
2146	IF (I .NE. NRM-1) GO TO 12	
2147	GP0=1.0	
2148	GRB=1.0	
2149	GRA=1.0	
2150	THG0=DRG(I1)	
2151	I0=2	
2152	JP=JJ+MP+MP/2	
2153	J0=JJ+MP/2	
2154	IF (JP .GT. NPM) JP=JP-NPM	
2155	CONTINUE	12
2156	P1=GR0+VMEFF(I1,JJ)+GRB+VMEFF(I1+K,JJ)	
2157	P2=GRA+VMEFF(I1-K,JJ)+GR0+VMEFF(I1,JJ)	
2158	P3=VMEFF(I1,JJ)+VMEFF(I0,JP)	

```

2159 P4=VMEFF(I0,J0)+VMEFF(II,JJ)
2160 PP=2.*GRO**2*THG0**2
2161 IF(1.EQ. NRM-1) GO TO 17
2162 P5=(P3+P4)/PP
2163 CK=-GK(I0,J0)*P4+GK(I0,JP)*P3/PP
2164 CE=-GE(I0,J0)*P4+GE(I0,JP)*P3/PP
2165 CONTINUE
2166 OR1=DRG(II-L1)
2167 OR2=DRG(II-L2)
2168 IF(1.EQ. NRM-1) OR2=OR1
2169 OR=(OR1+OR2)*GRO
2170 O1=OR1*OR
2171 O2=OR2*O1
2172 O3=OR2*OR
2173 AP=P1/O1
2174 AH=- (OR1*P2+OR2*P1)/O2+P5)
2175 HQ=P2/O3
2176 FK=(GE(II,JJ)-VMEFF(II,JJ)*UU(II,JJ))/GK(II,JJ)
2177 FE=(CE2*GE(II,JJ)-CE1*VMEFF(II,JJ)*UU(II,JJ))/GK(II,JJ)
2178 B(I)=AP/SIGK
2179 H(I)=AH/SIGK-FK/2.
2180 C(I)=HQ/SIGK
2181 F(I)=CK/SIGK
2182 IF(1.EQ. 1) F(I)=F(I)-B(I)*GK(II+1,JJ)
2183 IF(1.EQ. NM) F(I)=F(I)-C(I)*GK(II+1,JJ)
2184 B(I)=AP/SIGE
2185 A1(I)=AH/SIGE-FE/2.
2186 C1(I)=HQ/SIGE
2187 F1(I)=CE/SIGE
2188 IF(1.EQ. 1) F1(I)=F1(I)-B1(I)*GE(II+1,JJ)
2189 IF(1.EQ. NM) F1(I)=F1(I)-C1(I)*GE(II+1,JJ)
2190 CONTINUE
2191
2191C
2192C SOLVE FOR TRIDIAGONAL MATRIX EQUATIONS OF K AND E (XK AND XE).
2193C
2194 CALL TRIDIA(NM,A,B,C,F,XF)
2195 CALL TRIDIA(NM,A1,B1,C1,F1,XE)
2196 DO 8 I=1,NM
2197 IF(1.GT. NRM-1) GO TO 9
2198 I1=NRM-I

```

```

2199      JJ=J
2200      GO TO 10
2201  9    CONTINUE
2202      II=I-NRM+2
2203      JJ=J+MP
2204  10   CONTINUE
2205C
2206C      COMPUTE RELATIVE ERRORS.
2207C
2208      ERRK=ERRK+ABS(CXK(I)-GK(II,JJ))*100./GK(II,JJ)
2209      ERRE=ERRE+ABS(XE(I)-GE(II,JJ))*100./GE(II,JJ)
2210      IF(CXK(I).LT.0.0001) XK(I)=0.0001
2211      IF(XE(I).LT.0.0001) XE(I)=0.0001
2212C
2213C      OBTAIN UP-DATED SOLUTIONS WITH RELAXATION FACTOR, FACT.
2214C
2215      GK(II,JJ)=GK(II,JJ)+FACT*(CXK(I)-GK(II,JJ))
2216      GE(II,JJ)=GE(II,JJ)+FACT*(XE(I)-GE(II,JJ))
2217      VMEFF(II,JJ)=0.09*(CXK(I)+2/XE(I))+PMU
2218  8    CONTINUE
2219  100   FORMAT(9X,3F15.5)
2220  3    CONTINUE
2221      ERRK=ERRK/NM/MP
2222      ERRE=ERRE/NM/MP
2223      ERRT=ERRK+ERRE
2224      WRITE(6,100) ERRK,ERRE,ERRT
2225      IF(NSH.GE.NSHT) GO TO 20
2226      NSH=NSH+1
2227      GO TO 4
2228  20   CONTINUE
2229      RETURN
2230      END

```

APPENDIX B.

OPTIONAL "SEGMENTED VORTEX" ADDITION

An addition to the source code given in Appendix B includes the Segmented Vortex approach described in Ref. 8. In this approach, the vortex model derived in the standard Melick approach is divided into eight segments. This process allows for simulation of a nonlinear vortex, or a vortex ring. Theoretically, this should allow for more accurate modelling of the inlet flow distortion, for better results. The segmented vortex approach showed some improvement of the predicted peak instantaneous distortion contour map in certain cases (Reference 8). The User is free to experiment with this addition to the source code. The following page lists the addition, showing where it is to be inserted in the original code.


```

1621      IF (RAD.GT.670.0) RAD=670.0
1622C
1623C      DPT1 IS THE PRESSURE FLUCTUATION AT PROBE AR(J) AND ANGLUC(J,I)
1624C
1625      DPT1=2.0*VBAR*BASE/EXP(0.5*RAD)
1626 75      P(J,I)=PS(J,I)+DPT1*QDPT*TMAVGG
1627 80      CONTINUE
1628      GO TO 90
1629C
1630C      RESET STATIC PRESSURE RINGS TO STATIC PRESSURE.
1631C
1632 78      DO 79 I=1,NP
1633 79      P(J,I)=PS(J,I)
1634 90      CONTINUE
1635C
1636C      *** NEW "SEGMENTED" VORTEX METHOD BY STEPHEN R. DENNON ***
1637C      FIND PROBE LOCATION (RADLOC) NEAREST TO MEAN LINE
1638C
1639      DO 120 I=1,NP
1640      DDP(I) = 10.
1641      DO 110 J=1,NR
1642      DP(J,I) = ABS(TMAVGG - PS(J,I))
1643      IF (DP(J,I) .LE. DDP(I)) GO TO 100
1644      GO TO 110
1645 100      DDP(I) = DP(J,I)
1646      RADLOC(I) = RADLOC(J)
1647 110      CONTINUE
1648 120      CONTINUE
1649C
1650C      SOLVE FOR NEW PEAK INSTANTANEOUS PRESSURE ARRAY
1651C
1652      DO 140 I=1,NP
1653      DO 130 J=1,NR
1654      IF (J .LT. J1 .OR. J .GT. J2) GO TO 125
1655      DRR = ABS(RADLOC(I) - RADLOC(J))
1656      RRA = DRR/RT/ART
1657      RAD = RRA**2-1.
1658      DPT1 = ABS(2*VBAR*RRA*QDPT*TMAVGG/EXP(.5*RAD))
1659      IF (PS(J,I) .LE. TMAVGG) GO TO 121
1660      P(J,I) = PS(J,I) + DPT1
1661      GO TO 130
1662 121      P(J,I) = PS(J,I) - DPT1
1663      GO TO 130
1664 125      P(J,I) = PS(J,I)
1665 130      CONTINUE
1666 140      CONTINUE
1667C
1668      IF (IV=1) 91,91,92
1669 91      CALL PFIX (.TRUE.)
1670      CALL DISTR1
1671      GO TO 600
1672 92      CALL PRNT (2)
1673      CALL PFIX (.TRUE.)
1674      CALL DISTR1
1675      CALL PFIX (.FALSE.)
1676      CALL MAINLP
1677      CALL LNPOUT (1)
1678      WRITE (6,1995)
1679      WRITE (6,2000) VBAR,ART,G,B,AYRT,VL,RRT,TV
1680      WRITE (6,1999) VBM,VBO,AO

```

original
code

new
addition

original
code

APPENDIX C.

QUICK REFERENCE GUIDE

1. MAXIDYN Program Description
2. Input Data Description
3. Output Data Description

1. MAXIDYN Program Description

The MAXIDYN dynamic distortion program computes the most probable peak instantaneous distortion level given the steady-state distortion conditions, and generates a peak distortion map based on the predictions. The Melick convecting vortex model and statistical approach is used in this predictive analysis, with some modifications and improvements to enhance program flexibility. The complete FORTRAN program requires sufficient computer memory capacity for approximately 100,000 words, plus typically 5000 words per data set. Run time varies from system, but is generally limited only by the online printer output capacity on most main-frame systems.

Input data requirements include the rake and probe configuration used in the test, the steady-state static and total (stagnation) pressure measurements in the rake plane, some basic inlet flow parameters, and optionally the root mean square pressure fluctuation level measurements. The input data are described briefly in the next section, and formatting requirements are shown in the figure. Some of the input data are optional, that is they may be deleted from the input file. The program automatically assigns pre-defined default values, or as in the case of the rms levels, the data are computed based on other input data.

The printed output of the MAXIDYN program includes several pages of steady-state and dynamic distortion data. The input data are organized in groups printed in the first few pages, along with steady-state distortion computations, Melick vortex model parameters, and the steady-state map. The rms fluctuation levels and/or turbulence modelling data are printed in the next few pages, along with the statistical

predictions of the most probable peak instantaneous distortion levels. Finally, a dynamic distortion map is generated based on the peak instantaneous prediction. A brief description of the output data is given in the third part of this Appendix.

2. Input Data Description

The table below briefly defines the variables in the input data. Certain data may be deleted from the input file because they are considered optional and generally are not part of the computational procedure. Some of these data are assigned default values as needed within the program. All optional data are indicated with a "*" in the second column of the table below. In the Format column, "F" indicates a real number, "I" indicates an integer, and "A" indicates an alphanumeric array, according to standard FORTRAN rules. The arrangement of the input data is illustrated in Figure A1.

Data	*	Format	Definition
NR		I5	Number of pressure tap radial locations
NP		I5	Number of rakes
RADLOC		F10.5	Radial location of pressure taps
ANGLOC		F10.5	Angular location of rakes in degrees
KD		I5	Distortion factor selection index
			KD = 1: KTHETA
			2: KD2
			3: IDC
			4: IDR
			5: KRA
			6: KA2
			7: DSPR
			8: ID

Data	*	Format	Definition
T	*	F10.5	RMS fluctuation measurement time-on-point default = 1 sec.
FO	*	F10.5	Engine filter frequency, default = 500 Hz
FCO	*	F10.5	RMS cut-off filter frequency, 1000 Hz def.
TITLE	*	A80	Title block
BRP	*	F10.5	Base radial profile array, default = 1.0
PS		F10.5	Steady-state pressure array
ALPH	*	F5.3	Inlet angle of attack in degrees
PSI	*	F5.3	Inlet yaw angle (crosswind) in degrees
MO	*	F5.3	Freestream Mach number
U2		F5.3	Inlet flow velocity in fps
BF	*	F5.3	B-factor for weighting in KA2 computation default = 1.0
CKP	*	F5.3	Circumferential ID weighting factor, default = 16.4
RKP	*	F5.3	Radial ID weighting factor, default = 11.1
MFR	*	F5.3	Inlet mass flow ratio, default = 1.0
NTUR	*	I5	Dynamic data selection index NTUR = 0: Dynamic data (rms levels) input 1: Dynamic data synthesized
SPTRC	*	F5.3	Supersonic inlet pressure recovery, default = 1.0

The following data is required if NTUR = 0:

NPG		I5	Data run number
NPR		I5	Dynamic probe location number
RS	*	F5.3	Filtered rms level ÷ unfiltered rms level default = 0.5
SIG		F6.4	Unfiltered rms fluctuation level

155

3. Output Data Description

The printed output of the MAXIDYN program consists of several pages of data and computations. The first two pages are related to the steady-state distortion and some Melick vortex model parameters, the middle page or pages are related to the dynamic data and the statistical determination of the most probable peak instantaneous distortion, and the last two pages are related to the generation of the peak instantaneous distortion map. The contents of each of the pages of output are briefly defined below.

Page 1

At the top of the first page, immediately below the title blocks supplied by the user, is the steady-state PRESSURE ARRAY. This array is identical to the pressure array of the input data, except the static pressures have been deleted. Each column of the array represents a rake, while the rows represent probe locations of probes along the rake. Immediately below the pressure array is the BASE RADIAL PROFILE, also from the input file. The next table, the OVERALL FLOW DESCRIPTORS, provides some simple distortion parameters:

PTMIN is the minimum measured local pressure from the steady-state PRESSURE ARRAY.

PTMAX is the maximum pressure from the PRESSURE ARRAY.

PTAVG is the average pressure from the PRESSURE ARRAY.

PSAVG is the average static pressure.

QAVG is the average dynamic pressure.

The next table is a listing of the eight FLOW DISTORTION FACTORS and their values, along with weighting factors.

At the bottom of the first page, some of the Melick VORTEX PROPERTIES are given. These properties are:

- THMN - The rake showing minimum average pressure
- RKMN - The average pressure along rake THMN
- THMX - The rake with maximum average pressure
- RKMX - The average pressure along rake THMX
- DTH - The angular difference between THMX and THMN
- THETA - The angular location of the center of arc DTH
- A1 - The radius of the steady-state Melick vortex
- G1 - The orientation angle of the steady-state vortex

Page 2

The next page of printed output is a distortion contour map for the steady-state case. Relatively high and low pressure regions are indicated by symbols, which represent the percent difference from the average pressure, as indicated by the KEY TO MAPPING SYMBOLS immediately above the map. The average pressure is printed to the right of the map.

Page 3

Page three of the output includes a listing of some of the input data, including flow parameters, and the dynamic data, assuming dynamic data was included in the input file. If dynamic data was not included in the input file, the third page would include some data from internal turbulence calculations. The data on this page includes:

- T - The dynamic data time-on-point, in seconds
- FO - The engine filter frequency, in Hz.
- RT - The outer rake diameter at the static tap
- RI - The centerbody hub radius
- SPTRC - The supersonic inlet shock pressure recovery
- ALPH - The inlet angle of attack
- PSI - The inlet yaw/crosswind angle

MO - The freestream Mach number
ETA - The average pressure at the measurement plane
MFR - The inlet mass flow ratio
U2 - The inlet flow velocity at the measurement plane
QPT2 - The ratio of the dynamic to total pressure
FC - The rms filter cutoff frequency

If dynamic data is included in the input data file, these data are printed in a table. The terms in this table are:

PROBE - The dynamic probe location index
RS - The ratio of filtered-to-unfiltered rms level
SG/PT2 - The unfiltered rms fluctuation level
A/RT - The vortex radius resulting from the rms level

The rms fluctuation level and vortex size are given below the dynamic data table.

If dynamic data are excluded from the input file, these data must be synthesized by the turbulence modelling scheme. In this case, the dynamic data table is replaced by a table of DIMENSIONLESS VELOCITIES occurring at each of the probe locations, and a table of iterations of turbulent kinetic energies. These are provided for the convenience of the user and are not directly involved in the distortion analysis.

Page 4

The fourth page of output includes a listing of the DISTORTION FACTOR EXTREME VALUE computations. For each of the eight distortion factors, values of the most probable peak instantaneous distortion are presented. This table includes the STEADY STATE, MEAN INSTANTANEOUS, and peak instantaneous distortion at various statistical confidence levels. In addition, the filtered and unfiltered rms distortion levels are indicated; INF referring to the unfiltered case and FO representing the filtered case.

In the case where the turbulence modelling scheme is used to generate the dynamic data, the fourth page includes further results of the TURBULENCE CALCULATIONS. This table is similar to the dynamic data table as described in the third page of output, with the exception that the term RS is deleted, and velocity gradients (UU) and turbulent kinetic energy terms (K and E) are added. The unfiltered rms levels are presented in the last column. The DISTORTION FACTOR EXTREME VALUE table is moved to the fifth page in this case.

Page 5

The fifth page is arranged exactly like the first page, but with notable differences. All of the terms in the PRESSURE ARRAY, OVERALL FLOW DESCRIPTORS, and FLOW DISTORTION FACTORS tables refer to the peak instantaneous case rather than the steady-state case. In addition, the VORTEX properties table contains additional terms:

- VBAR - The vortex "strength", or maximum swirling velocity
- A/RT - The radius of the Melick vortex
- GAMMA - One of the vortex orientation angles
- BETA - The second vortex orientation angle
- AY/RT - (The same as A/RT)
- VL - The vortex length limit (generally "infinity")
- R/RT - The radial location of the vortex core
- VBMX - The maximum instantaneous vortex "strength"
- VBO - The approximated mean vortex strength found in an iteration of strengths and distortion factors.
- AO/RT - The vortex size indicated from the rms data.

Page 6

The sixth page is similar to the second page except the distortion map is for the peak instantaneous case.

VI. CONCLUSIONS & RECOMMENDATIONS

The subject computer program can be used to aid the prediction of maximum instantaneous distortion levels, and the peak instantaneous contour map, given the steady-state distortion data and, optionally, the dynamic rms pressure fluctuation data. There are some improvements which can be added to the program, at User's discretion.

One improvement currently being researched at the University of Kansas is the replacement of the single steady-state vortex model with a series of vortices whose axes lie approximately along the "mean line" of pressure recoveries at the compressor face. This effort is intended to improve the predicted peak distortion contour map to more closely resemble the experimental map produced by DYNADEC. Other methods of improving the accuracy of both the peak distortion level, and the corresponding contour map, with respect to experimental results, would be highly desirable.

The accuracy of the present analysis is discussed in References 5 and 6, along with the basic derivations in the theoretical analysis. In general, the Melick technique is reasonably accurate for preliminary design and analysis. The major benefit of the Melick method is its efficiency, and the general tendency to over-estimate the experimental or true peak distortion level, rather than under-estimate it. One of the primary difficulties with the Melick analysis is in predicting the distortion levels for inlets with separated flows. It would be desirable to try to improve the accuracy of the peak prediction for this extreme case, which can occur especially often in highly maneuverable aircraft, which operate at high angles of attack and yaw angles, and also tend to have complicated inlet duct shapes.

VII. REFERENCES

1. Ybarra, A. H., and Melick, H. C., "Computer Program Documentation, Estimating Maximum Instantaneous Distortion From Inlet Total Pressure RMS and PSD Measurements, Volume I. Definition of the Mean Size and Strength of the Vortices Creating Inlet Turbulent Flow" (Preliminary), Vought Systems Division of LTV Aerospace Corporation Technical Report No. 2-57110/5R-3210, 31 March 1975.
2. Ybarra, A. H. and Melick, H. C., "Computer Program Documentation, Estimating Maximum Instantaneous Distortion From Inlet Total Pressure RMS and PSD Measurements, Volume II. Estimating the Maximum Instantaneous Distortion" (Preliminary), VSD Technical Report No. 2-57110/5R-3210, 31 March 1975.
3. Melick, H. C., and Ybarra, A. H., "Estimating Maximum Instantaneous Distortion From Inlet Total Pressure RMS and PSD Measurements", VSD Technical Report No. 2-57110/5R-3209, 31 March 1975.
4. Schweikhard, W. G. and Chen, Yen-Sen, "Literature Search of Publications Concerning the Prediction of Dynamic Inlet Flow Distortion and Related Topics, NASA Contractor Report No. 3673, 1983.
5. Chen, Yen-Sen, "Statistical Prediction of Dynamic Distortion of Inlet Flow Using Minimum Dynamic Measurement - An Application to the Melick Method", Masters Thesis Diss., U. of Kansas, 1983.

6. Chen, Yes-Sen, "Inlet Flow Distortion Prediction -- Without RMS Measurements", PhD Thesis Dissertation, University of Kansas, 1984.
7. Marous, J.J., & Sedlock, D., "Dynamic Data Editing and Computing System (DYNADEC)", Proceedings of Air Force System Command Science and Engineering Symposium, AFSC-TR-003, Vol. 1, Oct. 1973.
8. Dennon, Stephen R., "Review and Evaluation of Recent Developments in Melick Inlet Dynamic Flow Distortion Prediction", Masters Thesis Dissertation, University of Kansas, 1986.